Fines reduction and energy optimisation in aggregates production

Matthew James Amor Ruszala

Supervisors:
Dr Neil Rowson
Mr Jon Aumônier
Dr Phil Robbins

MRes Chemical Engineering Sciences
The University of Birmingham

May 2013

ABSTRACT

Aggregates production is a huge global industry which uses an enormous amount of energy and produces a massive amount of unsaleable fines. By reducing the amount of energy used per tonne of material produced and/or the amount of fines produced, it would make a quarry more efficient and, therefore, more environmentally friendly and profitable. This research looks at modelling Mountsorrel Quarry, a granite quarry in the UK, using JKSimMet and Split-Desktop software packages in conjunction with the EU project, EE-Quarry. XRF analysis of Mountsorrel Quarry granite found that it contains a number of oxides, predominantly SiO_2 (63.3%) and Al_2O_3 (16.8%), and XRD analysis found it contains the crystalline structures of quartz (SiO_2) and albite, calcian, ordered $(Na,Ca)Al(Si,Al)_3O_8$). Samples submitted to drop-weight tests confirmed Mountsorrel Quarry granite as an extremely hard granite and rock fracture (t_{10}) data and energy of comminution (E_{cs}) data were obtained from analysing the results.

Split-Desktop image analysis software was utilised to determine the particle size distribution (PSD) of the primary crusher feed, as it contains particles too large to screen manually. It was also found that 0.8% of the feed is fines, which at Mountsorrel Quarry are classed as particles smaller than 5 mm, and that no particles were larger than 3810 mm. JKSimMet was used to create a flowsheet of Mountsorrel Quarry, and the crusher product PSDs were simulated and was found to have strong correlations with experimental data, especially in the fines region, with a mean difference of 1.0%. The simulated primary crusher product PSD showed that it contains 5.9% fines, and a simulation over the entire quarry showed the product to be within the size range produced at Mountsorrel Quarry, and with a simulated fines content of 13.4%. When the closed side setting on the primary crusher was altered from 165.1 mm (the operating size on site) to 100.0 mm, it increased the amount of fines produced by 45%, increased the power draw by 140.6 kW, but reduced the overall plant production of fines by 18%.

Two blasts were undertaken on adjacent rock faces which had identical blast designs, other than the order of deck detonation, with the first blast detonating the bottom deck before the top and vice versa in the second blast. For each blast, measurements of the feed PSD to the primary crusher, the number of particles that required secondary breakage on the quarry floor, acoustic levels and vibration readings were measured and no significant difference was identified between the two blasts in any of the parameters measured.

In conclusion, a working model of Mountsorrel Quarry has been made in JKSimMet that has been validated against data from site and Split-Desktop has been used to simulate the primary crusher feed PSD, something that was previously unknown. The effect of reversing the order of deck detonation in a two deck blast was also analysed but with no significant difference between the two blasts found.

ACKNOWLEDGMENTS

I would like to express my greatest gratitude to all the people who have helped and supported me throughout my project. I am truly thankful and indebted to my supervisor, Dr Neil Rowson from the University of Birmingham for his advice and direction throughout, as well as my secondary supervisor, Dr Phil Robbins. I would also like to thank Jon Aumônier, at MIRO, who provided the funding for this research and provided plenty of helpful ideas. I would not have been able to have completed this research wit out the help Ian Brown, Mick Collins, Simon Edwards, Steve Mee and everybody else at Lafarge Aggregates' Mountsorrel Quarry who very kindly explained the workings of the quarry and were extremely cooperative in helping me to collect my data while putting up with me interrupting their work. Moreover, I would like to thank Dr Rob Farnfield and Dr Mark Pegden from EPC, who helped to coordinate the blasting experiments and gave me help and advice in the field of explosives and blasting, and Christopher Bailey from JKSimMet and Brian Norton from Split-Desktop who helped me with my queries with their software. Last and by no means least I would like to thank Dr Richard Greenwood from the University of Birmingham for his help on and off site, Prof Sam Kingman of Nottingham University for kindly allowing me to use his drop-weight tester, and Jon Rowson for compiling some tables of data on JKSimMet.

TABLE OF CONTENTS

TABLE OF FIGURES

TABLE OF TABLES

TABLE OF EQUATIONS

TABLE OF ACRONYMS

BIF ore – Banded iron formation ore

CSS – Closed side settings

EE-Quarry – Energy Efficient Quarry

ET – Eccentric throw

EU – European Union

MIRO – Minerals Industry Research Organisation

MRes – Masters of Research

MSDS – Materials safety data sheet

N/A – Not applicable

PPE – Personal protective equipment

PSD – Particle size distribution

UK – United Kingdom

USA – United States of America

XRF – X-ray fluorescence

XRD – X-ray diffraction

1. INTRODUCTION

1.1 Background

Aggregates production is an extremely important process for modern life, with solid particle size reduction (crushing and milling) being a key procedure that is inefficient and consumes 5% of all electricity produced globally (Rhodes, 1998). As well as being inefficient with regards to energy consumption, crushing and milling also produce a large amount of fine particles (fines). Fines are classed varyingly depending upon the material that they are produced from, according to the European Aggregates Standards, which states that fines from concrete and general use are classed as particles that can pass through a 4 mm screen. The term ‘fines’, however, is often used in quarries to define site specific undersized or unsaleable particles (Manning, 2004). Since the introduction of the Landfill Tax in 1996 and the Aggregates Levy in 2002 (Martin & Scott, 2003), fines are generally stockpiled at the expense of the quarry operator as it is cheaper than paying for the fines to be sent to landfill. However stockpiling will increase the level of local land contamination due to aeolian transportation.

Because of the large amount of energy that is consumed during the crushing process and amount of fines produced in aggregate production in general, increasing efficiency, even by 1-2%, can have a profound beneficial effect. The results of greater efficiency would make the aggregate plant more environmentally friendly in addition to being financially beneficial to the operator by increasing the percentage of saleable product and reducing the production cost per tonne of saleable product.

Computer simulation packages are the most cost effective way of improving efficiency in an aggregates plant compared to physical methods. This is because they are less time consuming, can do trial and error tests without effecting production and will not cause any downtime of the plant before the point of implementation, unlike traditional methods where the plant, or part of it, has to be stopped and equipment settings altered and/or equipment added or removed.

There are a number of different computer simulation packages available commercially, including JKSimMet, USimPac and Bruno. JKSimMet was used in this research as it allows the input of site specific rock fracture data, unlike other software packages which use generic hard, medium and soft rock data. As well as being designed specifically for mineral processing operations, JKSimMet does not have the bias of being designed by a manufacturer to go specifically with their product and can be used in parallel with its sister product, JKSimBlast, to incorporate blasting into the model. How a rock face is blasted has a significant impact on the crushing processes downstream, so by being able to incorporate JKSimBlast it makes the JKTech software a powerful tool in aggregates production optimisation.

In plant design, and especially re-design, where alterations are made to an existing plant design, it is extremely important to know the tonnage and PSDs (particle size distributions) of the rock material throughout the plant. This information will aid the use of models and the predictions of what will happen further downstream, as the PSD will affect all downstream processes, including the amount of energy used and the amount of fines produced, amongst other factors. This is not normally an issue, as samples can be taken and screened by passing the material through various sieves that contain progressively smaller holes. The various fractions held by each sieve can then be weighed, converted to percentages and a PSD curve created. However this is not practical for pre-crushed material from the muck pile (i.e. the feed to the primary crusher) as particles are often too large to screen and thus causes an issue as the primary crusher feed PSD is unknown. There are a number of image analysis software packages that are commercially available that can be used in this situation, such as: CIAS, GoldSize, IPACS, FragScan, PowerSieve, Split-Desktop, TUCIPS and WipFrag (Siddiqui *et al*., 2009). Split-Desktop is being used in this research as it is linked with JKSimMet and has been validated by a number of experiments (Split-Desktop, 2001; Kemeny et al. 1999; Liu & Tran 1996).

To get a real understanding of what is happening in an aggregate plant, the concept of mine-to-mill was developed. The mine-to-mill concept looks at the entire aggregates process from blasting, all the way through crushing and screening, to the final product. By looking at everything in this way, a much more detailed representation of what is occurring is obtained, and it is possible to see how one aspect affects another e.g. the effect of blasting on the crushing and screening processes. By doing this, it can be ascertained where the greatest inefficiencies are, with respect to energy use and fines production. It may also be shown that spending more money in one area may cause savings in other areas, and result in a net gain. There have been a number of publications and reports that use the mine-to-mill approach, including Adel (2006), Jensan *et al*. (2009), Scott *et al*. (2000), Kanchibotla & Valery (2010) and Drew *et al*. (2011)

The research in this thesis is being conducted in conjunction with MIRO and the EU project EE-Quarry, with the ultimate aim of producing a top level model that can be used on any quarry to determine ways of reducing the amount of energy expended per tonne of saleable product. The EE-Quarry project takes into account all factors in aggregates production from blasting all the way through to delivery.

1.2 Aims and objectives

The aim of this research is to look at ways of reducing the amount of fines produced and the amount of energy used per tonne of saleable product from a working quarry in the UK whilst still producing saleable product. From these aims, the following hypotheses have been created:

1. Primary crusher feed PSDs can be calculated using Split-Desktop image analysis software.
2. UK aggregate quarries can be modelled using JKSimMet plant modelling software.
3. JKSimMet plant modelling software can be used to propose ways of reducing fines production in UK quarries.
4. There is a significant difference in blast PSDs when the order of deck detonation is changed.

To complete these aims and to address the hypotheses, the following objectives have been outlined:

- Model a working quarry within the UK using JKSimMet.
- Simulate optimisation within a working UK quarry using JKSimMet.
- Determine the primary crusher feed PSD using Split-Desktop.
- Determine the resultant PSDs of two blasts with different blast designs using Split-Desktop.

2. LITERATURE REVIEW

2.1 Introduction

A great deal has been written about aggregate production as it is a huge global business that requires a vast amount of energy and produces a large amount of waste, in the form of fines, in the process. As a result, aggregates production is an extremely inefficient process, with plenty of scope for improvement. Therefore, due to the colossal production of aggregates globally, if the amount of fines produced, or energy used, can be reduced, even by less than 1%, then the amount of profit on saleable product would increase, the amount of energy used per tonne of product would reduce and the operation would become more environmentally friendly by a significant amount.

To ascertain a way of optimising aggregate plants, there are two mains approaches that are undertaken. They are:

1. Changing the plant set up or working parameters to alter product PSDs and energy use.
2. Changing the blast design to alter the blast fragmentation.

Both of these approaches are generally simulated using computer software programmes. The findings from the software, that simulate a benefit to the aggregate plant, are then implemented, as this allows trial and error tests to be undertaken without affecting production. Once implemented, samples from site can be analysed to determine whether the implemented change is beneficial. For blast fragmentation however, this will usually require some form of image analysis software, as the blasted material will almost always contain particles that are too large to physically screen.

This literature is being analysed to determine what has been achieved, what has not been analysed, and to determine what could potentially be done to have a beneficial effect in reducing fines and to optimise energy usage in aggregates production. In particular, this literature review will analyse the historical and contemporary literature concerned with aggregate plant modelling software, rock fragmentation analysis and its uses in aggregate plants and the effects of blast design on fragmentation as well as downstream crushing processes.

2.2 Methodology

The information for this literature review was obtained through a number of sources, including:

- Books
- Online search engines
- Recommended papers and journals
- General reading around the topic

The online search engines used were ISI Web of Knowledge (http://wok.mimas.ac.uk/) and Google Scholar (http://scholar.google.co.uk/), and were used to locate historical and contemporary journals, articles and conference proceedings. These online search engines were utilised by using key words and phrases such as; aggregates, blast fragmentation, drop-weight, image analysis, JKSimMet, mine-to-mill and Split-Desktop.

Articles found were analysed and either excluded or included due to their content and if they came from a reputable source, such as a university or recognised journal. Once a useful article had been sourced, its citations, and other articles that had cited this article, were looked at and the process repeated.

Some articles were recommended from people in industry or academics in this field, whilst other articles came from reading news articles and following their sources or from books; however, all of these went through the same vetting process as the articles found using online search engines.

2.3 Results and discussion

The results from this literature review and their analysis are outlined below and have been split into three sections; aggregate plant modelling software, PSD determination by image analysis, and effects of blast design on fragmentation.

2.3.1 Aggregate plant modelling software

There is a lot of literature that utilises aggregate plant modelling software in their studies as aggregate plant modelling software packages have been commercially available for a number of years. They are produced, both by equipment manufacturers, such as BRUNO, which is produced by METSO, and independent companies, such as JKSimMet. With there being a number of different plant modelling software packages available, choosing which one to use can be a complicated process, or may be simply selected by cost. Lowndes *et al*. (2005) used both JKSimMet and USIM PAC and favoured JKSimMet due to unspecified issues in verifying USIM PAC.

The use of plant modelling software is for plant optimisation, whether that is fines reduction, energy use reduction, costs reductions, increased production of high value particle size fractions, or a combination of these factors (Lowndes *et al*., 2007). There are a number of ways that fines can be reduced and most simply, it has been found that fines can be reduced by up to 30% from doing an audit (Mitchell *et al*., 2008), and plant modelling software can be used to further reduce fines production on top of this (Mitchell, 2009). Drew *et al*. (2011) highlighted that there are two methods that can be undertaken to tackle the issue of fines:

1. Find a novel use or new market for the fines so that they are no longer a waste product.
2. Alter the plant to reduce the amount of fines produced.

Energy usage is another key factor which many studies have looked at optimising. Adel *et al*. (2006) used plant optimisation software and mine-to-mill concepts at two quarries in USA and found that energy use could be reduced by 1-5% at both sites. There are a number of other studies that have also successfully determined ways to optimise aggregate plants using plant analysis software, including: Drew *et al*. (2011) and Lowndes *et al*. (2007).

Energy optimisation in quarry plants has also been looked into by Cresswell (2011), however this was undertaken without plant modelling software and looked at general methods of energy reduction, concluding that as much equipment as possible should be included into studies and that fuel for mobile plant machines and transporting material around quarries is often the largest energy input.

The research undertaken by Lowndes *et al*. (2005) at Tunstead limestone quarry (UK) is a prime example of plant optimisation. The study used JKSimMet to combine fines reduction, costs reduction and energy use reduction to make the quarry more environmentally friendly. This has the benefit of making the quarry more efficient and more profitable and shows how useful these software packages can be in increasing profits and reducing the environmental impact of aggregate plants.

2.3.2 PSD determination by image analysis

Knowing the PSD at various parts of an aggregate plant is useful for quality control and is an essential parameter for plant modelling software (Hunter *et al*., 1990). Normally this is done by taking samples and screening them. However, sometimes this is not possible, due to the large size of the particles or because they are inaccessible and so no sample can be taken. Because of this, image analysis software tools have been developed, which also have the added benefit of not requiring the plant, or sections of it, to be stopped so that a sample can be taken.

Image analysis software works by employing the following steps (Kemeny *et al*., 1993):

- Take an image of the particles in question.
- Delineating the image using edge detection algorithms.
- Undertake statistical analysis to determine the amount of overlapping and ultimately the size of each particle.
- Produce a PSD curve.

Many image analysis systems require user input, however fully automated systems, using either photographs or videos, are also available. These have the benefits of lowering the man hours required. This will also allow quick and easy access to data at various points in the crushing and screening process and can therefore allow plant operators to adjust machinery parameters accordingly (Thurley, 2011; Salinas *et al*., 2005; Maerz *et al*., 1996). With these systems being fully automated, there is no human error, but there is also nobody checking that the delineations made by the software are correct. Consequently, the results can be skewed and the results produced inaccurate.

There is a lot of literature where PSD image analysis software is used for plant optimisation, such as Tamir *et al*. (2012), where image analysis was used to determine the PSDs at various points in a quarry to understand the downstream effects of different blast designs. Similarly, Paley (2010), used image analysis to determine the primary crusher product PSD to understand the effect of blast design on the resultant PSD. Kanchibotla (1999) however, used image analysis software to model fines.

There are limitations to using image analysis to determine PSDs. Possibly the most influential factor is the quality of the image taken, as it must be in focus and provide a good representation of the overall rock mass being analysed (Maerz, 1996). Once an image has been analysed, there will be, as with all computational analysis, some error between the computed (simulated) results and the experimental results obtained from site. Sanchidrián *et al*. (2009) found there to be a maximum error of 30% with particles large enough for the image analysis software to accurately identify them as individual particles, but with smaller particles, up to 100% error was found. This shows the importance of validating results against experimental results.

Another issue is the ability to account for perspective in an image, because if this is not accounted for, it can affect the results. To account for perspective, there are two methods that are undertaken by image analysis software. The first is to take two images from different angles, whilst the second is to apply multiple scales to the image (Fernlund, 2005; Split-Desktop, 2012).

2.3.3 Effects of blast design on fragmentation

During the process of preparing a blast and during the act of blasting, there are a number of inconsistencies that can occur. These can be due to drilling, actual explosives performance, explosives delivery quality and consistency, explosives loading consistency, geology and pyrotechnic detonator initiator accuracy (Barkley, 2011)

Electronic detonators are becoming ever more commonplace over their shock tube (non electrical) counterparts due to greater reliability, much more accurate timings and reported improvements in fragmentation and vibration control. However, electronic detonators are not being used by all aggregate plants currently as they cost more, but as the overall benefits are becoming clearer more quarries are adopting them (Lusk *et al*., 2011; Teowee, 2010; Migairou & Bickford, 2009; Teowee & Papillon, 2009; Bartley *et al*., 2003).

Paley (2010) looked at the effects of using electronic detonators on Red Dog mine in USA, and found that they gave an increased uniformity and that by changing the timings between detonating blast holes, the mean fragmentation varied from an increase of 20% to a decrease of 30%. This shows that there is a link between timings and blast fragmentation, and by using electronic detonators, it allows timings to be varied accurately which can then be changed to optimise a blast (Bernard, 2005).

Using DMCBLAST_3D, Preece & Chung (2005) found that changing delaying the timings in a blast design by varying amounts showed consistent changes in the way that the fragmented rock moved when blasted, which affects the shape of the muck pile and therefore can be optimised to a site to aid diggability. At higher powder factors, Workman & Eloranta (2009) found that particles became softer and therefore required less energy to break downstream. However this softening of the particles has the potential to reduce the quality of the final product and therefore must be analysed before implementing in every blast.

A number of studies have looked at generally optimising blasts to reduce fines, whilst still giving a good fragmentation, which is one of the key aspects of the mine-to-mill approach, such as Mirrabelli *et al*. (2009) and Glowe (2005). Similarly, Lilly *et al*. (2012) looked at different ways of optimising a plant, but used the Pareto principle to focus on the most important variables to simplify models. Other studies looked at specific quarries; Chavez *et al*. (2007) found that by relating the blast to the geology of the rock face, a blast could be designed to give better muck pile shapes. Cebrian (2010), on the other hand, looked at changing timings, stemming and spacing in a limestone quarry, however the results were not considered to be economically viable. On a broader scale Bremer *et al*. (2007) produced a blasting database that can be used as a guide and was found to give an increase in productivity in the region of 5-10% and overall cost savings.

Mine-to-mill optimisation has been adopted at mines and quarries globally, especially with the current economic climate to reduce cost, but along with the benefits there will often be some negatives, such as blast damage, dilution and ore loss. Nevertheless, the benefits often outweigh the costs and further optimisation can potentially reduce the negatives even further (Kanchibotla & Valery, 2010).

As shown, the effect of many factors of blast design on blast fragmentation have been analysed in the literature with the aim of optimising blast design either generically or for a specific site. However, nothing in the literature has addressed the effect of deck detonation order, which may have a significant effect on blast fragmentation.

2.4 Conclusions

In conclusion, there has been a lot of literature written in the fields of aggregate plant modelling, rock fragmentation analysis and the effects of blast design on fragmentation. The literature on plant modelling software looks at reducing fines, energy use, costs, increasing high profit particle size production or a combination of these aims. There are a number of software packages available and many studies have been undertaken on both generic and site specific solutions.

The use of image analysis to determine rock particle PSDs has been widely studied. It is an extremely useful tool for determining PSDs of particles that are too large to screen or inaccessible to sample and provides a method of determining the PSD without stopping sections of a plant. As a result, image analysis can be the only way to determine the PSDs required for input into plant modelling software.

Many parameters of blast design have been analysed to determine their effects on blast fragmentation, including detonation timings and powder factors. These parameters have been looked at on specific sites as well as generically, but no study has analysed the effects of the order of deck detonation.

3. MOUNTSORREL QUARRY

3.1 Background and location

Mountsorrel Quarry is a granite quarry run by Lafarge Aggregates Ltd and is located between Leicester and Loughborough in the UK. Mountsorrel Quarry is the largest granite quarry in Europe, producing in excess of 5,000,000 t of aggregate per annum (Lafarge Aggregates Ltd, 2006) and is being used as a case study for this research. The site design is set up so that the westernmost part is the quarry and the material flows in an easterly direction through the primary crusher, secondary and tertiary crushing, screening house, Ready-Mix cement plant (if the material is being made into Ready-Mix cement) and finally to the rail sidings if it is not being dispatched by road going vehicles, as shown in Figure 1. There are two types of granite in the region, both of which are found in Mountsorrel Quarry, which can be identified by the pink and grey feldspars that they contain (Miller & Podmore, 1961).

Figure 1: Site map of Mountsorrel Quarry with the quarry, primary crusher, stock area and rail sidings (inset) shown (Lafarge Aggregates Ltd, 2012).

Mountsorrel Quarry produces a variety of aggregate size fractions, with the largest being 63 mm and the smallest 5 mm. Any particles smaller than 5 mm are unsaleable and therefore classed as fines. There are a large amount of fines produced at Mountsorrel Quarry which are consequently stockpiled. Fines are however used to produce protective barriers around the quarry floor to make sure vehicle drivers do not accidently drive off of the edge of a quarry face and as markings around the blast holes.

When crushing the granite in to the required size fractions, Mountsorrel Quarry operates two types of crusher; cone and gyratory. Cone crushers work by feeding rock material into the top of the crusher into the crushing chamber where it is then compressed between a cone and a concave wall due to the eccentric throw (ET) of the cone causing the rock to break. This continues until the material is small enough to fit through the sizing gap and is then discharged from the machine (Figure 2). The ET can be altered which will affect the way the rock material is broken and thus the size of the rock particles that are discharged.

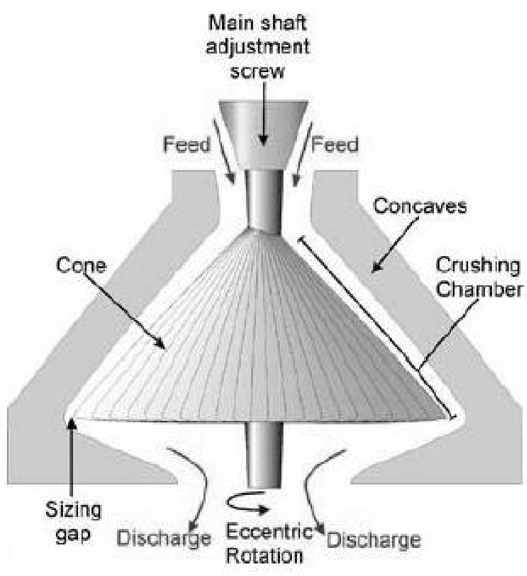

Figure 2: Diagram of a cone crusher where the rock material is fed into the top of the crusher and the eccentric rotation compresses the rock between the cone and the concaves until it is small enough to fit through the sizing gap (which is set at a specific width) and is discharged (British Geological Survey, n.d.).

Gyratory crushers are similar in design to cone crushers, where the rock material is added into the top of the crusher and it enters the crushing chamber. In the crushing chamber, the material is compressed between the lining of the crushing chamber and the main shaft due to its ET until it is small enough to pass through the sizing gap and be discharged (Figure 3). The main difference between gyratory crushers and cone crushers is that the angle of the crushing chamber in gyratory crushers is far less acute.

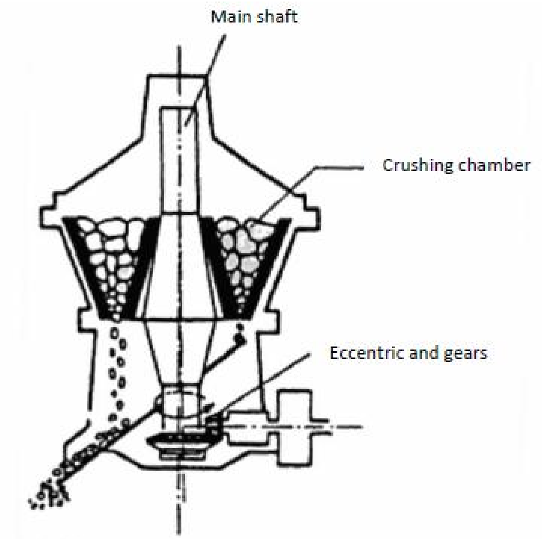

Figure 3: Diagram of a cone crusher where the rock is fed into the crushing chamber and the main shaft gyrates, thus compressing the rock against the liner wall until it is small enough to fit through the sizing gap (which is set at a specific width) and is discharged (Primel & Tourenq, 2000).

3.2 Mountsorrel granite

The granite extracted from Mountsorrel Quarry is an extremely hard granite and was formed around 400 million years ago (Meneisy & Miller, 1963). X -ray fluorescence (XRF) and x-ray diffraction (XRD) analyses were undertaken on samples to determine the elemental and crystal composition of the Mountsorrel Quarry granite, respectively. Samples were also exposed to drop-weight tests to determine the rock fracture data (t_{10} values; see section 3.2.2 Drop-weight tests) to understand how the Mountsorrel granite breaks up under pressure.

3.2.1 X-ray analysis

3.2.1.1 XRF

XRF is a technique that is used to classify the elemental content of an aggregate. This determination of elemental composition can be important to a company buying the aggregate if specific elements are desired or not wanted such as precious or rare earth metals (Brown *et al*. 1973). XRF spectrography works by firing x-rays at a test sample which causes backscattered (fluorescent) x-rays to be emitted, as shown in Figure 4.

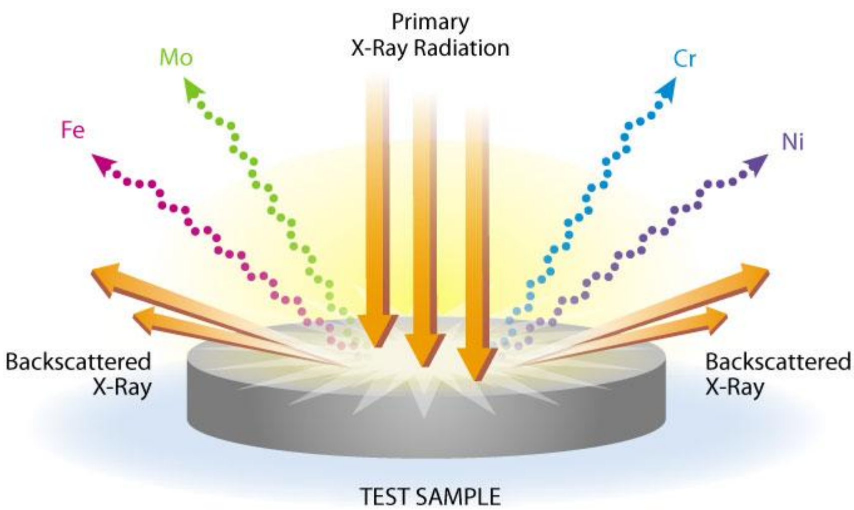

Figure 4: Schematic to show the basic principles of XRF spectrography, where x-rays are fired at a test sample and the resultant backscattered x-rays are recorded by a detector (Thermo Scientific, n.d.).

The backscattered x-rays are then recorded by a detector diode which determines the elemental composition of the sample as shown in the block diagram of an XRF spectrometer (Figure 5).

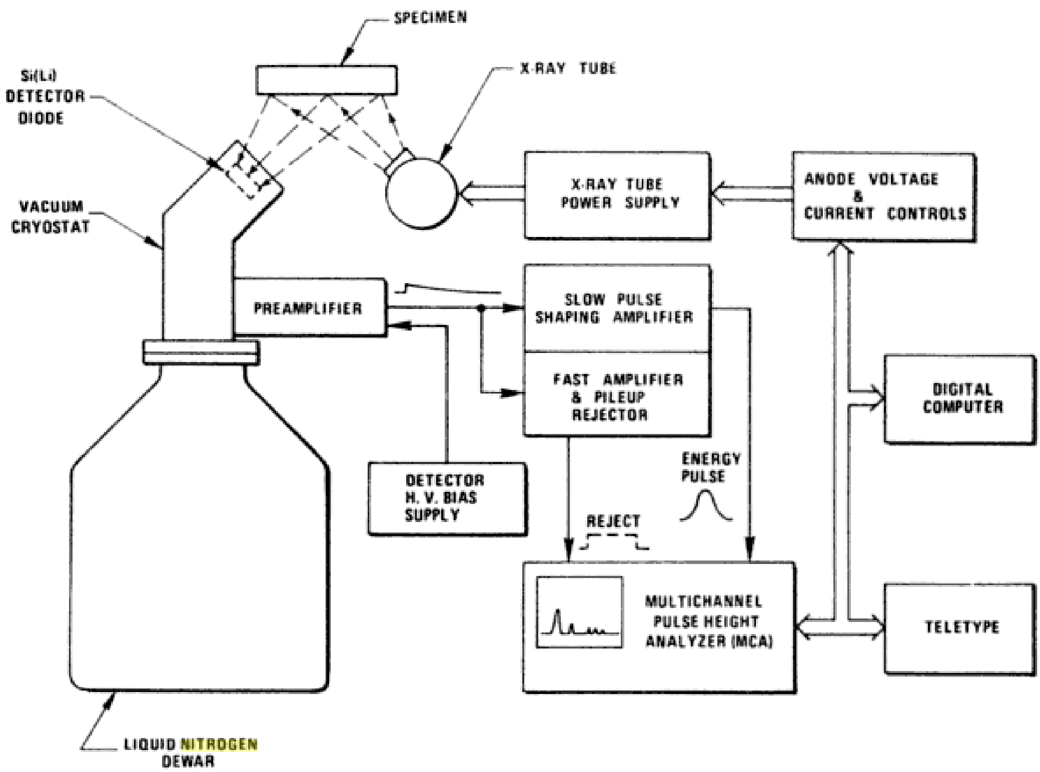

Figure 5: Diagram of an XRF spectrometer with the presentation and control equipment excluded (Jenkins *et al*., 1995).

There are two types of XRF spectrometer; single-channel and multichannel. Single-channel machines can only detect the presence of a single element at a time, which is useful to determine if a known impurity or wanted element is present, or the process can be repeated a number of times to detect numerous, different elements sequentially. Multichannel machines on the other hand can detect numerous elements simultaneously as they contain multiple detector diodes (channels), and each detector diode will be set up to detect a different element (Jenkins *et al*. 1995).

On an atomic scale, when the x-rays collide with the atoms within the sample, they cause electrons to be ejected from various shells. When these electrons are ejected, electrons from outer shells move to usurp the positions of the ejected electrons and in the process expel fluorescent x-rays, which are detected (Figure 6).

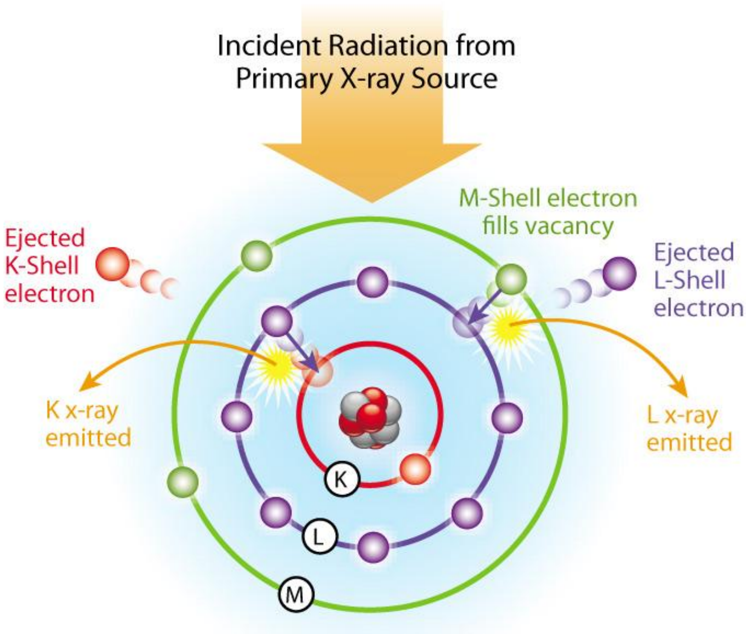

Figure 6: Schematic to show how XRF spectrography works. When the x-rays are fired at the sample, they collide with the atoms contained in the sample causing the ejection of electrons from various shells in the atoms and the emission of x-rays. The x-rays that are emitted are uniquely characteristic of the element from which they were emitted ad they can therefore be used to decipher what elements are present in a sample (Thermo Scientific, n.d.).

For this experiment, Mountsorrel granite was crushed into a fine powder and mixed with a wax in the ratio of 5:1 (powdered granite to wax powder), pressed into a pellet using a die, and then analysed using a Bruker (Billerica, Massachusetts, USA) S8 Tiger XRF multichannel spectrometer. The sample was crushed and pressed into a pellet, as this gives a much smoother surface and therefore much more accurate results. If the sample being analysed is not a powder or only a small quantity is owned and therefore too precious to crush into a powder, single particles and liquids can be used if appropriate.

The results from the XRF analysis are shown as the elemental detection (Figure 7), and as a table of the oxide compositions present (Table 1).

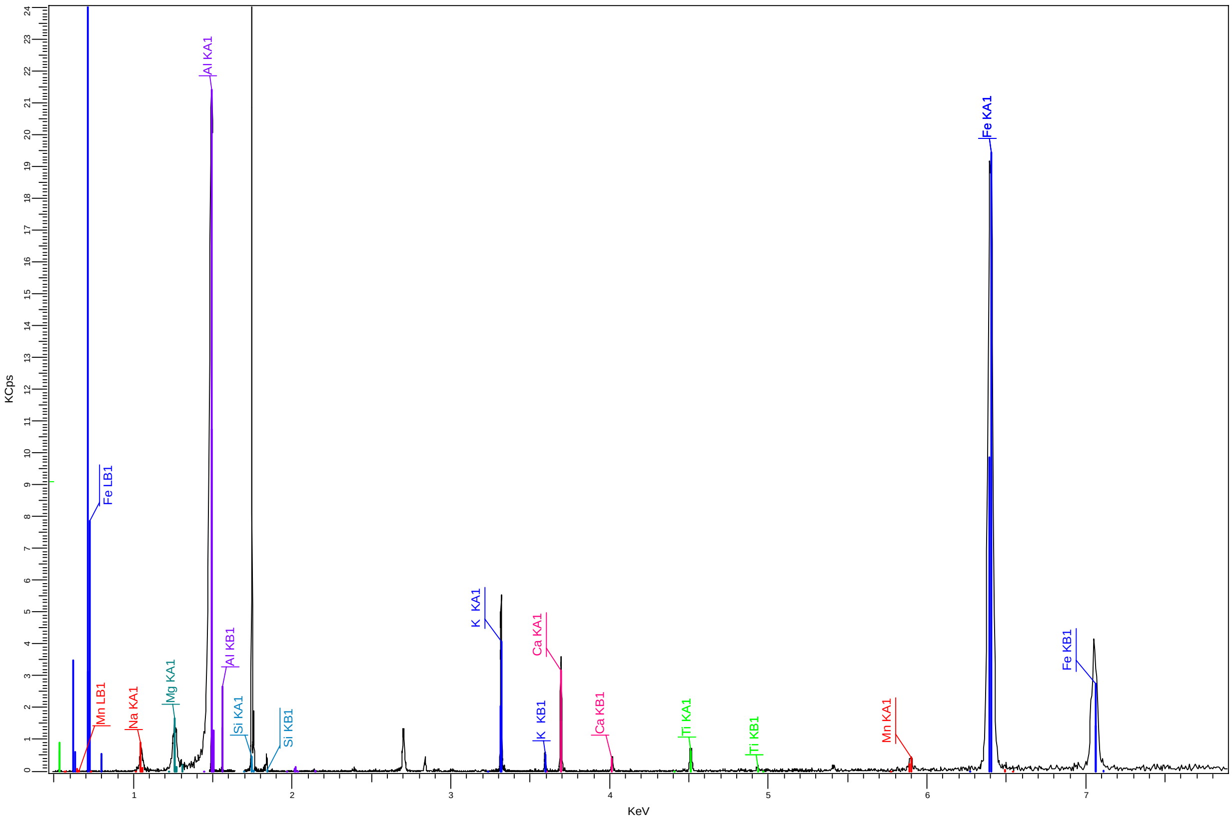

Figure 7: Plot of elements present in Mountsorrel granite obtained by XRF analysis.

Table 1: Formulae of the oxides and their respective concentrations found in Mountsorrel granite obtained by XRF analysis.

Formula	SiO_2	Al_2O_3	Na_2O	MgO	K_2O	Fe_2O_3	CaO	TiO_2
Concentration (weight % of oxides)	63.3	16.8	8.3	3.24	3.02	2.17	2.13	0.39
Formula	P_2O_5	BaO	MnO	Cl	Cr_2O_3	SrO	ZrO_2	RbO_2
Concentration (weight % of oxides)	0.36	0.064	0.054	0.05	0.029	0.021	0.013	0.008

As Figure 7 and Table 1 show, the Mountsorrel granite predominantly consists of SiO_2 (63.3%) and Al_2O_3 (16.8%). There is also Na_2O (8.3%), MgO (3.24%), K_2O (3.02%), Fe_2O_3 (2.17%) and CaO (2.13%)

present (all percentages are weight percent of oxides), along with trace amounts of other metal oxides (TiO_2, P_2O_5, BaO, MnO, Cl, Cr_2O_3, SrO, ZrO_2 and RbO_2) detected in the sample.

3.2.1.2 XRD

XRD analysis determines the crystal structures of a substance. It works according to the fact that every crystalline substance will give a unique pattern that does not vary between different particles of the same crystalline structure. This pattern is created by firing x-rays at a powdered sample, collecting the scattering using a detector and then analysing the scatter pattern. Where there is a mixture of crystalline substances, each substance will give its unique pattern independently of the other crystalline substances (Hull, 1919). By detecting these patterns, they can be compared to known patterns from crystalline substances and therefore the crystalline composition of a substance can be identified. This makes XRD a very useful technique for compositional identification and for the quality control of samples by determining if there are any impurities present. A schematic of an XRD machine is shown in Figure 8.

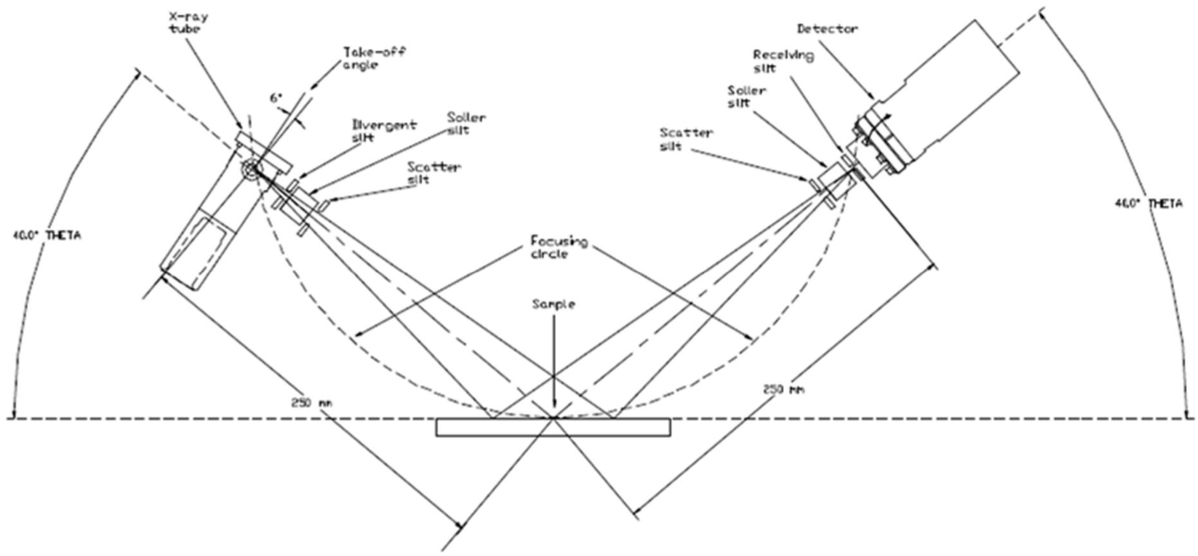

Figure 8: Schematic diagram of an XRD diffractometer (Thermo ARL, 1999).

A sample of Mountsorrel granite was ground into a fine powder and analysed using a Bruker D5005 diffractometer. The results of the XRD analysis are shown in Figure 9.

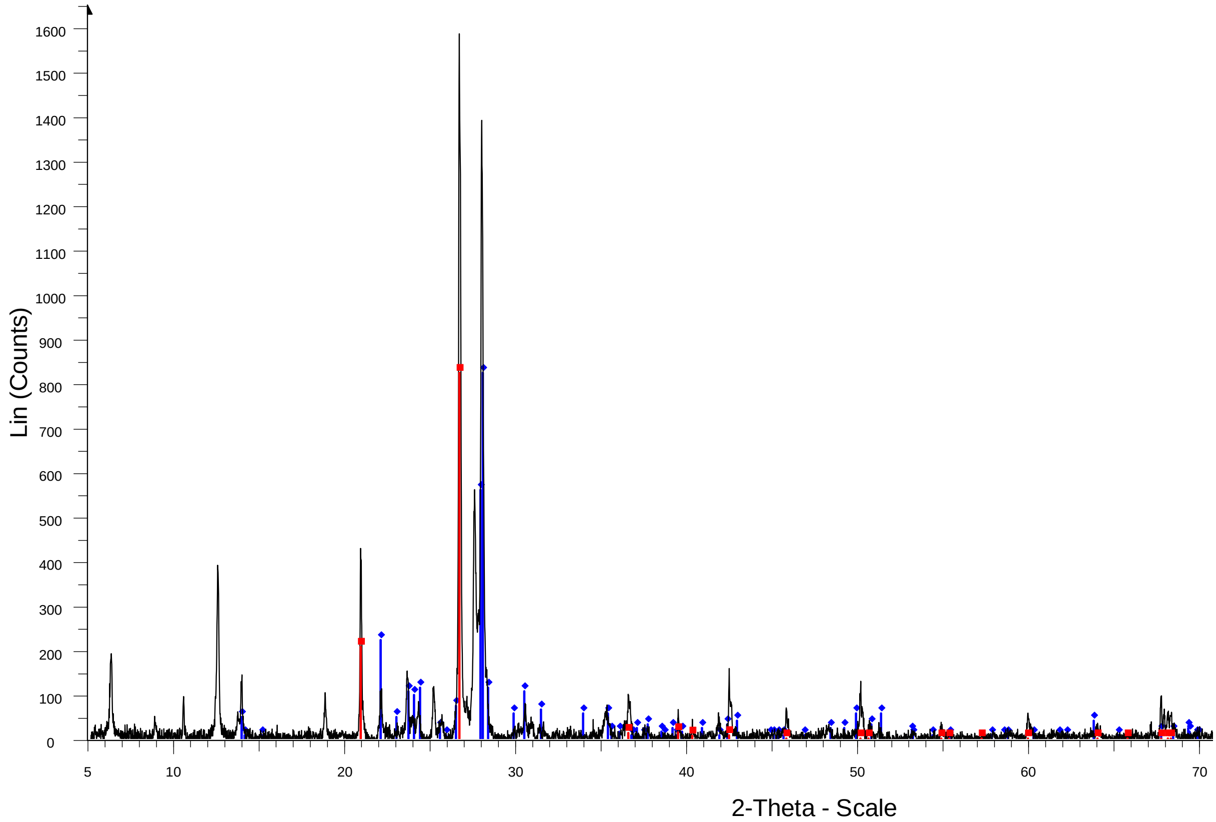

Figure 9: Overall compound spectrum (black peaks) with quartz (SiO_2; red lines) and albite, calcian, ordered $(Na,Ca)Al(Si,Al)_3O_8$; blue lines) obtained by XRD analysis.

As Figure 9 shows, the XRD analysis of Mountsorrel Quarry granite detected a number of compounds, and the peaks that correspond with quartz (SiO_2) and albite, calcian, ordered ($(Na,Ca)Al(Si,Al)_3O_8$) are shown with red and blue lines, respectively.

The main limitation of XRD is that it can only be used to analyse crystalline materials, meaning that any gas, liquid or amorphous solid samples cannot be analysed using this technique. Because this research is looking at solids, the issue of not being able to sample gases and liquids is eliminated, but the issue of amorphous solids, which account for about 5% of all solids, is still present (Thermo ARL, 1999).

3.2.2 Drop-weight tests

The composition and microstructure of rock particles will affect the amount of energy required to break them and the way in which they will break under force. This is because rocks particles contain internal planes of weakness which require less force to fracture than the rest of the rock particle and therefore dictate the ultimate shape of the aggregate produced as well as the particle size (Lajtai, 1968). Slate is an excellent example of this, having long parallel planes of weakness, making flat sheets of slate easy to produce.

Some aggregates, including granite, are made up of a composition of different interlocking minerals. Granite is composed of interlocking feldspars, quartz and micas, amongst other minerals, meaning that there are no naturally occurring large planes of weakness due to the construction of the granite. Geological activity and/or blasting can however give rise to large faults in a mass of hard rock such as granite. When a rock does fracture, there are three ways in which a fracture can be propagated (Figure 10).

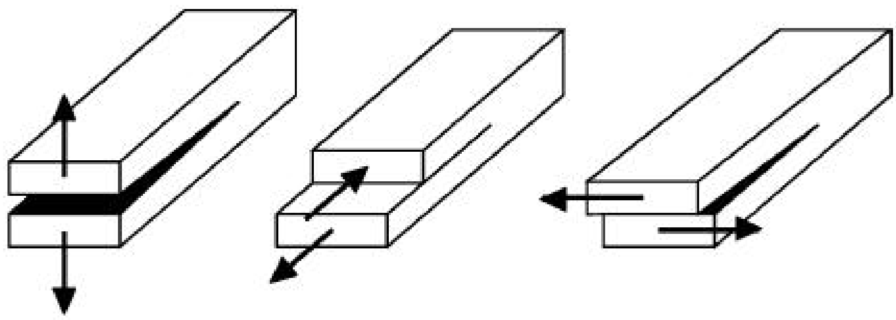

Figure 10: Diagram representing the three ways in which cracks can be propagated in a rock particle (Chang *et al*., 2002)

Some rocks contain networks of small intragranular cracks (sometimes referred to as microcracks or microfractures) which can occur from blasting or geological phenomenon, and have been found to make the rock particles more susceptible to breaking, whilst other samples have shown that intergranular cracks can strengthen a rock particle. This shows the complexity of rock microstructure, and the effects that can manifest because of it. Ultimately, the planar direction of microcracks within the rock will affect the toughness of the rock (Gallagher Jr *et al*., 1974; Tavares & das Neves, 2008; Xia *et al*., 2008). Under load, these intergranular and intragranular cracks can increase in size, as well as new ones being formed, and can lead to fractures with greater load leading to larger cracks (Zhang *et al*., 2000).

The toughness of the rock being crushed will also have an economical effect, as the tougher the rock, the more energy there will be required to crush it, and the crusher liners will have to be replaced more frequently due to an increased wear rate.

There are a number of tests that can be utilised to determine the hardness of a rock particle as outlined in Figure 11.

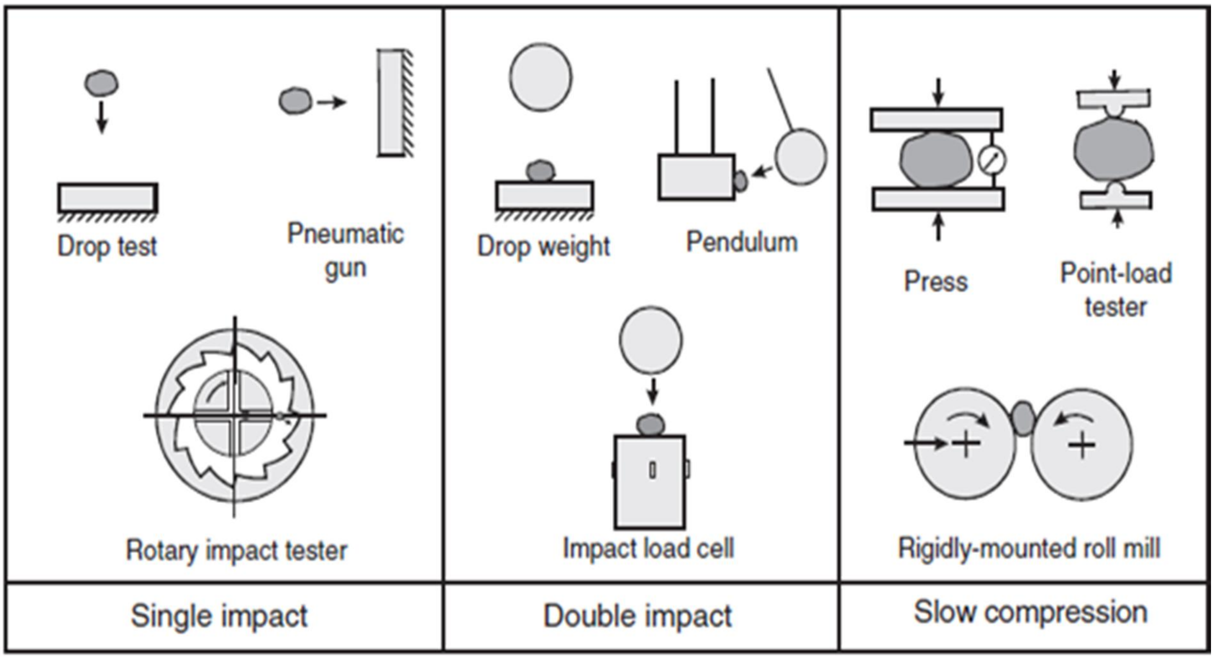

Figure 11: Diagram showing the various ways that single particle breakage tests can be undertaken, including single impact, double impact and slow compression methods (Tavares, 2007).

Drop-weight tests were undertaken to determine how the rock particles fracture under force in a manner that can be incorporated into JKSimMet. Drop-weight tests are performed by dropping known weights from known heights onto samples from five different particle size fractions using a drop-weight test machine (Figure 12) resulting in 15 size/weight groups with up to 30 samples in each group. These different heights lead to different levels of force being applied to the sample and, if the force is large enough, it will cause fractures to occur. These data can then be analysed and the fracture data of the sample calculated (Nataraja *et al*., 1999; Tavares & King, 2002).

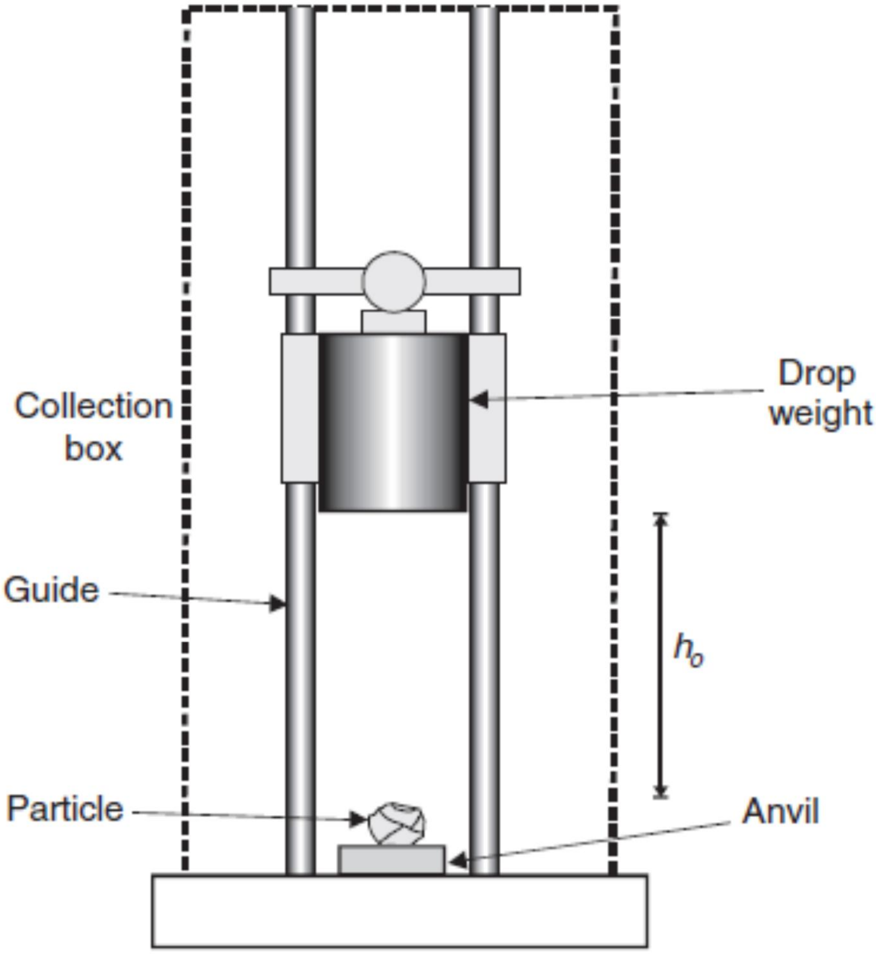

Figure 12: Schematic diagram of a drop-weight test machine where the drop-weight (of known weight) is raised to a set, known height above the particle sample (h_0) before being dropped onto the particle sample and compressing it between the drop-weight and the anvil which usually results in fracturing of the sample (Chau & Wu 2007).

When undertaking drop-weight tests, the amount of energy exerted by the drop-weight can be calculated using the Equation 1, where E_i = energy used for breakage, M = mass of the drop-weight, g = gravitational constant, h = initial height of the drop-weight above the anvil and x_M = final height of the drop-weight above the anvil (JKMRT, 2003).

Equation 1: Energy required for breakage equation, where, E_i = energy used for breakage, M = mass of the drop-weight, g = gravitational constant, h = initial height of the drop-weight above the anvil and x_M = final height of the drop-weight above the anvil (JKMRT, 2003).

$$E_i = Mg(h - x_M)$$

All of the fractured rock from each size/weight group is collected, along with any particles that do not fracture, and screened together to determine the t_{10} value (where t_{10} = amount of mass smaller than

1/10 original size). Similarly, values for t_2, t_4, t_{25}, t_{50} and t_{75} are calculated and these values can then be used in JKSimMet as rock fracture parameters.

The t_{10} values obtained from the drop-weight tests for Mountsorrel granite are shown in Table 2. This is the format required to enter the information into JKSimMet.

Table 2: Table to show the rock fracture data calculated for Mountsorrel granite obtained by submitting rock samples to drop-weight tests and analysing the data. When the value of t_{10} = 10, 20 or 30 (left hand column), the corresponding t_{75}, t_{50}, t_{25}, t_4 and t_2 are shown in their respective columns.

Rock fracture data (t_{10} values) for granite					
Value of t_{10}	t_{75}	t_{50}	t_{25}	t_4	t_2
10	3.0	3.7	5.7	21.5	53.2
20	5.8	7.5	11.4	42.7	82.4
30	8.9	11.5	17.3	61.8	94.9

Higher values in the t_{75} column will manifest themselves as a greater percentage of fines produced and this means that the rock in question will produce fewer fines than that of a rock that gives a lower value in the t_{75} column.

The t_{10} values collected can be related to the specific energy of comminution (E_{cs}; kW h t^{-1}) using Equation 2, where A and b are impact breakage parameters.

Equation 2: Equation relating breakage (t_{10}) to specific energy (E_{cs}) where A and b are impact breakage parameters (JKTech, 2011)

$$t_{10} = A\left(1 - e^{-bE_{cs}}\right)$$

From Equation 2, the E_{cs} data can be calculated and the data for Mountsorrel granite is shown in Table 3.

Table 3: Table to show the power data calculated for Mountsorrel Quarry granite obtained by submitting rock samples to drop-weight tests and analysing the data.

Power data					
	Mean Size (mm)				
	14.53	20.63	28.89	41.08	57.78
t_{10}	E_{cs} (kW h t^{-1})				
10	0.18	0.14	0.18	0.13	0.13
20	0.40	0.29	0.39	0.27	0.27
30	0.64	0.48	0.63	0.44	0.44

The E_{cs} data is inserted into JKSimMet and can be used to calculate the power draw of a crusher or mill. The biggest effect on the power draw is the closed side setting (CSS) on the crusher. The CSS is the size of the gap at the bottom of the crusher at its smallest point during the crushing process. This will dictate, along with the ET, the maximum size of particles that can pass through the crusher and into the product feed. An example of how varying the CSS can affect the power draw is shown in Figure 13.

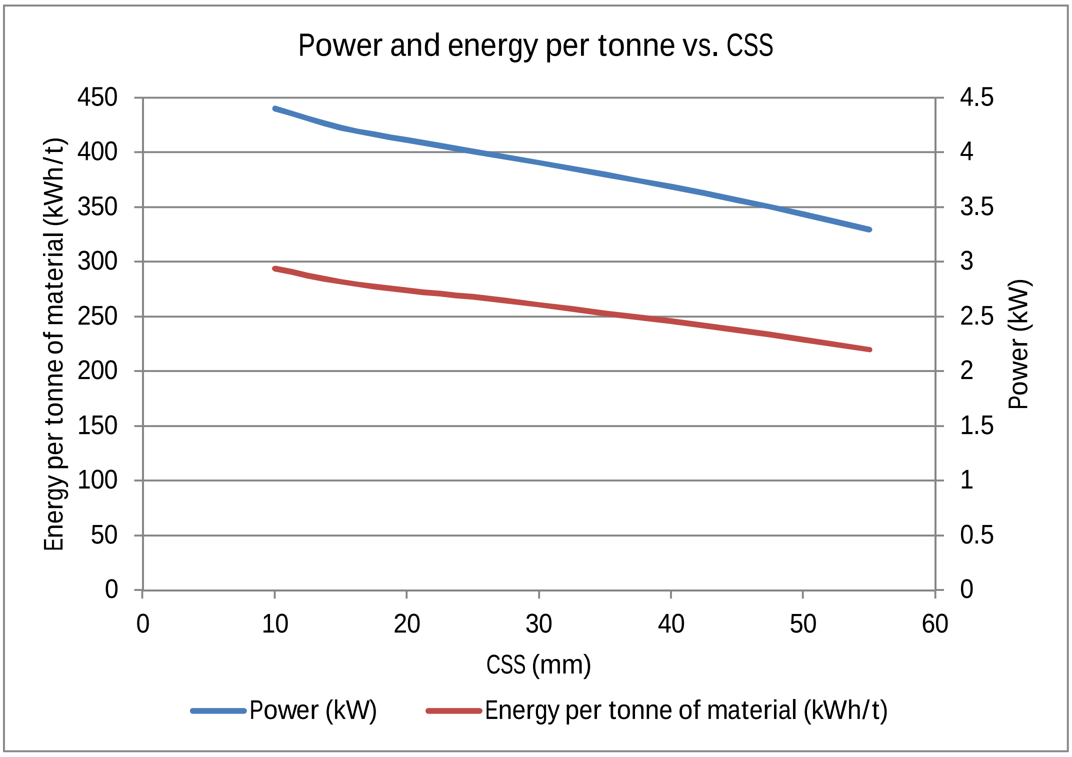

Figure 13: Graph showing the varying power draw and energy used per tonne of material crushed when the CSS is varied from 10 mm to 55 mm for Mountsorrel Quarry granite in a cone crusher with a feed rate of 150 t h^{-1}, ET of 25 mm and a fixed feed PSD calculated using JKSimMet.

Additional tables outlining the t_{10} values of other rock types and the effect of various parameters have on PSD can be seen in Appendix II – PSD and power data for EE-Quarry.

3.3 Health and safety

Before any work was undertaken, all the appropriate risk assessments and inductions were completed and great caution and awareness were adopted, especially when working around machinery. The main risk posed from the Mountsorrel granite is in the form of inhaling silica particles, which can lead to the development of silicosis, where nodules of silica build up in the lungs of the sufferer. Although silicosis can be fatal, it requires prolonged exposure for serious harm to be caused (Mossman & Churg, 1998). The correct personal protective equipment (PPE) was worn at all appropriate times to minimise the risk of harm, including high visibility clothing, hard hats, ear protection, gloves, dust masks and safety spectacles and the materials safety data sheets (MSDS) for granite are shown in Appendix I – MSDS.

3.4 Discussion

The elements detected by XRF analysis and the compounds identified by XRD analysis coincide with compounds that have been detected from the region in previous studies (Taylor, 1934; Sha & Chappell, 1999). Granite is a very diverse type of rock and can contain any of the following compounds and elements, amongst others; SiO_2, TiO_2, Al_2O_3, Fe_2O_3, FeO, MnO, MgO, CaO, NaO, K_2O, P_2O_5, S, H_2O^+,H_2O^-,CO_2,Ba, Rb, Sr, Pb, Th, U, Zr, Nb, Y, La, Ce, Nd, Sc, V, Cr, Mn, Co, Ni, Cu, Zn, Ga, As, Mo and Sn (Sha & Chappell, 1999).

The results from the drop-weight tests show lower values in the t_{75} column for the Mountsorrel granite when compared to a basalt (Table 4), which is also a hard rock. This difference will manifest itself as a greater percentage of fines produced and this means that the Mountsorrel granite will produce fewer fines than that of the basalt. This confirms that Mountsorrel granite is an extremely hard rock.

Table 4: Table to show the rock fracture data for a basalt (left; Bailey, 2009) and Mountsorrel granite (right).

Rock fracture data for basalt					
Value of t_{10}	t_{75}	t_{50}	t_{25}	t_4	t_2
10	3	3.6	5.3	23.5	53.3
20	6	7.4	10.8	44.8	82.9
30	9.2	11.4	16.5	63.2	95.7

Rock fracture data for Mountsorrel granite					
Value of t_{10}	t_{75}	t_{50}	t_{25}	t_4	t_2
10	3	3.7	5.7	21.5	53.2
20	5.8	7.5	11.4	42.7	82.4
30	8.9	11.5	17.3	61.8	94.9

The E_{cs} and the resultant crusher power draw data calculated for the Mountsorrel Quarry granite, when compared to a basalt, with the same ET, (Table 5) shows that the granite requires a lot more energy than the basalt with a mean of 148% more energy required across the various CSS settings.

Table 5: Table showing the varying power draw and energy used per tonne of material crushed when the CSS is varied from 10 mm to 55 mm for a basalt in a cone crusher with a feed rate of 150 t h^{-1}, ET of 25 mm and a fixed feed PSD calculated using JKSimMet. E_{cs} data obtained from Bailey (2009)

Closed Side Setting (mm)	10	15	20	25	30	35	40	45	50	55
Power (kW)	239.4	205.3	182.4	165.7	153.2	143.4	135.6	129.1	123.5	118.8
Energy per tonne of material (kWh/t)	1.60	1.37	1.22	1.10	1.02	0.96	0.90	0.86	0.82	0.79

The principal limitation of rock fracture analysis using the drop-weight test is that although it allows the amount of energy being inflicted upon the particle to be measured, there is no way of calculating what percentage of that energy is used to fracture the particle. This can however be estimated using a twin pendulum breaker that is connected to a computer; however this equipment was not available for this experiment (Tavares, 1999).

3.5 Conclusions

In conclusion, Mountsorrel Quarry is located between Leicester and Loughborough in the UK and is being used as a test site for the research in this thesis. Mountsorrel Quarry is the largest granite quarry in Europe and produces aggregates with various saleable size fractions between 63 mm and 5 mm, and particles smaller than 5 mm are unsaleable and classed as fines. The elemental composition of the granite was found from XRF analysis to contain a number of oxides with concentrations over 1%, with SiO_2, Al_2O_3, Na_2O, MgO, K_2O Fe_2O_3 and CaO being the most abundant, respectively. XRD analysis identified the presence of quartz and albite, calcian, ordered, amongst other crystal structures that lead the spectrum to contain too many peaks to allow the identification of other compounds. All of this elements and compounds found using XRD and XRF comply with other granite studies (Taylor, 1934; Sha & Chappell, 1999).

Drop-weight tests were undertaken and the results show that the Mountsorrel granite is an extremely hard granite, and analysis of the results has provided t_{10} and E_{cs} data. This data is required for input into JKSimMet for modelling Mountsorrel Quarry so that the software can accurately model breakage within the crushers.

4. SPLIT-DESKTOP IMAGE ANALYSIS SOFTWARE

Split-Desktop is a computer software package that allows the user to determine the PSD of objects in a picture by means of image analysis and, in the interest of this research, it can be used to determine the PSD of piles of rocks, whether it be a muck pile, stockpile, conveyor belt or any other selection of rocks that can be found at a quarry. This is very useful for determining the PSD of rocks that are hard to screen due to inaccessibility to obtain a sample or because the rocks are too large for the conventional screening method. At Mountsorrel Quarry the latter is the case and so Split-Desktop is being used to determine the primary crusher feed PSD.

It is recognised that the conventional screening method is not completely accurate as the fractions held by each screen will depend not only on the size of the rock particle but also the shape. This means that an elongated or heavily rounded particle of a size greater than that of the screen aperture is able to pass through the screen as Table 6 shows.

Table 6: Table showing the maximum size that particles with certain aspect ratios and shapes (angular and rounded) can fit through a 0.75” (1.905 cm) screen. A 1” (2.54 cm) rounded particle with an aspect ratio of 5:1 can fit through a 0.75” (1.905 cm) screen hole. These particles can also be much longer in the vertical axis and still pass through the screen (Maerz & Lusher, 2001).

Aspect Ratio	Angular fragments	Maximum Size	Rounded fragments	Maximum Size
1:1		0.75"	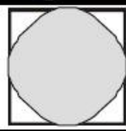	0.75"
2:1	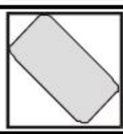	0.75"	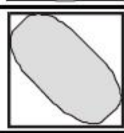	0.86"
3:1	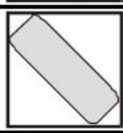	0.83"	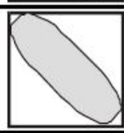	0.91"
4:1	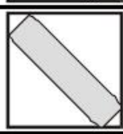	0.91"	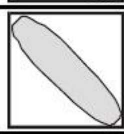	0.95"
5:1	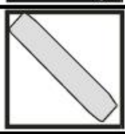	0.95"	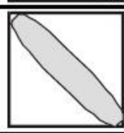	1.00"

Being able to determine the primary crusher feed PSD is important as it will have an effect on all downstream processes. Knowing the PSD of blast material can also be used to improve blast design using software such as JKSimBlast, as a well designed blast may cost more, but can significantly reduce costs and energy usage throughout downstream processes.

Split-Desktop works by taking an image of the aggregates in question and delineating the image into various sections using edge detection algorithms, with each section representing a rock particle. From these sections it uses various statistical equations to determine the dimensions of each particle. Equation 3 is used to determine the size of the particle from what is visible, where x_{minor} = the minor axis and x_{major} = the major axis. Equation 4 is used to determine what percentage of the particle is visible in the image (i.e. the particle size calculated in Equation 3 is not likely to be < 100% of the actual particle size and Equation 4 calculates what 100% of the particle size would be using probability) as most particles will be partially obscured, where p = the probability distribution and x = particle size measured from the edge detection algorithms. Equation 5 is used to determine the volume of the particles.

Equation 3: Equation for the particle size of a rock particle derived from its major axis (x_{minor}) and minor axis (x_{major}) as utilized by Split-Desktop (Kemeny, 1994).

$$particle\ size = 1.649x_{minor} + 0.004x_{major}$$

Equation 4: Equation for the probability distribution (p) for the actual particle size from the measured section from the edge detection algorithms (x) used in Split-Desktop (Kemeny, 1994).

$$p = -0.1245 + 27.1259x^{5.0562}\mathrm{e}^{-3.9071x}$$

Equation 5: Equation for the particle volume obtained from the particle area calculated from the edge detection algorithms and the particle size calculated from Equation 3 (Kemeny, 1994).

$$particle\ volume = particle\ area \times particle\ size$$

There are some limitations to Split-Desktop, namely the camera resolution, lighting and picture quality. Smaller particles and fines that have a resolution too low to accurately be detected by the camera subsequently cannot be delineated and as a result, Split-Desktop will estimate the sizes of these particles. This estimation is calculated by constructing a curve by calculating the sizes of the particles with a high enough resolution and utilizing either the Schumann or Rosin-Rammler distribution to determine the distribution of the smaller particles (Split-Desktop, 2012).

The lighting in an image can have a huge effect on the amount of manual editing involved because if the lighting is too bright, a lot of shadows can be cast, whilst if the lighting is too low then the image will have indistinct particle edges. Both of these scenarios will lead to the impairment of the edge detection algorithms used in Split-Desktop. Because of this, the best conditions for taking images is on overcast days as the light is not too bright and few shadows are cast. It may not however be possible to choose the conditions when the images are taken or the location, meaning that the images may have to be taken under imperfect lighting.

The quality of the image taken will also affect how well Split-Desktop can operate, because if the image is blurry, then the edge detection algorithms may not be able to pick out the edges accurately and may determine that a blurry particle is larger than it actually is. Blurriness in an image can occur due to a number of reasons, including shaky hands, vibrations from machinery causing a tripod to shake, from particles moving (e.g. particles being dumped into a crusher) or if the shutter speed is set too low on the camera.

There will also be the limitation of human error, as it is up to the operator to determine which delineations are erroneous and where delineations should be added. The degree of this will depend upon the user and how much editing is required, which is ultimately down to the quality of the image as outlined above.

Another potential issue for using Split-Desktop for analysing the PSD from dumper trucks is that it often occurs that not all of the particles are dumped into the crusher as, Figure 14 shows. This means that the same particle could potentially be imaged in more than one dump, which would affect the accuracy of the results. The amount of material that remains on a dumper truck in this manner, however, is minute in the scale of the overall material dumped and has been assumed to be insignificant.

Figure 14: Image of a dumper truck leaving the primary crusher at Mountsorrel Quarry after unloading but still carrying some rock particles.

Therefore, Split-Desktop can be used in a quarry in a number of ways, depending on what the quarry operator requires the PSD for. The main uses of Split-Desktop are for determining the PSD of blasted and pre-crushed material as it is often too large to screen and for quality control to monitor various parts of production.

Split-Desktop can be used with any number of images, however, the more images used, the more representative the resultant PSD obtained will be. This is especially the case when analysing blast material from dumper trucks, as the variance in PSD will be much greater than that of crushed and screened material, which will have had limitations enforced on the potential size (e.g. screen aperture and crusher CSS) resulting in greater variance between each truckload of material.

Split-Desktop has been validated by Liu & Tran (1996) and, more recently by Split-Desktop and Kemeny *et al*. (1999) by comparing separate Split-Desktop analyses against the manual screening of rock samples (Figure 15 and Figure 16).

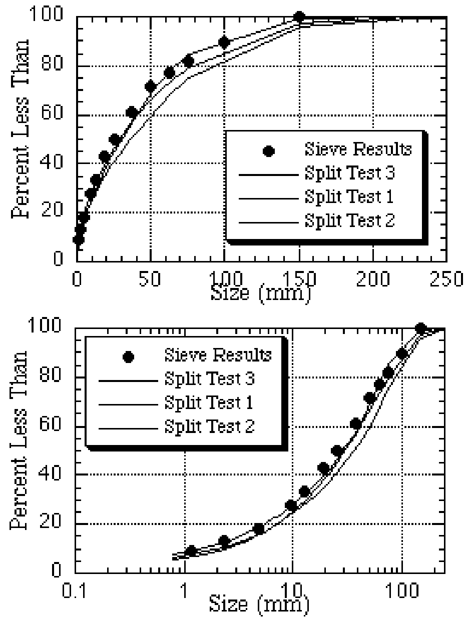

Figure 15: Split-Desktop validation curves of three tests against manual sieving data from Liu & Tran (1996; top) and a later study (bottom). Please note that the x axis on the top graph is linear whilst it is logarithmic on the bottom graph (Split-Desktop, 2001).

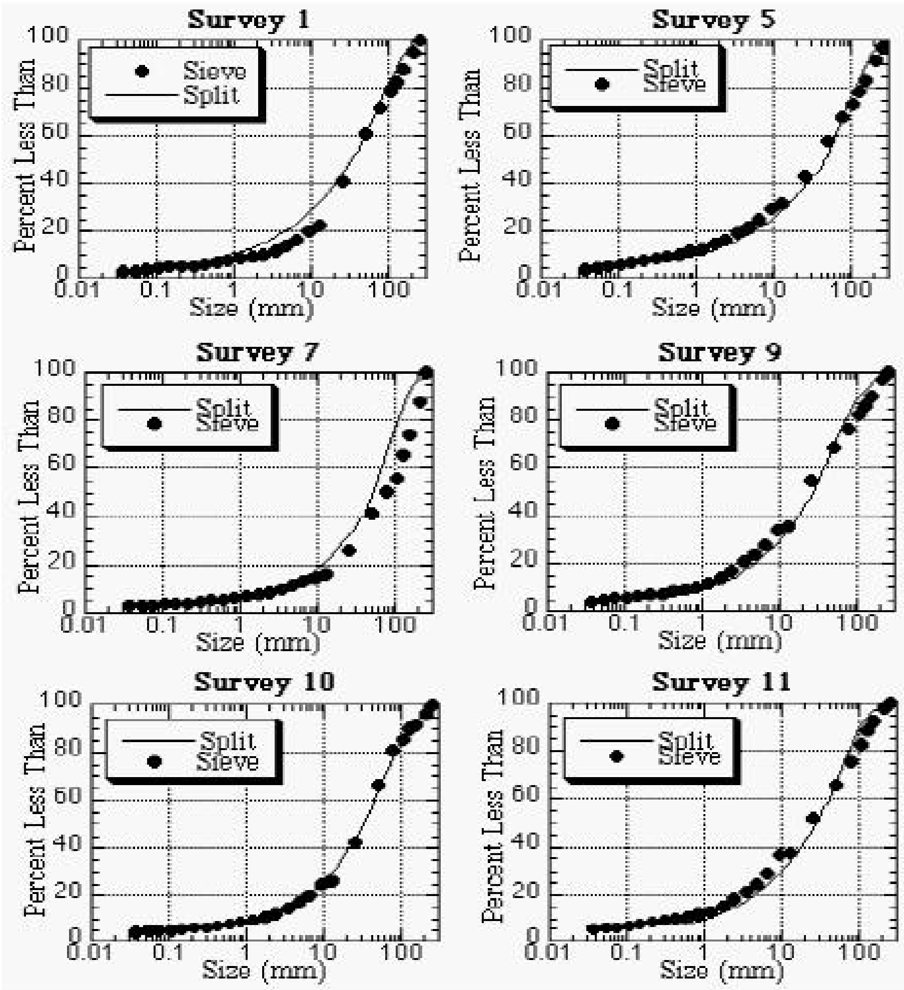

Figure 16: Comparison of PSDs obtained from Split-Desktop (line) and sieving (dots) over 6 surveys (Kemeny *et al.* 1999).

As Figure 15 and Figure 16 show, the accuracy is very high in the 1996 test and more so in the more recent validation tests where a newer version of Split-Desktop was used. In addition, through a number of experiments, the standard error for Split-Desktop has been found to not exceed 10% and is usually lower (Kemeny *et al*., 1999). This means that Split-Desktop is a reliable tool that can be used in particle size analysis.

4.1 Method

The initial step in using Split-Desktop is to take an image (preferably multiple) of the rock particles in question. An example is shown in Figure 17 of the primary crusher at Mountsorrel Quarry.

Figure 17: Initial image of a dumper unloading into the primary crusher at Mountsorrel Quarry before being analysed with Split-Desktop to determine the PSD.

Once the image is obtained it is imported into Split-Desktop and the software can be used to delineate the image. The amount of delineation can be varied (Figure 18) and it is up to the user to determine the most adequate level of delineation. The main factor that will influence this will be the lighting as outlined in section 4.

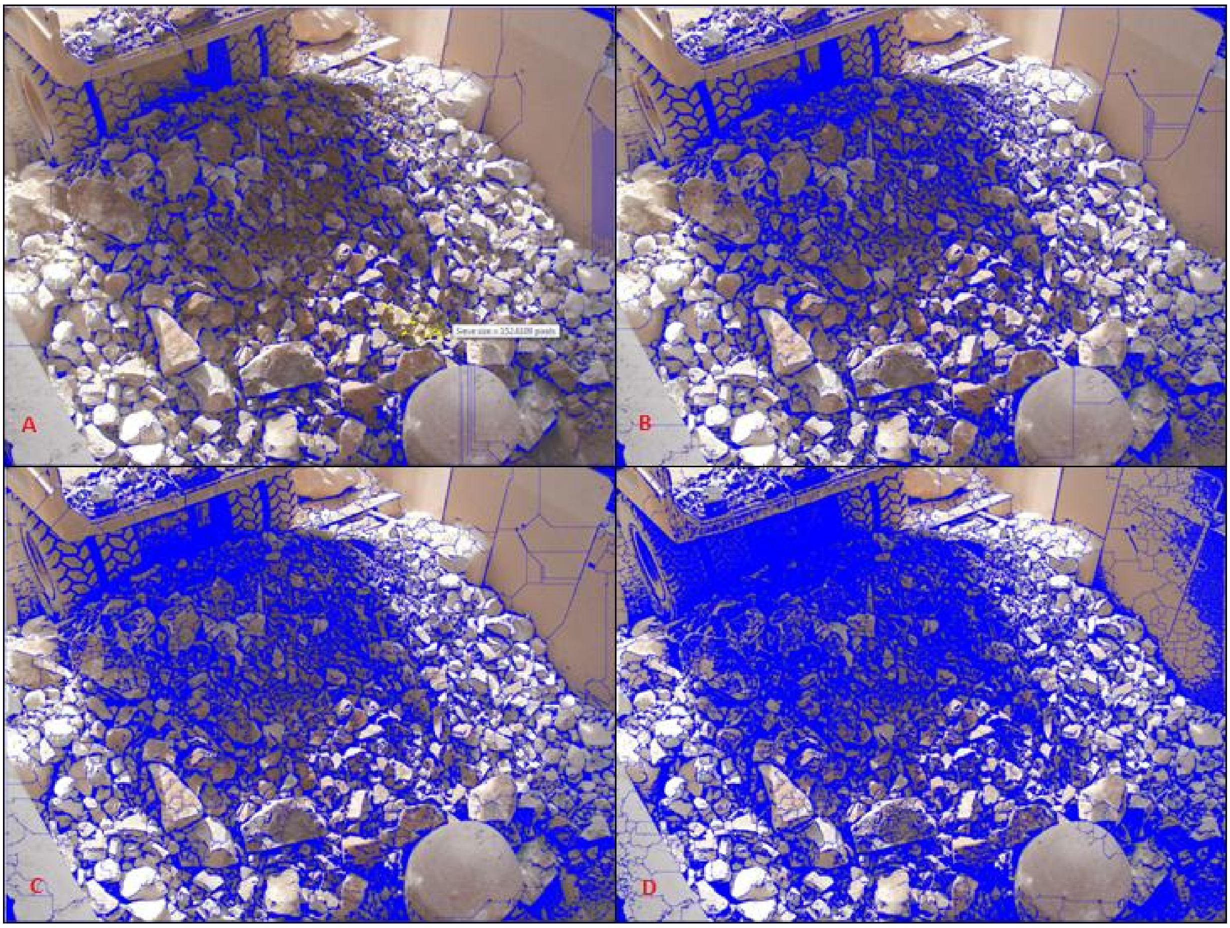

Figure 18: Various delineations (navy blue lines) of the initial picture where the amount of delineation is A<B<C<D.

Once the level of delineation has been chosen (in this case image B was chosen; Figure 18), scales are added (multiple scales will account for perspective), all the areas that are not of interest can be removed (e.g. dumper truck, walls, rock particles from previous dumps etc.), delineations can be added or removed depending upon errors made by the software and areas of fine material can be added where the particle size is not clear due to the resolution of the image (Figure 19).

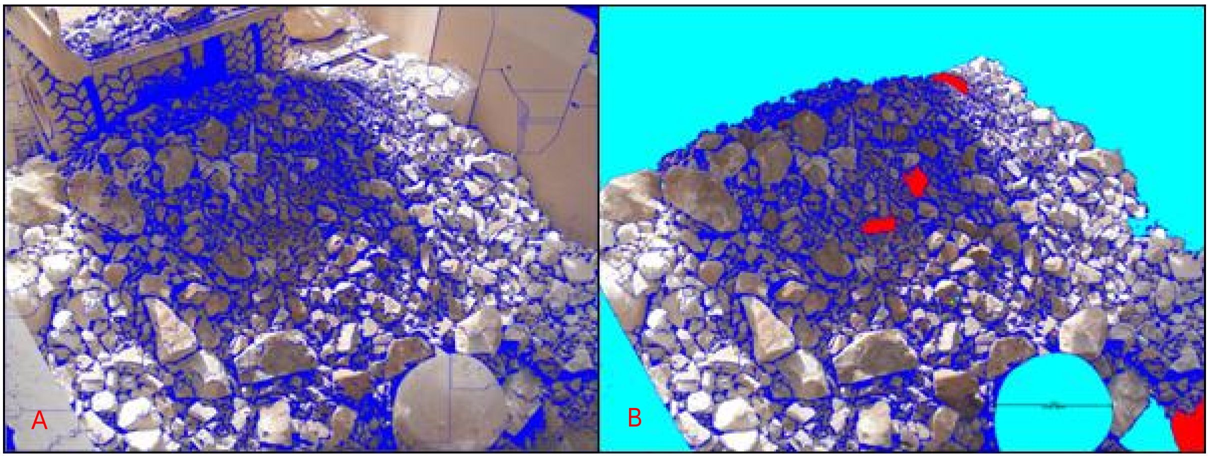

Figure 19: The delineated image of the feed to the primary crusher at Mountsorrel Quarry (A) and the image editing (B), with delineation (dark blue lines), scaling (black line spanning the crusher dome), fines addition (red) and areas that are not rock removed (light blue).

Split-Desktop assumes a normal distribution and can display the PSD data in three ways; as a cumulative curve (Figure 20A), as a histogram (Figure 20B) and as a table of raw data (Table 7). Please note that the copy of Split-Desktop being used for this research is on an academic licence, hence the watermarks. The raw data (Table 7) however can be exported to create graphs without the watermark in software such as Microsoft Excel. In the above example, the scale was added to the tyres of the dumper truck in the background and to the dome of the crusher (looks like a concrete ball in the foreground).

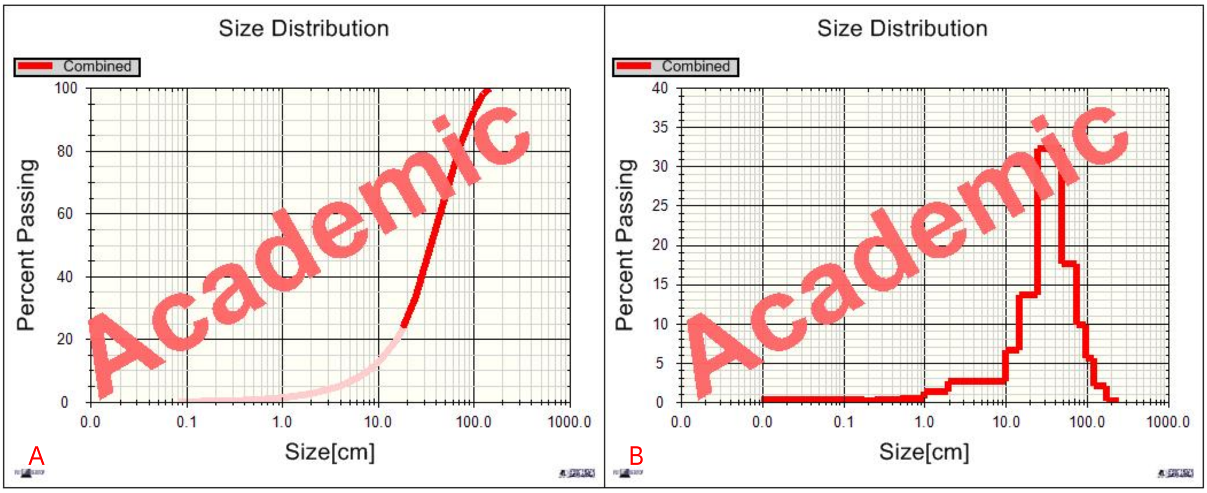

Figure 20: PSD cumulative curve (left) and PSD histogram (right) obtained using Split-Desktop and plotted with a logarithmic x axis.

Table 7: PSD cumulative percent passing in number form with sieve sizes from 444.5 mm down to 0.2032 cm.

Particle size (mm)	Cumulative % passing
444.5	100
317.5	98.06
254	92.52
190.5	82.75
127	65.24
63.5	32.99
38.1	19.39
25.4	12.84
20.32	10.28
15.24	7.76
10.16	5.27
5.08	2.78
2.54	1.5
1.905	1.17
1.27	0.83
0.9652	0.65
0.635	0.46
0.4826	0.36
0.2032	0.18

This process was repeated for a number of images and Split-Desktop calculated a PSD curve from all the images analysed. The results obtained from Split-Desktop in the form of Table 7 can be inserted into JKSimMet as the combiner (feed) size distribution to a crusher (Figure 21).

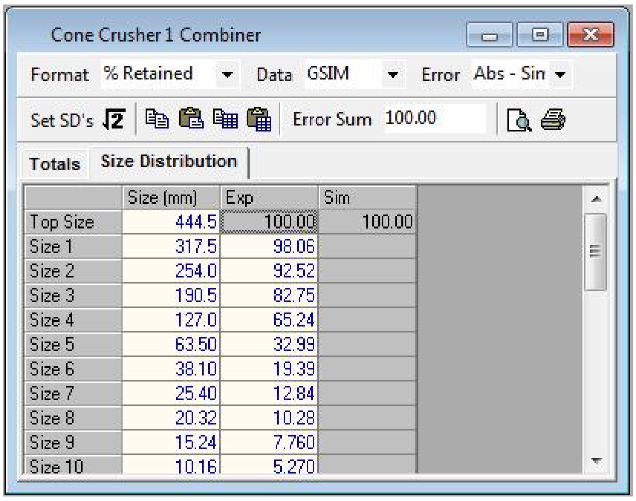

Figure 21: Image of the PSD feed for a crusher in JKSimMet.

By using JKSimMet with Split-Desktop in this way, any changes in PSD calculated from Split-Desktop can be entered into JKSimMet and the resultant product PSD from the crusher simulated. The product PSD would be different and as a result it would affect all of the downstream processes and these affects can also be analysed.

4.2 Results

The results obtained using Split-Desktop for the primary crusher feed PSD are shown in Table 8 as the percentage retained of each size fraction and in Figure 22 as a cumulative percent passing curve.

Table 8: Table of the retained size fractions of the primary crusher feed obtained using Split-Desktop.

Particle size (mm)	Percent retained
1905	2.352
1270	8.443
635	27.715
381	21.378
254	12.656
203.2	4.698
152.4	4.678
101.6	5.364
50.8	5.685
25.4	3.081
19.05	0.831
12.7	0.875
9.652	0.465
6.35	0.495
4.826	0.264
2.032	0.505

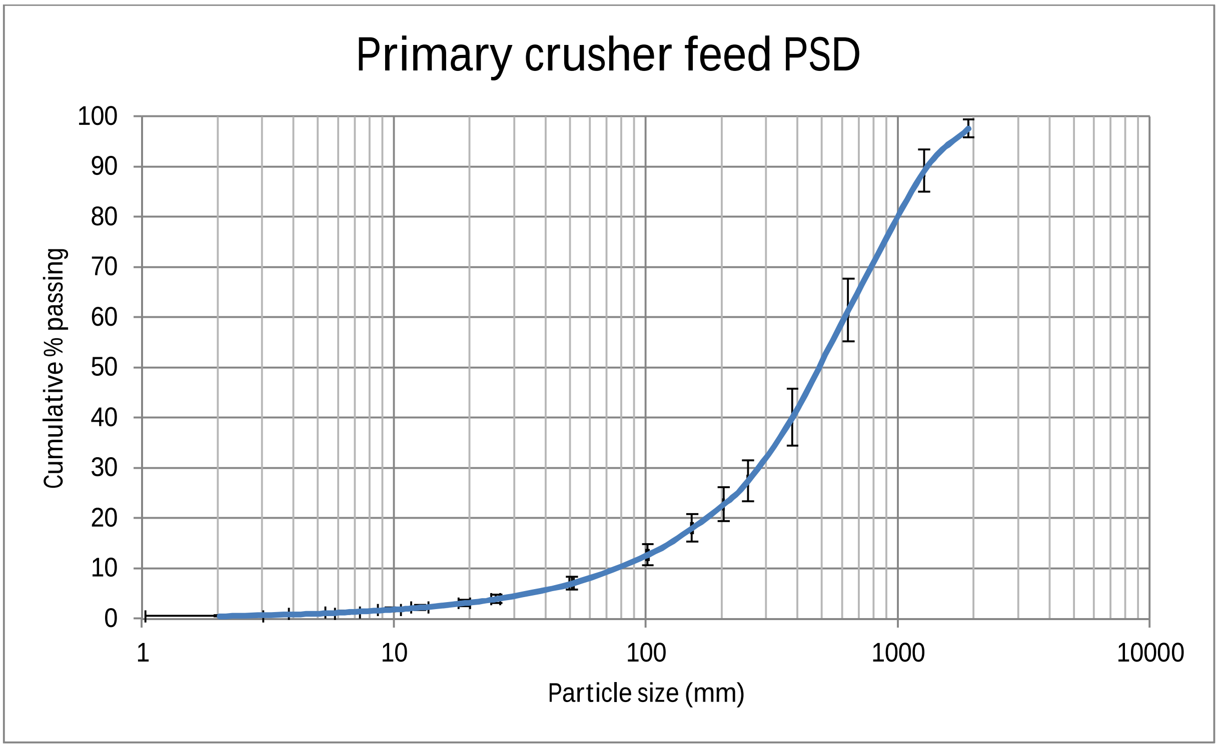

Figure 22: PSD of the feed to the primary crusher at Mountsorrel Quarry obtained using Split-Desktop. The error bars represent standard error.

As Table 8 and Figure 22 show, more particles fall in the size fraction of 635 mm < x < 1270 mm than any other fraction at 27.7%. It also shows that all particle size fractions smaller than 25.4 mm account for less than 1% each of the total mass of particles with 4.826 mm < x < 6.35 mm particles being the smallest fraction at 0.264%. The results also show that 2.352% of particles are larger than 1905 mm, that 72.5% of particles are greater in size than 254 mm and that 0.8% of particles are fines.

The greatest variance between the dumps analysed was in the 635 mm < x < 1270 mm fraction and the least variance being found in the 0 mm < x < 2.032 mm size fraction.

4.3 Discussion

As the results show, 0.8% of the primary crusher feed at Mountsorrel Quarry are fines. This may not seem significant, but with Mountsorrel Quarry having an annual production rate in excess of 5,000,000 t (Lafarge Aggregates Ltd, 2006), 0.8% equates to more than 40,000 t of fines produced pre-crushing annually. That is a huge amount of waste and, as a result of creating it, a huge amount of wasted energy. Some of the fines in the primary crusher feed will, however, be from protective barriers that are placed for safety reasons around the quarry (resulting in the recirculation of some of the fines produced.). These figures highlight that even a small reduction in the amount of fines can have a significant effect, as a 0.1% reduction in fines from blasting would reduce the amount of wasted material pre-crushing by more than 5,000 t per annum. This extra material would then increase the tonnage in the crushing process and therefore increase the amount of saleable product. With this increased tonnage in the crushing process, the total amount of fines could possibly be increased through primary, secondary and tertiary crushing if the difference was great enough, but it would lead to a lowering in the lifetime of the crusher liners due to increased tonnage. As there would be a greater product to waste ratio from this increased throughput in the crushing process, the sales would offset the cost of having to replace the crusher liners more frequently.

The results obtained for the primary crusher feed at Mountsorrel Quarry do not, however, account for secondary breakage on the quarry floor, which means that it cannot be truly indicative of the blast fragmentation. The fact that the images are from a number of different blasts will account for some variation in geology and any differences in blast design (e.g. variance in the number of blast holes).

The value of comparing the primary crusher feed PSD obtained for Mountsorrel Quarry to that of other quarries is questionable, as every quarry will use different blast designs which will affect fragmentation, use different equipment for blasting, excavating and transporting, which will affect breakage through attrition and abrasion, have a different primary crusher set up which is likely to be a completely different model or have different settings and will therefore be able to receive different maximum size particles and feed rates and, most importantly the geology will be different, which will have a huge effect on the way that the rock breaks up under the explosive forces. Even in the unlikely scenario that all of these variables are similar, the subtle differences will combine to have a significant effect on the blast and primary crusher feed PSDs. The value of the results from this experiment is therefore site specific for Mountsorrel Quarry and will be used to model Mountsorrel

Quarry using JKSimMet (see section 5) as the model requires a primary crusher feed PSD to model the quarry accurately.

Ultimately, having a well designed blast that does not create too many very large boulders or a huge amount of fines will have a significant and positive effect on the amount of saleable product produced at a quarry. It would also reduce the amount of energy used per tonne of saleable product and reduce the percentage of fines produced. This would reduce unwanted expenditure by reducing the stockpiles of fines which would lower the quantity of fines that are transported and would lead to the quarry operator to savings on fuel, vehicle repairs and man hours.

4.4 Conclusions

In conclusion, Split-Desktop is a highly useful image analysis software package that allows the user to determine the PSD of rock piles, including primary crusher feed PSDs. This software has been utilised for this research to determine the PSD of the primary crusher feed at Mountsorrel Quarry, as it is impractical to screen the feed due to the large size of many of the particles.

It was found that 0.8% of the feed was fines, although some of this will be from protective barriers placed around the quarry for safety reasons and, if a blast design could be produced to reduce this percentage, then it would lead to a more profitable quarry.

The hypothesis that primary crusher feed PSDs can be calculated using Split-Desktop image analysis software can be accepted.

5. JKSIMMET PLANT MODELLING SOFTWARE

JKSimMet is a computer modelling software package that allows the user to model individual pieces of aggregate production equipment, including crushers, screens and hydrocyclones. These individual pieces can be combined to model an entire plant. However, JKSimMet does not incorporate conveyor belts, so the energy used by conveyor belts cannot be calculated.

JKSimMet works by utilising a number of models to predict how rock particles will break and behave in a variety of quarry machines. The Whiten model (Equation 6) is used to simulate crushing, which works by breaking the process of crushing into two elements; the selection of the particles for breakage and the breakage of the selected particles. The selection of the particles will depend primarily upon the particle size relative to the CSS of the crusher, the ET and the choke feeding, whilst the product PSD will also depend upon how hard the rock material is (JKMRT, 2003).

Equation 6: Whiten model, where, p = product size distribution vector, I = unit matrix, C = classification function, A = appearance function and f = feed size distribution vector (JKMRT, 2003).

$$p = (I - C) \times (I - A \times C)^{-1} \times f$$

Equation 6 shows the whiten model, where p = product size distribution vector, I = unit matrix, C = classification function, A = appearance function and f = feed size distribution vector. The feed size distribution vector can be obtained from site by analysing the particles in the blast pile or feed to a crusher.

The Andersen model is then used to simulate how the rock particles that have been selected for breakage under the Whiten model will fracture under crushing. However, for the Anderson model to be used, rock fracture data needs to be obtained for the type of rock being looked at. This is obtained by undertaking drop-weight tests (see section 3.2.2 Drop-weight tests). The Anderson model combines the rock fracture data with the following crusher parameters (Adel *et al.*, 2006):

- CSS (mm)
- Crusher feed 80% passing
- Crusher product 80% passing
- ET (mm)
- Length of the liner (mm)
- Life of the liner (h)

Once the rock fracture data has been identified, the Awachie model can be used to determine the typical size distribution after breaking. This is done by calculating a value for the parameter t_{10}, which is the cumulative percent passing one tenth of the geometric mean size of the test particle. This is done similarly for t_n, where n = 2, 4, 10, 25, 50 and 75, and thus allowing a full size distribution to be simulated (JKMRT, 2003).

When all of these data have been entered, along with the feed PSD, JKSimMet can then simulate how a crusher will crush rocks and simulate product PSDs. These simulated product PSDs are then compared to the experimental product PSDs obtained from site to determine if the model is simulating accurately. The various crusher and material parameters can be altered to produce a different simulated product PSD, which can be analysed to determine if it is beneficial.

5.1 Method

The initial step in modelling Mountsorrel Quarry using JKSimMet is to create a flowsheet of the plant by combining the feed, primary gyratory crusher, screens, secondary and tertiary cone crushers, stock piles, bins and final products in the correct order (Figure 23; mass balance shown in Table 9). With this done, the parameters outlined in section 5, and the parameters outlined below are entered so the software will run accurate simulations:

- Material flow (t h^{-1})
- Feed and product PSDs
- Rock density (t m^{-3})
- Rock fracture data (t_{10} values)
- Energy data (E_{cs} values)
- Rock moisture content (%)

These parameters were obtained from data collected from analysing samples. The exception to this is the primary crusher feed which was obtained by using Split-Desktop as described in section 4.1 Method.

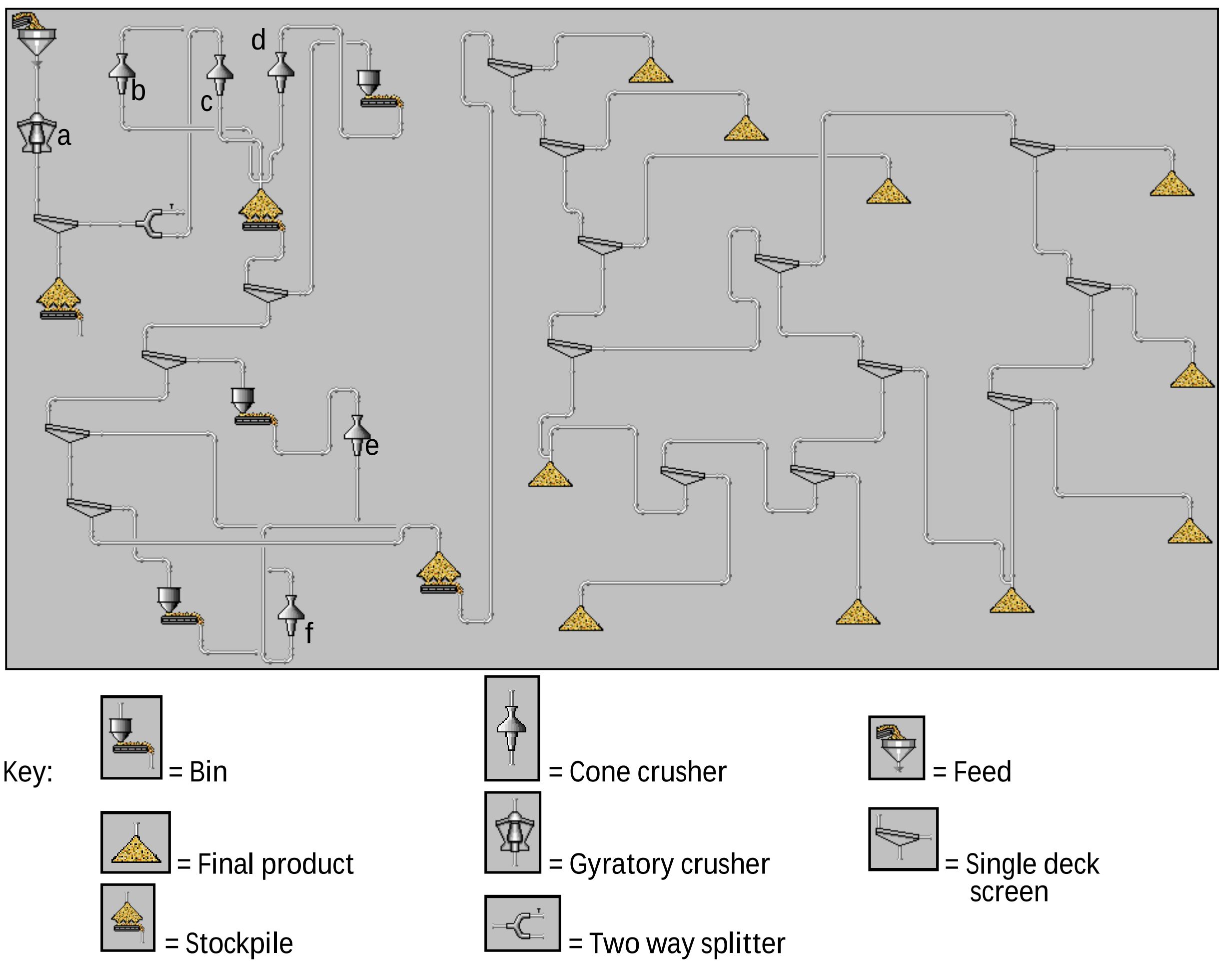

Figure 23: Flowsheet of Mountsorrel Quarry created using JKSimMet with key, , where a = primary gyratory crusher, b = cone crusher 1A, c = cone crusher 1B, d = cone crusher 2, e = cone crusher 3 and f = cone crusher 4.

As Figure 23 shows, the design of Mountsorrel Quarry consists of the blasted material entering the primary crusher, after which, the scalpings are removed before the rock is sent to two cone crushers (1A and 1B) which work in parallel. After this the rock is screened and any +70 mm particles are sent to cone crusher 2 in a feedback loop. With the -70 mm particles from cone crushers 1A, 1B and 2, any 63 mm < x < 70 mm particles are sent to cone crusher 3 and any 12 mm < x < 36 mm particles are sent to cone crusher 4. The products from cone crushers 3 and 4, along with -12 mm and 36 mm < x < 63 mm particles are sent to be screened and separated into their final product fractions of:

- -3 mm
- 3 mm < x < 4 mm
- 4 mm < x < 5 mm

Fines

- 5 mm < x < 6 mm
- 10 mm < x < 14 mm
- 14 mm < x < 20 mm
- 20 mm < x < 28 mm
- 28 mm < x < 40 mm
- 40 mm < x < 63 mm

Table 9: Mass input for each crusher at Mountsorrel Quarry. The mass output will be the same as JKSimMet assumes no loss or accumulation of mass.

Crusher	Mass input ($t\ h^{-1}$)
Primary gyratory crusher	2750
Cone crusher 1A	1100
Cone crusher 1B	900
Cone crusher 2	750
Cone crusher 3	443
Cone crusher 4	482

There are also four cone crushers (crushers 5, 6, 7 and 8) which are used for re-crushing material when there is a demand for smaller particles. However as these are rarely used they have been omitted from the flowsheet.

Once the t_{10} and E_{cs} data have been obtained from the drop-weight tests (see section 3.2.2 Drop-weight tests), the data is entered into the JKSimMet flowsheet for each crusher (Figure 24 and Figure 25, respectively). This ability allows for much more accurate results to be obtained as the crushers will model the crushing to site-specific rock data, not just generic hard, medium or soft rock data that most other aggregate plant modelling software allows.

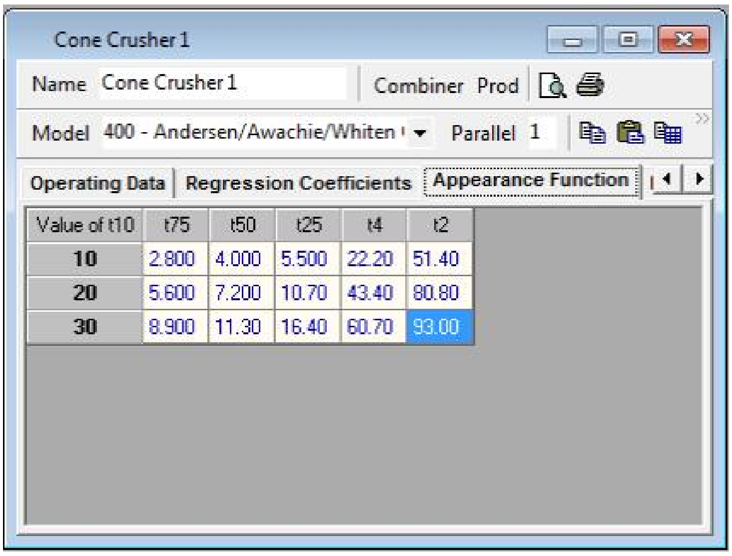

Figure 24: Image of the input field of the rock fracture data (t_{10}) in JKSimMet.

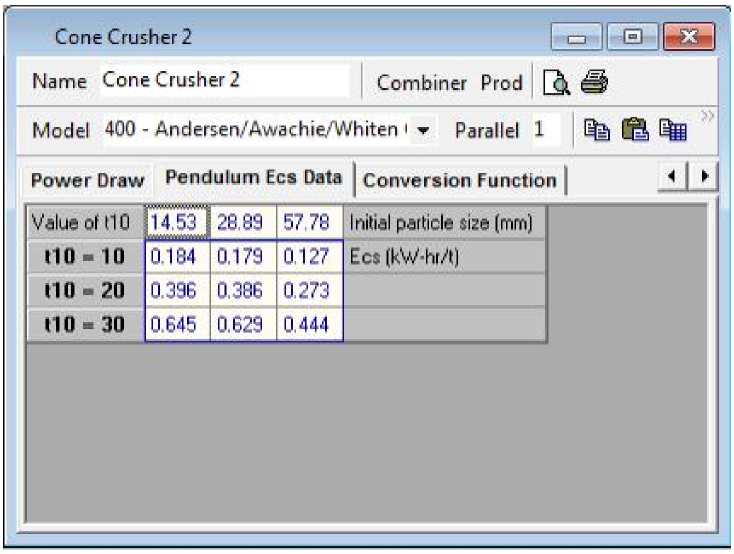

Figure 25: Image of the input field of the energy of comminution data (E_{cs}) in JKSimMet

Once the flowsheet has been created and all of the necessary data entered, JKSimMet utilises the Andersen, Awachie and Whiten models to simulate crushing and rock breakage (JKMRT, 2003).

The simulated product can then be compared to the experimental data obtained from screening samples from site. If the simulated product and experimental product PSDs have a strong correlation, the model is verified, and various parameters can be varied, and the resultant change in simulated product PSDs can be analysed to determine if the change has a positive effect.

5.2 Results

All the information collected from site (feed and product PSDs, CSSs, ETs etc.) has been entered into the JKSimMet flowsheet of Mountsorrel Quarry and the product PSDs of each crusher has been simulated to validate the model.

The simulated product PSD for the primary crusher, simulated using the feed PSD obtained using Split-Desktop, is shown in Figure 26.

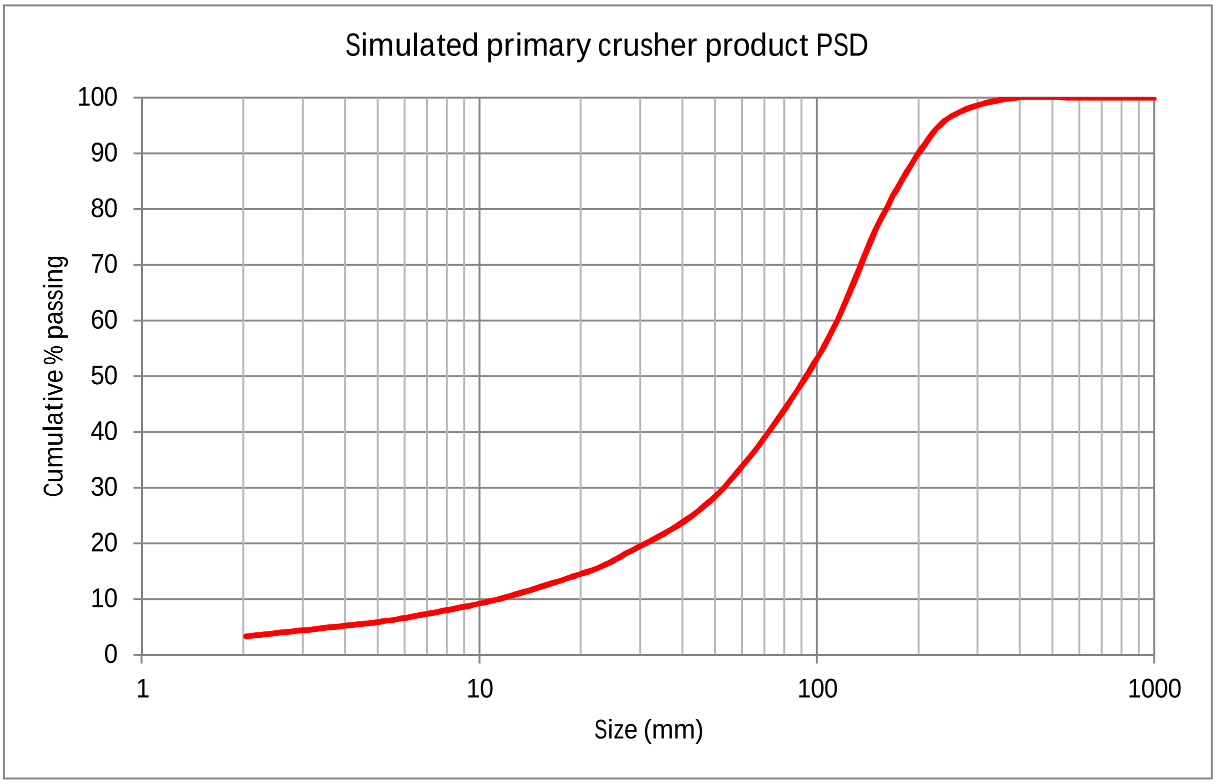

Figure 26: Graph to show the simulated Mountsorrel Quarry primary crusher product PSD obtained using JKSimMet.

Figure 26 shows the product PSD of the primary crusher at Mountsorrel Quarry, simulated in JKSimMet using the feed PSD obtained from using Split-Desktop (Section 4). As this curve shows, roughly 50% of the product is smaller than 90 mm, no particles are larger than 635 mm and it was simulated that 5.9% of the product is fines.

The experimental product PSDs from site are plotted against the simulated product PSDs from JKSimMet for crushers 1A, 1B, 2, 3 and 4 in Figure 27, Figure 28,

Figure 29, Figure 30 and Figure 31, respectively.

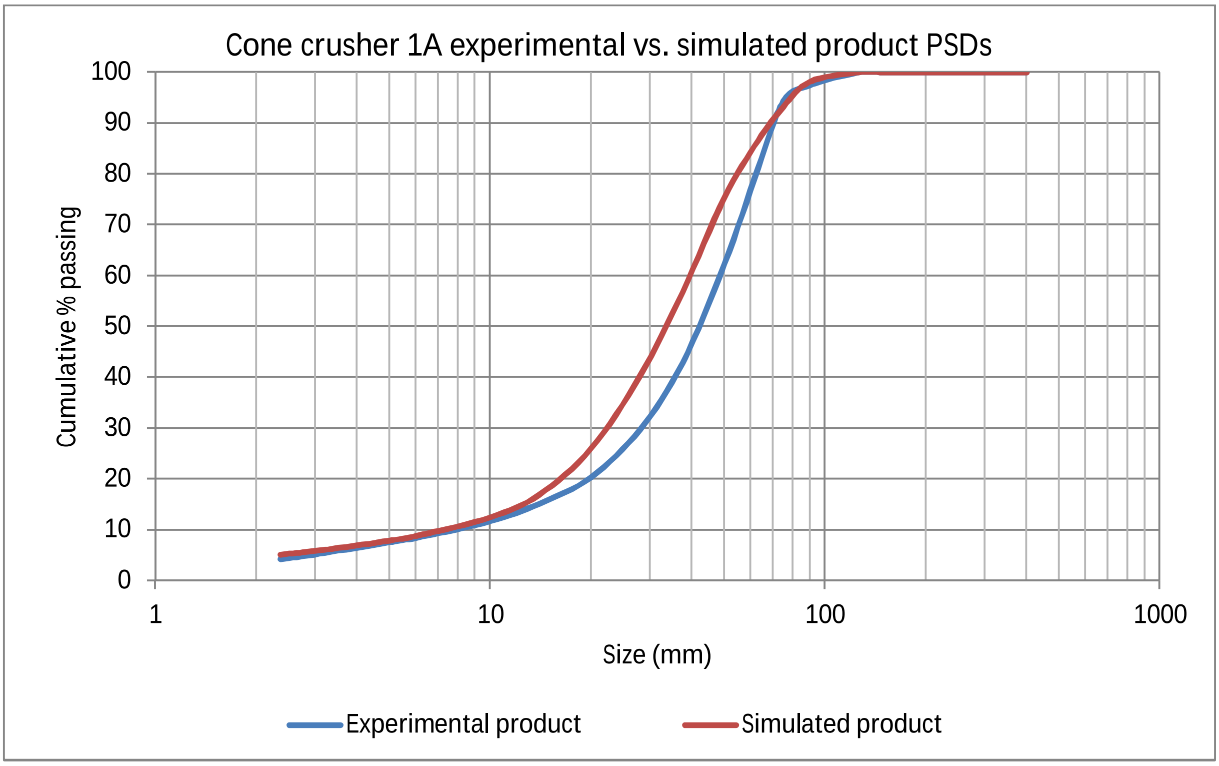

Figure 27: Graph to show the simulated (red) and experimental (blue) output PSDs from cone crusher 1A at Mountsorrel Quarry.

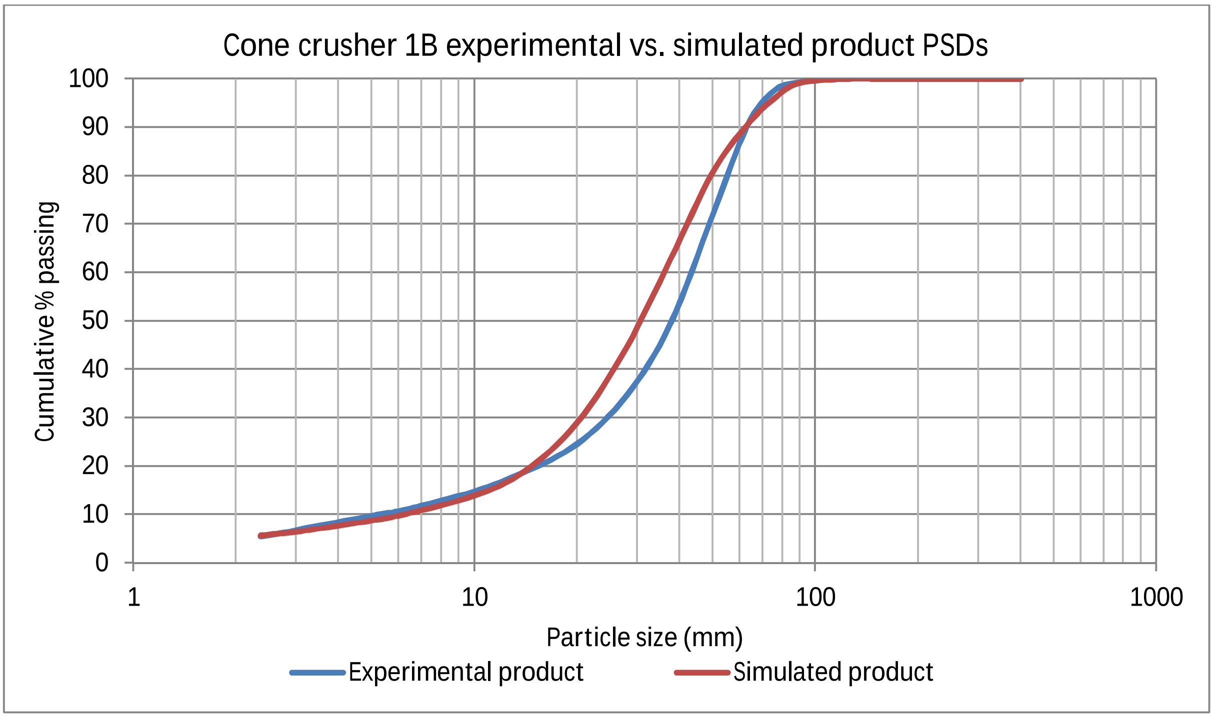

Figure 28: Graph to show the simulated (red) and experimental (blue) output PSDs from cone crusher 1B at Mountsorrel Quarry.

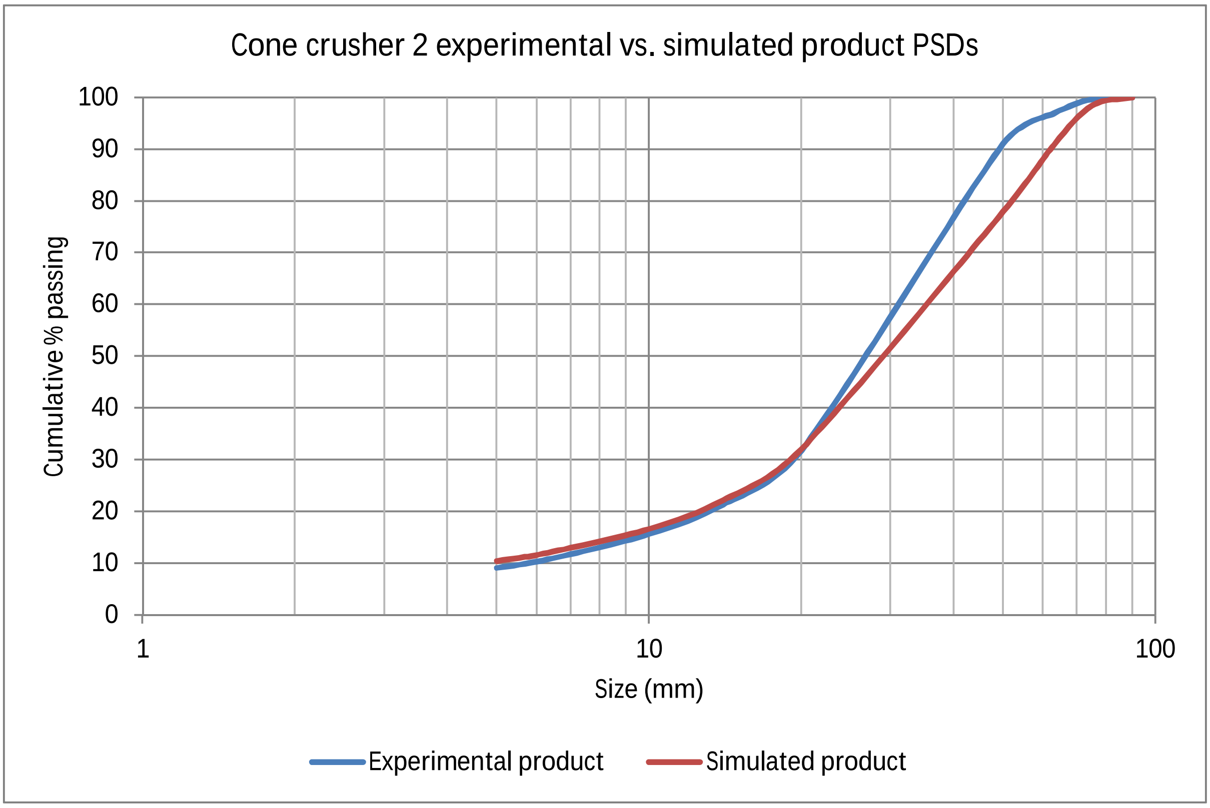

Figure 29: Graph to show the simulated (red) and experimental (blue) output PSDs from cone crusher 2 at Mountsorrel Quarry.

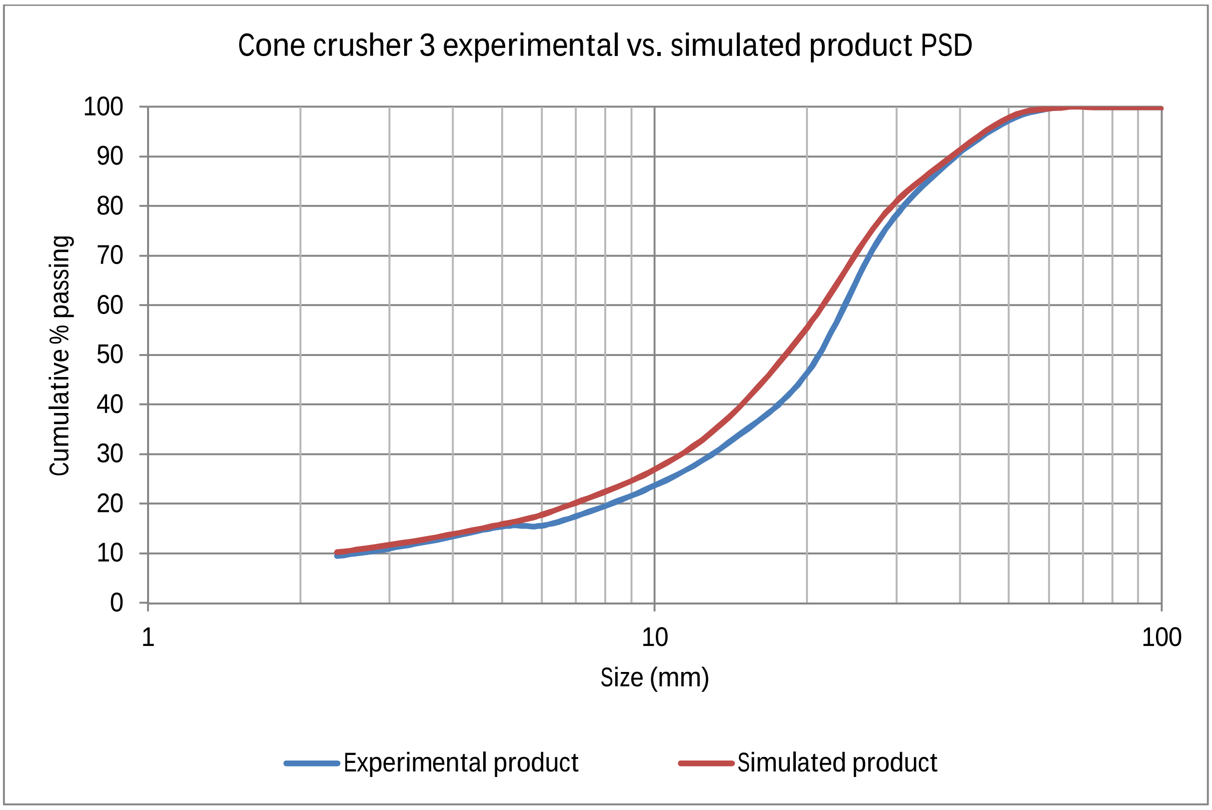

Figure 30: Graph to show the simulated (red) and experimental (blue) output PSDs from cone crusher 3 at Mountsorrel Quarry.

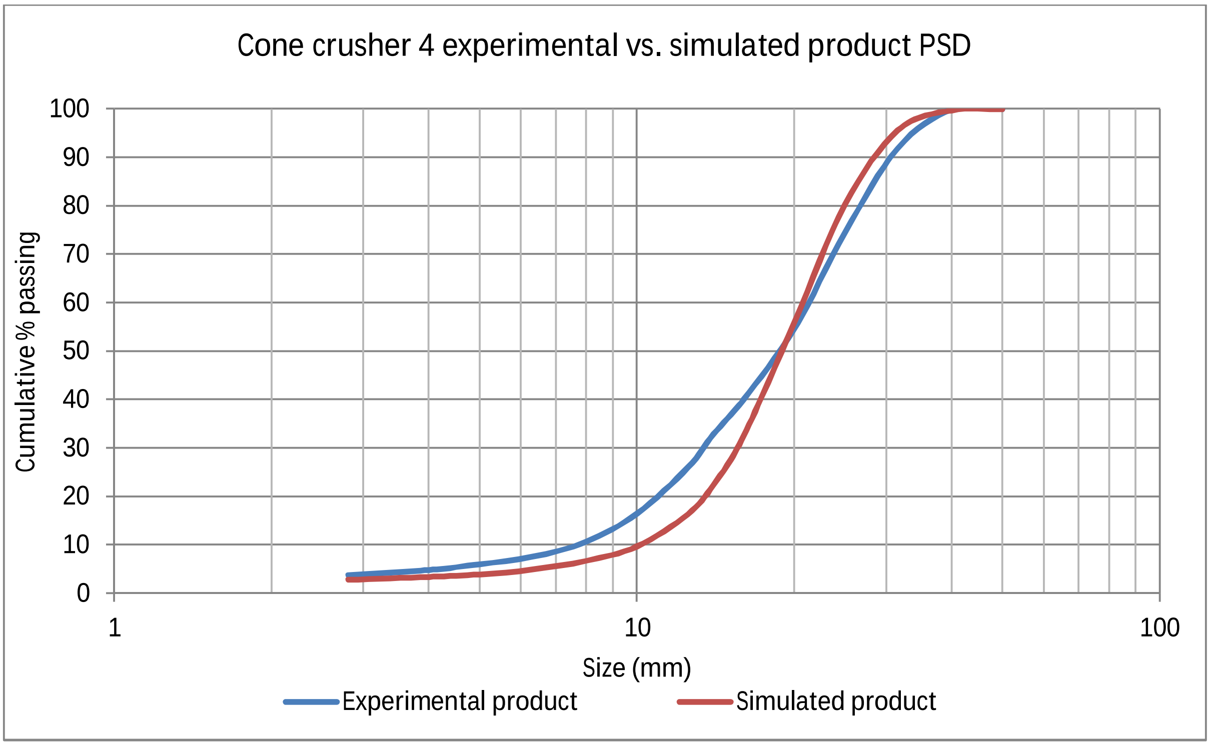

Figure 31: Graph to show the simulated (red) and experimental (blue) output PSDs from cone crusher 4 at Mountsorrel Quarry.

As Figure 27, 28, 29, 30 and 31 respectively show, there is a strong correlation between the simulated and experimental product PSDs from crushers 1A, 1B, 2, 3 and 4. The correlation is especially strong at the finer and larger ends of the scales. There is some difference in the middle ranged sizes for all crushers. The largest differences between the simulated and experimental PSDs for crushers 1A, 1B, 2, 3 and 4 and the maximum simulated particle sizes are shown in Table 10.

Table 10: Table outlining the largest differences between the simulated and experimental PSDs and the maximum simulated particle sizes for crushers 1A, 1B, 2, 3 and 4.

Crusher	Largest difference between simulated and experimental product		Maximum simulated particle size (mm)
	Size (mm)	Difference (%)	
Cone crusher 1A	37.5	13.96	150
Cone crusher 1B	37.5	13.26	125
Cone crusher 2	50	13.10	90
Cone crusher 3	20	19.17	63
Cone crusher 4	14	10.51	40

As Table 10 shows, all of the largest differences are in the middle ranged sizes and the maximum particle sizes are what would be expected. Table 11 outlines the percentage of fines calculated from experimental and simulated methods for all the crushers, as well as the differences between the two.

Table 11: Table to show the amount of fines produced by each crusher obtained from site (experimental) and simulated using JKSimMet (Simulated). The difference between the experimental and simulated data and mean values are also shown.

Crusher	Experimental fines (%)	Simulated fines (%)	% Difference
Primary gyratory crusher	N/A	5.9	N/A
Cone crusher 1A	7.6	7.9	3.8
Cone crusher 1B	9.8	8.8	11.4
Cone crusher 2	9.1	10.4	12.5
Cone crusher 3	15.5	15.0	3.3
Cone crusher 4	6.0	3.9	53.8

AS Table 11 shows, the largest percentage of fines (excluding the primary crusher) produced is by cone crusher 3 with 15.5%, followed by crushers 1B, 2, 1A 7% and 4 with 9.8%, 9.1%, 7.6% and 6.0%, respectively. The simulated percentage of fines produced follows a similar pattern, with crusher 3 > crusher 2 > crusher 1B > crusher 1A > crusher 4, with 15.0%, 10.4%, 8.8%, 7.9% and 3.9%, respectively. The difference between the experimental and simulated fines percentages varies from 3.3% for crusher 3 to 53.8% for crusher 4.

Table 12 outlines the power draws, feed rates and the energy used per tonne of material crushed for each of the crushers at Mountsorrel Quarry. These power draw values were simulated using JKSimMet whilst the feed rates were obtained from site and the energy used per tonne of material crushed values calculated by dividing the power draw by the feed rate.

Table 12: Table outlining the power draws (kW), feed rates (t h^{-1}) and the amount of power used per tonne of material crushed (kW h t^{-1}) for each of the crushers at Mountsorrel Quarry obtained using JKSimMet.

Crusher	Power draw (kW)	Feed rate (t h^{-1})	Energy per tonne of material crushed (kW h t^{-1})
Primary gyratory crusher	332.0	2750	0.12
Cone crusher 1A	205.6	1100	0.19
Cone crusher 1B	198.9	900	0.22
Cone crusher 2	232.5	750	0.31
Cone crusher 3	207.1	443	0.47
Cone crusher 4	102.1	482	0.21
Net	1278.2	N/A	1.52

As Table 12 shows, the primary crusher has the greatest power draw at 332.0 kW, followed by cone crushers 2, 3, 1A, 1B and 4 which use 232.5 kW, 207.1 kW, 205.6 kW, 198.9 kW and 102.1 kW, respectively. Table 12 also shows that cone crusher 3 at Mountsorrel Quarry uses the greatest amount of power per tonne of material crushed at 0.47 kW h t^{-1}, followed by cone crushers 2, 1B, 4, 1A and the primary crusher which use 0.31 kW h t^{-1}, 0.22 kW h t^{-1}, 0.21 kW h t^{-1}, and 0.19 kW h t^{-1}, and 0.12 kW h t^{-1} respectively. The net power draw and energy used per tonne of material crushed across all the crushers is 1278.2 kW and 1.52 kW h t^{-1}, respectively.

The JKSimMet flowsheet was also used to simulate the overall product PSD of Mountsorrel Quarry, and the results are shown in Figure 32.

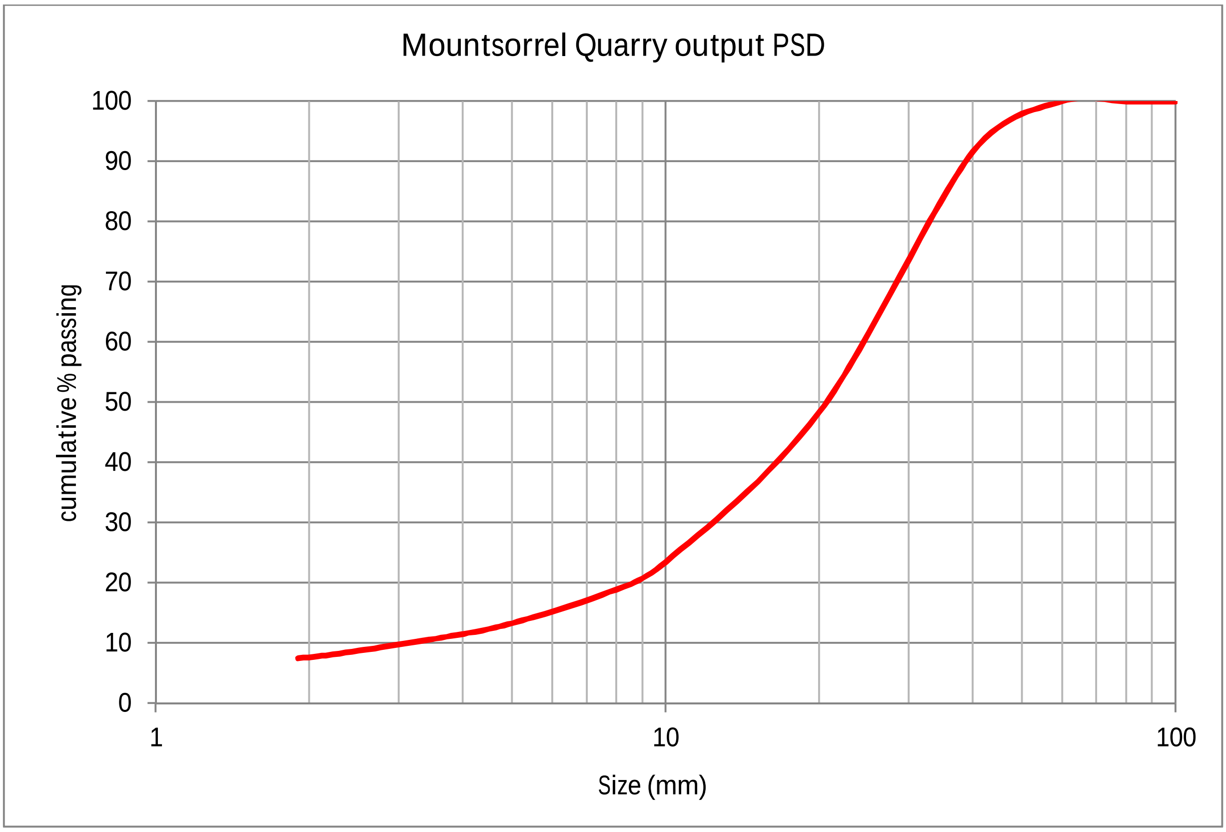

Figure 32: The overall output PSD of Mountsorrel Quarry simulated using JKSimMet.

AS Figure 32 shows, the simulated overall plant production at Mountsorrel Quarry has a fines percentage of 13.4%, with the largest size fraction being 20.0 mm < x < 40.0 mm, and there are no particles larger than 60.0 mm.

When the CSS of the primary crusher is reduced from 165.1 mm (which is used on site) to 100.0 mm the product PSD changes as a result. This simulated product PSDs for the primary crusher for these two CSS settings is shown in Figure 33.

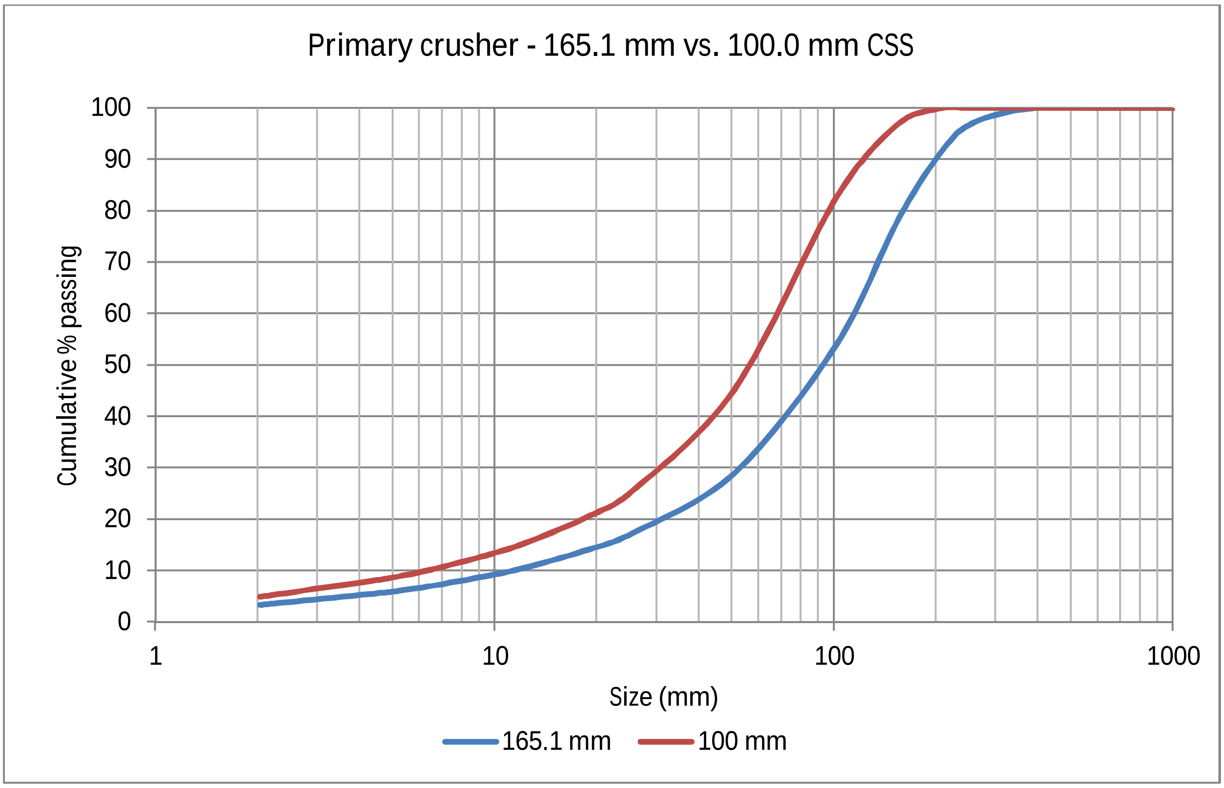

Figure 33: Product PSDs for the primary gyratory crusher at Mountsorrel Quarry, with CSS settings of 165.1 mm (the operating gap; blue) and 100 mm (red), simulated using JKSimMet.

As Figure 33 shows, when the CSS is reduced from 165.1 mm to 100 mm there are fewer larger particles in the product and the overall percentage of fines increases from 6% to 8.7%, which equates to a 45% increase in fines production. The largest simulated difference occurs in the 101.6 mm < x < 152.4 mm size fraction with the product from the 100.0 mm CSS simulation containing 28.6% more.

The differences in power draw and energy used per tonne of material crushed for the two CSS settings on the primary crusher was simulated and are stated in Table 13.

Table 13: Table outlining the difference in power draw and energy usage, for the primary gyratory crusher at Mountsorrel Quarry, when the CSS is varied from 165.1 mm (the operating gap) to 100.0 mm, simulated using JKSimMet.

Primary crusher CSS (mm)	Power draw (kW)	Energy per tonne of material crushed (kW h t^{-1})
165.1	332.0	0.12
100.0	472.6	0.17
Difference	140.6	0.05

As Table 13 shows, when the CSS is reduced from 165.1 mm to 100.0 mm, the power draw increases by 140.6 kW, and the energy per tonne of material crushed increases by 0.05 kW h t^{-1}.

The effect of the change in primary crusher CSS from its operating size of 165.1 mm to 100.0 mm on the overall product PSD of Mountsorrel Quarry is shown in Figure 34.

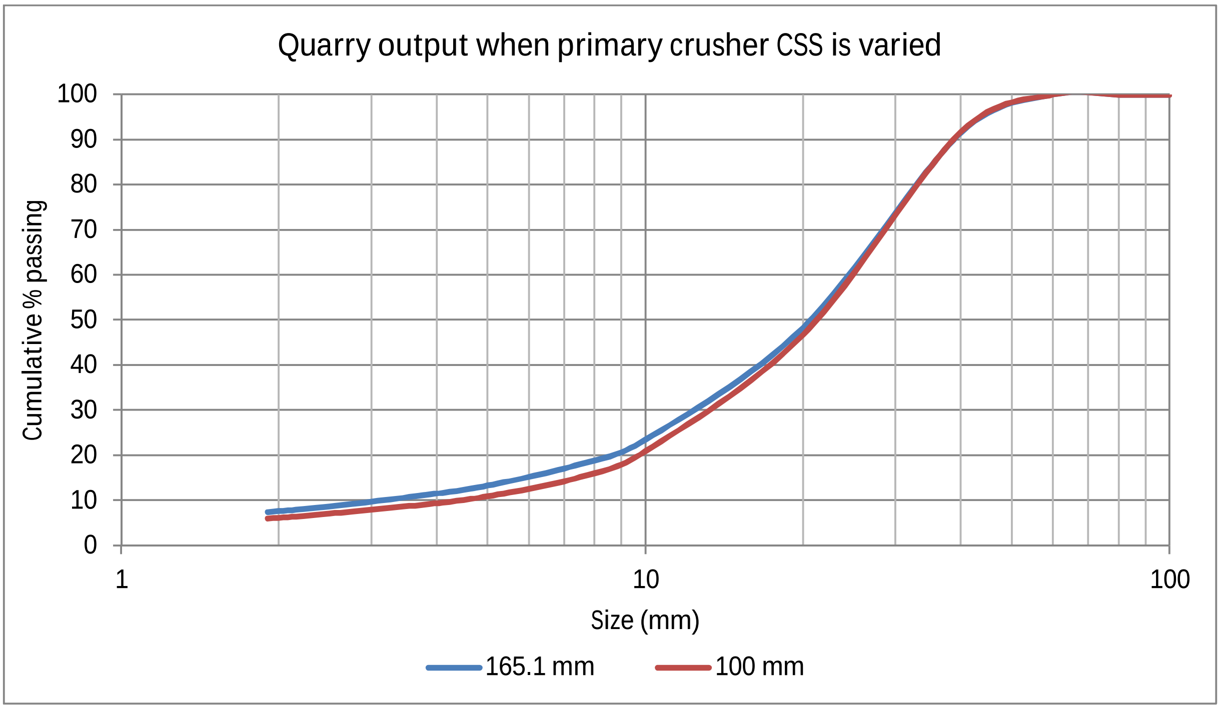

Figure 34: The output PSD of Mountsorrel Quarry when the primary crusher CSS is 165.1 mm (the operating gap; blue) and 100 mm (red), simulated using JKSimMet.

As Figure 34 shows, the quarry output PSDs are similar, but there are fewer smaller particles produced and the overall production of fines is 18% lower when the primary crusher CSS is set to 100.0 mm when compared to 165.1 mm. The biggest difference was found in the 7.5 mm < x < 10.0 mm size fraction at 15.5%.

5.3 Discussion

The simulated product PSD of the primary crusher shows that 5.9% of the product is fines, which equates to more than 162 t h^{-1}. Fines are produced every time a rock particle is fractured, and with the number of large particles entering the crusher, needing to be crushed multiple times before they become small enough to pass through the operating gap of the crusher, there will be a large amount of fines produced. Some of these fines will be due to fines used as protective barriers around the quarry floor, some of which will get mixed up with the muck pile and become part of the primary crusher feed.

The simulation of crushers 1A, 1B, 2, 3 and 4 all show strong correlation with the experimental data, with the largest difference being in the size 37.5 mm > x > 50 mm fraction on crusher 1A at 13.96%, and a mean difference between simulated and experimental data of 3.33%. These larger differences are in the mid-ranged particles sizes, but what is important is that the model is accurately simulating the amount of fines produced across all the crushers because the ultimate aim of this research is to reduce fines production. This means that as the fines are being simulated accurately, when any parameters which affect the product PSDs that are changed, the model will accurately simulate the resultant change in fines production. Across crushers 1A, 1B, 2, 3 and 4, the least accurate simulation of fines was 2.1% off the experimental data on crusher 4, whilst the most accurate was crusher 1A with 0.3% and the mean over all the crushers was 1.0%. This accuracy means that the JKSimMet model can be used to predict fines production.

The difference in power draw between the crushers varied from 102.1 kW, on cone crusher 4, to 332 kW on the primary crusher. The simulated power draw is a function of two main factors; CSS and rock fracture data (Bearman *et al*., 1991). Because the same material is being used in all the crushers, the rock fracture data will not influence the difference between the power draws. This suggests that the CSS will determine the power draw, and Table 14 shows the CSS settings used on site and the power draws simulated using JKSimMet.

Table 14: Table highlighting the power draw and energy per tonne of material crushed for each crusher at Mountsorrel simulated using JKSimMet and the CSS used on site.

Crusher	Power draw (kW)	Energy per tonne of material crushed (kW h t^{-1})	CSS (mm)
Primary gyratory crusher	332.0	0.12	165.1
Cone crusher 1A	205.6	0.19	55.0
Cone crusher 1B	198.9	0.22	50.0
Cone crusher 2	232.5	0.31	42.0
Cone crusher 3	207.1	0.47	28.0
Cone crusher 4	102.1	0.21	28.0

As Table 14 shows, there is a rough correlation between CSS and power draw, with the larger the CSS, the greater the power draw. Cone crusher 2, however, does not fit this pattern and cone crusher 4 has a power draw less than half that of cone crusher 3, even though they both have the same CSS. This suggests that there are other factors that can influence the power draw. One of these factors will be the crusher type; however this will only factor a difference for the primary crusher, as it is a gyratory crusher, whilst all of the other crushers are cone crushers, and JKSimMet does not allow the entry of specific models, just crusher type. Therefore the crusher type can be ignored for these anomalies. Another factor is the feed PSD and feed rate (Cleary, 1998), and this is most likely what has caused these differences in power draw. It is worth noting that the CSS of some of the crushers are reduced as the crusher liners wear to compensate for the increasing gap. Therefore, the CSS settings used in this model are the CSS settings used when the liners are new.

The energy used per tonne of material crushed (Table 14) is a factor of the power draw and the feed rate, and the primary crusher is by far the most efficient crusher, simulated as operating at 0.12 kW h t^{-1}. Although the primary crusher has the largest power draw (332.0 kW), it also has by far the greatest feed rate at 2750 t h^{-1}, which is two and a half times that of the second highest feed rate of cone crusher 1A (1100 t h^{-1}). It is therefore because of this high feed rate that the primary crusher is the most efficient. The primary crusher has the highest feed rate because all material that Mountsorrel Quarry processes goes through the primary crusher, but after the primary crusher, the material is split between crushers 1A and 1B and with some material going into the scalping. Crusher 3 is the least efficient crusher, operating at 0.47 kW h t^{-1} as it has the lowest feed rate and the highest simulated power draw at 207.1 kW and 443 t h^{-1}, respectively. The energy per tonne of material crushed is the most useful parameter to analyse with respect to energy efficiency and the greater the throughput, the more efficient the crusher will be operating.

It may be expected that crushers 1A and 1B would show the same product PSDs and power draws as both of these crushers have the same feed PSDs and both are 7' short head crushers, however their feed rates and CSS settings are different. Cone crusher 1A has a feed rate of 1100 t h^{-1} and a CSS of 55 mm, whilst cone crusher 1B has a feed rate of 900 t h^{-1} and a CSS of 50 mm. The feed rate, however, will have an insignificant effect on the product PSD but does explain the difference in energy used per tonne of material crushed between the two crushers, as crusher 1A is processing more material for a similar power draw and is therefore using less energy per tonne. The difference in CSS on the other hand explains why there are two different product PSDs created by these two crushers, as the smaller CSS on cone crusher 1B will mean that more particles are being crushed, especially particles in the size range of 50 mm < x < 55 mm, which are more likely to fall straight through on cone crusher 1A.

The simulated overall product of Mountsorrel Quarry shows that 13.4% of the overall product is fines and that there are no particles larger than 60.0 mm. This is possibly suggesting that the model is predicting slightly more breakage occurring than actually happens, as the largest particle produced at Mountsorrel Quarry is 63 mm. However, this supports that the JKSimMet model is simulating the overall product within the size ranges that are produced on site.

The effect of changing the CSS of the primary crusher from 165.1 mm to 100.0 mm on the primary crusher product PSD, which resulted in fewer larger particles and more fines, is not a surprising find. This is because, by reducing the CSS, it reduces the maximum gap at the bottom of the crusher, and therefore reduces the maximum size of a particle that can pass through the gap. This will reduce the amount of larger particles produced, compared to when the crusher has a larger CSS. This smaller gap will also mean that larger particles will be broken more times before they are able to pass through the gap, and with each fracture, fines will be produced and, ultimately, more fines will be produced.

The effect of reducing the primary crusher CSS on the overall plant product PSD however, was to give an overall reduction in fines. This is because fewer larger particles are being produced by the primary crusher, meaning fewer particles will be crushed downstream in crushers 1A, 1B, 2, 3 and 4, as there will be more smaller particles that are able to pass straight through the crusher or will be screened out prior to crushers 3 and 4. As a result, fewer breakages downstream will result in fewer fines produced, and in this simulation, the difference is great enough to outweigh the amount of extra fines produced by the primary crusher to result in fewer fines overall. As a negative effect, reducing the primary crusher CSS increases the power draw of the primary crusher so a cost benefit analysis would need to be undertaken to determine if the effects of changing the CSS is beneficial.

In reality, the primary crusher at Mountsorrel Quarry cannot physically reduce its CSS to 100.0 mm, but these simulations outline how JKSimMet can be utilised to reduce fines and how complex aggregate production is.

This model can now be used to optimise the quarry to produce fewer fines, use less energy or produce more of a certain size range. The latter is useful if one size range is more profitable or in higher demand. However, all of these factors will have positive and adverse effects, such as reducing the amount of fines and increase energy usage (as shown above), so a cost benefit analysis would need to be undertaken to determine whether an alteration to the plant settings is beneficial. Further research into this aspect is planned to be undertaken by a Masters of Research (MRes) student.

5.4 Conclusions

In conclusion, a working flowsheet of Mountsorrel Quarry has been created using JKSimMet, and the primary crusher product has been simulated using the feed PSD obtained using Split-Desktop. Moreover, all the cone crushers at Mountsorrel Quarry (except the crushers used for re-crushing) have been successfully modelled and validated, with particular accuracy in the amount of fines produced. The power draws and amount of energy use per tonne of material crushed for these crushers has also been simulated. It was found that the primary crusher has the highest power draw, but is the most efficient due to its large feed rate, whilst cone crusher 3 is the least efficient crusher due to its high power draw and low feed rate. The JKSimMet model has also been used to produce an overall product PSD for Mountsorrel Quarry which falls within the product size range of the plant, with no particles simulated to be larger than 63 mm.

By reducing the primary crusher's CSS from 165.1 mm to 100.0 mm, the effects of changing one crusher parameters on the product PSD, of both a single crusher and the entire plant, has been shown. This simulation resulted in an increase of 45% in fines produced by the primary crusher, but due to the different primary crusher product PSD, the downstream processes created an overall reduction in fines of 18%. This, however, is a theoretical example, as the primary crusher at Mountsorrel Quarry is unable to reduce its CSS to 100.0 mm, but it does highlight how JKSimMet can be used to optimise a quarry and shows how complex the processes is.

The flowsheet created in JKSimMet can be used to optimise Mountsorrel Quarry to produce fewer fines, lower energy usage or to produce more of a certain size fraction. This can be accomplished by altering equipment settings and/or by adding or removing equipment, and is planned to be undertaken by another MRes student who is continuing this research.

From the results obtained, the hypotheses that UK aggregate quarries can be modelled using JKSimMet plant modelling software can be accepted and that JKSimMet can be used to propose ways of reducing fines production in UK quarries can be accepted as it has been shown how changing the CSS of the primary crusher can reduce the total amount of fines across the entire quarry.

6. BLAST DESIGN

Excluding the excavation of unwanted material above a reserve, blasting is the initial stage in aggregates production and the resultant PSD of the muck pile will affect the efficiency, energy usage and the amount of fines produced throughout all the crushing and screening processes downstream. An ideal blast would lead to all particles being of a saleable size, resulting in no need no crushing and the muck pile would just require screening into its various size fractions. This however, will never happen as there will always be fines and oversized particles produced. Some particles from a blast will be so large that they will not fit into the primary crusher or potentially cause the crusher to stall, and it is up to the discretion of the excavator operator to determine which particles fall into this category. These particles need to be broken into smaller particles. At Mountsorrel quarry this is achieved by using the excavator to drop a large metal ball onto any particle that requires this secondary breakage on the quarry floor, until it is broken into suitably smaller particles. Consequently this process takes time and as a result slows down the feed rate into the primary crusher, however the amount of time wasted will be less than if the crusher stalls or if a digger needs to be called in to remove the particle from the primary crusher.

To reduce the amount of these large boulders in the first place, larger amounts of explosives can be used; however this will produce more fines. Therefore, to reduce the amount of fines produced, a lesser amount of explosives can be used; however this will produce more boulders requiring secondary breakage on the quarry floor. Because of this a compromise needs to be achieved and, as a result, an intermediate amount of fines and large boulders will be produced.

Further breakage can occur post blasting whilst excavating and transporting the muck pile. This occurs through the force of the excavators bucket or through attrition and abrasion caused by contact between particles and with the dumper. The effect of these processes however are minimal in the scale of the tonnage blasted and are assumed to be insignificant.

Once the blast holes have been excavated, quarries can either fill the blast holes completely with explosives, or they can add decking, as illustrated in Figure 35.

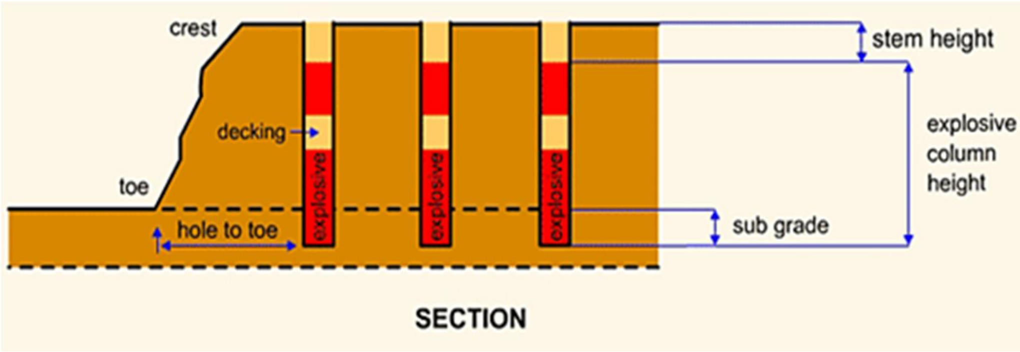

Figure 35: Diagram to illustrate the concept of decking in blast holes (Farnfield, 2007).

When undertaking a decked blast, quarries either stagger the detonation timings of the decks, or detonate them all together. In the scenario of a two deck blast, which is what Mountsorrel Quarry do and is illustrated in Figure 35, quarries will often blast the bottom deck first, as it will intuitively give a better blast fragmentation. This is because if the top deck is detonated first, a lot of energy will be spent in expelling the rock into the atmosphere, and likewise with the bottom deck. If however the bottom deck is detonated first, then a lot more energy will be used in fragmenting the rock and will also affect the top half of the rock face, increasing the fragmentation.

To date there have been no experiments conducted to determine the effects of deck detonation order on blast fragmentation. This experiment will look to determine whether the order of deck detonation has any significant effect on the primary crusher feed PSD, number particles that require secondary breakage on the quarry floor, acoustic levels and vibration readings.

6.1 Method

Two blasts were conducted at Mountsorrel Quarry to determine the effects of the order of deck detonation on fragmentation. The two blasts were undertaken on adjacent faces to minimise any geological variation between the two blasts and the blast designs are shown in Table 15 and Figure 36.

Table 15: Table outlining the number of blast holes, the timings between holes, decks and rows, the offset timing, the type of detonator used and the order of deck detonation for blast 1 and blast 1.

Parameter	Blast 1	Blast2
Number of blast holes	19	19
Timing between holes (ms)	16	16
Timing between decks (ms)	24	24
Timing between rows (ms)	120	120
Offset to the right (ms)	28	28
Type of detonator	Electronic	Electronic
Order of deck detonation	Bottom then top	Top then bottom

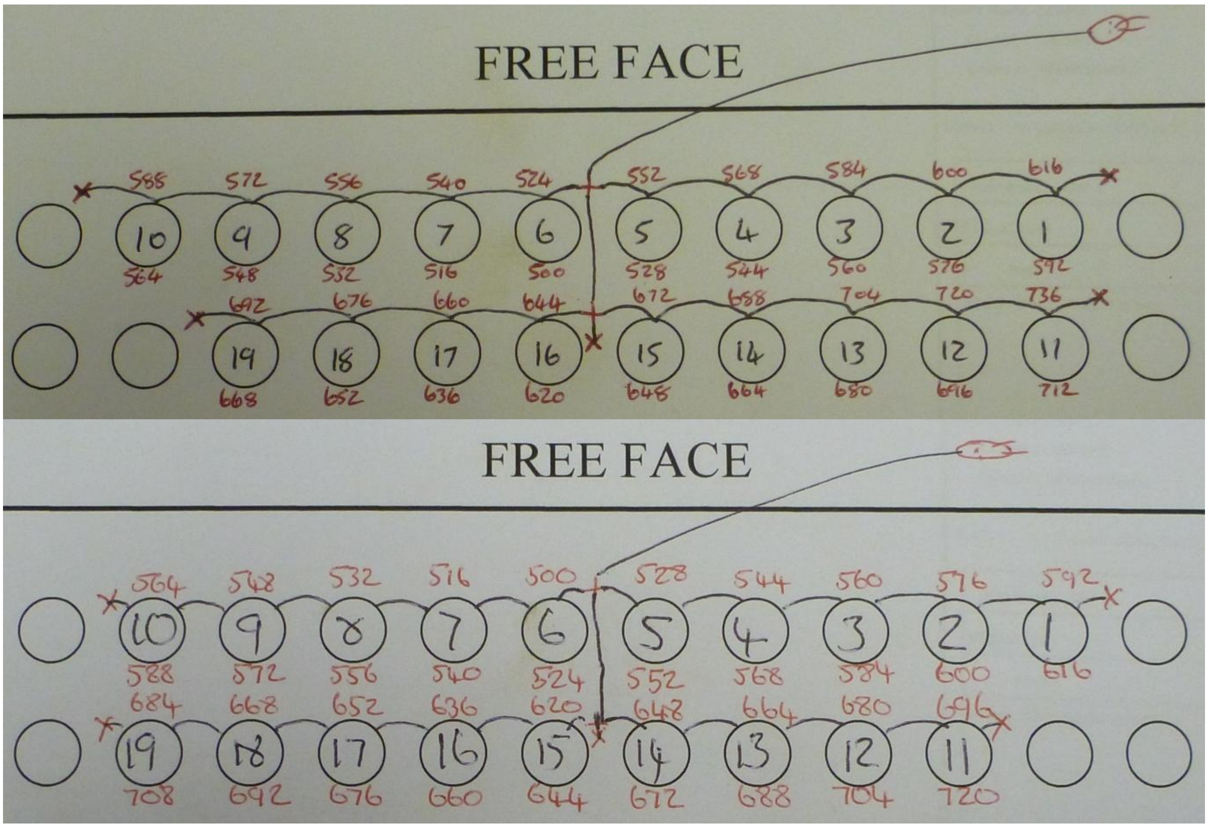

Figure 36: Blast design for blast 1 (top) and blast 2 (bottom) undertaken at Mountsorrel Quarry on 24th July and 31st July 2012, respectively, where x = End plugs, + = Row controllers, | = Extenders,  = Bench controllers, Black numbers (e.g. 7) = Hole number and red numbers (e.g. 676) = detonation time (ms).

As Table 15 and Figure 36 show, both blasts contain the same number of holes, used the same timings and were detonated using electronic detonators as electronic detonators have much more accurate timings than shock tube (non-electric) detonators (Paley, 2010; Teowee, 2010). The only difference in blast design was the order of deck detonation, with the first blast (blast 1) having the bottom deck detonated before the top deck, which is the usual design at Mountsorrel Quarry and vice versa in the second blast (blast 2).

Images were taken from above the primary crusher control room as the two muck piles were dumped into the primary crusher. Split-Desktop was utilised as described in section 4.1 Method to determine the PSDs of the two different blasts so that they could be compared. Because analysing the material being dumped into the primary crusher does not account for particles that require secondary breakage on the quarry floor, it therefore does not truly represent the blast fragmentation. Because of this, the number of particles that required secondary breakage was recorded.

Due to the proximity of residents living near Mountsorrel Quarry, the noise and vibrations created by every blast need to be monitored using a seismograph. The acoustic levels and vibration readings from blasts 1 and 2 were recorded to determine if there was any significant difference between them.

6.2 Results

The simulated primary crusher feed PSDs obtained using Split-Desktop for blasts 1 and 2 are shown in Figure 37.

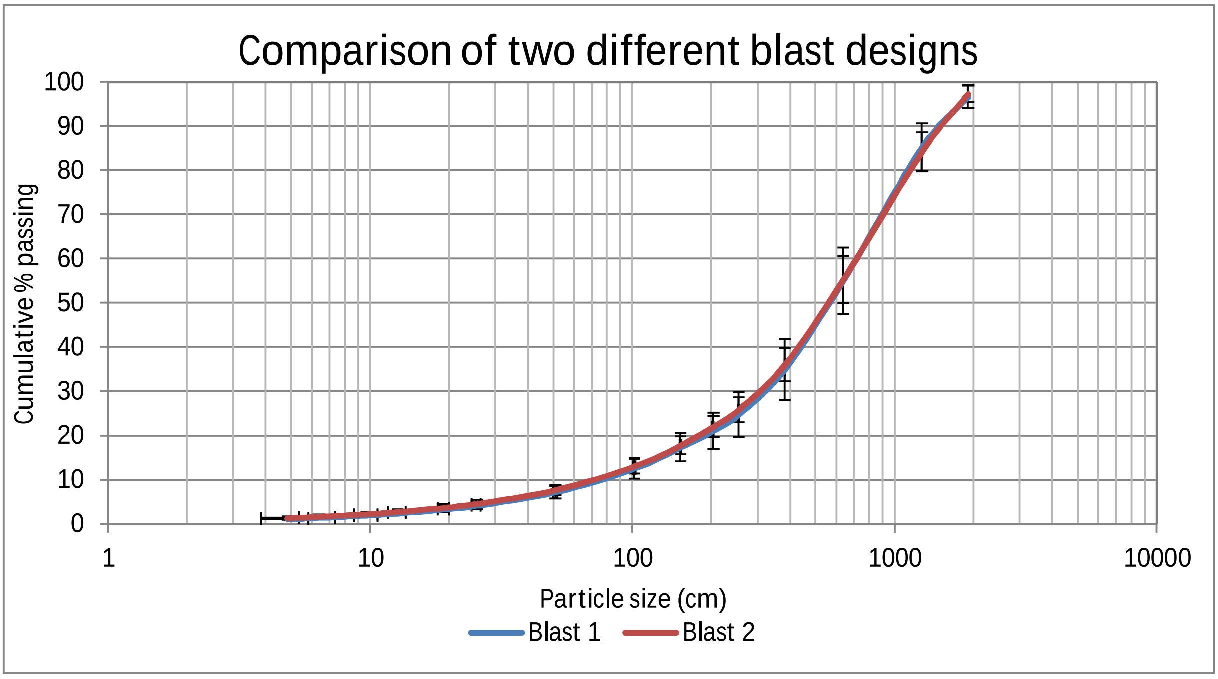

Figure 37: Graph the show the primary crusher feed PSDs from blast 1 (blue) and blast 2 (red) obtained using Split-Desktop. The error bars represent standard error.

As Figure 37 shows, there is very little difference between the primary crusher feed PSDs of blasts 1 and 2 with the largest difference occurring in the 254 mm < x < 381 mm size fraction at 1.14%. These results show that Blast 1 created 0.26% fewer fines than blast 2. As well as showing the similarity of the two primary crusher feed PSDs, Figure 37 also shows that all of the error bars (standard error) overlap, meaning that there is statistically no significant difference between the primary crusher feeds from blasts 1 and 2.

Because the primary crusher feed PSDs do not truly represent the blast fragmentation PSDs, during the course of a day's excavation of the muck piles of blasts 1 and 2 the number of particles that required secondary breakage were recorded. The results from this, along with the acoustic and vibration readings from the two blasts, are shown in Table 16. The full acoustic and vibration readings are shown in Appendix III – Blast vibration and acoustic readings.

Table 16: Table outlining the amount of secondary breakage recorded for the blast piles of blast 1 and blast 2 over the course of one day's excavation.

Parameter	Blast 1	Blast 1	Difference
Particles requiring secondary breakage	12	14	2
Acoustic level (dB)	124	121	3
Radial vibration (mm s^{-1})	3.239	2.858	0.381
Vertical vibration (mm s^{-1})	9.906	11.684	1.778
Transverse vibration (mm s^{-1})	4.001	4.064	0.063

As Table 16 shows, there were more particles that required secondary breakage in blast 2 than blast 1, with 14 and 12 particles recorded respectively and blast 2 created a greater amount of noise than blast 1, with 124 dB and 121 dB recorded respectively. Blast 1 created greater vibrations in the radial plane, whilst blast 2 created greater vibrations in the vertical and transverse planes. The greatest difference in vibrations was found in the vertical plane with a difference of 1.778 mm s^{-1}.

6.3 Discussion

As shown in Figure 37, the primary crusher feed PSDs for blasts 1 and 2, although having different blast designs, are statistically indifferent. The reasons for such close similarities could be because of any of the following reasons:

- The difference in geology of the two faces that were blasted.
- The order of deck detonation has no effect in blast fragmentation.
- The difference in the number of particles that required secondary breakage on the quarry floor which could have affected the primary crusher feed PSD.
- The fact that not every single dump from the blasts was analysed.

It is unlikely that the difference in the geology of the two faces would act in a way to nullify the effect that the order of deck detonation has on the blast fragmentation, as although there will be some difference in geology between the two faces, the fact that they were adjacent to each other means that they would be unlikely to differ by such a significant amount. It is untrue that the order of deck detonation has no effect, as the two blasts resulted in different numbers of particles that required secondary breakage on the quarry floor, so this possibility can be discarded.

The difference in the number of particles that required secondary breakage on the quarry floor will have affected the primary crusher feed PSD as these were broken before the images were taken and analysed meaning that the primary crusher feed PSD will not be the same as the muck pile PSD. As blast 2 contained more of these large particles, it would have had a PSD with a larger percentage of larger particles compared to blast 1.

What is most likely to have had an effect on the similarities of the two crusher feed PSDs is that not every dumper that unloaded truckloads of blast material was analysed. Because of this, the results obtained may not be a true representation of what the two feed PSDs were. As a result, if this experiment were to be repeated, it would be advised that every single truckload of material from each blast was imaged and analysed to obtain more representative results.

During the course of a day there were 12 rock particles from blast 1 that underwent secondary breakage on the quarry floor, whilst there were 14 for blast 2. Therefore there were 16.7% more rock particles that required secondary breakage in blast 2 than blast 1; however this cannot be concluded as significantly different as these results are just comparing two blasts, and more blasts would be required to obtain more useful statistical data. The difference in acoustics and vibrations between the two blasts was also found to be insignificant, and well within the limits imposed on Mountsorrel Quarry.

The lack of difference found between the crusher feed PSDs, number of particles requiring secondary breakage on the quarry floor, acoustic levels and vibration reading between the two blasts, shows that the altering of the order of deck detonation on a two deck blast design has no effect on these factor. This may or may not be because not every dump load of each blast was analysed. However, altering the deck detonation order may have an effect on other factors that were not measured, such as diggability and shape of the rock particles.

Because an experiment looking at the effect of deck detonation order has not been undertaken before, these results cannot be compared to anything in the literature. If this experiment was undertaken in a quarry with a different rock type (e.g. limestone) then the geology may have an effect, which means that it is more beneficial to detonate one deck before the other, but further experiments, in different quarries, would need to be undertaken to determine this. Another interesting factor of blast design would be to look at the diggability of the muck pile, as this will affect how efficiently the excavator can work and ultimately the fuel consumption of the excavator.

6.4 Conclusions

In conclusion, two blasts were undertaken at Mountsorrel Quarry with identical blast designs except for the order of deck detonation, with blast 1 having the bottom deck detonated before the top deck, and blast 2 having the top deck detonated before the bottom deck. The blasts were undertaken on adjacent faces to minimise geological variations, the muck piles were analysed as they were dumped into the primary crusher using Split-Desktop, and the number of particles that required secondary breakage on the quarry floor was recorded, along with acoustic levels and vibration readings.

It was determined that there was no statistical difference in the primary crusher feed, the number of rocks requiring secondary breakage, acoustic levels or vibrations levels between the two blasts. This is most likely due to the order of deck detonation having no significant effect on these parameters, but could be due to the fact that not every truckload of material from each blast was analysed.

The hypothesis that there is a significant difference in blast PSD when the order of deck detonation is changed can neither be accepted nor rejected, as although there was no significant difference found in the parameters measured of the two blasts, the order of deck detonation may have a significant effect on other factors, such as diggability or particle shape. The effect of rock type may also give different results with the different blast designs, but as this experiment was only undertaken on granite, this is not known.

7. SUMMARY OF RESULTS AND CONCLUSIONS

7.1 Summary of results

A summary of the results obtained for the physical properties of Mountsorrel Quarry granite, the primary crusher feed, the JKSimMet model of Mountsorrel Quarry and the effects of altering the order of deck detonation in the blast design are outlined below.

7.1.1 Mountsorrel Quarry granite

The granite at Mountsorrel Quarry was found to be an extremely hard granite whose oxide composition, determined using XRF, is predominantly: SiO_2, Al_2O_3, Na_2O, MgO, K_2O, Fe_2O_3 and CaO with their respective weight percent of oxides being: 63.3%, 16.8%, 8.3%, 3.24%, 3.02%, 2.17% and 2.13%. XRD analysis showed that the granite contained the crystalline structures of quartz (SiO_2) and albite, calcian, ordered $(Na,Ca)Al(Si,Al)_3O_8)$, amongst other unidentified compounds.

E_{cs} and t_{10} data were also obtained for input into JKSimMet through the analysis of data acquired by submitting samples to drop-weight tests. Both the t_{10} and E_{cs} data confirmed that the Mountsorrel Quarry granite is a very hard rock type.

These findings from the XRF, XRD and drop-weight test analyses correspond with the elements and compounds found in other studies on granite and geology in the area.

7.1.2 Primary crusher feed

The primary crusher feed PSD at Mountsorrel Quarry was obtained using Split-Desktop image analysis software because the particles are too large to obtain a PSD using conventional screening methods. It was found that 0.8% of the feed is fines and that more particles fall into the 635 mm < x < 1270 mm size fraction than any other at 27.7%. It also showed that no particles are larger than 3810 mm, and although it may not be 100% accurate, it does give an indication of what the PSD is entering the primary crusher as no studies have been undertaken previously at Mountsorrel Quarry to determining this.

7.1.3 JKSimMet model of Mountsorrel Quarry

A flowsheet of the Mountsorrel Quarry aggregate plant was created using JKSimMet and utilised to simulate various parts of the quarry. The product PSD of the primary crusher has been simulated using the feed PSD simulated using Split-Desktop. This showed that the primary crusher produces 5.9% fines and no particles larger than 635 mm. Cone crushers 1A, 1B, 2, 3 and 4 at Mountsorrel Quarry have been modelled with a strong correlation between the simulated and experimental product PSD. This correlation is very accurate in fines simulations, with a mean difference between simulated and experimental data of 1%. Mountsorrel Quarry as a whole has also been successfully modelled using JKSimMet, with the simulated product corresponding with the product size ranges produced on site and a simulation of 13.4% of the final product being fines.

The theoretical effect of changing parameters has been shown using JKSimMet. This was accomplished by changing the CSS on the primary crusher from 165.1 mm (the operating CSS on site) to 100.0 mm, which caused the primary crusher to produce 45% more fines. The effect of the different primary crusher product PSD on the downstream processes (crushers 1A, 1B, 2, 3 and 4 and screens) however, meant that the quarry as a whole created 18% fewer fines. This reduction in fines, however, increase the power draw of the primary crusher from 332.0 kW to 472.6, kW and therefore a cost benefit analysis would need to be undertaken to determine whether the change would be profitable.

The power draw and energy use per tonne of material crushed were also simulated for each crusher. This found that although the primary crusher has the greatest power draw, it uses the least amount of energy per tonne of material crushed at 0.12 kW h t^{-1}, and is therefore the most efficient, whilst crusher 3 is the most inefficient crusher at 0.47 kW h t^{-1}, due to its high power draw and low feed rate.

7.1.4 Blast design

Two blasts were undertaken to determine whether the order of deck detonation has an effect on any of the following parameters:

- Resultant primary crusher feed PSDs
- Number of rocks requiring secondary breakage
- The acoustic levels (dB)
- Vibration readings (mm s^{-1})

The two blasts were undertaken on adjacent rock faces to minimise any variations in geology between the two rock faces and they both had the same blasts designs other than the order that the decks were detonated (in blast 1 the bottom deck was detonated before the top deck and vice versa in blast 2).

It was found that there was no significant difference between the two blast designs in any of the aforementioned parameters. Therefore, it has been determined that the order of deck detonation has no significant effect on the aforementioned parameters when conducted in a granite quarry. The order of deck detonation may, however, have an effect on other parameters, such as muck pile shape and diggability. It may have a significant effect on one of the parameters measured in this experiment if undertaken on a different type of rock. Further experiments will need to be undertaken to determine this.

7.2 Conclusions

In conclusion, this research has looked at various aspects of Mountsorrel Quarry, including the rock parameters and blast design. This research has also used JKSimMet plant modelling software to create a working model of Mountsorrel Quarry that has been validated against data from site, and Split-Desktop image analysis software has been used to simulate the primary crusher feed PSD, which was previously unknown. The model was used to simulate various crusher product and feed

PSDs, as well as the overall plant product PSD, and it was used to determine the effect of changing parameters on said PSDs. From the experiments undertaken, and the results thus obtained, it has been determined that the following hypotheses can be accepted.

- Primary crusher feed PSDs can be calculated using Split-Desktop image analysis software.
- UK aggregate quarries can be modelled using JKSimMet plant modelling software.
- JKSimMet plant modelling software can be used to propose ways of reducing fines production in UK quarries.

However, the hypothesis that there is a significant difference in blast PSDs when the order of deck detonation is changed can neither be accepted nor rejected.

8. Future work

From undertaking this research and analysing the results, a number of areas that would benefit from future work have been identified. With respect to the EE-Quarry project, this research is planned to be continued by another MRes student. This student will be using this research as a basis, along with further information collected to produce a matrix and/or a code using MatLab code writing software that allows the abilities of JKSimMet to be utilised in the EE-Quarry top level model. The top level model, once completed, will be able to be used on any quarry to make it more energy efficient. This will be accomplished using the newest version of JKSimMet which is due to be released towards the end of 2012, and it will have the new ability of being able to run batch files, amongst other new features.

As for the blast design comparison, it would be extremely interesting to continue looking at the comparative fragmentations of different blast sequencing and in different geologies to determine the effects that they have on muck pile PSDs as well as the downstream effects of fines production, energy and cost.

9. REFERENCES

Adel, G., Kojovic, T. and Thornton, D. (2006). *Mine-to-Mill Optimization of Aggregate Production*. JKTech Report No. DE-FC26-04NT42084

Barkley, T. L. (2011). The Fundamentals of a Good Electronic Initiation System Program. *International Society of Explosives Engineers*: 12 pages

Bartley, D. A., McClure, R. and Trousselle, R. (2003). Electronic Detonator Technology in Open Pit Mining. In: *Proceedings of the EFEE 2nd World Conference, Prague, Czech Republic, 10-12 September 2003*: 165-171

Bearman, R. A., Barley, R. W. and Hitchcock, A. (1991). Prediction of Power Consumption and Product Size in Cone Crushing. *Minerals Engineering* 4(12): 1243-1256

Bernard, T. (2005). How has Electronic Initiation Changed the Rules of Blast Design? *International Society of Explosives Engineering*: 10 pages

Bremer, D., Ethier, R. and Lilly, D. P. (2007). Factors Driving Continuous Blasting Improvement at the Lafarge Ravena Plant. *Proceedings of the Annual Conference on Explosives and Blasting Technique* 33(1): 97-106

British Geological Survey, (n.d.). *Resources*. [Online] Available at: <http://www.bgs.ac.uk/planning4minerals/Resources_21.htm> [Accessed 8th November 2011]

Brown, G. C., Hughes, D. J. and Esson, J. (1973). New X.R.F. Data Retrieval Techniques and Their Application to U.S.G.S. Standard Rocks. *Chemical Geology* 11(3): 223-229

Cebrian, B. (2010). Blast optimisation at limestone quarry operations – good fragmentation, less fines. *International Society of Explosives Engineering*: 9 pages

Chang, S. -H., Lee, C. -I. and Seokwon, J. (2002). Measurement of Rock Fracture Toughness under Modes I and II and Mixed-Mode Conditions by Using Disc-Type Specimens. *Engineering Geology* 66(1–2): 79-97

Chau, K. T. and Wu, S. (2007). Chapter 2 Impact Breakage of Single Particles: Double Impact Test. *Handbook of Powder Technology*. Agba M.G., Salman D. and Michael J.H., Elsevier Science B.V. 12: 69-85

Chavez, R., Leclercq, F and McClure, R. (2007). Applying up-to-date Blasting Technology and Mine to Mill Concept in Quarries. *Proceedings of the Annual Conference on Explosives and Blasting Technique* 33(1): 329-340

Cleary, P. W. (1998). Predicting Charge Motion, Power Draw, Segregation and Wear in Ball Mills Using Discrete Element Methods. *Minerals Engineering* 11(11): 1061-1080

Cresswell, D. (2011). *Measuring Energy Consumption of Quarrying Operations*. Report No. EEQ-MIRO-WP2-2.2

Drew, A., Ghazireh, N. Rowson, N., Ghataora, G., Wardrop, D., Huxtable, P., James, B., Barritt, J., Stock, H., Freeman, S., Farnfield, R., Rollo, A., Stratford, G., Eldred, S., Hutchinson, R., South, J., O'Nyons, P., Holmes, D., Shuttlewood, A., McCurdy, S., Hutchinson, R., Barnes, G., Blackburn, S. & Robbins, P. (2011). *Towards Meeting the Challenges of Sustainable Aggregates Production; Mine-To-Mill Process*. Tarmac Ltd Report No. MA/7/G/5/004

Farnfield, R. (2007). Blasting Practice for Hard Rock Quarries. *PREN5650-5 Blasting & Drilling*. University of Leeds, Unpublished

Fernlund, J. M. R. (2005). Image Analysis Method for Determining 3-D Shape of Coarse Aggregate. *Cement and Concrete Research* 35(8): 1629-1637

Gallagher Jr, J. J., M. Friedman, Handin, J. and Sowers, G. M. (1974). Experimental Studies Relating to Microfracture in Sandstone. *Tectonophysics* 21(3): 203-247

Glowe, R. (2005). Blasting Results Compared Using Crusher Power Consumption and Tonnage of Rock Produced. *International Society of Explosives Engineering*: 15 pages

Hull, A. W. (1919). A New Method of Chemical Analysis. *Journal of the American Chemical Society* 41(8): 1168-1175

Hunter, G. C., McDermott, C., Miles, N. J., Singh, A. and Scoble, M. J. (1990). A Review of Image Analysis Techniques for Measuring Blast Fragmentation. *Mining Science and Technology* 11(1): 19-36

Jansen, W. M., Morrison, R. D., Wortley, M. and Rivett, T. (2009). Tracer-based mine-mill ore tracking via process hold ups at Northparkes mine. In: Tenth Mill Operators' Conference - Proceedings. *Tenth Mill Operators' Conference, Adelaide, Australia, 12th-14th October, 2009*: 345-356

Jenkins, R., Gould, R. W. and Gedcke, D. (1995). Quantitative X-ray spectrometry, Second edition. *Practical Spectroscopy Series* 20

JKMRT (2003). *JKSimMet User Manual; Steady State Mineral Processing Simulator*

Kanchibotla, S. S. and Valery, W. (2012). Mine to Mill Process Integration and Optimisation – Benefits and Challenges. In: 2010 Volume I General Proceedings Collection. *International Society of Explosives Engineering*: 14 pages

Kanchibotla, S. S., Valery, W. and Morrell, S. (1999) Modelling fines in blast fragmentation and its impact on crushing and grinding. In: *Proceedings of Explo'99—A Conference on Rock Breaking. The Australasian Institute of Mining and Metallurgy, Kalgoorlie, Australia*: 137–144

Kemeny, J. M. (1994). Practical Technique for Determining the Size Distribution of Blasted Benches, Waste Dumps and Heap Leach Sites. *Mining Engineering* 46(11): 1281-1284

Kemeny, J., Devgan, A., Hagaman, R. and Wu, X. (1993). Analysis of Rock Fragmentation Using Digital Image Processing. *Journal of Geotechnical Engineering* 119(7): 1144-1160

Kemeny, J., Girdner, K., Bobo, T. and Norton, B. (1999) Improvements for Fragmentation Measurement by Digital Imaging: Accurate Estimation of Fines. *Proceedings of the 6th International Symposium for Rock Fragmentation by Blasting, South African Institute of Mining and Metallurgy, Johannesburg*: 103-110

Lafarge Aggregates Ltd (2006). *A Guide to Mountsorrel Quarry*. [Online] Available at: <http://www.lafarge.co.uk/pdf/A_Guide_to_Mountsorrel_Quarry.pdf> [Access 8th November 2011]

Lafarge Aggregates Ltd (2012). *Mountsorrel Quarry: Past Present and Future*. [Online] Available at: <http://www.lafarge.co.uk/pdf/MSQ_Planning_Document_Rev_5.pdf> [Accessed 17th September 2012]

Lajtai, E. Z. (1969). Shear Strength of Weakness Planes in Rock. *International Journal of Rock Mechanics and Mining Sciences & Geomechanics Abstracts* 6(5): 499-515

Lilly, D., Tamir, R. and Cory, J. (2012). Blasting Related Aggregate Size Optimization. *International Society of Explosives Engineers*: 14 pages

Liu, Q., and Tran, H. 1996. "Comparing systems - Validation of Fragscan, WipFrag, and Split, Measurement of Blast Fragmentation", J. Franklin and T. Katsabanis eds, AA Balkema: 151-155

Lowndes, I. and Jeffry, K. (2007). *Optimising the Efficiency of Primary Aggregate Production*. [Online] Available at: <http://www.sustainableaggregates.com/library/docs/mist/l0022_t2b_oepap.pdf> [Accessed 25th September 2012]

Lowndes, I., Kingman, S., Silvester, S. A., Jones, A., Jackson, K., Docx, J., Gora, S., Steele, S., McCallum, K., Berry, J and Wooton, R. (2005). *Cleaner Quarries: Methods to Reduce the Environmental Impact of Quarry Operations.* The University of Nottingham Report No. MA 4/1/002

Lusk, B. T., Hoffman, J. and Wedding, W. C. (2011). Electronic Detonator and Modern Non-Electric Shocktube Detonator Accuracy. *International Society of Explosives Engineers*: 14 pages

Maerz, N. H. (1996). Image Sampling Techniques and Requirements for Automated Image Analysis of Rock Fragmentation. In: *Proceedings of the FRAGBLAST 5 Workshop on Measurement of Blast Fragmentation, Montreal, Canada, 23-24 August*: 115-120

Maerz, N. H. And Lusher, M. (2001). Measurement of Flat and Elongation of Coarse Aggregate Using Digital Image Processing. Paper No. 01-0177, Transportation Research Board 80th Annual Meeting, January 7–11, 2001: 14 pp.

Maerz, N. H., Palangio, T. C., and Franklin, J. A., 1996. WipFrag Image Based Granulometry System. In: *Proceedings of the FRAGBLAST 5 Workshop on Measurement of Blast Fragmentation, Montreal, Canada, 23-24 August*: 91-99

Meneisy, M. Y. and Miller, J. A. (1963). A Geochronological Study of the Crystalline Rocks of Charnwood Forest, England. *Geological Magazine* 100(6): 507-523

Migairou, P. -L. and Bickford, D. (2009). Case Studies Demonstrating Electronic Initiation Versatility. *International Society of Explosives Engineering*: 11 pages

Miller, J. A. and Podmore, J. S. (1961). Age of Mountsorrel Granite. *Geological Magazine* 98(1): 86-88

Mirabelli, L. J., Hissem, W. and Veltrop, G. (2009). Missouri Quarry Productivity Improvement – Casework. In: *14th PA Drilling and Blasting Conference*. Pennsylvania, USA 12-13 November 2009: 11 pages

Mitchell, C. (2009). Quarry fines and waste. In: *Quarries & Mines 2009.* Ten Alps: 63-67

Mitchell, C. J., Mitchell, P. and Pascoe, R. D. (2008). Quarry fines Minimisation: Can We Really Have 10mm Aggregate with No Fines? In: *Proceedings of the 14th Extractive industry geology conference.* EIG Conferences: 37-44

Mossman, B. T. and Churg, A. (1998). Mechanisms in the Pathenogenesis of Asbestosis and Silicosis. *American Journal of Respiratory and Critical Care Medicine* 157(5): 1666-1680

Nataraja, M.C., Dhang, N. and Gupta, A.P. (1999). Statistical Variations in Impact Resistance of Steel Fiber-Reinforced Concrete Subjected to Drop Weight Test. *Cement and Concrete Research* 29(7): 989-995

Paley, N. (2010). Testing Electronic Detonators to Increase SAG Mill Throughput at the Red Dog Mine. In: 2010 Volume I General Proceedings Collection. *International Society of Explosives Engineering*: 14 pages

Preece, D. Chung, S. (2005). The Effect of Electronic Detonators and Precise Detonation Timing on Blasting Induced Rock Movement. In: *Proceedings of the Annual Conference on Explosives and Blasting Technique* 31(1): 321-328

Primel, L. and Tourenq, C. (2000). *Aggregates: Geology, Prospection, Environment, Testing, Specifications, Extraction, Processing Plants, Equipments, Quality Control*. Rotterdam: A.A. Balkema

Rhodes, M. (1998) *Introduction to Particle Technology.* John Wiley and Sons, Chichester

Ritger, P. L. and N. A. Peppas (1987). A Simple Equation for Description of Solute Release I. Fickian and Non-Fickian Release from Non-Swellable Devices in the Form of Slabs, Spheres, Cylinders or Discs. *Journal of Controlled Release* 5(1): 23-36

Salinas, R. A., Raff, U. and Farfan, C. (2005). "Automated estimation of rock fragment distributions using computer vision and its application in mining." *Vision, Image and Signal Processing, IEE* Proceedings 152(1): 1-8

Sanchidrián, J. A., Segarra, P., Ouchterlony, F. and López, L. M. (2009). On the Accuracy of Fragment Size Measurement by Image Analysis in Combination with Some Distribution Functions. *Rock Mechanics and Rock Engineering* 42(1): 95-116

Scott, A., Segui, J. and Kanchibotla, S. S. (2000). Ore characterisation for mine to mill fragmentation. In: Proceedings 4th International Mining Geology Conference. Coolum, Australia, 14th-17th May 2000: 247-253

Sha, L. -K. and Chappell, B. W. (1999). Apatite Chemical Composition, Determined by Electron Microprobe and Laser-Ablation Inductively Coupled Plasma Mass Spectrometry, as a Probe into Granite Petrogenesis. *Geochimica et Cosmochimica Acta* 63(22): 3861-3881

Siddiqui F. I., Ali Shah, S. M. And Behan, M. Y. (2009). Measure of Size Distribution of Blasted Rock Using Digital Image Procesing. *Journal of King Abdulaziz University: Engineering Sciences* 20(2): 81-93

Split-Desktop (2012). Software, version 3.1. Split Engineering LLC, Tucson

Split-Engineering (2001). *Validation & Accuracy* [Online] Available at: <http://www.soft-blast.com/Split/Accuracy.htm> [Accessed 20 August 2012]

Tamir, R., Mirabelli, L. J. and McGough, J. P. (2012). Utilizing Continuous Photo Analysis of Fragmentation as a Blast / Crush Improvement Tool. In: *2012 Cambridge Business & Economics Conference June 27-28, 2012. Cambridge, UK*: 15 pages

Tavares, L. M. (1999). Energy Absorbed in Breakage of Single Particles in Drop Weight Testing. *Minerals Engineering* 12(1): 43-50

Tavares, L. M. (2007). Chapter 1 Breakage of Single Particles: Quasi-Static. *Handbook of Powder Technology*. M. G. Agba D. Salman and J. H. Michael, Elsevier Science B.V. 12: 3-68

Tavares, L. M. and das Neves, P. B. (2008). Microstructure of Quarry Rocks and Relationships to Particle Breakage and Crushing. *International Journal of Mineral Processing* 87(1–2): 28-41

Tavares, L.M. and King R.P. (2002). Modeling Of Particle Fracture by Repeated Impacts Using Continuum Damage Mechanics. *Powder Technology* 123(2-3): 138-146

Taylor, J. H. (1934). The Mountsorrel Granodiorite and Associated Igneous Rocks. *Geological Magazine* 71(1): 1-16

Teowee, G. (2010). Firing Reliability of Electronic Detonators. *International Society of Explosives Engineers*: 9 pages

Teowee, G. and Papillon, B. (2009). RF Susceptibility of Electronic Detonators. *International Society of Explosives Engineering*: 11 pages

Thermo ARL (1999). *Basics of X-ray Diffraction*. [Online] Available at: <http://www.vscht.cz/clab/rtg/dokumenty/thermo/xrd/Introduction%20to%20powder%20diffraction.pdf> [Accessed 14th September 2012]

Thermo Scientific (n.d.). *How XRF Works*. [Online] Available at: <http://www.niton.com/portable-xrf-technology/how-xrf-works.aspx?sflang=en> [Accessed 15th January 2012]

Thurley, M. J. (2011). Automated Online Measurement of Limestone Particle Size Distributions Using 3D Range Data. *Journal of Process Control* 21(2): 254-262

Workman, L. and Eloranta, A. (2009). Considerations on the Effect of Blasting on Downstream Performance. *International Society of Explosives Engineers*: 14 pages

Xia, K., Nasseri, M. H. B., Mohanty, B., Lu, F., Chen, R. and Luo, S. N. (2008). Effects of Microstructures on Dynamic Compression of Barre Granite. *International Journal of Rock Mechanics and Mining Sciences* 45(6): 879-887

Zhang, Z. X., Kou, S. Q., Jiang, L. G. and Lindqvist, P. A. (2000). Effects of Loading Rate on Rock Fracture: Fracture Characteristics and Energy Partitioning. *International Journal of Rock Mechanics and Mining Sciences* 37(5): 745-762

Appendix II – PSD and power data for EE-Quarry

BIF Ore

Table 17: Rock fracture data for BIF ore (Bailey, 2009).

Rock fracture data (t_{10} values)					
Value of t_{10}	t_{75}	t_{50}	t_{25}	t_4	t_2
10	2.4	3.0	4.9	23.7	59.8
20	4.7	6.0	9.6	45.0	87.9
30	7.2	9.2	14.7	62.8	96.4

Table 18: PSD, power draw and energy used per tonne of rock crushed for various CSS values for BIF ore calculated using JKSimMet.

Size distribution (cumulative % passing)											
Closed Side Setting (mm)		10	15	20	25	30	35	40	45	50	55
Screen size (mm)	150	100	100	100	100	100	100	100	100	100	100
	125	100	100	100	100	100	100	100	99.99	99.85	99.98
	90	100	100	100	100	100	99.99	99.95	99.51	98.39	96.67
	80	100	100	100	100	100	99.94	99.74	98.78	97	93.78
	75	100	100	100	100	100	99.86	99.46	98.12	95.93	92.21
	63	100	100	100	99.98	99.89	99.15	97.56	95.03	91.63	87.46
	50	100	100	100	99.65	98.36	95.54	91.59	87.05	81.77	76.27
	31.5	100	99.86	97.16	91.09	83.12	74.48	65.88	58.27	51.81	46.34
	25	100	98.37	91.2	81.29	70.46	60.74	52.54	45.92	40.57	36.3
	20	99.79	93.58	82.04	69.05	57.49	48.67	42.03	36.82	32.61	29.26
	14	94.82	78.47	61.22	48.66	40.28	34.2	29.74	26.28	23.46	21.19
	10	82.36	58.81	44.12	35.2	29.44	25.28	22.19	19.76	17.76	16.14
	6.3	55.48	37.13	28.2	22.88	19.37	16.78	14.81	13.25	11.94	10.87
	5	44.08	29.86	22.94	18.74	15.94	13.85	12.24	10.97	9.89	9.007
	4	35.67	24.61	19.12	15.73	13.45	11.73	10.4	9.344	8.439	7.7
	2	19.77	14.27	11.37	9.502	8.22	7.232	6.45	5.831	5.287	4.846
	1	11.86	8.795	7.117	6.008	5.244	4.643	4.155	3.772	3.424	3.145
	0	0	0	0	0	0	0	0	0	0	0
Power (kW)		248.4	213.9	192	176.1	164.1	154.3	146.4	139.6	133.7	128.4
Energy per tonne of material (kWh/t)		1.66	1.43	1.28	1.17	1.09	1.03	0.98	0.93	0.89	0.86
Energy for fines (kWh/t)		0.73	0.43	0.29	0.22	0.17	0.14	0.12	0.10	0.09	0.08

The size-distribution block carries the vertical label "Size distribution (cumulative % passing)".

Copper carbonatitie

Table 19: Rock fracture data for copper carbonatitie (Lowndes, 2005).

Rock fracture data (t_{10} values)					
Value of t_{10}	t_{75}	t_{50}	t_{25}	t_{4}	t_{2}
10	2.6	3.4	5.2	21.4	51.4
20	5.4	7.0	10.7	43.4	82.1
30	8.7	11.0	16.5	63.8	97.2

Table 20: PSD for various CSS values for copper carbonatite calculated using JKSimMet.

Size distribution (cumulative % passing)										
Closed Side Setting (mm)	10	15	20	25	30	35	40	45	50	55
Screen size (mm) / Size distribution (cumulative % passing)										
150	100	100	100	100	100	100	100	100	100	100
125	100	100	100	100	100	100	100	99.99	99.88	99.98
90	100	100	100	100	100	99.98	99.95	99.48	98.29	96.45
80	100	100	100	100	100	99.91	99.71	98.63	96.67	93.2
75	100	100	100	100	99.99	99.81	99.38	97.85	95.42	91.38
63	100	100	100	99.99	99.86	99	97.2	94.31	90.54	85.98
50	100	100	100	99.65	98.25	95.21	90.94	86.02	80.41	74.6
31.5	100	99.85	96.98	90.58	82.3	73.44	64.79	57.16	50.81	45.45
25	100	98.25	90.66	80.36	69.37	59.72	51.77	45.32	40.17	35.98
20	99.78	93.2	81.19	68.06	56.7	48.16	41.85	36.8	32.74	29.39
14	94.58	77.76	60.64	48.5	40.48	34.61	30.29	26.83	24.04	21.71
10	81.75	58.47	44.45	35.92	30.28	26.15	23.1	20.61	18.59	16.88
6.3	55.51	38.1	29.47	24.2	20.64	17.97	15.98	14.3	12.94	11.76
5	44.81	31.24	24.44	20.22	17.32	15.12	13.47	12.07	10.93	9.931
4	36.97	26.24	20.76	17.3	14.89	13.04	11.65	10.46	9.492	8.634
2	21.66	16.05	12.98	10.96	9.504	8.356	7.499	6.739	6.131	5.577
1	13.48	10.16	8.256	6.977	6.039	5.286	4.742	4.242	3.857	3.498
0	0	0	0	0	0	0	0	0	0	0

Talc de luzenac

Table 21: Rock fracture data for talc de luzenac (Lowndes, 2005).

Rock frackture data (t_{10} values)					
Value of t_{10}	t_{75}	t_{50}	t_{25}	t_4	t_2
10	3.0	3.6	5.4	19.9	50.0
20	5.8	7.3	11.0	39.6	82.0
30	8.8	11.2	16.8	57.5	98.4

Table 22: PSD for various CSS values for hard talc calculated using JKSimMet.

Size distribution (cumulative % passing)												
Closed Side Setting (mm)			10	15	20	25	30	35	40	45	50	55
Screen size (mm)	150	Size distribution (cumulative % passing)	100	100	100	100	100	100	100	100	100	100
	125		100	100	100	100	100	100	100	99.99	99.88	99.98
	90		100	100	100	100	100	99.99	99.95	99.48	98.3	96.47
	80		100	100	100	100	100	99.93	99.71	98.63	96.68	93.23
	75		100	100	100	100	99.99	99.83	99.38	97.85	95.42	91.4
	63		100	100	100	99.98	99.86	99	97.16	94.26	90.46	85.87
	50		100	100	100	99.62	98.18	95.05	90.63	85.6	79.87	73.94
	31.5		100	99.85	96.88	90.24	81.65	72.48	63.49	55.66	49.17	43.74
	25		100	98.19	90.35	79.67	68.28	58.34	50.12	43.57	38.38	34.22
	20		99.77	92.97	80.55	66.96	55.25	46.55	40.11	35.08	31.08	27.83
	14		94.42	77.07	59.45	47.05	38.98	33.2	28.94	25.62	22.95	20.73
	10		81.28	57.41	43.21	34.73	29.25	25.32	22.35	20	18.07	16.42
	6.3		54.63	37.23	28.86	23.81	20.41	17.89	15.91	14.31	12.97	11.79
	5		43.97	30.7	24.2	20.16	17.37	15.28	13.61	12.25	11.1	10.08
	4		36.33	26.04	20.82	17.48	15.13	13.35	11.91	10.73	9.731	8.838
	2		22.03	16.63	13.6	11.53	10.02	8.866	7.911	7.13	6.469	5.868
	1		14.49	11.1	9.119	7.743	6.736	5.974	5.332	4.809	4.367	3.953
	0		0	0	0	0	0	0	0	0	0	0

Lead-zinc ore

Table 23: Rock fracture data for lead-zinc ore (Lowndes, 2005).

Rock frackture data (t_{10} values)					
Value of t_{10}	t_{75}	t_{50}	t_{25}	t_4	t_2
10	3.2	3.9	5.5	23.9	53.2
20	6.5	7.9	11.2	44.8	84.5
30	10.0	12.1	17.0	62.6	99.1

Table 24: PSD for various CSS values for lead-zinc ore calculated using JKSimMet.

Size distribution (cumulative % passing)												
Closed Side Setting (mm)			10	15	20	25	30	35	40	45	50	55
Screen size (mm)	150	Size distribution (cumulative % passing)	100	100	100	100	100	100	100	100	100	100
	125		100	100	100	100	100	100	100	99.99	99.87	99.98
	90		100	100	100	100	100	99.98	99.95	99.48	98.3	96.49
	80		100	100	100	100	100	99.92	99.71	98.66	96.73	93.32
	75		100	100	100	100	99.99	99.83	99.39	97.91	95.53	91.56
	63		100	100	100	99.99	99.87	99.05	97.29	94.52	90.85	86.4
	50		100	100	100	99.66	98.32	95.41	91.27	86.54	81.08	75.42
	31.5		100	99.86	97.08	90.9	82.9	74.31	65.85	58.38	52.08	46.75
	25		100	98.32	90.98	81.01	70.32	60.87	53	46.61	41.42	37.21
	20		99.79	93.44	81.81	69.01	57.84	49.38	43.05	37.98	33.84	30.45
	14		94.76	78.43	61.64	49.58	41.54	35.61	31.19	27.67	24.79	22.42
	10		82.29	59.44	45.44	36.8	31.06	26.84	23.69	21.15	19.06	17.32
	6.3		56.48	38.98	30.16	24.74	21.09	18.36	16.3	14.62	13.21	12.03
	5		45.8	32	25.01	20.66	17.69	15.46	13.76	12.37	11.19	10.2
	4		37.91	26.92	21.27	17.71	15.26	13.4	11.97	10.8	9.792	8.946
	2		22.54	16.8	13.68	11.62	10.16	9.015	8.119	7.373	6.712	6.153
	1		14.63	11.29	9.356	8.019	7.044	6.26	5.641	5.121	4.653	4.261
	0		0	0	0	0	0	0	0	0	0	0

Limestone

Table 25: Rock fracture data for limestone (Bailey, 2009).

Rock fracture data (t_{10} values)					
Value of t_{10}	t_{75}	t_{50}	t_{25}	t_4	t_2
10	2.7	3.3	5.0	23.3	52.7
20	5.7	6.9	10.3	43.3	81.7
30	9.0	10.8	15.9	60.1	94.2

Table 26: PSD for various CSS values for limestone calculated using JKSimMet.

Size distribution (cumulative % passing)												
Closed Side Setting (mm)			10	15	20	25	30	35	40	45	50	55
Screen size (mm)	150	Size distribution (cumulative % passing)	100	100	100	100	100	100	100	100	100	100
	125		100	100	100	100	100	100	100	100	99.87	99.98
	90		100	100	100	100	100	99.98	99.95	99.95	98.28	96.45
	80		100	100	100	100	100	99.91	99.71	99.71	96.67	93.22
	75		100	100	100	100	99.99	99.81	99.38	99.38	95.43	91.41
	63		100	100	100	99.99	99.86	99.01	97.22	97.22	90.62	86.09
	50		100	100	100	99.66	98.28	95.3	91.08	91.08	80.7	74.95
	31.5		100	99.85	97.03	90.74	82.6	73.89	65.36	65.36	51.53	46.18
	25		100	98.27	90.8	80.67	69.84	60.32	52.45	52.45	40.9	36.68
	20		99.78	93.28	81.45	68.51	57.27	48.8	42.51	42.51	33.36	29.97
	14		94.63	78	61.05	48.99	40.97	35.07	30.7	30.7	24.36	21.99
	10		81.89	58.78	44.78	36.21	30.5	26.31	23.21	23.21	18.64	16.9
	6.3		55.69	38.2	29.44	24.09	20.48	17.78	15.76	15.76	12.73	11.55
	5		44.91	31.16	24.23	19.95	17.02	14.82	13.16	13.16	10.66	9.669
	4		36.94	26	20.42	16.93	14.51	12.69	11.3	11.3	9.202	8.359
	2		21.39	15.71	12.66	10.69	9.277	8.193	7.356	7.356	6.064	5.524
	1		13.48	10.23	8.41	7.197	6.297	5.594	5.047	5.047	4.182	3.804
	0		0	0	0	0	0	0	0	0	0	0

Porphyry copper

Table 27: Rock fracture data for lead-zinc ore (Bailey, 2009).

Rock fracture data (t_{10} values)					
Value of t_{10}	t_{75}	t_{50}	t_{25}	t_4	t_2
10	3.1	3.7	5.4	23.3	55.4
20	6.5	7.8	11.2	44.4	85.1
30	10.1	12.2	17.3	62.5	96.9

Table 28: PSD, power draw and energy used per tonne of rock crushed for various CSS values for porphyry copper calculated using JKSimMet.

Size distribution (cumulative % passing)												
Closed Side Setting (mm)			10	15	20	25	30	35	40	45	50	55
Screen size (mm)	150	Size distribution (cumulative % passing)	100	100	100	100	100	100	100	100	100	100
	125		100	100	100	100	100	100	100	99.99	99.86	99.98
	90		100	100	100	100	100	99.99	99.95	99.49	98.33	96.55
	80		100	100	100	100	100	99.93	99.72	98.7	96.82	93.48
	75		100	100	100	100	100	99.84	99.41	97.98	95.66	91.78
	63		100	100	100	99.99	99.88	99.08	97.38	94.68	91.09	86.73
	50		100	100	100	99.66	98.32	95.42	91.33	86.63	81.2	75.57
	31.5		100	99.86	97.09	90.9	82.84	74.17	65.61	58.04	51.66	46.27
	25		100	98.33	91.01	80.98	70.17	60.57	52.55	46.05	40.8	36.58
	20		99.79	93.46	81.8	68.85	57.5	48.88	42.44	37.31	33.16	29.8
	14		94.77	78.38	61.37	49.11	40.96	34.99	30.59	27.1	24.25	21.94
	10		82.3	59.17	44.94	36.23	30.53	26.35	23.25	20.76	18.69	17.01
	6.3		56.18	38.46	29.67	24.32	20.75	18.07	16.05	14.4	13	11.86
	5		45.33	31.5	24.59	20.31	17.42	15.22	13.55	12.18	11	10.05
	4		37.36	26.46	20.91	17.41	15.02	13.17	11.77	10.61	9.598	8.788
	2		22.15	16.5	13.42	11.38	9.952	8.804	7.93	7.191	6.526	6.004
	1		14.47	11.14	9.229	7.911	6.976	6.196	5.604	5.093	4.619	4.257
	0		0	0	0	0	0	0	0	0	0	0
Power (kW)			213.4	181.6	160.3	145.4	134.7	126.6	120.3	115.2	110.9	107.4
Energy per tonne of material (kWh/t)			1.42	1.21	1.07	0.97	0.90	0.84	0.80	0.77	0.74	0.72
Energy for fines (kWh/t)			0.64	0.38	0.26	0.20	0.16	0.13	0.11	0.09	0.08	0.07

Jaw crusher then variable CSS cone crusher – basalt

Table 29: Product PSDs for basalt going into a jaw crusher, then a cone crusher for various CSS settings. Power draw is shown and all values were simulated using JKSimMet; continued overleaf.

Value of t10	t75	t50	t25	t4	t2
10	2.8	4	5.5	22.2	51.4
20	5.6	7.2	10.7	43.4	80.8
30	8.9	11.3	16.4	60.7	93

Jaw crusher	
CSS (mm)	76
Feed rate ($t\,h^{-1}$)	333.3
Power draw (kW)	111.5

Cone crusher

CSS (mm)	16	18	20	22	24	26	28	30	32	34	36	38	40	42
Size (mm)	% retained													
460	0.000	0.000	0.000	0.000	0.000	0.000	0.000	0.000	0.000	0.000	0.000	0.000	0.000	0.000
290	0.000	0.000	0.000	0.000	0.000	0.000	0.000	0.000	0.000	0.000	0.000	0.000	0.000	0.000
230	0.000	0.000	0.000	0.000	0.000	0.000	0.000	0.000	0.000	0.000	0.000	0.000	0.000	0.000
145	0.000	0.000	0.000	0.000	0.000	0.000	0.000	0.000	0.000	0.000	0.000	0.000	0.000	0.000
115	0.000	0.000	0.000	0.000	0.000	0.000	0.000	0.000	0.000	0.000	0.000	0.000	0.000	0.000
87	0.000	0.000	0.000	0.000	0.000	0.000	0.000	0.000	0.001	0.001	0.001	0.001	0.005	0.014
50	0.001	0.001	0.001	0.008	0.086	0.288	0.639	1.146	1.799	2.579	3.465	4.439	5.483	6.581
45	0.000	0.000	0.000	0.078	0.314	0.660	1.081	1.548	2.039	2.534	3.024	3.500	3.958	4.396
37.5	0.008	0.165	0.658	1.305	2.310	3.377	4.450	5.492	6.482	7.410	8.270	9.061	9.783	10.440
31.5	0.224	0.929	1.936	3.273	4.442	5.576	6.635	7.603	8.476	9.215	9.786	10.200	10.480	10.640
26.5	1.571	2.914	4.265	5.536	6.690	7.713	8.602	9.360	9.994	10.460	10.730	10.830	10.800	10.670
22.4	3.492	5.071	6.532	7.808	8.847	9.544	9.935	10.070	9.991	9.798	9.567	9.314	9.051	8.783
19	5.666	7.185	8.422	9.378	10.030	10.290	10.240	9.978	9.557	9.099	8.686	8.314	7.976	7.670
16	8.168	9.403	10.010	10.100	9.849	9.475	9.043	8.584	8.120	7.684	7.299	6.959	6.658	6.394
13.2	11.030	11.700	11.600	11.000	10.180	9.443	8.795	8.223	7.717	7.271	6.881	6.540	6.244	5.987
11.2	11.090	10.600	9.991	9.356	8.748	8.223	7.776	7.398	7.078	6.802	6.561	6.350	6.166	6.007
9.5	10.960	9.955	9.109	8.389	7.774	7.258	6.827	6.468	6.169	5.913	5.688	5.492	5.320	5.171
8	8.737	7.817	7.074	6.472	5.979	5.566	5.220	4.931	4.692	4.487	4.308	4.151	4.015	3.896
6.3	9.472	8.366	7.491	6.799	6.242	5.774	5.382	5.055	4.782	4.549	4.343	4.163	4.005	3.867
4.75	6.924	6.019	5.298	4.726	4.265	3.877	3.551	3.279	3.051	2.856	2.685	2.535	2.403	2.288
3.35	6.296	5.516	4.894	4.401	4.002	3.666	3.383	3.145	2.947	2.776	2.626	2.494	2.379	2.278
2.36	3.802	3.282	2.866	2.534	2.264	2.036	1.843	1.680	1.544	1.427	1.323	1.231	1.151	1.080
1.18	4.677	4.090	3.617	3.236	2.924	2.659	2.433	2.242	2.079	1.938	1.812	1.700	1.600	1.511
0.6	2.798	2.505	2.262	2.057	1.883	1.728	1.593	1.473	1.366	1.271	1.185	1.106	1.035	0.970
0.3	1.982	1.771	1.587	1.428	1.288	1.166	1.058	0.963	0.880	0.807	0.741	0.682	0.630	0.583
0.15	1.256	1.100	0.971	0.862	0.770	0.690	0.622	0.562	0.511	0.466	0.426	0.390	0.358	0.330
0	1.849	1.612	1.416	1.252	1.114	0.994	0.891	0.802	0.725	0.657	0.597	0.544	0.496	0.453

CSS (mm)	44	46	48	50	52	54	56	58	60
Size (mm)	% retained								
460	0.000	0.000	0.000	0.000	0.000	0.000	0.000	0.000	0.000
290	0.000	0.000	0.000	0.000	0.000	0.000	0.000	0.000	0.000
230	0.000	0.000	0.000	0.000	0.000	0.000	0.000	0.000	0.000
145	0.000	0.000	0.000	0.000	0.000	0.000	0.000	0.000	0.000
115	0.001	0.001	0.001	0.001	0.003	0.006	0.011	0.018	0.028
87	0.065	0.144	0.250	0.382	0.538	0.715	0.913	1.127	1.356
50	7.681	8.782	9.866	10.920	11.940	12.910	13.840	14.720	15.560
45	4.810	5.197	5.536	5.821	6.055	6.242	6.384	6.484	6.547
37.5	11.030	11.550	11.970	12.280	12.490	12.620	12.680	12.670	12.610
31.5	10.690	10.650	10.570	10.470	10.360	10.240	10.110	9.978	9.846
26.5	10.440	10.160	9.885	9.635	9.408	9.201	9.013	8.842	8.686
22.4	8.516	8.254	8.013	7.797	7.602	7.428	7.272	7.135	7.013
19	7.392	7.139	6.912	6.709	6.528	6.368	6.226	6.102	5.994
16	6.161	5.956	5.773	5.609	5.463	5.333	5.219	5.118	5.031
13.2	5.764	5.571	5.399	5.245	5.108	4.986	4.878	4.784	4.702
11.2	5.870	5.751	5.646	5.552	5.469	5.395	5.330	5.273	5.224
9.5	5.041	4.929	4.828	4.738	4.657	4.585	4.521	4.465	4.416
8	3.794	3.705	3.627	3.556	3.493	3.437	3.388	3.345	3.308
6.3	3.747	3.642	3.549	3.464	3.389	3.321	3.261	3.208	3.161
4.75	2.189	2.102	2.024	1.955	1.892	1.837	1.787	1.744	1.706
3.35	2.190	2.113	2.044	1.983	1.928	1.878	1.835	1.796	1.762
2.36	1.019	0.964	0.916	0.872	0.833	0.797	0.766	0.738	0.713
1.18	1.432	1.361	1.297	1.239	1.185	1.137	1.093	1.053	1.018
0.6	0.911	0.857	0.809	0.764	0.723	0.687	0.653	0.623	0.596
0.3	0.541	0.504	0.471	0.440	0.413	0.388	0.366	0.346	0.328
0.15	0.305	0.283	0.262	0.244	0.227	0.213	0.199	0.187	0.177
0	0.416	0.382	0.352	0.324	0.299	0.277	0.257	0.239	0.223

CSS (mm)	Calculated Power (kW)
16	208.887
18	190.467
20	175.071
22	162.271
24	151.556
26	142.392
28	134.643
30	128.11
32	122.571
34	117.807
36	113.614
38	109.91
40	106.67
42	103.842
44	101.361
46	99.206
48	97.284
50	95.545

Jaw crusher then variable CSS cone crusher – BIF ore

Table 30: Product PSDs for BIF ore going into a jaw crusher, then a cone crusher for various CSS settings. Power draw is shown and all values were simulated using JKSimMet; continued overleaf.

Value of t10	t75	t50	t25	t4	t2
10	2.40	3.00	4.90	23.70	59.80
20	4.70	6.00	9.60	45.00	87.90
30	7.20	9.20	14.70	62.80	96.40

Jaw crusher	
CSS (mm)	76
Feed rate ($t\ h^{-1}$)	333.3
Power draw (kW)	107.345

Cone crusher

CSS (mm)	16	18	20	22	24	26	28	30	32	34	36	38	40	42
Size (mm)	% retained													
460	0.000	0.000	0.000	0.000	0.000	0.000	0.000	0.000	0.000	0.000	0.000	0.000	0.000	0.000
290	0.000	0.000	0.000	0.000	0.000	0.000	0.000	0.000	0.000	0.000	0.000	0.000	0.000	0.000
230	0.000	0.000	0.000	0.000	0.000	0.000	0.000	0.000	0.000	0.000	0.000	0.000	0.000	0.000
145	0.000	0.000	0.000	0.000	0.000	0.000	0.000	0.000	0.000	0.000	0.000	0.000	0.000	0.000
115	0.000	0.000	0.000	0.000	0.000	0.000	0.000	0.000	0.000	0.000	0.000	0.000	0.000	0.000
87	0.000	0.000	0.000	0.000	0.000	0.000	0.000	0.000	0.001	0.001	0.001	0.001	0.005	0.013
50	0.001	0.001	0.001	0.008	0.081	0.272	0.604	1.084	1.702	2.441	3.281	4.208	5.204	6.256
45	0.000	0.000	0.000	0.075	0.300	0.631	1.036	1.487	1.962	2.447	2.929	3.402	3.861	4.303
37.5	0.008	0.161	0.641	1.259	2.231	3.266	4.311	5.333	6.313	7.240	8.109	8.916	9.660	10.340
31.5	0.208	0.863	1.799	3.068	4.177	5.269	6.304	7.268	8.153	8.922	9.537	10.010	10.350	10.570
26.5	1.439	2.670	3.918	5.112	6.223	7.235	8.138	8.929	9.613	10.140	10.480	10.660	10.700	10.630
22.4	3.275	4.797	6.243	7.544	8.639	9.416	9.896	10.120	10.120	9.997	9.814	9.591	9.340	9.071
19	5.426	6.955	8.243	9.275	10.020	10.370	10.410	10.220	9.853	9.432	9.037	8.666	8.316	7.986
16	7.982	9.329	10.080	10.310	10.170	9.872	9.474	9.017	8.529	8.057	7.635	7.259	6.923	6.626
13.2	10.940	11.790	11.860	11.400	10.660	9.959	9.306	8.699	8.136	7.628	7.183	6.795	6.458	6.167
11.2	11.430	11.070	10.520	9.866	9.202	8.622	8.126	7.705	7.349	7.042	6.773	6.539	6.335	6.159
9.5	11.400	10.450	9.595	8.815	8.122	7.540	7.058	6.660	6.332	6.053	5.809	5.595	5.408	5.247
8	9.273	8.273	7.457	6.792	6.247	5.793	5.415	5.103	4.847	4.630	4.439	4.273	4.128	4.002
6.3	10.040	8.791	7.815	7.053	6.450	5.947	5.527	5.179	4.892	4.648	4.432	4.243	4.077	3.932
4.75	7.263	6.277	5.500	4.891	4.409	4.003	3.664	3.382	3.149	2.950	2.774	2.618	2.482	2.364
3.35	6.435	5.615	4.966	4.455	4.047	3.703	3.413	3.170	2.968	2.795	2.640	2.504	2.384	2.279
2.36	3.758	3.226	2.800	2.461	2.186	1.953	1.755	1.587	1.446	1.325	1.216	1.119	1.034	0.958
1.18	4.406	3.802	3.311	2.914	2.587	2.307	2.068	1.864	1.690	1.539	1.404	1.284	1.178	1.083
0.6	2.372	2.064	1.810	1.602	1.430	1.282	1.155	1.046	0.954	0.874	0.802	0.738	0.681	0.631
0.3	1.441	1.268	1.125	1.007	0.909	0.823	0.750	0.686	0.631	0.582	0.539	0.499	0.464	0.432
0.15	0.933	0.831	0.745	0.672	0.609	0.555	0.507	0.465	0.429	0.397	0.367	0.341	0.318	0.296
0	1.965	1.756	1.579	1.428	1.300	1.187	1.088	1.002	0.926	0.860	0.799	0.745	0.696	0.652

CSS (mm)	44	46	48	50	52	54	56	58	60
Size (mm)	% retained								
460	0.000	0.000	0.000	0.000	0.000	0.000	0.000	0.000	0.000
290	0.000	0.000	0.000	0.000	0.000	0.000	0.000	0.000	0.000
230	0.000	0.000	0.000	0.000	0.000	0.000	0.000	0.000	0.000
145	0.000	0.000	0.000	0.000	0.000	0.000	0.000	0.000	0.000
115	0.001	0.001	0.001	0.001	0.002	0.005	0.009	0.015	0.024
87	0.060	0.131	0.228	0.348	0.490	0.652	0.832	1.028	1.238
50	7.318	8.387	9.445	10.480	11.490	12.460	13.390	14.290	15.140
45	4.725	5.124	5.477	5.779	6.032	6.237	6.399	6.519	6.601
37.5	10.960	11.520	11.970	12.320	12.570	12.730	12.820	12.840	12.810
31.5	10.680	10.700	10.670	10.620	10.540	10.440	10.330	10.210	10.080
26.5	10.480	10.250	10.020	9.806	9.603	9.411	9.231	9.060	8.899
22.4	8.791	8.506	8.242	8.002	7.786	7.592	7.418	7.264	7.128
19	7.675	7.383	7.119	6.884	6.675	6.490	6.328	6.187	6.064
16	6.362	6.129	5.922	5.736	5.571	5.425	5.297	5.185	5.088
13.2	5.915	5.700	5.509	5.338	5.186	5.051	4.933	4.830	4.741
11.2	6.007	5.878	5.764	5.662	5.571	5.491	5.421	5.360	5.308
9.5	5.107	4.987	4.879	4.783	4.697	4.621	4.554	4.495	4.443
8	3.895	3.802	3.720	3.646	3.581	3.523	3.472	3.428	3.390
6.3	3.806	3.697	3.600	3.512	3.433	3.362	3.300	3.244	3.196
4.75	2.260	2.170	2.090	2.018	1.953	1.896	1.845	1.799	1.760
3.35	2.187	2.107	2.035	1.970	1.912	1.860	1.814	1.773	1.737
2.36	0.892	0.834	0.781	0.733	0.690	0.652	0.618	0.587	0.560
1.18	1.000	0.927	0.861	0.802	0.748	0.700	0.657	0.619	0.586
0.6	0.586	0.547	0.512	0.480	0.451	0.425	0.401	0.380	0.362
0.3	0.404	0.379	0.356	0.335	0.316	0.299	0.283	0.269	0.257
0.15	0.277	0.260	0.245	0.231	0.218	0.206	0.196	0.187	0.178
0	0.613	0.578	0.546	0.517	0.490	0.466	0.445	0.425	0.408

CSS (mm)	Calculated Power (kW)
16	202.078
18	184.731
20	170.201
22	158.126
24	148.033
26	139.373
28	132.038
30	125.852
32	120.615
34	116.105
36	112.115
38	108.573
40	105.465
42	102.747
44	100.362
46	98.291
48	96.443
50	94.771
52	93.279
54	91.952
56	90.769
58	89.731
60	88.824

Jaw crusher then variable CSS cone crusher – granite

Table 31: Product PSDs for granite going into a jaw crusher, then a cone crusher for various CSS settings. Power draw is shown and all values were simulated using JKSimMet; continued overleaf.

Value of t10	t75	t50	t25	t4	t2
10	2.964	3.749	5.671	21.53	53.2
20	5.828	7.491	11.36	42.73	82.41
30	8.929	11.51	17.29	61.81	94.94

Jaw crusher	
CSS (mm)	76
Feed rate ($t\,h^{-1}$)	333.3
Power draw (kW)	109.3

Cone crusher

CSS (mm)	16	18	20	22	24	26	28	30	32	34	36	38	40	42
Size (mm)	% retained													
460	0.000	0.000	0.000	0.000	0.000	0.000	0.000	0.000	0.000	0.000	0.000	0.000	0.000	0.000
290	0.000	0.000	0.000	0.000	0.000	0.000	0.000	0.000	0.000	0.000	0.000	0.000	0.000	0.000
230	0.000	0.000	0.000	0.000	0.000	0.000	0.000	0.000	0.000	0.000	0.000	0.000	0.000	0.000
145	0.000	0.000	0.000	0.000	0.000	0.000	0.000	0.000	0.000	0.000	0.000	0.000	0.000	0.000
115	0.000	0.000	0.000	0.000	0.000	0.000	0.000	0.000	0.000	0.000	0.000	0.000	0.000	0.000
87	0.000	0.000	0.000	0.000	0.000	0.000	0.000	0.000	0.001	0.001	0.001	0.001	0.005	0.014
50	0.001	0.001	0.001	0.008	0.086	0.289	0.642	1.151	1.807	2.591	3.483	4.464	5.516	6.625
45	0.000	0.000	0.000	0.078	0.314	0.660	1.081	1.549	2.040	2.537	3.030	3.510	3.972	4.415
37.5	0.008	0.165	0.658	1.302	2.304	3.368	4.439	5.482	6.474	7.407	8.275	9.074	9.804	10.470
31.5	0.221	0.917	1.911	3.236	4.396	5.526	6.585	7.558	8.440	9.190	9.775	10.210	10.500	10.670
26.5	1.543	2.862	4.192	5.449	6.599	7.625	8.523	9.293	9.943	10.420	10.710	10.830	10.810	10.690
22.4	3.460	5.038	6.509	7.805	8.868	9.591	10.000	10.160	10.090	9.903	9.671	9.412	9.138	8.855
19	5.650	7.186	8.450	9.434	10.110	10.390	10.360	10.100	9.686	9.224	8.802	8.415	8.061	7.735
16	8.201	9.478	10.120	10.240	10.000	9.630	9.186	8.706	8.215	7.752	7.341	6.979	6.659	6.377
13.2	11.110	11.830	11.760	11.180	10.360	9.604	8.932	8.329	7.788	7.308	6.890	6.527	6.213	5.941
11.2	11.250	10.760	10.140	9.469	8.817	8.257	7.783	7.383	7.048	6.762	6.513	6.296	6.109	5.949
9.5	11.120	10.100	9.218	8.457	7.801	7.254	6.802	6.429	6.123	5.864	5.637	5.440	5.268	5.120
8	8.818	7.842	7.058	6.428	5.919	5.495	5.145	4.858	4.623	4.424	4.251	4.100	3.970	3.857
6.3	9.497	8.323	7.408	6.697	6.136	5.669	5.282	4.963	4.700	4.477	4.282	4.110	3.961	3.831
4.75	6.733	5.818	5.102	4.545	4.105	3.738	3.432	3.179	2.970	2.792	2.635	2.497	2.377	2.272
3.35	6.008	5.260	4.671	4.210	3.843	3.534	3.274	3.057	2.875	2.719	2.581	2.459	2.351	2.257
2.36	3.556	3.077	2.695	2.390	2.142	1.931	1.752	1.600	1.471	1.359	1.259	1.169	1.090	1.020
1.18	4.482	3.929	3.478	3.107	2.799	2.532	2.301	2.102	1.931	1.780	1.644	1.523	1.414	1.316
0.6	2.785	2.471	2.208	1.986	1.797	1.631	1.487	1.362	1.252	1.155	1.068	0.990	0.919	0.856
0.3	1.895	1.683	1.505	1.354	1.225	1.112	1.014	0.928	0.854	0.788	0.729	0.676	0.628	0.585
0.15	1.250	1.110	0.992	0.893	0.808	0.734	0.670	0.613	0.565	0.521	0.482	0.447	0.416	0.388
0	2.414	2.147	1.922	1.732	1.569	1.428	1.304	1.197	1.103	1.020	0.946	0.879	0.819	0.765

CSS (mm)	44	46	48	50	52	54	56	58	60
Size (mm)	% retained								
460	0.000	0.000	0.000	0.000	0.000	0.000	0.000	0.000	0.000
290	0.000	0.000	0.000	0.000	0.000	0.000	0.000	0.000	0.000
230	0.000	0.000	0.000	0.000	0.000	0.000	0.000	0.000	0.000
145	0.000	0.000	0.000	0.000	0.000	0.000	0.000	0.000	0.000
115	0.001	0.001	0.001	0.001	0.002	0.005	0.009	0.016	0.025
87	0.065	0.142	0.246	0.376	0.529	0.703	0.897	1.108	1.333
50	7.738	8.856	9.958	11.030	12.070	13.070	14.020	14.930	15.790
45	4.834	5.227	5.572	5.862	6.102	6.293	6.439	6.543	6.608
37.5	11.070	11.600	12.030	12.340	12.560	12.700	12.760	12.760	12.700
31.5	10.730	10.700	10.620	10.530	10.420	10.300	10.160	10.030	9.889
26.5	10.470	10.200	9.928	9.680	9.451	9.241	9.047	8.868	8.704
22.4	8.570	8.289	8.029	7.796	7.586	7.399	7.232	7.084	6.954
19	7.436	7.160	6.913	6.692	6.497	6.324	6.172	6.039	5.924
16	6.130	5.914	5.721	5.548	5.396	5.261	5.142	5.038	4.949
13.2	5.708	5.508	5.330	5.172	5.031	4.907	4.798	4.703	4.620
11.2	5.811	5.694	5.591	5.499	5.418	5.346	5.284	5.230	5.183
9.5	4.993	4.883	4.785	4.698	4.620	4.550	4.489	4.435	4.388
8	3.761	3.678	3.605	3.539	3.481	3.430	3.385	3.345	3.311
6.3	3.718	3.620	3.533	3.454	3.383	3.319	3.263	3.213	3.169
4.75	2.180	2.100	2.029	1.965	1.907	1.855	1.809	1.769	1.733
3.35	2.174	2.101	2.035	1.976	1.922	1.875	1.832	1.794	1.760
2.36	0.957	0.902	0.852	0.806	0.764	0.727	0.693	0.663	0.636
1.18	1.229	1.151	1.081	1.016	0.958	0.905	0.857	0.814	0.776
0.6	0.800	0.749	0.703	0.662	0.624	0.589	0.559	0.531	0.506
0.3	0.547	0.513	0.482	0.453	0.428	0.404	0.383	0.365	0.348
0.15	0.363	0.340	0.320	0.301	0.284	0.269	0.255	0.243	0.232
0	0.717	0.674	0.635	0.599	0.567	0.538	0.511	0.488	0.467

CSS (mm)	Calculated Power (kW)
16	208.163
18	189.888
20	174.611
22	161.915
24	151.293
26	142.2
28	134.51
30	128.025
32	122.528
34	117.796
36	113.625
38	109.932
40	106.698
42	103.872
44	101.39
46	99.233
48	97.307
50	95.564
52	94.008
54	92.624
56	91.389
58	90.302
60	89.352

Jaw crusher then variable CSS cone crusher – hard talc

Table 32: Product PSDs for hard talc going into a jaw crusher, then a cone crusher for various CSS settings. Power draw is shown and all values were simulated using JKSimMet; continued overleaf.

Value of t10	t75	t50	t25	t4	t2
10	3.00	3.60	5.40	19.90	50.00
20	5.80	7.30	11.00	39.60	82.00
30	8.80	11.20	16.80	57.50	98.40

Jaw crusher	
CSS (mm)	76
Feed rate ($t\,h^{-1}$)	333.3
Power draw (kW)	111.4

Cone crusher

CSS (mm)	16	18	20	22	24	26	28	30	32	34	36	38	40	42
Size (mm)	% retained													
460	0	0	0	0	0	0	0	0	0	0	-	0	0	0
290	0	0	0	0	0	0	0	0	0	0	-	0	0	0
230	0	0	0	0	0	0	0	0	0	0	-	0	0	0
145	0	0	0	0	0	0	0	0	0	0	-	0	0	0
115	0	0	0	0	0	0	0	0	0	0	-	0	0	0
87	0	0	0	0	0	0	0	0	0.001	0.001	-	0.001	0.005	0.014
50	0.001	0.001	0.001	0.008	0.087	0.292	0.649	1.164	1.827	2.62	-	4.514	5.578	6.698
45	0	0	0	0.08	0.319	0.67	1.097	1.572	2.071	2.575	-	3.56	4.028	4.475
37.5	0.009	0.167	0.666	1.323	2.34	3.421	4.508	5.565	6.571	7.515	-	9.197	9.931	10.6
31.5	0.226	0.938	1.956	3.308	4.492	5.645	6.723	7.711	8.603	9.359	-	10.37	10.65	10.81
26.5	1.582	2.935	4.297	5.582	6.754	7.796	8.704	9.478	10.13	10.6	-	10.98	10.95	10.81
22.4	3.564	5.187	6.696	8.019	9.096	9.82	10.22	10.35	10.26	10.05	-	9.511	9.215	8.914
19	5.819	7.392	8.677	9.668	10.34	10.6	10.54	10.26	9.81	9.320	-	8.468	8.097	7.757
16	8.457	9.748	10.37	10.46	10.18	9.768	9.286	8.774	8.256	7.770	-	6.965	6.634	6.345
13.2	11.41	12.11	11.99	11.35	10.47	9.678	8.970	8.34	7.777	7.281	-	6.479	6.158	5.883
11.2	11.47	10.92	10.24	9.514	8.823	8.234	7.740	7.328	6.986	6.696	-	6.227	6.041	5.882
9.5	11.24	10.15	9.224	8.427	7.746	7.183	6.721	6.344	6.037	5.779	-	5.361	5.194	5.050
8	8.824	7.793	6.975	6.327	5.808	5.381	5.031	4.747	4.517	4.325	-	4.014	3.89	3.784
6.3	9.403	8.185	7.247	6.528	5.968	5.506	5.127	4.817	4.565	4.353	-	4.006	3.866	3.745
4.75	6.49	5.569	4.859	4.315	3.892	3.542	3.253	3.016	2.822	2.658	-	2.388	2.278	2.183
3.35	5.684	4.959	4.396	3.960	3.618	3.332	3.092	2.893	2.728	2.587	-	2.351	2.254	2.168
2.36	3.274	2.827	2.473	2.193	1.967	1.774	1.611	1.473	1.355	1.253	-	1.081	1.008	0.943
1.18	4.117	3.609	3.192	2.850	2.563	2.315	2.099	1.913	1.751	1.609	-	1.366	1.262	1.170
0.6	2.575	2.275	2.023	1.810	1.629	1.471	1.335	1.217	1.114	1.024	-	0.872	0.808	0.751
0.3	1.732	1.534	1.370	1.232	1.116	1.015	0.927	0.851	0.785	0.726	-	0.626	0.584	0.546
0.15	1.187	1.061	0.955	0.864	0.787	0.718	0.659	0.607	0.561	0.521	-	0.451	0.422	0.395
0	2.931	2.639	2.391	2.180	1.998	1.839	1.700	1.578	1.473	1.376	-	1.213	1.144	1.082

CSS (mm)	44	46	48	50	52	54	56	58	60
Size (mm)	% retained								
460	0	0	0	0	0	0	0	0	0
290	0	0	0	0	0	0	0	0	0
230	0	0	0	0	0	0	0	0	0
145	0	0	0	0	0	0	0	0	0
115	0.001	0.001	0.001	0.001	0.003	0.006	0.011	0.018	0.027
87	0.067	0.147	0.255	0.39	0.548	0.729	0.93	1.149	1.383
50	7.822	8.949	10.06	11.14	12.18	13.18	14.14	15.04	15.9
45	4.898	5.293	5.639	5.93	6.168	6.356	6.499	6.599	6.66
37.5	11.2	11.73	12.15	12.46	12.67	12.8	12.85	12.84	12.77
31.5	10.86	10.81	10.73	10.62	10.49	10.36	10.22	10.07	9.922
26.5	10.58	10.28	9.998	9.736	9.496	9.275	9.072	8.885	8.714
22.4	8.613	8.317	8.046	7.802	7.583	7.389	7.217	7.065	6.931
19	7.445	7.160	6.905	6.677	6.476	6.299	6.144	6.009	5.893
16	6.092	5.872	5.677	5.503	5.35	5.215	5.096	4.994	4.905
13.2	5.648	5.448	5.272	5.114	4.975	4.853	4.746	4.653	4.573
11.2	5.747	5.634	5.534	5.445	5.367	5.299	5.239	5.188	5.144
9.5	4.927	4.822	4.729	4.646	4.572	4.506	4.449	4.398	4.354
8	3.693	3.616	3.549	3.488	3.435	3.388	3.346	3.31	3.279
6.3	3.64	3.550	3.469	3.396	3.331	3.273	3.221	3.175	3.135
4.75	2.1	2.028	1.964	1.906	1.854	1.808	1.766	1.73	1.697
3.35	2.093	2.027	1.968	1.914	1.866	1.822	1.783	1.748	1.717
2.36	0.886	0.835	0.788	0.746	0.707	0.672	0.641	0.612	0.587
1.18	1.087	1.013	0.946	0.885	0.83	0.78	0.735	0.695	0.659
0.6	0.7	0.655	0.614	0.576	0.543	0.512	0.485	0.46	0.438
0.3	0.511	0.481	0.453	0.427	0.404	0.383	0.364	0.346	0.331
0.15	0.371	0.350	0.33	0.312	0.296	0.281	0.268	0.256	0.245
0	1.025	0.975	0.929	0.887	0.849	0.814	0.783	0.755	0.73

CSS (mm)	Calculated Power (kW)
16	211.169
18	192.324
20	176.602
22	163.556
24	152.654
26	143.34
28	135.475
30	128.853
32	123.246
34	118.424
36	114.178
38	110.423
40	107.138
42	104.269
44	101.751
46	99.563
48	97.61
50	95.844
52	94.266
54	92.864
56	91.613
58	90.512
60	89.549

Jaw crusher then variable CSS cone crusher – lead-zinc ore

Table 33: Product PSDs for lead-zinc ore going into a jaw crusher, then a cone crusher for various CSS settings. Power draw is shown and all values were simulated using JKSimMet; continued overleaf

Value of t10	t75	t50	t25	t4	t2
10	3.20	3.90	5.50	23.90	53.20
20	6.50	7.90	11.20	44.80	84.50
30	10.00	12.10	17.00	62.60	99.10

Jaw crusher	
CSS (mm)	76
Feed rate (t h^{-1})	333.3
Power draw (kW)	111.5

Cone crusher

CSS (mm)	16	18	20	22	24	26	28	30	32	34	36	38	40	42
Size (mm)	% retained													
460	0.000	0.000	0.000	0.000	0.000	0.000	0.000	0.000	0.000	0.000	0.000	0.000	0.000	0.000
290	0.000	0.000	0.000	0.000	0.000	0.000	0.000	0.000	0.000	0.000	0.000	0.000	0.000	0.000
230	0.000	0.000	0.000	0.000	0.000	0.000	0.000	0.000	0.000	0.000	0.000	0.000	0.000	0.000
145	0.000	0.000	0.000	0.000	0.000	0.000	0.000	0.000	0.000	0.000	0.000	0.000	0.000	0.000
115	0.000	0.000	0.000	0.000	0.000	0.000	0.000	0.000	0.000	0.000	0.000	0.000	0.000	0.000
87	0.000	0.000	0.000	0.000	0.000	0.000	0.000	0.000	0.001	0.001	0.001	0.001	0.005	0.014
50	0.001	0.001	0.001	0.008	0.082	0.275	0.610	1.095	1.719	2.464	3.313	4.246	5.247	6.302
45	0.000	0.000	0.000	0.076	0.304	0.639	1.048	1.502	1.980	2.464	2.944	3.412	3.864	4.296
37.5	0.008	0.162	0.645	1.275	2.259	3.305	4.359	5.384	6.360	7.279	8.133	8.922	9.644	10.300
31.5	0.217	0.901	1.877	3.181	4.321	5.432	6.474	7.431	8.300	9.041	9.622	10.050	10.350	10.530
26.5	1.520	2.820	4.130	5.368	6.500	7.512	8.399	9.162	9.808	10.290	10.580	10.710	10.710	10.600
22.4	3.390	4.933	6.371	7.639	8.683	9.398	9.816	9.979	9.935	9.772	9.566	9.334	9.087	8.831
19	5.527	7.030	8.268	9.237	9.912	10.200	10.190	9.959	9.568	9.134	8.740	8.380	8.052	7.751
16	8.009	9.263	9.904	10.040	9.840	9.503	9.097	8.656	8.203	7.774	7.393	7.055	6.756	6.491
13.2	10.880	11.600	11.560	11.020	10.240	9.532	8.901	8.337	7.832	7.384	6.991	6.649	6.350	6.091
11.2	11.070	10.630	10.070	9.451	8.851	8.330	7.885	7.506	7.185	6.909	6.666	6.453	6.268	6.108
9.5	11.000	10.040	9.216	8.501	7.883	7.363	6.929	6.566	6.264	6.006	5.779	5.580	5.406	5.255
8	8.840	7.928	7.188	6.584	6.088	5.671	5.322	5.031	4.788	4.581	4.400	4.241	4.103	3.982
6.3	9.619	8.506	7.624	6.925	6.362	5.889	5.492	5.159	4.882	4.645	4.436	4.252	4.091	3.950
4.75	7.044	6.131	5.402	4.822	4.354	3.960	3.628	3.350	3.119	2.920	2.745	2.592	2.457	2.340
3.35	6.346	5.555	4.923	4.420	4.014	3.670	3.381	3.139	2.935	2.761	2.607	2.472	2.354	2.250
2.36	3.741	3.211	2.786	2.446	2.170	1.936	1.738	1.572	1.432	1.311	1.205	1.111	1.028	0.956
1.18	4.395	3.793	3.308	2.918	2.598	2.327	2.096	1.901	1.736	1.594	1.467	1.355	1.256	1.169
0.6	2.469	2.177	1.937	1.741	1.577	1.435	1.312	1.206	1.114	1.034	0.961	0.896	0.837	0.785
0.3	1.703	1.526	1.376	1.248	1.137	1.040	0.955	0.881	0.815	0.757	0.704	0.657	0.614	0.576
0.15	1.212	1.087	0.981	0.890	0.811	0.742	0.681	0.628	0.581	0.539	0.502	0.468	0.438	0.410
0	3.011	2.701	2.436	2.209	2.013	1.841	1.690	1.557	1.441	1.337	1.243	1.159	1.083	1.015

CSS (mm)	44	46	48	50	52	54	56	58	60
Size (mm)	% retained								
460	0.000	0.000	0.000	0.000	0.000	0.000	0.000	0.000	0.000
290	0.000	0.000	0.000	0.000	0.000	0.000	0.000	0.000	0.000
230	0.000	0.000	0.000	0.000	0.000	0.000	0.000	0.000	0.000
145	0.000	0.000	0.000	0.000	0.000	0.000	0.000	0.000	0.000
115	0.001	0.001	0.001	0.001	0.003	0.006	0.011	0.019	0.029
87	0.063	0.139	0.242	0.371	0.522	0.695	0.886	1.095	1.317
50	7.361	8.422	9.468	10.490	11.470	12.420	13.320	14.180	14.990
45	4.707	5.093	5.432	5.719	5.957	6.148	6.295	6.402	6.471
37.5	10.900	11.430	11.860	12.170	12.400	12.540	12.610	12.620	12.570
31.5	10.600	10.580	10.520	10.440	10.350	10.240	10.120	10.000	9.878
26.5	10.400	10.140	9.888	9.655	9.442	9.246	9.067	8.902	8.751
22.4	8.572	8.316	8.080	7.866	7.674	7.502	7.349	7.213	7.092
19	7.474	7.222	6.994	6.790	6.609	6.448	6.306	6.182	6.073
16	6.258	6.053	5.869	5.704	5.557	5.427	5.312	5.211	5.123
13.2	5.866	5.672	5.498	5.343	5.205	5.082	4.974	4.879	4.796
11.2	5.969	5.849	5.743	5.649	5.564	5.490	5.424	5.367	5.317
9.5	5.123	5.009	4.907	4.815	4.733	4.660	4.596	4.539	4.489
8	3.878	3.788	3.709	3.637	3.573	3.517	3.467	3.424	3.386
6.3	3.828	3.721	3.626	3.540	3.462	3.393	3.332	3.278	3.230
4.75	2.238	2.149	2.070	1.999	1.935	1.878	1.828	1.784	1.745
3.35	2.159	2.081	2.011	1.947	1.891	1.841	1.796	1.756	1.722
2.36	0.893	0.838	0.788	0.743	0.703	0.667	0.635	0.607	0.582
1.18	1.092	1.024	0.963	0.908	0.858	0.813	0.773	0.737	0.705
0.6	0.738	0.695	0.657	0.622	0.590	0.561	0.535	0.512	0.490
0.3	0.541	0.510	0.482	0.456	0.433	0.411	0.392	0.375	0.359
0.15	0.386	0.363	0.343	0.325	0.308	0.293	0.279	0.267	0.256
0	0.954	0.899	0.848	0.803	0.761	0.723	0.689	0.658	0.631

CSS (mm)	Calculated Power (kW)
16	205.3
18	187.398
20	172.422
22	159.971
24	149.553
26	140.634
28	133.089
30	126.73
32	121.343
34	116.712
36	112.632
38	109.025
40	105.87
42	103.117
44	100.704
46	98.611
48	96.744
50	95.056
52	93.55
54	92.212
56	91.019
58	89.971
60	89.056

Jaw crusher then variable CSS cone crusher – porphyry copper

Table 34: Product PSDs for porphyry copper going into a jaw crusher, then a cone crusher for various CSS settings. Power draw is shown and all values were simulated using JKSimMet; continued overleaf.

Value of t10	t75	t50	t25	t4	t2
10	3.10	3.70	5.40	23.30	55.40
20	6.50	7.80	11.20	44.40	85.10
30	10.10	12.20	17.30	62.50	96.90

Jaw crusher	
CSS (mm)	76
Feed rate ($t\,h^{-1}$)	333.3
Power draw (kW)	109.1

Cone crusher

CSS (mm)	16	18	20	22	24	26	28	30	32	34	36	38	40	42
Size (mm)	% retained													
460	0.000	0.000	0.000	0.000	0.000	0.000	0.000	0.000	0.000	0.000	0.000	0.000	0.000	0.000
290	0.000	0.000	0.000	0.000	0.000	0.000	0.000	0.000	0.000	0.000	0.000	0.000	0.000	0.000
230	0.000	0.000	0.000	0.000	0.000	0.000	0.000	0.000	0.000	0.000	0.000	0.000	0.000	0.000
145	0.000	0.000	0.000	0.000	0.000	0.000	0.000	0.000	0.000	0.000	0.000	0.000	0.000	0.000
115	0.000	0.000	0.000	0.000	0.000	0.000	0.000	0.000	0.000	0.000	0.000	0.000	0.000	0.000
87	0.000	0.000	0.000	0.000	0.000	0.000	0.000	0.000	0.001	0.001	0.001	0.001	0.005	0.014
50	0.001	0.001	0.001	0.008	0.083	0.278	0.617	1.107	1.738	2.493	3.352	4.298	5.313	6.384
45	0.000	0.000	0.000	0.076	0.305	0.642	1.052	1.509	1.989	2.477	2.960	3.433	3.890	4.328
37.5	0.008	0.162	0.646	1.276	2.259	3.305	4.360	5.387	6.368	7.292	8.154	8.950	9.681	10.350
31.5	0.215	0.892	1.859	3.156	4.290	5.399	6.443	7.407	8.284	9.037	9.631	10.080	10.390	10.580
26.5	1.498	2.780	4.074	5.303	6.432	7.448	8.343	9.118	9.778	10.280	10.580	10.720	10.730	10.630
22.4	3.366	4.910	6.358	7.644	8.710	9.448	9.887	10.070	10.040	9.879	9.675	9.439	9.184	8.917
19	5.517	7.036	8.297	9.291	9.990	10.300	10.300	10.080	9.691	9.255	8.854	8.484	8.142	7.825
16	8.041	9.332	10.010	10.180	9.988	9.653	9.240	8.785	8.311	7.859	7.457	7.100	6.784	6.505
13.2	10.950	11.720	11.710	11.180	10.410	9.689	9.040	8.452	7.919	7.442	7.026	6.664	6.348	6.075
11.2	11.220	10.800	10.220	9.583	8.949	8.399	7.930	7.532	7.196	6.907	6.654	6.434	6.242	6.077
9.5	11.150	10.180	9.335	8.587	7.935	7.388	6.934	6.557	6.245	5.980	5.747	5.544	5.367	5.213
8	8.959	8.003	7.227	6.597	6.083	5.652	5.294	4.997	4.752	4.545	4.362	4.204	4.065	3.946
6.3	9.707	8.534	7.614	6.892	6.318	5.837	5.435	5.102	4.826	4.591	4.383	4.201	4.042	3.903
4.75	6.998	6.062	5.322	4.740	4.277	3.887	3.561	3.289	3.064	2.872	2.702	2.553	2.422	2.308
3.35	6.234	5.447	4.823	4.330	3.936	3.603	3.323	3.088	2.893	2.724	2.576	2.445	2.329	2.228
2.36	3.637	3.122	2.711	2.383	2.117	1.891	1.700	1.539	1.403	1.285	1.181	1.089	1.007	0.935
1.18	4.278	3.694	3.222	2.839	2.525	2.256	2.027	1.831	1.665	1.521	1.393	1.278	1.177	1.088
0.6	2.366	2.071	1.829	1.629	1.464	1.321	1.198	1.093	1.003	0.925	0.854	0.792	0.736	0.686
0.3	1.548	1.377	1.235	1.116	1.015	0.927	0.851	0.784	0.726	0.674	0.627	0.585	0.546	0.512
0.15	1.103	0.992	0.898	0.817	0.747	0.684	0.630	0.581	0.539	0.501	0.466	0.435	0.407	0.382
0	3.197	2.881	2.610	2.376	2.173	1.994	1.835	1.696	1.573	1.463	1.364	1.274	1.192	1.119

CSS (mm)	44	46	48	50	52	54	56	58	60
Size (mm)	% retained								
460	0.000	0.000	0.000	0.000	0.000	0.000	0.000	0.000	0.000
290	0.000	0.000	0.000	0.000	0.000	0.000	0.000	0.000	0.000
230	0.000	0.000	0.000	0.000	0.000	0.000	0.000	0.000	0.000
145	0.000	0.000	0.000	0.000	0.000	0.000	0.000	0.000	0.000
115	0.001	0.001	0.001	0.001	0.002	0.005	0.010	0.016	0.025
87	0.063	0.137	0.239	0.365	0.514	0.684	0.872	1.077	1.297
50	7.462	8.545	9.613	10.660	11.670	12.640	13.570	14.460	15.300
45	4.744	5.136	5.481	5.774	6.017	6.213	6.364	6.474	6.546
37.5	10.950	11.490	11.930	12.250	12.480	12.630	12.700	12.710	12.660
31.5	10.660	10.650	10.600	10.520	10.430	10.320	10.200	10.070	9.944
26.5	10.450	10.190	9.943	9.712	9.497	9.299	9.115	8.944	8.786
22.4	8.645	8.373	8.121	7.893	7.689	7.505	7.342	7.196	7.068
19	7.531	7.260	7.015	6.796	6.602	6.430	6.279	6.146	6.031
16	6.258	6.040	5.846	5.673	5.518	5.382	5.261	5.156	5.064
13.2	5.839	5.636	5.456	5.295	5.151	5.024	4.913	4.815	4.730
11.2	5.935	5.813	5.705	5.609	5.523	5.448	5.382	5.324	5.274
9.5	5.080	4.965	4.862	4.770	4.688	4.615	4.550	4.493	4.444
8	3.843	3.754	3.676	3.605	3.543	3.487	3.439	3.396	3.359
6.3	3.782	3.677	3.583	3.499	3.423	3.355	3.294	3.241	3.194
4.75	2.209	2.123	2.046	1.977	1.914	1.859	1.810	1.767	1.729
3.35	2.140	2.063	1.994	1.932	1.877	1.827	1.782	1.743	1.709
2.36	0.872	0.817	0.767	0.722	0.681	0.644	0.612	0.583	0.557
1.18	1.009	0.939	0.877	0.820	0.769	0.723	0.682	0.646	0.614
0.6	0.641	0.602	0.566	0.534	0.504	0.478	0.454	0.432	0.413
0.3	0.481	0.453	0.428	0.404	0.383	0.364	0.346	0.330	0.316
0.15	0.359	0.338	0.319	0.302	0.286	0.272	0.259	0.247	0.236
0	1.053	0.993	0.938	0.888	0.842	0.801	0.763	0.730	0.699

CSS (mm)	Calculated Power (kW)
16	204.933
18	187.14
20	172.25
22	159.874
24	149.52
26	140.649
28	133.141
30	126.81
32	121.446
34	116.83
36	112.757
38	109.15
40	105.99
42	103.229
44	100.806
46	98.702
48	96.825
50	95.127
52	93.61
54	92.262
56	91.06
58	90.003
60	89.08

Jaw crusher then variable CSS cone crusher –copper carbonatitie

Table 35: Product PSDs for copper carbonatitie going into a jaw crusher, then a cone crusher for various CSS settings. Power draw is shown and all values were simulated using JKSimMet; continued overleaf.

Value of t10	t75	t50	t25	t4	t2
10	2.60	3.40	5.20	21.40	51.40
20	5.40	7.00	10.70	43.40	82.10
30	8.70	11.00	16.50	63.80	97.20

Jaw crusher	
CSS (mm)	76
Feed rate ($t\,h^{-1}$)	333.3
Power draw (kW)	110.9

Cone crusher

CSS (mm)	16	18	20	22	24	26	28	30	32	34	36	38	40	42
Size (mm)	% retained													
460	0.000	0.000	0.000	0.000	0.000	0.000	0.000	0.000	0.000	0.000	0.000	0.000	0.000	0.000
290	0.000	0.000	0.000	0.000	0.000	0.000	0.000	0.000	0.000	0.000	0.000	0.000	0.000	0.000
230	0.000	0.000	0.000	0.000	0.000	0.000	0.000	0.000	0.000	0.000	0.000	0.000	0.000	0.000
145	0.000	0.000	0.000	0.000	0.000	0.000	0.000	0.000	0.000	0.000	0.000	0.000	0.000	0.000
115	0.000	0.000	0.000	0.000	0.000	0.000	0.000	0.000	0.000	0.000	0.000	0.000	0.000	0.000
87	0.000	0.000	0.000	0.000	0.000	0.000	0.000	0.000	0.001	0.001	0.001	0.001	0.005	0.014
50	0.001	0.001	0.001	0.008	0.087	0.290	0.644	1.155	1.813	2.600	3.494	4.477	5.531	6.641
45	0.000	0.000	0.000	0.079	0.315	0.663	1.085	1.555	2.047	2.545	3.037	3.516	3.977	4.417
37.5	0.008	0.166	0.659	1.308	2.314	3.383	4.457	5.501	6.494	7.426	8.290	9.085	9.811	10.470
31.5	0.223	0.928	1.933	3.269	4.437	5.573	6.634	7.606	8.483	9.227	9.803	10.220	10.510	10.670
26.5	1.565	2.903	4.250	5.519	6.674	7.701	8.594	9.357	9.996	10.470	10.740	10.840	10.820	10.680
22.4	3.494	5.078	6.549	7.837	8.887	9.595	9.993	10.130	10.050	9.859	9.624	9.365	9.094	8.817
19	5.684	7.215	8.465	9.433	10.090	10.360	10.310	10.050	9.626	9.161	8.741	8.360	8.013	7.697
16	8.225	9.481	10.100	10.200	9.949	9.569	9.127	8.655	8.176	7.726	7.328	6.977	6.667	6.394
13.2	11.120	11.810	11.720	11.120	10.280	9.535	8.871	8.283	7.759	7.297	6.894	6.543	6.239	5.975
11.2	11.220	10.720	10.100	9.442	8.812	8.269	7.809	7.420	7.093	6.813	6.568	6.355	6.170	6.010
9.5	11.070	10.050	9.182	8.440	7.805	7.274	6.833	6.467	6.165	5.907	5.682	5.485	5.313	5.165
8	8.816	7.865	7.101	6.485	5.985	5.566	5.219	4.931	4.694	4.493	4.316	4.163	4.029	3.914
6.3	9.519	8.378	7.484	6.782	6.223	5.756	5.366	5.042	4.774	4.546	4.344	4.168	4.014	3.879
4.75	6.877	5.966	5.247	4.682	4.231	3.852	3.535	3.272	3.053	2.865	2.700	2.555	2.428	2.317
3.35	6.188	5.422	4.815	4.336	3.951	3.626	3.353	3.124	2.932	2.767	2.621	2.493	2.380	2.280
2.36	3.683	3.180	2.778	2.456	2.194	1.972	1.783	1.623	1.488	1.371	1.267	1.174	1.092	1.020
1.18	4.547	3.968	3.496	3.112	2.794	2.521	2.287	2.086	1.915	1.764	1.630	1.510	1.403	1.307
0.6	2.732	2.421	2.161	1.944	1.759	1.598	1.458	1.335	1.229	1.134	1.049	0.973	0.904	0.843
0.3	1.842	1.635	1.460	1.311	1.184	1.072	0.975	0.891	0.817	0.752	0.694	0.642	0.595	0.554
0.15	1.182	1.044	0.929	0.832	0.749	0.678	0.616	0.562	0.515	0.474	0.437	0.404	0.375	0.348
0	2.008	1.773	1.577	1.412	1.272	1.150	1.045	0.954	0.874	0.805	0.742	0.686	0.636	0.591

CSS (mm)	44	46	48	50	52	54	56	58	60
Size (mm)	% retained								
460	0.000	0.000	0.000	0.000	0.000	0.000	0.000	0.000	0.000
290	0.000	0.000	0.000	0.000	0.000	0.000	0.000	0.000	0.000
230	0.000	0.000	0.000	0.000	0.000	0.000	0.000	0.000	0.000
145	0.000	0.000	0.000	0.000	0.000	0.000	0.000	0.000	0.000
115	0.001	0.001	0.001	0.001	0.003	0.006	0.010	0.017	0.027
87	0.066	0.144	0.251	0.383	0.540	0.718	0.916	1.131	1.361
50	7.753	8.868	9.965	11.030	12.060	13.050	14.000	14.890	15.740
45	4.834	5.224	5.566	5.853	6.089	6.276	6.419	6.520	6.583
37.5	11.060	11.590	12.010	12.320	12.530	12.660	12.720	12.710	12.650
31.5	10.720	10.680	10.600	10.500	10.380	10.260	10.130	9.992	9.855
26.5	10.460	10.180	9.902	9.650	9.420	9.210	9.017	8.841	8.681
22.4	8.540	8.268	8.017	7.792	7.590	7.409	7.247	7.105	6.979
19	7.408	7.144	6.907	6.696	6.508	6.342	6.195	6.067	5.955
16	6.154	5.944	5.756	5.588	5.439	5.307	5.190	5.088	4.999
13.2	5.747	5.550	5.376	5.220	5.081	4.958	4.850	4.755	4.672
11.2	5.873	5.755	5.651	5.559	5.476	5.403	5.340	5.284	5.236
9.5	5.036	4.925	4.825	4.736	4.657	4.586	4.523	4.468	4.419
8	3.814	3.729	3.653	3.585	3.524	3.470	3.423	3.382	3.346
6.3	3.762	3.660	3.569	3.487	3.413	3.347	3.288	3.235	3.189
4.75	2.221	2.137	2.061	1.994	1.933	1.878	1.830	1.787	1.750
3.35	2.193	2.117	2.049	1.987	1.932	1.882	1.838	1.799	1.764
2.36	0.956	0.900	0.849	0.803	0.762	0.724	0.690	0.660	0.634
1.18	1.222	1.147	1.078	1.015	0.959	0.908	0.861	0.820	0.783
0.6	0.787	0.738	0.693	0.652	0.614	0.581	0.550	0.523	0.499
0.3	0.516	0.483	0.453	0.426	0.401	0.378	0.358	0.340	0.324
0.15	0.325	0.304	0.285	0.268	0.252	0.238	0.226	0.214	0.204
0	0.552	0.516	0.484	0.455	0.428	0.404	0.383	0.364	0.346

CSS (mm)	Calculated Power (kW)
16	209.156
18	190.705
20	175.288
22	162.477
24	151.759
26	142.59
28	134.838
30	128.302
32	122.761
34	117.994
36	113.796
38	110.083
40	106.834
42	103.996
44	101.505
46	99.34
48	97.408
50	95.66
52	94.099
54	92.711
56	91.472
58	90.382
60	89.429

Variable CSS jaw crusher, screen, then cone crusher – basalt

Table 36: Product PSDs for basalt entering a jaw crusher with variable CSSs, then into a cone crusher or with a screen in between (denoted with (s)). Power data is shown and values were calculated using JKSimMet. CC = cone crusher product and U/S = screen undersize product.

Value of t10	t75	t50	t25	t4	t2
10	2.80	4.00	5.50	22.20	51.40
20	5.60	7.20	10.70	43.40	80.80
30	8.90	11.30	16.40	60.70	93.00

Cone crusher	
CSS (mm)	50
Feed rate (t h^{-1})	333.3
Power draw (kW)	109.31

Screen aperture (mm)	50

Jaw crusher

CSS (mm)	90	90 (s)		95	95 (s)		100	100 (s)		105	105 (s)		110	110 (s)		115	115 (s)		120	120 (s)	
		CC	U/S		CC	U/S		CC	U/S		CC	U/S		CC	U/S		CC	U/S		CC	U/S
Size (mm)	% retained																				
460	0.000	0.000	0.000	0.000	0.000	0.000	0.000	0.000	0.000	0.000	0.000	0.000	0.000	0.000	0.000	0.000	0.000	0.000	0.000	0.000	0.000
290	0.000	0.000	0.000	0.000	0.000	0.000	0.000	0.000	0.000	0.000	0.000	0.000	0.000	0.000	0.000	0.000	0.000	0.000	0.000	0.000	0.000
230	0.000	0.000	0.000	0.000	0.000	0.000	0.000	0.000	0.000	0.000	0.000	0.000	0.000	0.000	0.000	0.000	0.000	0.000	0.000	0.000	0.000
145	0.000	0.000	0.000	0.000	0.000	0.000	2.217	0.000	0.000	0.000	0.000	0.000	0.000	0.000	0.000	0.000	0.000	0.000	0.000	0.000	0.000
115	0.005	0.006	0.000	0.007	0.008	0.000	13.910	0.011	0.000	0.014	0.015	0.000	0.017	0.019	0.000	0.021	0.023	0.000	0.024	0.026	0.000
87	1.232	1.554	0.000	1.309	1.620	0.000	26.580	1.665	0.000	1.414	1.692	0.000	1.447	1.707	0.000	1.471	1.714	0.000	1.488	1.715	0.000
50	21.030	25.770	0.001	20.880	25.140	0.001	32.700	24.570	0.001	20.530	24.040	0.001	20.380	23.560	0.001	20.240	23.150	0.001	20.120	22.780	0.001
45	7.308	7.925	1.454	7.279	7.798	1.711	4.520	7.690	2.002	7.231	7.596	2.328	7.210	7.513	2.708	7.191	7.438	3.148	7.174	7.372	3.653
37.5	13.260	13.700	18.120	13.220	13.560	18.420	6.122	13.440	18.720	13.160	13.340	19.020	13.140	13.250	19.310	13.120	13.170	19.570	13.100	13.100	19.820
31.5	9.345	8.785	10.870	9.323	8.846	10.680	2.625	8.902	10.500	9.301	8.953	10.320	9.295	8.998	10.130	9.289	9.038	9.937	9.284	9.072	9.733
26.5	7.865	7.090	11.230	7.854	7.193	10.980	1.802	7.285	10.730	7.851	7.369	10.490	7.852	7.444	10.250	7.854	7.511	9.996	7.855	7.570	9.737
22.4	5.965	5.448	7.936	5.967	5.531	7.771	1.270	5.605	7.610	5.982	5.671	7.456	5.991	5.731	7.297	5.999	5.784	7.131	6.006	5.830	6.963
19	5.009	4.551	6.693	5.016	4.626	6.568	1.039	4.693	6.445	5.038	4.753	6.327	5.049	4.807	6.203	5.059	4.856	6.075	5.068	4.898	5.942
16	4.063	3.775	5.080	4.076	3.837	4.985	0.799	3.892	4.892	4.105	3.942	4.800	4.119	3.986	4.705	4.132	4.026	4.605	4.144	4.061	4.503
13.2	3.782	3.513	4.687	3.798	3.573	4.607	0.735	3.626	4.526	3.832	3.675	4.446	3.848	3.718	4.362	3.862	3.757	4.273	3.876	3.792	4.182
11.2	2.459	2.347	2.819	2.475	2.386	2.769	0.447	2.422	2.720	2.506	2.455	2.670	2.520	2.484	2.618	2.533	2.510	2.564	2.545	2.533	2.508
9.5	2.134	2.022	2.467	2.149	2.058	2.427	0.390	2.090	2.386	2.178	2.119	2.345	2.191	2.146	2.302	2.203	2.169	2.256	2.215	2.190	2.210
8	1.795	1.697	2.115	1.811	1.727	2.103	0.344	1.755	2.091	1.841	1.779	2.081	1.855	1.802	2.071	1.868	1.822	2.061	1.879	1.839	2.051
6.3	2.101	1.947	2.609	2.120	1.983	2.616	0.429	2.015	2.624	2.159	2.045	2.634	2.176	2.072	2.645	2.192	2.096	2.658	2.207	2.117	2.673
4.75	1.994	1.702	3.130	2.017	1.734	3.232	0.548	1.763	3.339	2.060	1.790	3.451	2.080	1.814	3.570	2.097	1.836	3.694	2.114	1.856	3.823
3.35	2.074	1.552	4.189	2.097	1.586	4.380	0.751	1.617	4.572	2.137	1.647	4.762	2.154	1.674	4.956	2.170	1.699	5.154	2.183	1.722	5.350
2.36	1.808	1.190	4.362	1.816	1.225	4.512	0.762	1.258	4.641	1.827	1.291	4.747	1.831	1.321	4.848	1.833	1.348	4.946	1.835	1.374	5.037
1.18	2.823	1.929	6.533	2.812	1.990	6.566	1.078	2.047	6.569	2.791	2.102	6.540	2.782	2.151	6.503	2.773	2.196	6.461	2.764	2.236	6.413
0.6	1.694	1.356	3.068	1.693	1.389	3.049	0.496	1.421	3.026	1.695	1.450	2.999	1.697	1.476	2.969	1.699	1.500	2.938	1.700	1.521	2.904
0.3	0.977	0.857	1.442	0.983	0.877	1.433	0.233	0.896	1.422	0.996	0.914	1.409	1.002	0.930	1.395	1.008	0.944	1.380	1.014	0.957	1.365
0.15	0.546	0.514	0.654	0.553	0.526	0.650	0.106	0.538	0.645	0.566	0.548	0.639	0.573	0.558	0.633	0.578	0.567	0.626	0.584	0.575	0.619
0	0.734	0.771	0.543	0.752	0.789	0.540	0.088	0.806	0.535	0.784	0.822	0.531	0.798	0.837	0.525	0.812	0.850	0.520	0.824	0.862	0.514

CSS (mm)	125	125 (s)		130	130 (s)		135	135 (s)		140	140 (s)	
		CC	U/S		CC	U/S		CC	U/S		CC	U/S
Size (mm)	% retained											
460	0.000	0.000	0.000	0.000	0.000	0.000	0.000	0.000	0.000	0.000	0.000	0.000
290	0.000	0.000	0.000	0.000	0.000	0.000	0.000	0.000	0.000	0.000	0.000	0.000
230	0.000	0.000	0.000	0.000	0.000	0.000	0.000	0.000	0.000	0.000	0.000	0.000
145	0.000	0.000	0.000	0.000	0.000	0.000	0.000	0.000	0.000	0.000	0.000	0.000
115	0.027	0.029	0.000	0.029	0.031	0.000	0.030	0.032	0.000	0.031	0.033	0.000
87	1.500	1.711	0.000	1.507	1.704	0.000	1.503	1.694	0.000	1.508	1.682	0.000
50	20.010	22.470	0.001	19.930	22.200	0.001	19.860	21.980	0.001	19.810	21.790	0.001
45	7.159	7.313	4.218	7.145	7.262	4.834	7.134	7.218	5.482	7.125	7.181	6.133
37.5	13.090	13.030	20.030	13.070	12.980	20.220	13.060	12.930	20.370	13.050	12.890	20.490
31.5	9.279	9.101	9.527	9.275	9.125	9.323	9.272	9.145	9.129	9.268	9.160	8.955
26.5	7.856	7.622	9.480	7.857	7.665	9.229	7.858	7.702	8.992	7.858	7.732	8.780
22.4	6.012	5.871	6.793	6.018	5.906	6.628	6.023	5.935	6.471	6.026	5.958	6.329
19	5.076	4.935	5.808	5.084	4.967	5.676	5.090	4.994	5.550	5.095	5.016	5.435
16	4.155	4.092	4.399	4.164	4.118	4.297	4.172	4.140	4.199	4.179	4.158	4.110
13.2	3.887	3.822	4.090	3.898	3.848	3.998	3.907	3.870	3.909	3.915	3.888	3.828
11.2	2.556	2.553	2.452	2.565	2.570	2.397	2.574	2.585	2.344	2.581	2.597	2.296
9.5	2.224	2.208	2.163	2.233	2.224	2.116	2.241	2.238	2.071	2.248	2.249	2.031
8	1.890	1.855	2.042	1.899	1.868	2.034	1.908	1.879	2.027	1.915	1.889	2.023
6.3	2.220	2.136	2.689	2.232	2.152	2.706	2.242	2.166	2.724	2.251	2.178	2.744
4.75	2.128	1.873	3.954	2.141	1.889	4.084	2.152	1.903	4.208	2.162	1.915	4.322
3.35	2.194	1.743	5.538	2.204	1.763	5.713	2.211	1.781	5.866	2.215	1.798	5.987
2.36	1.835	1.397	5.116	1.834	1.419	5.178	1.833	1.438	5.219	1.830	1.456	5.232
1.18	2.757	2.273	6.360	2.750	2.304	6.302	2.743	2.333	6.238	2.738	2.357	6.170
0.6	1.702	1.540	2.869	1.703	1.557	2.833	1.705	1.572	2.796	1.706	1.585	2.760
0.3	1.019	0.969	1.348	1.023	0.979	1.331	1.027	0.988	1.314	1.031	0.996	1.297
0.15	0.588	0.582	0.611	0.593	0.588	0.604	0.597	0.593	0.596	0.600	0.598	0.588
0	0.835	0.872	0.508	0.845	0.882	0.501	0.854	0.890	0.495	0.862	0.897	0.488

	Calculated power (kW)	
CSS (mm)	Jaw crusher	Cone crusher
90	152.766	114.659
90(s)	152.745	114.181
95	149.008	115.871
95(s)	148.897	115.416
100	145.438	116.977
100(s)	145.419	116.544
105	142.042	117.989
105(s)	142.023	117.574
110	138.847	118.92
110(s)	138.829	118.524
115	135.857	119.774
115(s)	135.84	119.393
120	133.072	120.549
120(s)	133.056	120.182
125	130.489	121.244
125(s)	130.474	120.89
130	128.108	121.858
130(s)	128.094	121.516
135	125.929	122.391
135(s)	125.915	122.059
140	123.951	122.842
140(s)	123.938	122.518

Variable CSS jaw crusher, screen, then cone crusher – BIF ore

Table 37: Product PSDs for BIF ore entering a jaw crusher with variable CSSs, then into a cone crusher or with a screen in between (denoted with (s)). Power data is shown and values were calculated using JKSimMet. CC = cone crusher product and U/S = screen undersize product; continued overleaf.

Value of t10	t75	t50	t25	t4	t2
10	2.40	3.00	4.90	23.70	59.80
20	4.70	6.00	9.60	45.00	87.90
30	7.20	9.20	14.70	62.80	96.40

Cone crusher	
CSS (mm)	50
Feed rate ($t\ h^{-1}$)	333.3
Power draw (kW)	

Screen aperture (mm)	50

Jaw crusher

CSS (mm)	90	90 (s)		95	95 (s)		100	100 (s)		105	105 (s)		110	110 (s)		115	115 (s)		120	120 (s)	
		CC	U/S		CC	U/S		CC	U/S		CC	U/S		CC	U/S		CC	U/S		CC	U/S
Size (mm)	% retained																				
460	0.000	0.000	0.000	0.000	0.000	0.000	0.000	0.000	0.000	0.000	0.000	0.000	0.000	0.000	0.000	0.000	0.000	0.000	0.000	0.000	0.000
290	0.000	0.000	0.000	0.000	0.000	0.000	0.000	0.000	0.000	0.000	0.000	0.000	0.000	0.000	0.000	0.000	0.000	0.000	0.000	0.000	0.000
230	0.000	0.000	0.000	0.000	0.000	0.000	0.000	0.000	0.000	0.000	0.000	0.000	0.000	0.000	0.000	0.000	0.000	0.000	0.000	0.000	0.000
145	0.000	0.000	0.000	0.000	0.000	0.000	0.000	0.000	0.000	0.000	0.000	0.000	0.000	0.000	0.000	0.000	0.000	0.000	0.000	0.000	0.000
115	0.005	0.005	0.000	0.007	0.007	0.000	0.009	0.011	0.000	0.013	0.015	0.000	0.017	0.019	0.000	0.022	0.024	0.000	0.026	0.028	0.000
87	1.146	1.435	0.000	1.223	1.500	0.000	1.280	1.542	0.000	1.317	1.563	0.000	1.342	1.572	0.000	1.360	1.573	0.000	1.372	1.568	0.000
50	20.090	24.430	0.001	19.930	23.810	0.001	19.770	23.280	0.001	19.620	22.810	0.001	19.490	22.380	0.001	19.370	22.010	0.001	19.270	21.670	0.001
45	7.335	7.858	1.569	7.305	7.741	1.858	7.275	7.637	2.177	7.243	7.542	2.522	7.214	7.456	2.928	7.187	7.379	3.409	7.164	7.310	3.970
37.5	13.440	13.750	19.240	13.400	13.630	19.510	13.360	13.510	19.760	13.320	13.400	20.020	13.280	13.300	20.270	13.240	13.220	20.500	13.210	13.140	20.710
31.5	9.816	9.333	11.270	9.794	9.396	11.030	9.780	9.450	10.810	9.772	9.497	10.610	9.766	9.540	10.400	9.761	9.577	10.170	9.755	9.609	9.936
26.5	8.325	7.647	11.470	8.315	7.751	11.180	8.314	7.844	10.900	8.319	7.927	10.650	8.325	8.002	10.390	8.330	8.070	10.120	8.335	8.130	9.832
22.4	6.364	5.905	8.098	6.371	5.986	7.945	6.381	6.056	7.803	6.394	6.119	7.674	6.407	6.175	7.540	6.419	6.226	7.398	6.430	6.272	7.250
19	5.312	4.897	6.785	5.324	4.969	6.683	5.338	5.033	6.588	5.354	5.089	6.501	5.369	5.140	6.410	5.383	5.187	6.312	5.395	5.228	6.210
16	4.306	3.976	5.470	4.324	4.036	5.426	4.341	4.089	5.384	4.360	4.137	5.343	4.377	4.181	5.300	4.393	4.220	5.252	4.407	4.256	5.202
13.2	3.970	3.640	5.140	3.990	3.698	5.121	4.010	3.750	5.101	4.029	3.797	5.079	4.048	3.840	5.054	4.065	3.879	5.027	4.080	3.914	4.996
11.2	2.652	2.404	3.564	2.669	2.444	3.577	2.685	2.480	3.587	2.700	2.514	3.592	2.714	2.544	3.595	2.727	2.572	3.598	2.739	2.596	3.599
9.5	2.283	2.050	3.161	2.299	2.086	3.179	2.313	2.118	3.194	2.327	2.148	3.203	2.340	2.176	3.212	2.351	2.201	3.219	2.362	2.223	3.226
8	1.958	1.730	2.835	1.971	1.762	2.861	1.984	1.791	2.882	1.996	1.818	2.895	2.007	1.843	2.907	2.017	1.866	2.919	2.026	1.886	2.928
6.3	2.261	1.975	3.389	2.277	2.013	3.424	2.292	2.049	3.451	2.306	2.081	3.468	2.318	2.111	3.484	2.330	2.139	3.498	2.340	2.164	3.510
4.75	2.058	1.774	3.193	2.071	1.811	3.217	2.083	1.845	3.231	2.094	1.877	3.231	2.103	1.906	3.228	2.112	1.933	3.223	2.121	1.957	3.214
3.35	1.916	1.651	2.979	1.926	1.687	2.985	1.936	1.720	2.980	1.944	1.751	2.962	1.953	1.779	2.941	1.960	1.805	2.917	1.967	1.828	2.891
2.36	1.397	1.216	2.123	1.405	1.242	2.124	1.412	1.265	2.121	1.420	1.287	2.114	1.426	1.307	2.105	1.433	1.325	2.095	1.439	1.341	2.085
1.18	1.787	1.534	2.810	1.802	1.568	2.846	1.817	1.600	2.877	1.831	1.630	2.902	1.844	1.657	2.927	1.857	1.683	2.953	1.868	1.706	2.977
0.6	1.096	0.898	1.918	1.107	0.922	1.954	1.117	0.944	1.984	1.126	0.966	2.007	1.135	0.986	2.029	1.143	1.004	2.051	1.151	1.020	2.073
0.3	0.769	0.616	1.414	0.776	0.632	1.441	0.782	0.648	1.463	0.788	0.663	1.480	0.793	0.677	1.496	0.798	0.690	1.513	0.803	0.701	1.529
0.15	0.530	0.415	1.013	0.533	0.426	1.033	0.537	0.437	1.049	0.540	0.447	1.060	0.543	0.456	1.072	0.546	0.465	1.084	0.549	0.473	1.095
0	1.182	0.858	2.562	1.184	0.881	2.610	1.186	0.903	2.650	1.189	0.924	2.681	1.191	0.943	2.710	1.193	0.961	2.740	1.194	0.977	2.769

CSS (mm)	125	125 (s)		130	130 (s)		135	135 (s)		140	140 (s)	
		CC	U/S		CC	U/S		CC	U/S		CC	U/S
Size (mm)	% retained											
460	0.000	0.000	0.000	0.000	0.000	0.000	0.000	0.000	0.000	0.000	0.000	0.000
290	0.000	0.000	0.000	0.000	0.000	0.000	0.000	0.000	0.000	0.000	0.000	0.000
230	0.000	0.000	0.000	0.000	0.000	0.000	0.000	0.000	0.000	0.000	0.000	0.000
145	0.000	0.000	0.000	0.000	0.000	0.000	0.000	0.000	0.000	0.000	0.000	0.000
115	0.029	0.032	0.000	0.032	0.035	0.000	0.034	0.037	0.000	0.035	0.037	0.000
87	1.378	1.560	0.000	1.381	1.550	0.000	1.381	1.539	0.000	1.379	1.527	0.000
50	19.180	21.380	0.001	19.100	21.130	0.001	19.040	20.930	0.001	18.990	20.760	0.001
45	7.143	7.250	4.606	7.126	7.198	5.304	7.113	7.156	6.034	7.103	7.121	6.749
37.5	13.190	13.070	20.880	13.160	13.010	21.020	13.150	12.960	21.120	13.140	12.920	21.210
31.5	9.751	9.637	9.693	9.747	9.660	9.454	9.745	9.678	9.231	9.742	9.691	9.038
26.5	8.339	8.183	9.544	8.342	8.227	9.264	8.345	8.263	9.004	8.347	8.291	8.779
22.4	6.440	6.312	7.100	6.448	6.345	6.952	6.455	6.373	6.813	6.460	6.395	6.689
19	5.406	5.265	6.104	5.416	5.296	5.998	5.424	5.322	5.897	5.430	5.342	5.806
16	4.420	4.287	5.149	4.431	4.313	5.094	4.440	4.336	5.041	4.447	4.354	4.989
13.2	4.094	3.945	4.963	4.106	3.971	4.928	4.115	3.994	4.892	4.123	4.012	4.854
11.2	2.749	2.618	3.598	2.758	2.637	3.595	2.766	2.654	3.588	2.771	2.667	3.577
9.5	2.371	2.243	3.230	2.379	2.261	3.232	2.386	2.275	3.230	2.391	2.288	3.223
8	2.034	1.904	2.936	2.041	1.920	2.940	2.046	1.934	2.939	2.050	1.945	2.932
6.3	2.349	2.186	3.519	2.357	2.205	3.523	2.363	2.222	3.521	2.368	2.235	3.511
4.75	2.127	1.978	3.201	2.133	1.997	3.183	2.138	2.013	3.160	2.141	2.027	3.132
3.35	1.972	1.848	2.862	1.978	1.866	2.831	1.982	1.881	2.798	1.985	1.894	2.765
2.36	1.444	1.356	2.074	1.449	1.368	2.062	1.453	1.379	2.050	1.456	1.388	2.039
1.18	1.879	1.727	3.000	1.888	1.745	3.019	1.896	1.762	3.033	1.902	1.776	3.039
0.6	1.158	1.035	2.093	1.164	1.049	2.110	1.169	1.060	2.123	1.173	1.070	2.130
0.3	0.807	0.712	1.543	0.810	0.721	1.556	0.814	0.729	1.566	0.816	0.736	1.571
0.15	0.551	0.480	1.106	0.553	0.486	1.115	0.555	0.491	1.122	0.556	0.496	1.125
0	1.195	0.992	2.795	1.196	1.005	2.818	1.197	1.016	2.836	1.197	1.026	2.845

	Calculated power (kW)	
CSS (mm)	Jaw crusher	Cone crusher
90	142.825	112.823
90(s)	142.806	112.331
95	139.561	113.974
95(s)	139.543	113.51
100	136.476	115.014
100(s)	136.459	114.574
105	133.546	115.955
105(s)	133.53	115.536
110	130.753	116.835
110(s)	130.737	116.435
115	128.109	117.653
115(s)	128.095	117.271
120	125.631	118.402
120(s)	125.617	118.036
125	123.331	119.077
125(s)	123.318	118.725
130	121.224	119.671
130(s)	121.211	119.332
135	119.317	120.181
135(s)	119.305	119.853
140	117.619	120.603
140(s)	117.608	120.283

Variable CSS jaw crusher, screen, then cone crusher – granite

Table 38: Product PSDs for granite entering a jaw crusher with variable CSSs, then into a cone crusher or with a screen in between (denoted with (s)). Power data is shown and values were calculated using JKSimMet. CC = cone crusher product and U/S = screen undersize product; continued overleaf.

Value of t10	t75	t50	t25	t4	t2
10	2.96	3.75	5.67	21.53	53.20
20	5.83	7.49	11.36	42.73	82.41
30	8.93	11.51	17.29	61.81	94.94

Cone crusher	
CSS (mm)	50
Feed rate (t h^{-1})	333.3
Power draw (kW)	

Screen aperture (mm)	50

Jaw crusher

CSS (mm)	90	90 (s)		95	95 (s)		100	100 (s)		105	105 (s)		110	110 (s)		115	115 (s)		120	120 (s)	
		CC	U/S		CC	U/S		CC	U/S		CC	U/S		CC	U/S		CC	U/S		CC	U/S
Size (mm)	% retained																				
460	0.000	0.000	0.000	0.000	0.000	0.000	0.000	0.000	0.000	0.000	0.000	0.000	0.000	0.000	0.000	0.000	0.000	0.000	0.000	0.000	0.000
290	0.000	0.000	0.000	0.000	0.000	0.000	0.000	0.000	0.000	0.000	0.000	0.000	0.000	0.000	0.000	0.000	0.000	0.000	0.000	0.000	0.000
230	0.000	0.000	0.000	0.000	0.000	0.000	0.000	0.000	0.000	0.000	0.000	0.000	0.000	0.000	0.000	0.000	0.000	0.000	0.000	0.000	0.000
145	0.000	0.000	0.000	0.000	0.000	0.000	0.000	0.000	0.000	0.000	0.000	0.000	0.000	0.000	0.000	0.000	0.000	0.000	0.000	0.000	0.000
115	0.005	0.005	0.000	0.007	0.007	0.000	0.009	0.010	0.000	0.013	0.014	0.000	0.017	0.019	0.000	0.021	0.023	0.000	0.025	0.027	0.000
87	1.239	1.541	0.000	1.320	1.610	0.000	1.380	1.657	0.000	1.421	1.681	0.000	1.450	1.693	0.000	1.471	1.697	0.000	1.484	1.695	0.000
50	21.180	25.600	0.001	20.990	24.960	0.001	20.810	24.400	0.001	20.630	23.890	0.001	20.460	23.440	0.001	20.320	23.040	0.001	20.190	22.690	0.001
45	7.422	7.975	2.093	7.393	7.861	2.467	7.365	7.761	2.874	7.339	7.673	3.311	7.314	7.592	3.816	7.292	7.520	4.404	7.272	7.454	5.075
37.5	13.440	13.800	18.380	13.400	13.680	18.530	13.370	13.570	18.670	13.340	13.480	18.810	13.310	13.400	18.930	13.290	13.320	19.010	13.270	13.250	19.060
31.5	9.465	9.107	10.240	9.445	9.163	9.965	9.432	9.211	9.715	9.424	9.252	9.489	9.419	9.288	9.254	9.413	9.320	9.006	9.408	9.346	8.749
26.5	7.941	7.385	10.500	7.932	7.480	10.180	7.929	7.563	9.887	7.932	7.636	9.614	7.936	7.702	9.334	7.939	7.760	9.041	7.941	7.812	8.743
22.4	5.882	5.525	7.260	5.887	5.596	7.090	5.895	5.656	6.935	5.906	5.709	6.796	5.916	5.757	6.653	5.926	5.800	6.503	5.935	5.837	6.350
19	4.904	4.565	6.125	4.914	4.629	6.009	4.926	4.684	5.902	4.939	4.733	5.807	4.952	4.778	5.708	4.963	4.817	5.604	4.974	4.853	5.496
16	3.906	3.627	4.931	3.922	3.679	4.882	3.938	3.726	4.837	3.954	3.768	4.795	3.970	3.806	4.752	3.984	3.840	4.706	3.997	3.870	4.658
13.2	3.616	3.323	4.703	3.635	3.375	4.682	3.653	3.421	4.662	3.672	3.463	4.642	3.689	3.502	4.621	3.705	3.537	4.597	3.719	3.568	4.572
11.2	2.392	2.148	3.350	2.408	2.185	3.370	2.424	2.218	3.388	2.438	2.249	3.402	2.452	2.277	3.416	2.465	2.303	3.429	2.477	2.326	3.442
9.5	2.088	1.850	3.045	2.103	1.884	3.072	2.117	1.915	3.096	2.131	1.943	3.116	2.144	1.969	3.136	2.156	1.993	3.155	2.166	2.015	3.173
8	1.808	1.556	2.847	1.822	1.588	2.887	1.835	1.617	2.920	1.847	1.644	2.947	1.859	1.669	2.973	1.869	1.692	2.998	1.879	1.712	3.022
6.3	2.137	1.808	3.530	2.154	1.847	3.584	2.170	1.883	3.630	2.185	1.918	3.664	2.199	1.949	3.698	2.211	1.978	3.730	2.222	2.004	3.760
4.75	2.018	1.669	3.515	2.033	1.710	3.557	2.047	1.748	3.585	2.059	1.785	3.597	2.071	1.818	3.605	2.081	1.849	3.609	2.091	1.877	3.610
3.35	1.985	1.650	3.429	1.998	1.694	3.442	2.011	1.735	3.440	2.023	1.773	3.422	2.034	1.809	3.399	2.044	1.842	3.373	2.054	1.872	3.343
2.36	1.551	1.324	2.522	1.563	1.360	2.523	1.576	1.392	2.518	1.588	1.423	2.506	1.600	1.452	2.493	1.611	1.478	2.478	1.622	1.502	2.463
1.18	2.194	1.900	3.444	2.220	1.950	3.485	2.246	1.997	3.521	2.271	2.041	3.549	2.294	2.082	3.577	2.316	2.119	3.604	2.336	2.153	3.630
0.6	1.446	1.211	2.461	1.463	1.244	2.506	1.479	1.274	2.542	1.493	1.303	2.569	1.507	1.329	2.596	1.520	1.354	2.622	1.531	1.376	2.647
0.3	1.024	0.823	1.900	1.033	0.846	1.935	1.042	0.866	1.963	1.049	0.886	1.984	1.057	0.904	2.005	1.064	0.921	2.025	1.070	0.936	2.044
0.15	0.708	0.544	1.427	0.712	0.559	1.453	0.716	0.573	1.474	0.719	0.586	1.490	0.723	0.598	1.505	0.726	0.609	1.520	0.729	0.619	1.535
0	1.654	1.063	4.299	1.646	1.091	4.377	1.639	1.118	4.441	1.632	1.144	4.489	1.625	1.167	4.534	1.618	1.189	4.580	1.612	1.208	4.623

CSS (mm)	125	125 (s)		130	130 (s)		135	135 (s)		140	140 (s)	
		CC	U/S		CC	U/S		CC	U/S		CC	U/S
Size (mm)	% retained											
460	0.000	0.000	0.000	0.000	0.000	0.000	0.000	0.000	0.000	0.000	0.000	0.000
290	0.000	0.000	0.000	0.000	0.000	0.000	0.000	0.000	0.000	0.000	0.000	0.000
230	0.000	0.000	0.000	0.000	0.000	0.000	0.000	0.000	0.000	0.000	0.000	0.000
145	0.000	0.000	0.000	0.000	0.000	0.000	0.000	0.000	0.000	0.000	0.000	0.000
115	0.028	0.031	0.000	0.031	0.033	0.000	0.032	0.035	0.000	0.033	0.036	0.000
87	1.493	1.688	0.000	1.496	1.679	0.000	1.496	1.667	0.000	1.493	1.654	0.000
50	20.090	22.380	0.001	20.000	22.120	0.001	19.920	21.900	0.001	19.870	21.730	0.001
45	7.254	7.397	5.822	7.238	7.347	6.628	7.225	7.304	7.458	7.215	7.268	8.266
37.5	13.250	13.190	19.080	13.230	13.130	19.050	13.220	13.090	19.010	13.200	13.050	18.960
31.5	9.403	9.368	8.491	9.399	9.386	8.240	9.395	9.399	8.009	9.391	9.407	7.811
26.5	7.943	7.856	8.446	7.945	7.893	8.160	7.946	7.923	7.898	7.947	7.946	7.672
22.4	5.942	5.870	6.196	5.949	5.898	6.047	5.954	5.920	5.908	5.958	5.938	5.788
19	4.983	4.884	5.387	4.992	4.910	5.280	4.998	4.932	5.179	5.004	4.949	5.089
16	4.008	3.897	4.608	4.018	3.920	4.558	4.026	3.940	4.509	4.033	3.956	4.464
13.2	3.732	3.595	4.544	3.743	3.619	4.516	3.752	3.639	4.486	3.759	3.656	4.456
11.2	2.487	2.346	3.452	2.496	2.364	3.460	2.503	2.380	3.464	2.509	2.393	3.463
9.5	2.176	2.034	3.190	2.184	2.051	3.203	2.191	2.065	3.212	2.197	2.078	3.215
8	1.887	1.731	3.043	1.894	1.747	3.060	1.900	1.762	3.071	1.905	1.774	3.073
6.3	2.232	2.028	3.785	2.241	2.049	3.805	2.248	2.067	3.816	2.254	2.083	3.816
4.75	2.099	1.902	3.606	2.107	1.925	3.595	2.113	1.944	3.576	2.117	1.962	3.547
3.35	2.062	1.898	3.311	2.070	1.922	3.276	2.077	1.943	3.238	2.083	1.960	3.198
2.36	1.631	1.523	2.446	1.640	1.542	2.430	1.648	1.558	2.413	1.655	1.572	2.397
1.18	2.354	2.183	3.653	2.370	2.210	3.672	2.384	2.234	3.684	2.395	2.254	3.688
0.6	1.541	1.396	2.669	1.550	1.414	2.688	1.558	1.429	2.701	1.564	1.443	2.706
0.3	1.075	0.949	2.061	1.080	0.962	2.076	1.084	0.972	2.086	1.087	0.981	2.090
0.15	0.731	0.628	1.548	0.733	0.636	1.558	0.735	0.643	1.566	0.736	0.649	1.569
0	1.606	1.226	4.663	1.600	1.241	4.695	1.594	1.255	4.718	1.589	1.267	4.728

	Calculated power (kW)	
CSS (mm)	Jaw crusher	Cone crusher
90	147.303	114.815
90(s)	147.283	114.348
95	143.794	116.012
95(s)	143.775	115.571
100	140.477	117.094
100(s)	140.458	116.674
105	137.322	118.076
105(s)	137.305	117.676
110	134.324	118.991
110(s)	134.307	118.608
115	131.494	119.837
115(s)	131.479	119.471
120	128.845	120.61
120(s)	128.831	120.259
125	126.388	121.305
125(s)	126.374	120.966
130	124.13	121.917
130(s)	124.116	121.59
135	122.078	122.444
135(s)	122.065	122.126
140	120.236	122.882
140(s)	120.224	122.572

Variable CSS jaw crusher, screen, then cone crusher – hard talc

Table 39: Product PSDs for hard talc entering a jaw crusher with variable CSSs, then into a cone crusher or with a screen in between (denoted with (s)). Power data is shown and values were calculated using JKSimMet. CC = cone crusher product and U/S = screen undersize product; continued overleaf.

Value of t10	t75	t50	t25	t4	t2
10	3.00	3.60	5.40	19.90	50.00
20	5.80	7.30	11.00	39.60	82.00
30	8.80	11.20	16.80	57.50	98.40

Cone crusher	
CSS (mm)	50
Feed rate ($t\ h^{-1}$)	333.3
Power draw (kW)	

Screen aperture (mm)	50

Jaw crusher

CSS (mm)	90	90 (s)		95	95 (s)		100	100 (s)		105	105 (s)		110	110 (s)		115	115 (s)		120	120 (s)	
		CC	U/S		CC	U/S		CC	U/S		CC	U/S		CC	U/S		CC	U/S		CC	U/S
Size (mm)	% retained																				
460	0.000	0.000	0.000	0.000	0.000	0.000	0.000	0.000	0.000	0.000	0.000	0.000	0.000	0.000	0.000	0.000	0.000	0.000	0.000	0.000	0.000
290	0.000	0.000	0.000	0.000	0.000	0.000	0.000	0.000	0.000	0.000	0.000	0.000	0.000	0.000	0.000	0.000	0.000	0.000	0.000	0.000	0.000
230	0.000	0.000	0.000	0.000	0.000	0.000	0.000	0.000	0.000	0.000	0.000	0.000	0.000	0.000	0.000	0.000	0.000	0.000	0.000	0.000	0.000
145	0.000	0.000	0.000	0.000	0.000	0.000	0.000	0.000	0.000	0.000	0.000	0.000	0.000	0.000	0.000	0.000	0.000	0.000	0.000	0.000	0.000
115	0.005	0.006	0.000	0.007	0.008	0.000	0.010	0.011	0.000	0.014	0.015	0.000	0.018	0.019	0.000	0.021	0.023	0.000	0.025	0.027	0.000
87	1.263	1.567	0.000	1.341	1.632	0.000	1.400	1.676	0.000	1.440	1.700	0.000	1.469	1.712	0.000	1.489	1.716	0.000	1.504	1.715	0.000
50	21.520	25.960	0.001	21.370	25.370	0.001	21.220	24.850	0.001	21.080	24.390	0.001	20.950	23.970	0.001	20.840	23.610	0.001	20.740	23.290	0.001
45	7.611	8.210	2.139	7.590	8.101	2.516	7.568	8.004	2.932	7.547	7.917	3.381	7.527	7.839	3.897	7.509	7.768	4.492	7.492	7.705	5.164
37.5	13.720	14.130	18.320	13.690	14.010	18.480	13.660	13.910	18.620	13.640	13.820	18.760	13.620	13.740	18.870	13.600	13.670	18.960	13.580	13.600	19.010
31.5	9.658	9.358	10.160	9.640	9.410	9.899	9.627	9.453	9.651	9.619	9.490	9.423	9.612	9.521	9.188	9.606	9.548	8.942	9.600	9.571	8.691
26.5	8.059	7.542	10.430	8.049	7.631	10.120	8.044	7.708	9.823	8.045	7.775	9.548	8.046	7.836	9.267	8.047	7.889	8.978	8.047	7.935	8.685
22.4	5.878	5.532	7.218	5.878	5.594	7.048	5.882	5.649	6.891	5.888	5.696	6.748	5.893	5.738	6.602	5.899	5.775	6.451	5.903	5.808	6.298
19	4.859	4.518	6.096	4.864	4.575	5.978	4.871	4.625	5.869	4.879	4.669	5.770	4.887	4.708	5.668	4.895	4.743	5.561	4.901	4.774	5.452
16	3.793	3.502	4.887	3.803	3.548	4.834	3.813	3.589	4.785	3.824	3.626	4.739	3.834	3.660	4.691	3.844	3.690	4.640	3.852	3.716	4.588
13.2	3.478	3.168	4.656	3.490	3.214	4.631	3.502	3.255	4.605	3.515	3.293	4.580	3.527	3.327	4.553	3.538	3.358	4.525	3.547	3.385	4.494
11.2	2.251	1.995	3.283	2.262	2.028	3.297	2.273	2.058	3.309	2.284	2.086	3.319	2.294	2.111	3.327	2.303	2.134	3.335	2.312	2.154	3.342
9.5	1.958	1.709	2.982	1.968	1.739	3.004	1.979	1.767	3.023	1.989	1.793	3.039	1.998	1.817	3.054	2.007	1.838	3.068	2.015	1.858	3.081
8	1.675	1.419	2.757	1.685	1.448	2.790	1.696	1.475	2.818	1.705	1.500	2.841	1.714	1.523	2.862	1.723	1.544	2.882	1.730	1.563	2.900
6.3	1.977	1.645	3.411	1.990	1.681	3.458	2.002	1.715	3.497	2.015	1.747	3.527	2.026	1.776	3.555	2.036	1.803	3.581	2.045	1.827	3.604
4.75	1.862	1.522	3.346	1.875	1.561	3.380	1.887	1.598	3.401	1.899	1.634	3.408	1.910	1.666	3.411	1.920	1.696	3.411	1.929	1.723	3.407
3.35	1.847	1.532	3.231	1.860	1.574	3.237	1.872	1.614	3.230	1.884	1.651	3.208	1.895	1.686	3.182	1.905	1.717	3.153	1.914	1.746	3.122
2.36	1.451	1.243	2.359	1.462	1.276	2.357	1.473	1.306	2.349	1.484	1.334	2.336	1.495	1.359	2.322	1.504	1.383	2.307	1.513	1.404	2.291
1.18	2.023	1.738	3.256	2.045	1.781	3.298	2.066	1.822	3.334	2.087	1.861	3.365	2.106	1.896	3.396	2.125	1.928	3.426	2.141	1.958	3.454
0.6	1.339	1.094	2.422	1.354	1.125	2.469	1.368	1.154	2.508	1.382	1.181	2.539	1.394	1.207	2.569	1.406	1.230	2.598	1.416	1.251	2.626
0.3	0.995	0.781	1.951	1.004	0.803	1.989	1.013	0.825	2.021	1.020	0.845	2.046	1.028	0.863	2.070	1.034	0.880	2.094	1.041	0.895	2.116
0.15	0.726	0.547	1.530	0.731	0.563	1.559	0.735	0.578	1.584	0.739	0.592	1.604	0.743	0.605	1.623	0.746	0.617	1.641	0.749	0.627	1.659
0	2.052	1.282	5.550	2.042	1.319	5.657	2.033	1.353	5.748	2.025	1.386	5.819	2.017	1.417	5.888	2.009	1.444	5.955	2.002	1.469	6.019

CSS (mm)	125	125 (s)		130	130 (s)		135	135 (s)		140	140 (s)	
		CC	U/S		CC	U/S		CC	U/S		CC	U/S
Size (mm)	% retained											
460	0.000	0.000	0.000	0.000	0.000	0.000	0.000	0.000	0.000	0.000	0.000	0.000
290	0.000	0.000	0.000	0.000	0.000	0.000	0.000	0.000	0.000	0.000	0.000	0.000
230	0.000	0.000	0.000	0.000	0.000	0.000	0.000	0.000	0.000	0.000	0.000	0.000
145	0.000	0.000	0.000	0.000	0.000	0.000	0.000	0.000	0.000	0.000	0.000	0.000
115	0.028	0.030	0.000	0.030	0.033	0.000	0.032	0.034	0.000	0.032	0.034	0.000
87	1.512	1.709	0.000	1.517	1.701	0.000	1.518	1.691	0.000	1.516	1.679	0.000
50	20.660	23.010	0.001	20.590	22.770	0.001	20.540	22.580	0.001	20.500	22.420	0.001
45	7.478	7.650	5.907	7.465	7.601	6.704	7.455	7.559	7.526	7.446	7.523	8.333
37.5	13.560	13.540	19.020	13.550	13.490	19.000	13.540	13.440	18.960	13.530	13.400	18.910
31.5	9.595	9.589	8.440	9.589	9.603	8.197	9.585	9.613	7.973	9.580	9.618	7.778
26.5	8.047	7.974	8.396	8.047	8.007	8.118	8.046	8.033	7.862	8.045	8.053	7.640
22.4	5.907	5.836	6.145	5.911	5.860	5.997	5.913	5.879	5.860	5.915	5.894	5.739
19	4.907	4.801	5.342	4.912	4.824	5.235	4.916	4.843	5.133	4.919	4.859	5.042
16	3.860	3.740	4.534	3.866	3.760	4.480	3.872	3.777	4.428	3.877	3.791	4.380
13.2	3.556	3.409	4.462	3.564	3.430	4.428	3.570	3.448	4.394	3.575	3.463	4.360
11.2	2.319	2.173	3.346	2.326	2.189	3.349	2.331	2.203	3.348	2.336	2.215	3.343
9.5	2.022	1.875	3.092	2.028	1.890	3.100	2.033	1.904	3.104	2.038	1.915	3.104
8	1.737	1.580	2.916	1.743	1.595	2.927	1.748	1.609	2.933	1.752	1.621	2.932
6.3	2.054	1.850	3.624	2.061	1.870	3.637	2.067	1.887	3.643	2.072	1.903	3.639
4.75	1.937	1.748	3.397	1.944	1.770	3.381	1.950	1.789	3.358	1.955	1.807	3.327
3.35	1.922	1.771	3.087	1.930	1.793	3.050	1.936	1.813	3.010	1.942	1.830	2.969
2.36	1.521	1.422	2.275	1.529	1.439	2.259	1.535	1.453	2.243	1.541	1.465	2.228
1.18	2.156	1.984	3.479	2.170	2.008	3.500	2.181	2.029	3.514	2.191	2.048	3.521
0.6	1.426	1.270	2.651	1.434	1.287	2.673	1.441	1.303	2.688	1.448	1.316	2.696
0.3	1.046	0.909	2.137	1.051	0.921	2.154	1.055	0.932	2.166	1.058	0.942	2.173
0.15	0.752	0.637	1.675	0.754	0.646	1.688	0.756	0.653	1.698	0.758	0.660	1.703
0	1.995	1.492	6.077	1.988	1.512	6.125	1.981	1.531	6.161	1.975	1.547	6.179

	Calculated power (kW)	
CSS (mm)	**Jaw crusher**	**Cone crusher**
90	152.508	115.473
90(s)	152.486	115.011
95	148.725	116.689
95(s)	148.705	116.252
100	145.138	117.798
100(s)	145.119	117.382
105	141.726	118.811
105(s)	141.708	118.415
110	138.507	119.748
110(s)	138.49	119.369
115	135.488	120.61
115(s)	135.472	120.246
120	132.672	121.393
120(s)	132.656	121.044
125	130.06	122.097
125(s)	130.045	121.76
130	127.655	122.719
130(s)	127.641	122.393
135	125.457	123.259
135(s)	125.443	122.943
140	123.466	123.716
140(s)	123.453	123.407

Variable CSS jaw crusher, screen, then cone crusher – lead-zinc ore

Table 40: Product PSDs for lead-zinc ore entering a jaw crusher with variable CSSs, then into a cone crusher or with a screen in between (denoted with (s)). Power data is shown and values were calculated using JKSimMet. CC = cone crusher product and U/S = screen undersize product; continued overleaf.

Value of t10	t75	t50	t25	t4	t2
10	3.20	3.90	5.50	23.90	53.20
20	6.50	7.90	11.20	44.80	84.50
30	10.00	12.10	17.00	62.60	99.10

Cone crusher	
CSS (mm)	50
Feed rate (t h^{-1})	333.3
Power draw (kW)	

Screen aperture (mm)	50

Jaw crusher

CSS (mm)	90	90 (s)		95	95 (s)		100	100 (s)		105	105 (s)		110	110 (s)		115	115 (s)		120	120 (s)	
		CC	U/S		CC	U/S		CC	U/S		CC	U/S		CC	U/S		CC	U/S		CC	U/S
Size (mm)	% retained																				
460	0.000	0.000	0.000	0.000	0.000	0.000	0.000	0.000	0.000	0.000	0.000	0.000	0.000	0.000	0.000	0.000	0.000	0.000	0.000	0.000	0.000
290	0.000	0.000	0.000	0.000	0.000	0.000	0.000	0.000	0.000	0.000	0.000	0.000	0.000	0.000	0.000	0.000	0.000	0.000	0.000	0.000	0.000
230	0.000	0.000	0.000	0.000	0.000	0.000	0.000	0.000	0.000	0.000	0.000	0.000	0.000	0.000	0.000	0.000	0.000	0.000	0.000	0.000	0.000
145	0.000	0.000	0.000	0.000	0.000	0.000	0.000	0.000	0.000	0.000	0.000	0.000	0.000	0.000	0.000	0.000	0.000	0.000	0.000	0.000	0.000
115	0.006	0.006	0.000	0.008	0.009	0.000	0.011	0.012	0.000	0.014	0.016	0.000	0.018	0.020	0.000	0.021	0.023	0.000	0.024	0.027	0.000
87	1.181	1.520	0.000	1.254	1.580	0.000	1.311	1.621	0.000	1.352	1.643	0.000	1.382	1.655	0.000	1.405	1.659	0.000	1.421	1.658	0.000
50	20.090	25.070	0.001	19.970	24.460	0.001	19.840	23.910	0.001	19.700	23.400	0.001	19.580	22.950	0.001	19.470	22.560	0.001	19.380	22.210	0.001
45	7.136	7.864	1.213	7.116	7.737	1.414	7.096	7.626	1.641	7.078	7.529	1.896	7.062	7.442	2.191	7.047	7.365	2.532	7.034	7.297	2.921
37.5	13.080	13.680	17.080	13.050	13.540	17.410	13.020	13.410	17.730	13.000	13.300	18.060	12.990	13.210	18.390	12.970	13.120	18.710	12.960	13.040	19.020
31.5	9.361	8.812	10.700	9.343	8.870	10.560	9.331	8.923	10.420	9.324	8.971	10.290	9.318	9.013	10.140	9.313	9.050	9.996	9.308	9.082	9.841
26.5	7.948	7.137	11.230	7.937	7.237	11.020	7.933	7.328	10.810	7.933	7.411	10.610	7.933	7.485	10.400	7.934	7.550	10.190	7.934	7.608	9.974
22.4	6.130	5.520	8.265	6.129	5.603	8.134	6.131	5.676	8.005	6.137	5.742	7.881	6.142	5.801	7.752	6.147	5.854	7.619	6.151	5.900	7.483
19	5.177	4.626	7.070	5.180	4.701	6.971	5.186	4.768	6.873	5.194	4.828	6.779	5.202	4.882	6.680	5.208	4.930	6.577	5.214	4.972	6.471
16	4.269	3.851	5.671	4.276	3.912	5.602	4.284	3.968	5.534	4.294	4.017	5.466	4.303	4.062	5.395	4.311	4.101	5.321	4.318	4.136	5.245
13.2	3.994	3.591	5.339	4.003	3.650	5.284	4.014	3.704	5.229	4.025	3.752	5.173	4.035	3.796	5.114	4.045	3.835	5.052	4.053	3.869	4.987
11.2	2.658	2.408	3.488	2.667	2.448	3.458	2.676	2.484	3.427	2.685	2.516	3.396	2.694	2.545	3.362	2.701	2.571	3.327	2.708	2.594	3.290
9.5	2.308	2.077	3.078	2.317	2.112	3.056	2.326	2.145	3.033	2.334	2.174	3.009	2.342	2.200	2.983	2.350	2.224	2.956	2.356	2.245	2.927
8	1.944	1.749	2.599	1.952	1.779	2.587	1.960	1.806	2.573	1.968	1.831	2.559	1.976	1.853	2.543	1.982	1.873	2.526	1.989	1.890	2.507
6.3	2.252	2.007	3.078	2.263	2.043	3.071	2.273	2.076	3.062	2.283	2.106	3.050	2.292	2.132	3.038	2.301	2.156	3.024	2.308	2.177	3.009
4.75	2.006	1.760	2.860	2.016	1.791	2.870	2.026	1.820	2.878	2.036	1.847	2.884	2.044	1.871	2.890	2.052	1.892	2.895	2.059	1.911	2.899
3.35	1.880	1.592	2.898	1.889	1.623	2.927	1.899	1.651	2.953	1.908	1.678	2.976	1.916	1.702	2.999	1.924	1.723	3.021	1.931	1.743	3.043
2.36	1.432	1.159	2.425	1.440	1.185	2.459	1.448	1.209	2.490	1.455	1.232	2.516	1.462	1.254	2.541	1.469	1.273	2.566	1.475	1.290	2.590
1.18	2.074	1.615	3.769	2.086	1.659	3.821	2.097	1.700	3.866	2.109	1.739	3.903	2.120	1.774	3.937	2.130	1.807	3.971	2.139	1.836	4.003
0.6	1.431	1.109	2.627	1.439	1.140	2.663	1.448	1.169	2.693	1.456	1.197	2.717	1.463	1.222	2.741	1.470	1.245	2.763	1.476	1.266	2.785
0.3	1.049	0.815	1.920	1.055	0.838	1.945	1.062	0.859	1.967	1.068	0.879	1.985	1.073	0.898	2.002	1.079	0.915	2.019	1.083	0.930	2.035
0.15	0.747	0.582	1.362	0.752	0.598	1.381	0.756	0.613	1.396	0.760	0.627	1.409	0.765	0.641	1.421	0.768	0.653	1.433	0.772	0.663	1.444
0	1.847	1.447	3.330	1.859	1.487	3.375	1.871	1.525	3.413	1.882	1.561	3.444	1.893	1.594	3.474	1.903	1.624	3.503	1.912	1.651	3.530

CSS (mm)	125	125 (s)		130	130 (s)		135	135 (s)		140	140 (s)	
		CC	U/S		CC	U/S		CC	U/S		CC	U/S
Size (mm)	% retained											
460	0.000	0.000	0.000	0.000	0.000	0.000	0.000	0.000	0.000	0.000	0.000	0.000
290	0.000	0.000	0.000	0.000	0.000	0.000	0.000	0.000	0.000	0.000	0.000	0.000
230	0.000	0.000	0.000	0.000	0.000	0.000	0.000	0.000	0.000	0.000	0.000	0.000
145	0.000	0.000	0.000	0.000	0.000	0.000	0.000	0.000	0.000	0.000	0.000	0.000
115	0.027	0.030	0.000	0.029	0.032	0.000	0.030	0.033	0.000	0.031	0.034	0.000
87	1.432	1.653	0.000	1.438	1.645	0.000	1.441	1.635	0.000	1.440	1.623	0.000
50	19.300	21.920	0.001	19.240	21.660	0.001	19.190	21.450	0.001	19.150	21.270	0.001
45	7.022	7.236	3.355	7.011	7.184	3.828	7.003	7.138	4.327	6.995	7.100	4.831
37.5	12.940	12.970	19.300	12.930	12.910	19.570	12.920	12.860	19.810	12.910	12.810	20.020
31.5	9.304	9.109	9.684	9.300	9.131	9.529	9.296	9.149	9.380	9.293	9.163	9.245
26.5	7.934	7.658	9.758	7.934	7.701	9.548	7.933	7.737	9.349	7.933	7.767	9.169
22.4	6.154	5.940	7.346	6.157	5.974	7.212	6.160	6.003	7.085	6.161	6.026	6.968
19	5.219	5.009	6.364	5.224	5.041	6.258	5.227	5.067	6.156	5.230	5.089	6.062
16	4.325	4.167	5.167	4.330	4.193	5.090	4.335	4.215	5.015	4.339	4.233	4.945
13.2	4.061	3.899	4.921	4.067	3.925	4.855	4.073	3.947	4.790	4.077	3.965	4.729
11.2	2.714	2.614	3.252	2.720	2.631	3.214	2.724	2.646	3.176	2.727	2.658	3.140
9.5	2.362	2.263	2.896	2.367	2.279	2.866	2.371	2.292	2.835	2.375	2.304	2.805
8	1.994	1.906	2.488	1.998	1.919	2.469	2.002	1.931	2.449	2.005	1.940	2.429
6.3	2.315	2.196	2.993	2.321	2.212	2.976	2.325	2.226	2.958	2.329	2.238	2.940
4.75	2.065	1.928	2.902	2.071	1.943	2.904	2.075	1.955	2.904	2.079	1.966	2.902
3.35	1.937	1.760	3.062	1.943	1.776	3.079	1.948	1.789	3.092	1.952	1.802	3.099
2.36	1.480	1.306	2.611	1.484	1.321	2.629	1.488	1.334	2.642	1.492	1.345	2.650
1.18	2.147	1.863	4.031	2.154	1.887	4.055	2.160	1.908	4.072	2.165	1.927	4.081
0.6	1.482	1.284	2.804	1.487	1.301	2.820	1.492	1.316	2.832	1.495	1.329	2.837
0.3	1.088	0.944	2.049	1.091	0.956	2.060	1.095	0.967	2.069	1.097	0.977	2.073
0.15	0.775	0.673	1.454	0.778	0.682	1.462	0.780	0.690	1.468	0.782	0.697	1.471
0	1.920	1.675	3.554	1.928	1.697	3.575	1.934	1.717	3.589	1.939	1.734	3.597

	Calculated power (kW)	
CSS (mm)	Jaw crusher	Cone crusher
90	152.549	113.341
90(s)	152.527	112.857
95	148.834	114.525
95(s)	148.813	114.065
100	145.301	115.611
100(s)	145.281	115.172
105	141.938	116.607
105(s)	141.919	116.186
110	138.87	117.524
110(s)	138.762	117.12
115	135.828	118.363
115(s)	135.811	117.975
120	133.079	119.125
120(s)	133.063	118.752
125	130.531	119.81
125(s)	130.516	119.449
130	128.181	120.417
130(s)	128.166	120.067
135	126.028	120.946
135(s)	126.014	120.606
140	124.073	121.396
140(s)	124.06	121.064

Variable CSS jaw crusher, screen, then cone crusher – porphyry copper

Table 41: Product PSDs for porphyry copper entering a jaw crusher with variable CSSs, then into a cone crusher or with a screen in between (denoted with (s)). Power data is shown and values were calculated using JKSimMet. CC = cone crusher product and U/S = screen undersize product; continued overleaf.

Value of t10	t75	t50	t25	t4	t2
10	3.10	3.70	5.40	23.30	55.40
20	6.50	7.80	11.20	44.40	85.10
30	10.10	12.20	17.30	62.50	96.90

Cone crusher	
CSS (mm)	50
Feed rate ($t\ h^{-1}$)	333.3
Power draw (kW)	

Screen aperture (mm)	50

Jaw crusher

CSS (mm)	90	90 (s)		95	95 (s)		100	100 (s)		105	105 (s)		110	110 (s)		115	115 (s)		120	120 (s)	
		CC	U/S		CC	U/S		CC	U/S		CC	U/S		CC	U/S		CC	U/S		CC	U/S
Size (mm)	% retained																				
460	0.000	0.000	0.000	0.000	0.000	0.000	0.000	0.000	0.000	0.000	0.000	0.000	0.000	0.000	0.000	0.000	0.000	0.000	0.000	0.000	0.000
290	0.000	0.000	0.000	0.000	0.000	0.000	0.000	0.000	0.000	0.000	0.000	0.000	0.000	0.000	0.000	0.000	0.000	0.000	0.000	0.000	0.000
230	0.000	0.000	0.000	0.000	0.000	0.000	0.000	0.000	0.000	0.000	0.000	0.000	0.000	0.000	0.000	0.000	0.000	0.000	0.000	0.000	0.000
145	0.000	0.000	0.000	0.000	0.000	0.000	0.000	0.000	0.000	0.000	0.000	0.000	0.000	0.000	0.000	0.000	0.000	0.000	0.000	0.000	0.000
115	0.005	0.006	0.000	0.007	0.008	0.000	0.010	0.011	0.000	0.013	0.015	0.000	0.017	0.019	0.000	0.021	0.023	0.000	0.025	0.027	0.000
87	1.192	1.503	0.000	1.269	1.568	0.000	1.326	1.610	0.000	1.365	1.632	0.000	1.393	1.641	0.000	1.412	1.643	0.000	1.425	1.639	0.000
50	20.370	24.940	0.001	20.210	24.310	0.001	20.050	23.760	0.001	19.890	23.270	0.001	19.750	22.830	0.001	19.630	22.440	0.001	19.520	22.090	0.001
45	7.278	7.876	1.495	7.253	7.759	1.758	7.229	7.654	2.051	7.204	7.561	2.373	7.181	7.477	2.749	7.160	7.401	3.189	7.142	7.334	3.697
37.5	13.290	13.720	18.250	13.260	13.590	18.540	13.230	13.470	18.820	13.200	13.370	19.100	13.180	13.280	19.370	13.150	13.200	19.630	13.130	13.120	19.870
31.5	9.549	9.057	10.880	9.529	9.116	10.680	9.515	9.168	10.490	9.507	9.213	10.320	9.500	9.253	10.130	9.494	9.288	9.933	9.488	9.319	9.728
26.5	8.081	7.372	11.220	8.071	7.472	10.960	8.067	7.560	10.710	8.068	7.639	10.480	8.071	7.711	10.240	8.072	7.775	9.984	8.074	7.831	9.725
22.4	6.150	5.647	8.038	6.152	5.725	7.889	6.157	5.793	7.748	6.165	5.854	7.617	6.173	5.908	7.481	6.180	5.957	7.338	6.186	6.000	7.190
19	5.156	4.700	6.801	5.163	4.771	6.696	5.172	4.833	6.595	5.183	4.888	6.501	5.193	4.938	6.402	5.203	4.983	6.298	5.211	5.022	6.189
16	4.184	3.830	5.441	4.195	3.888	5.382	4.207	3.939	5.324	4.220	3.985	5.267	4.233	4.027	5.208	4.244	4.065	5.144	4.254	4.098	5.077
13.2	3.882	3.534	5.120	3.897	3.591	5.080	3.911	3.641	5.040	3.926	3.687	4.999	3.940	3.728	4.955	3.953	3.765	4.908	3.964	3.799	4.858
11.2	2.570	2.330	3.434	2.582	2.369	3.424	2.594	2.403	3.413	2.606	2.435	3.399	2.617	2.463	3.383	2.627	2.489	3.366	2.636	2.512	3.346
9.5	2.227	2.003	3.048	2.239	2.037	3.045	2.251	2.069	3.041	2.262	2.097	3.033	2.272	2.124	3.024	2.282	2.147	3.014	2.290	2.168	3.002
8	1.885	1.681	2.648	1.896	1.711	2.654	1.907	1.739	2.657	1.917	1.764	2.656	1.926	1.787	2.654	1.935	1.808	2.651	1.943	1.827	2.646
6.3	2.189	1.931	3.164	2.203	1.968	3.177	2.216	2.001	3.186	2.228	2.032	3.189	2.239	2.060	3.190	2.250	2.086	3.190	2.259	2.109	3.188
4.75	1.969	1.717	2.939	1.982	1.752	2.953	1.993	1.783	2.961	2.004	1.813	2.961	2.014	1.840	2.959	2.023	1.864	2.956	2.031	1.886	2.950
3.35	1.845	1.593	2.828	1.856	1.626	2.840	1.867	1.657	2.844	1.876	1.686	2.841	1.885	1.712	2.836	1.894	1.736	2.829	1.901	1.758	2.820
2.36	1.374	1.173	2.161	1.382	1.199	2.174	1.390	1.222	2.184	1.398	1.243	2.189	1.405	1.263	2.193	1.411	1.281	2.197	1.417	1.297	2.200
1.18	1.853	1.530	3.144	1.867	1.567	3.190	1.881	1.601	3.230	1.895	1.634	3.264	1.908	1.664	3.297	1.920	1.692	3.330	1.931	1.717	3.362
0.6	1.236	0.980	2.279	1.247	1.008	2.320	1.258	1.035	2.355	1.269	1.061	2.383	1.279	1.085	2.411	1.289	1.107	2.438	1.297	1.126	2.465
0.3	0.941	0.740	1.763	0.949	0.762	1.795	0.958	0.783	1.822	0.966	0.802	1.844	0.973	0.821	1.865	0.980	0.837	1.886	0.986	0.853	1.907
0.15	0.702	0.550	1.326	0.708	0.566	1.350	0.714	0.581	1.370	0.720	0.596	1.386	0.725	0.610	1.402	0.730	0.622	1.418	0.735	0.633	1.434
0	2.064	1.588	4.021	2.080	1.635	4.094	2.096	1.680	4.156	2.110	1.722	4.206	2.124	1.761	4.254	2.137	1.797	4.302	2.149	1.830	4.349

CSS (mm)	125	125 (s)		130	130 (s)		135	135 (s)		140	140 (s)	
		CC	U/S		CC	U/S		CC	U/S		CC	U/S
Size (mm)	% retained											
460	0.000	0.000	0.000	0.000	0.000	0.000	0.000	0.000	0.000	0.000	0.000	0.000
290	0.000	0.000	0.000	0.000	0.000	0.000	0.000	0.000	0.000	0.000	0.000	0.000
230	0.000	0.000	0.000	0.000	0.000	0.000	0.000	0.000	0.000	0.000	0.000	0.000
145	0.000	0.000	0.000	0.000	0.000	0.000	0.000	0.000	0.000	0.000	0.000	0.000
115	0.028	0.031	0.000	0.031	0.034	0.000	0.033	0.035	0.000	0.033	0.036	0.000
87	1.432	1.632	0.000	1.436	1.622	0.000	1.437	1.610	0.000	1.434	1.597	0.000
50	19.430	21.790	0.001	19.360	21.540	0.001	19.300	21.330	0.001	19.250	21.160	0.001
45	7.125	7.274	4.269	7.111	7.223	4.894	7.099	7.179	5.547	7.090	7.142	6.195
37.5	13.110	13.050	20.080	13.090	13.000	20.250	13.080	12.940	20.400	13.070	12.900	20.530
31.5	9.483	9.344	9.519	9.478	9.365	9.313	9.473	9.381	9.119	9.470	9.393	8.949
26.5	8.075	7.880	9.465	8.075	7.922	9.212	8.076	7.956	8.977	8.075	7.982	8.769
22.4	6.192	6.038	7.041	6.197	6.070	6.895	6.200	6.096	6.757	6.203	6.117	6.633
19	5.218	5.057	6.078	5.225	5.087	5.968	5.230	5.112	5.863	5.234	5.132	5.767
16	4.263	4.127	5.009	4.270	4.152	4.940	4.277	4.173	4.873	4.282	4.190	4.810
13.2	3.974	3.828	4.806	3.983	3.853	4.753	3.990	3.874	4.700	3.996	3.892	4.649
11.2	2.644	2.532	3.326	2.651	2.550	3.303	2.657	2.565	3.280	2.662	2.577	3.255
9.5	2.298	2.187	2.988	2.304	2.203	2.973	2.310	2.217	2.955	2.314	2.229	2.937
8	1.949	1.843	2.639	1.955	1.858	2.630	1.960	1.870	2.619	1.964	1.880	2.605
6.3	2.267	2.129	3.183	2.274	2.147	3.176	2.280	2.163	3.165	2.285	2.175	3.150
4.75	2.038	1.905	2.942	2.044	1.923	2.930	2.049	1.937	2.914	2.053	1.950	2.895
3.35	1.908	1.777	2.810	1.913	1.793	2.797	1.918	1.808	2.782	1.922	1.820	2.764
2.36	1.423	1.312	2.203	1.428	1.325	2.203	1.432	1.336	2.203	1.435	1.345	2.200
1.18	1.941	1.740	3.392	1.950	1.761	3.418	1.958	1.779	3.437	1.965	1.796	3.448
0.6	1.305	1.144	2.489	1.312	1.161	2.510	1.318	1.175	2.527	1.323	1.188	2.536
0.3	0.992	0.867	1.926	0.997	0.879	1.942	1.002	0.890	1.955	1.006	0.900	1.962
0.15	0.739	0.644	1.448	0.743	0.653	1.460	0.746	0.661	1.470	0.749	0.668	1.475
0	2.159	1.860	4.393	2.169	1.886	4.430	2.177	1.910	4.459	2.184	1.931	4.475

	Calculated power (kW)	
CSS (mm)	Jaw crusher	Cone crusher
90	146.904	113.633
90(s)	146.884	113.152
95	143.443	114.804
95(s)	143.424	114.348
100	140.167	115.865
100(s)	140.149	115.432
105	137.05	116.831
105(s)	137.033	116.417
110	134.091	117.73
110(s)	134.075	117.333
115	131.303	118.561
115(s)	131.288	118.181
120	128.695	119.319
120(s)	128.681	118.954
125	126.276	120.001
125(s)	126.262	119.65
130	124.053	120.604
130(s)	124.039	120.263
135	122.031	121.123
135(s)	122.018	120.792
140	120.214	121.556
140(s)	120.202	121.234

Variable CSS jaw crusher, screen, then cone crusher – copper carbonatitie

Table 42: Product PSDs for copper carbonatitie entering a jaw crusher with variable CSSs, then into a cone crusher or with a screen in between (denoted with (s)). Power data is shown and values were calculated using JKSimMet. CC = cone crusher product and U/S = screen undersize product; continued overleaf.

Value of t10	t75	t50	t25	t4	t2
10	2.60	3.40	5.20	21.40	51.40
20	5.40	7.00	10.70	43.40	82.10
30	8.70	11.00	16.50	63.80	97.20

Cone crusher	
CSS (mm)	50
Feed rate ($t\ h^{-1}$)	333.3
Power draw (kW)	

Screen aperture (mm)	50

Jaw crusher

CSS (mm)	90	90 (s)		95	95 (s)		100	100 (s)		105	105 (s)		110	110 (s)		115	115 (s)		120	120 (s)	
		CC	U/S		CC	U/S		CC	U/S		CC	U/S		CC	U/S		CC	U/S		CC	U/S
Size (mm)	% retained																				
460	0.000	0.000	0.000	0.000	0.000	0.000	0.000	0.000	0.000	0.000	0.000	0.000	0.000	0.000	0.000	0.000	0.000	0.000	0.000	0.000	0.000
290	0.000	0.000	0.000	0.000	0.000	0.000	0.000	0.000	0.000	0.000	0.000	0.000	0.000	0.000	0.000	0.000	0.000	0.000	0.000	0.000	0.000
230	0.000	0.000	0.000	0.000	0.000	0.000	0.000	0.000	0.000	0.000	0.000	0.000	0.000	0.000	0.000	0.000	0.000	0.000	0.000	0.000	0.000
145	0.000	0.000	0.000	0.000	0.000	0.000	0.000	0.000	0.000	0.000	0.000	0.000	0.000	0.000	0.000	0.000	0.000	0.000	0.000	0.000	0.000
115	0.005	0.006	0.000	0.007	0.008	0.000	0.010	0.011	0.000	0.013	0.015	0.000	0.017	0.019	0.000	0.021	0.023	0.000	0.024	0.027	0.000
87	1.246	1.557	0.000	1.325	1.624	0.000	1.386	1.670	0.000	1.428	1.695	0.000	1.459	1.709	0.000	1.481	1.714	0.000	1.497	1.714	0.000
50	21.220	25.760	0.001	21.050	25.130	0.001	20.870	24.560	0.001	20.680	24.040	0.001	20.520	23.580	0.001	20.370	23.160	0.001	20.250	22.810	0.001
45	7.382	7.953	1.756	7.352	7.833	2.067	7.325	7.730	2.412	7.301	7.641	2.789	7.279	7.561	3.227	7.259	7.488	3.734	7.241	7.424	4.313
37.5	13.360	13.740	18.390	13.320	13.610	18.630	13.290	13.500	18.860	13.260	13.410	19.090	13.240	13.330	19.300	13.220	13.250	19.490	13.200	13.180	19.650
31.5	9.408	8.944	10.610	9.388	9.004	10.380	9.375	9.057	10.170	9.370	9.104	9.970	9.365	9.146	9.763	9.361	9.183	9.545	9.358	9.215	9.320
26.5	7.900	7.235	10.910	7.891	7.335	10.630	7.889	7.423	10.360	7.893	7.503	10.100	7.897	7.574	9.845	7.900	7.637	9.577	7.903	7.693	9.304
22.4	5.941	5.490	7.705	5.946	5.568	7.546	5.955	5.636	7.398	5.966	5.697	7.260	5.977	5.751	7.118	5.987	5.800	6.970	5.996	5.843	6.819
19	4.970	4.560	6.514	4.980	4.630	6.403	4.993	4.692	6.298	5.007	4.748	6.200	5.020	4.797	6.098	5.032	4.842	5.992	5.043	4.881	5.882
16	4.029	3.714	5.201	4.044	3.772	5.143	4.060	3.824	5.086	4.077	3.870	5.032	4.092	3.913	4.975	4.107	3.950	4.915	4.119	3.984	4.852
13.2	3.746	3.431	4.913	3.764	3.488	4.877	3.783	3.539	4.841	3.801	3.585	4.804	3.818	3.627	4.765	3.833	3.664	4.723	3.847	3.698	4.679
11.2	2.493	2.268	3.353	2.509	2.307	3.352	2.525	2.343	3.348	2.539	2.375	3.342	2.553	2.404	3.335	2.566	2.431	3.327	2.577	2.455	3.317
9.5	2.169	1.953	3.003	2.184	1.988	3.009	2.198	2.021	3.013	2.212	2.050	3.014	2.224	2.077	3.013	2.236	2.102	3.012	2.246	2.123	3.009
8	1.866	1.650	2.724	1.880	1.682	2.744	1.894	1.711	2.761	1.906	1.738	2.774	1.918	1.762	2.787	1.928	1.784	2.798	1.938	1.804	2.808
6.3	2.190	1.906	3.338	2.206	1.944	3.372	2.222	1.979	3.402	2.237	2.012	3.425	2.251	2.042	3.447	2.264	2.069	3.468	2.275	2.094	3.488
4.75	2.048	1.723	3.398	2.064	1.761	3.448	2.078	1.795	3.491	2.091	1.828	3.524	2.104	1.857	3.556	2.115	1.884	3.588	2.125	1.909	3.617
3.35	2.011	1.639	3.580	2.025	1.678	3.634	2.038	1.714	3.679	2.050	1.749	3.713	2.061	1.780	3.745	2.071	1.809	3.776	2.081	1.835	3.805
2.36	1.597	1.274	2.973	1.608	1.308	3.014	1.618	1.339	3.046	1.628	1.370	3.068	1.637	1.397	3.088	1.646	1.423	3.107	1.653	1.445	3.124
1.18	2.324	1.862	4.298	2.340	1.913	4.345	2.355	1.961	4.380	2.369	2.006	4.401	2.383	2.047	4.418	2.395	2.085	4.435	2.406	2.118	4.448
0.6	1.483	1.206	2.665	1.493	1.237	2.691	1.501	1.265	2.711	1.510	1.292	2.722	1.518	1.317	2.732	1.525	1.339	2.741	1.532	1.360	2.749
0.3	0.966	0.787	1.729	0.972	0.807	1.746	0.978	0.825	1.759	0.984	0.843	1.767	0.989	0.859	1.773	0.993	0.873	1.779	0.998	0.886	1.784
0.15	0.608	0.495	1.088	0.612	0.508	1.099	0.615	0.519	1.107	0.619	0.530	1.112	0.622	0.540	1.116	0.625	0.549	1.120	0.628	0.558	1.123
0	1.032	0.840	1.848	1.039	0.861	1.866	1.045	0.881	1.880	1.051	0.900	1.888	1.056	0.917	1.895	1.061	0.932	1.901	1.066	0.946	1.906

CSS (mm)	125	125 (s)		130	130 (s)		135	135 (s)		140	140 (s)	
		CC	U/S		CC	U/S		CC	U/S		CC	U/S
Size (mm)	% retained											
460	0.000	0.000	0.000	0.000	0.000	0.000	0.000	0.000	0.000	0.000	0.000	0.000
290	0.000	0.000	0.000	0.000	0.000	0.000	0.000	0.000	0.000	0.000	0.000	0.000
230	0.000	0.000	0.000	0.000	0.000	0.000	0.000	0.000	0.000	0.000	0.000	0.000
145	0.000	0.000	0.000	0.000	0.000	0.000	0.000	0.000	0.000	0.000	0.000	0.000
115	0.027	0.030	0.000	0.030	0.032	0.000	0.031	0.034	0.000	0.032	0.034	0.000
87	1.507	1.709	0.000	1.512	1.701	0.000	1.513	1.690	0.000	1.511	1.678	0.000
50	20.140	22.490	0.001	20.050	22.230	0.001	19.980	22.010	0.001	19.920	21.830	0.001
45	7.225	7.367	4.958	7.211	7.318	5.656	7.199	7.275	6.382	7.189	7.239	7.102
37.5	13.190	13.120	19.780	13.170	13.070	19.880	13.160	13.020	19.950	13.150	12.980	20.010
31.5	9.354	9.241	9.094	9.351	9.263	8.873	9.348	9.280	8.666	9.346	9.292	8.485
26.5	7.906	7.741	9.033	7.908	7.782	8.771	7.910	7.815	8.527	7.911	7.842	8.313
22.4	6.004	5.880	6.668	6.011	5.912	6.521	6.016	5.938	6.382	6.021	5.959	6.259
19	5.052	4.916	5.770	5.060	4.946	5.661	5.067	4.970	5.556	5.073	4.990	5.461
16	4.131	4.013	4.788	4.140	4.038	4.723	4.149	4.060	4.661	4.155	4.077	4.602
13.2	3.860	3.727	4.632	3.871	3.753	4.585	3.880	3.774	4.537	3.887	3.792	4.491
11.2	2.587	2.476	3.305	2.596	2.494	3.292	2.603	2.509	3.277	2.609	2.523	3.260
9.5	2.256	2.143	3.004	2.264	2.159	2.997	2.270	2.174	2.988	2.276	2.186	2.977
8	1.946	1.822	2.816	1.953	1.837	2.822	1.959	1.850	2.824	1.964	1.862	2.822
6.3	2.285	2.115	3.505	2.293	2.134	3.518	2.300	2.151	3.526	2.306	2.165	3.527
4.75	2.134	1.931	3.644	2.141	1.950	3.665	2.147	1.967	3.679	2.152	1.982	3.685
3.35	2.089	1.859	3.830	2.096	1.880	3.849	2.102	1.898	3.861	2.107	1.915	3.863
2.36	1.660	1.466	3.138	1.666	1.485	3.147	1.671	1.501	3.150	1.675	1.516	3.146
1.18	2.416	2.149	4.457	2.424	2.176	4.461	2.431	2.199	4.458	2.437	2.220	4.447
0.6	1.537	1.378	2.754	1.543	1.394	2.755	1.547	1.408	2.753	1.550	1.420	2.745
0.3	1.001	0.898	1.787	1.005	0.908	1.788	1.007	0.918	1.786	1.010	0.925	1.782
0.15	0.630	0.565	1.125	0.632	0.572	1.125	0.634	0.577	1.124	0.635	0.582	1.121
0	1.070	0.959	1.910	1.073	0.970	1.911	1.076	0.980	1.909	1.078	0.988	1.904

	Calculated power (kW)	
CSS (mm)	Jaw crusher	Cone crusher
90	151.241	114.98
90(s)	151.219	114.509
95	147.539	116.184
95(s)	147.519	115.738
100	144.029	117.278
100(s)	144.01	116.854
105	140.69	118.277
105(s)	140.672	117.871
110	137.538	119.199
110(s)	137.52	118.811
115	134.58	120.047
115(s)	134.563	119.675
120	131.819	120.818
120(s)	131.804	120.46
125	129.26	121.509
125(s)	129.245	121.165
130	126.903	122.12
130(s)	126.889	121.786
135	124.751	122.647
135(s)	124.738	122.223
140	122.805	123.091
140(s)	122.792	122.775

Jaw crusher – basalt

Table 43: Product PSDs for basalt entering a jaw crusher with variable CSSs. Power Values were calculated using JKSimMet; continued overleaf.

Jaw crusher

CSS (mm)	10	12	14	16	18	20	22	24	26	28	30	32	34	36	38	40	42	44	46	48	50
Size (mm)	% retained																				
460	0	0	0	0	0	0	0	0	0	0	0	0	0	0	0	0	0	0	0	0	0
290	0	0	0	0	0	0	0	0	0	0	0	0	0	0	0	0	0	0	0	0	0
230	0	0	0	0	0	0	0	0	0	0	0	0	0	0	0	0	0	0	0	0	0
145	0	0	0	0	0	0	0	0	0	0	0	0	0	0	0	0	0	0	0	0	0
115	0	0	0.001	0.001	0.001	0.002	0.003	0	0.01	0.011	0.016	0.02	0.03	0.04	0.053	0.068	0.09	0.11	0.13	0.16	0.19
87	0.04	0.05	0.078	0.106	0.14	0.18	0.225	0.28	0.33	0.399	0.471	0.55	0.64	0.73	0.831	0.941	1.06	1.18	1.31	1.45	1.6
50	2.73	2.99	3.268	3.556	3.856	4.165	4.484	4.81	5.15	5.49	5.838	6.19	6.55	6.91	7.271	7.63	7.98	8.33	8.68	9.01	9.34
45	1.41	1.51	1.606	1.706	1.808	1.911	2.014	2.12	2.22	2.324	2.427	2.53	2.63	2.73	2.816	2.888	2.94	2.98	3	3	2.98
37.5	3.47	3.65	3.843	4.033	4.222	4.41	4.596	4.78	4.96	5.138	5.311	5.48	5.64	5.8	5.94	6.036	6.09	6.11	6.09	6.03	5.95
31.5	3.78	3.94	4.094	4.245	4.391	4.531	4.665	4.79	4.91	5.004	5.058	5.08	5.06	5.02	4.947	4.876	4.8	4.73	4.65	4.58	4.5
26.5	4.35	4.49	4.62	4.747	4.867	4.978	5.081	5.18	5.26	5.306	5.302	5.25	5.16	5.03	4.875	4.739	4.62	4.51	4.41	4.32	4.25
22.4	4.6	4.71	4.809	4.902	4.985	5.04	5.043	5	4.91	4.806	4.703	4.6	4.5	4.4	4.309	4.224	4.15	4.08	4.02	3.96	3.91
19	4.85	4.94	5.011	5.075	5.129	5.149	5.105	5	4.85	4.695	4.555	4.43	4.32	4.23	4.148	4.073	4.01	3.95	3.89	3.84	3.8
16	4.45	4.47	4.469	4.42	4.322	4.198	4.073	3.95	3.82	3.707	3.605	3.51	3.44	3.37	3.306	3.251	3.2	3.16	3.12	3.08	3.05
13.2	4.73	4.71	4.672	4.558	4.375	4.171	3.996	3.85	3.72	3.617	3.522	3.44	3.36	3.3	3.244	3.194	3.15	3.11	3.07	3.04	3.01
11.2	4.36	4.27	4.131	3.991	3.862	3.746	3.646	3.56	3.49	3.431	3.378	3.33	3.29	3.25	3.222	3.193	3.17	3.14	3.12	3.11	3.09
9.5	4.4	4.29	4.122	3.971	3.846	3.741	3.652	3.58	3.51	3.46	3.412	3.37	3.33	3.3	3.273	3.248	3.23	3.21	3.19	3.17	3.16
8	4.54	4.4	4.262	4.15	4.057	3.98	3.914	3.86	3.81	3.774	3.738	3.71	3.68	3.66	3.637	3.618	3.6	3.59	3.57	3.56	3.55
6.3	6	5.79	5.64	5.514	5.41	5.324	5.25	5.19	5.14	5.093	5.054	5.02	4.99	4.96	4.94	4.919	4.9	4.88	4.87	4.85	4.84
4.75	5.51	5.36	5.251	5.159	5.084	5.022	4.969	4.92	4.89	4.855	4.826	4.8	4.78	4.76	4.742	4.727	4.71	4.7	4.69	4.68	4.67
3.35	8.55	8.43	8.34	8.268	8.208	8.159	8.116	8.08	8.05	8.025	8.002	7.98	7.96	7.95	7.934	7.922	7.91	7.9	7.89	7.88	7.88
2.36	7.61	7.54	7.483	7.44	7.405	7.375	7.349	7.33	7.31	7.294	7.279	7.27	7.26	7.25	7.238	7.23	7.22	7.22	7.21	7.2	7.2
1.18	8.18	8.11	8.054	8.01	7.973	7.941	7.913	7.89	7.87	7.847	7.829	7.81	7.8	7.78	7.768	7.755	7.74	7.73	7.72	7.71	7.7
0.6	4.75	4.71	4.679	4.65	4.623	4.597	4.573	4.55	4.53	4.506	4.486	4.47	4.45	4.43	4.412	4.396	4.38	4.37	4.35	4.34	4.33
0.3	1.54	1.51	1.472	1.441	1.413	1.386	1.362	1.34	1.32	1.302	1.286	1.27	1.26	1.25	1.234	1.224	1.22	1.21	1.2	1.19	1.19
0.15	0.69	0.66	0.639	0.619	0.602	0.586	0.573	0.56	0.55	0.543	0.535	0.53	0.52	0.52	0.511	0.507	0.5	0.5	0.5	0.49	0.49
0	9.5	9.47	9.454	9.436	9.422	9.409	9.398	9.39	9.38	9.373	9.366	9.36	9.36	9.35	9.346	9.343	9.34	9.34	9.33	9.33	9.33

CSS (mm)	52	54	56	58	60	62	64	66	68	70	72	74	76
Size (mm)	% retained												
460	0	0	0	0	0	0	0	0	0	0	0	0	0
290	0	0	0	0	0	0	0	0	0	0	0	0	0
230	0	0	0	0	0	0	0	0	0	0	0	0	0
145	0	0	0.003	0.005	0.008	0.012	0.017	0.02	0.03	0.041	0.053	0.07	0.08
115	0.23	0.19	0.233	0.286	0.344	0.407	0.476	0.55	0.63	0.718	0.81	0.91	1.01
87	1.76	2	2.169	2.342	2.52	2.704	2.892	3.09	3.28	3.483	3.687	3.89	4.09
50	9.66	9.94	10.19	10.39	10.57	10.7	10.81	10.9	10.9	10.92	10.9	10.9	10.8
45	2.95	2.91	2.878	2.843	2.809	2.777	2.745	2.72	2.69	2.659	2.633	2.61	2.59
37.5	5.83	5.71	5.602	5.499	5.403	5.313	5.228	5.15	5.08	5.007	4.943	4.88	4.83
31.5	4.43	4.36	4.294	4.233	4.175	4.121	4.07	4.02	3.98	3.937	3.898	3.86	3.83
26.5	4.18	4.12	4.063	4.009	3.959	3.912	3.867	3.83	3.79	3.75	3.716	3.68	3.65
22.4	3.87	3.84	3.801	3.767	3.736	3.706	3.678	3.65	3.63	3.605	3.584	3.56	3.55
19	3.77	3.73	3.701	3.672	3.644	3.618	3.594	3.57	3.55	3.53	3.512	3.49	3.48
16	3.03	3	2.981	2.959	2.939	2.92	2.903	2.89	2.87	2.856	2.843	2.83	2.82
13.2	2.99	2.96	2.943	2.923	2.905	2.887	2.871	2.86	2.84	2.828	2.816	2.8	2.79
11.2	3.08	3.06	3.052	3.041	3.031	3.021	3.011	3	3	2.987	2.98	2.97	2.97
9.5	3.14	3.13	3.123	3.113	3.103	3.095	3.086	3.08	3.07	3.064	3.058	3.05	3.05
8	3.54	3.53	3.525	3.518	3.511	3.504	3.498	3.49	3.49	3.482	3.477	3.47	3.47
6.3	4.83	4.82	4.814	4.806	4.798	4.79	4.783	4.78	4.77	4.764	4.759	4.75	4.75
4.75	4.66	4.66	4.649	4.643	4.637	4.631	4.626	4.62	4.62	4.613	4.609	4.61	4.6
3.35	7.87	7.86	7.859	7.854	7.849	7.845	7.84	7.84	7.83	7.829	7.826	7.82	7.82
2.36	7.2	7.19	7.187	7.183	7.18	7.176	7.172	7.17	7.17	7.162	7.159	7.16	7.15
1.18	7.68	7.67	7.662	7.652	7.641	7.631	7.621	7.61	7.6	7.59	7.58	7.57	7.56
0.6	4.32	4.31	4.3	4.291	4.282	4.274	4.266	4.26	4.25	4.244	4.237	4.23	4.23
0.3	1.18	1.18	1.171	1.167	1.163	1.159	1.155	1.15	1.15	1.144	1.141	1.14	1.14
0.15	0.49	0.49	0.483	0.481	0.479	0.477	0.475	0.47	0.47	0.47	0.469	0.47	0.47
0	9.33	9.32	9.322	9.321	9.319	9.318	9.316	9.32	9.31	9.312	9.311	9.31	9.31

Jaw crusher – BIF ore

Table 44: Product PSDs for BIF ore entering a jaw crusher with variable CSSs. Power data is shown and values were calculated using JKSimMet; continued overleaf.

Value of t10	t75	t50	t25	t4	t2
10	2.40	3.00	4.90	23.70	59.80
20	4.70	6.00	9.60	45.00	87.90
30	7.20	9.20	14.70	62.80	96.40

Jaw crusher	
CSS (mm)	
Feed rate ($t\,h^{-1}$)	333.3
Power draw (kW)	

Jaw crusher

CSS (mm)	10	12	14	16	18	20	22	24	26	28	30	32	34	36	38	40	42	44	46	48	50
Size (mm)	% retained																				
460	0.000	0.000	0.000	0.000	0.000	0.000	0.000	0.000	0.000	0.000	0.000	0.000	0.000	0.000	0.000	0.000	0.000	0.000	0.000	0.000	0.000
290	0.000	0.000	0.000	0.000	0.000	0.000	0.000	0.000	0.000	0.000	0.000	0.000	0.000	0.000	0.000	0.000	0.000	0.000	0.000	0.000	0.000
230	0.000	0.000	0.000	0.000	0.000	0.000	0.000	0.000	0.000	0.000	0.000	0.000	0.000	0.000	0.000	0.000	0.000	0.000	0.000	0.000	0.000
145	0.000	0.000	0.000	0.000	0.000	0.000	0.000	0.000	0.000	0.000	0.000	0.000	0.000	0.000	0.000	0.000	0.000	0.000	0.000	0.000	0.000
115	0.001	0.001	0.001	0.001	0.001	0.001	0.003	0.004	0.006	0.009	0.016	0.019	0.026	0.034	0.044	0.057	0.071	0.089	0.109	0.133	0.160
87	0.030	0.046	0.066	0.090	0.119	0.152	0.191	0.235	0.285	0.340	0.471	0.471	0.546	0.629	0.718	0.814	0.918	1.030	1.149	1.276	1.410
50	2.409	2.652	2.908	3.177	3.458	3.751	4.055	4.371	4.698	5.036	5.838	5.739	6.105	6.478	6.856	7.238	7.621	8.004	8.387	8.767	9.144
45	1.287	1.384	1.483	1.586	1.691	1.798	1.908	2.019	2.133	2.247	2.427	2.480	2.598	2.715	2.825	2.917	2.988	3.039	3.070	3.080	3.068
37.5	3.216	3.411	3.610	3.811	4.015	4.221	4.428	4.636	4.845	5.053	5.311	5.467	5.672	5.874	6.055	6.190	6.277	6.319	6.316	6.270	6.182
31.5	3.603	3.780	3.956	4.131	4.304	4.474	4.640	4.802	4.958	5.084	5.058	5.209	5.210	5.171	5.106	5.034	4.959	4.880	4.798	4.715	4.631
26.5	4.211	4.378	4.540	4.699	4.852	4.999	5.139	5.271	5.395	5.474	5.302	5.457	5.366	5.224	5.059	4.907	4.769	4.644	4.532	4.432	4.345
22.4	4.581	4.724	4.860	4.988	5.107	5.193	5.217	5.182	5.092	4.981	4.703	4.753	4.638	4.524	4.413	4.312	4.221	4.139	4.067	4.003	3.949
19	4.904	5.022	5.130	5.228	5.316	5.362	5.330	5.225	5.055	4.876	4.555	4.571	4.444	4.331	4.231	4.140	4.058	3.985	3.921	3.865	3.818
16	4.600	4.647	4.671	4.632	4.531	4.395	4.254	4.110	3.963	3.826	3.605	3.596	3.503	3.422	3.352	3.288	3.231	3.179	3.134	3.095	3.063
13.2	4.954	4.961	4.936	4.819	4.613	4.377	4.171	3.995	3.846	3.716	3.522	3.501	3.414	3.341	3.278	3.220	3.168	3.122	3.081	3.046	3.017
11.2	4.565	4.478	4.314	4.150	3.995	3.854	3.735	3.635	3.554	3.484	3.378	3.368	3.322	3.283	3.249	3.218	3.191	3.166	3.144	3.125	3.109
9.5	4.612	4.494	4.292	4.111	3.960	3.832	3.724	3.635	3.564	3.503	3.412	3.402	3.362	3.328	3.298	3.272	3.248	3.226	3.207	3.190	3.176
8	4.712	4.543	4.382	4.247	4.137	4.047	3.971	3.908	3.857	3.814	3.738	3.743	3.714	3.690	3.669	3.650	3.632	3.617	3.603	3.591	3.580
6.3	6.193	5.949	5.763	5.612	5.491	5.393	5.310	5.242	5.188	5.141	5.054	5.064	5.032	5.005	4.982	4.961	4.941	4.924	4.908	4.894	4.882
4.75	5.641	5.461	5.332	5.229	5.146	5.079	5.022	4.975	4.936	4.903	4.826	4.846	4.823	4.803	4.785	4.768	4.753	4.739	4.727	4.716	4.706
3.35	8.630	8.493	8.395	8.315	8.250	8.197	8.151	8.112	8.080	8.052	8.002	8.003	7.983	7.965	7.949	7.934	7.920	7.907	7.896	7.885	7.876
2.36	7.616	7.537	7.479	7.430	7.390	7.356	7.326	7.300	7.278	7.258	7.279	7.224	7.209	7.196	7.184	7.172	7.162	7.152	7.143	7.135	7.128
1.18	8.040	7.957	7.893	7.837	7.789	7.747	7.710	7.677	7.648	7.622	7.829	7.576	7.556	7.539	7.522	7.507	7.493	7.481	7.469	7.459	7.449
0.6	4.507	4.465	4.430	4.400	4.373	4.350	4.329	4.311	4.296	4.282	4.486	4.258	4.248	4.239	4.231	4.224	4.217	4.211	4.205	4.200	4.195
0.3	1.333	1.309	1.289	1.273	1.258	1.246	1.235	1.225	1.217	1.209	1.286	1.195	1.189	1.184	1.179	1.174	1.170	1.166	1.162	1.159	1.155
0.15	0.615	0.601	0.590	0.580	0.571	0.563	0.556	0.550	0.544	0.538	0.535	0.529	0.525	0.521	0.517	0.514	0.511	0.508	0.505	0.503	0.500
0	9.740	9.708	9.680	9.656	9.633	9.613	9.595	9.579	9.564	9.550	9.366	9.526	9.515	9.506	9.497	9.488	9.480	9.473	9.466	9.460	9.454

CSS (mm)	52	54	56	58	60	62	64	66	68	70	72	74	76
Size (mm)	% retained												
460	0.000	0.000	0.000	0.000	0.000	0.000	0.000	0.000	0.000	0.000	0.000	0.000	0.000
290	0.000	0.000	0.000	0.000	0.000	0.000	0.000	0.000	0.000	0.000	0.000	0.000	0.000
230	0.000	0.000	0.000	0.000	0.000	0.000	0.000	0.000	0.000	0.000	0.000	0.000	0.000
145	0.000	0.001	0.002	0.004	0.006	0.010	0.014	0.019	0.026	0.035	0.045	0.056	0.070
115	0.191	0.156	0.197	0.242	0.292	0.347	0.407	0.472	0.543	0.618	0.700	0.787	0.880
87	1.552	1.771	1.926	2.088	2.257	2.433	2.616	2.804	2.999	3.200	3.406	3.615	3.822
50	9.515	9.855	10.160	10.420	10.650	10.830	10.990	11.100	11.170	11.210	11.220	11.190	11.160
45	3.037	3.001	2.965	2.928	2.892	2.857	2.822	2.789	2.756	2.725	2.695	2.666	2.638
37.5	6.057	5.930	5.810	5.696	5.589	5.489	5.394	5.305	5.221	5.143	5.069	5.000	4.933
31.5	4.547	4.467	4.391	4.320	4.253	4.191	4.133	4.078	4.028	3.981	3.938	3.898	3.860
26.5	4.269	4.198	4.131	4.068	4.009	3.954	3.902	3.854	3.810	3.770	3.733	3.698	3.665
22.4	3.903	3.861	3.821	3.783	3.748	3.715	3.684	3.656	3.630	3.606	3.584	3.563	3.544
19	3.778	3.742	3.708	3.676	3.646	3.618	3.591	3.567	3.545	3.525	3.506	3.489	3.472
16	3.035	3.010	2.987	2.964	2.943	2.924	2.906	2.889	2.873	2.859	2.846	2.833	2.822
13.2	2.992	2.970	2.949	2.929	2.910	2.892	2.876	2.861	2.847	2.834	2.822	2.811	2.800
11.2	3.096	3.083	3.072	3.061	3.050	3.040	3.031	3.023	3.015	3.007	3.000	2.994	2.988
9.5	3.165	3.154	3.144	3.134	3.125	3.116	3.108	3.100	3.093	3.086	3.080	3.074	3.069
8	3.571	3.563	3.555	3.548	3.540	3.534	3.527	3.521	3.516	3.511	3.506	3.501	3.497
6.3	4.872	4.863	4.853	4.845	4.836	4.829	4.821	4.814	4.807	4.801	4.795	4.790	4.784
4.75	4.697	4.689	4.682	4.674	4.667	4.660	4.654	4.648	4.642	4.636	4.631	4.626	4.621
3.35	7.867	7.859	7.852	7.845	7.838	7.831	7.824	7.818	7.812	7.807	7.801	7.796	7.791
2.36	7.121	7.115	7.109	7.104	7.098	7.093	7.088	7.083	7.078	7.074	7.070	7.066	7.062
1.18	7.441	7.433	7.426	7.419	7.412	7.406	7.400	7.394	7.389	7.384	7.379	7.375	7.371
0.6	4.191	4.187	4.184	4.180	4.177	4.173	4.170	4.167	4.164	4.161	4.159	4.156	4.154
0.3	1.153	1.150	1.147	1.145	1.142	1.140	1.138	1.135	1.133	1.131	1.129	1.127	1.125
0.15	0.498	0.496	0.494	0.493	0.491	0.489	0.487	0.486	0.484	0.483	0.482	0.480	0.479
0	9.449	9.444	9.439	9.434	9.430	9.426	9.421	9.417	9.414	9.410	9.406	9.403	9.400

CSS (mm)	Calculated Power (kW)
10	123.132
12	120.870
14	118.876
16	117.078
18	115.449
20	113.933
22	112.546
24	111.278
26	110.097
28	109.003
30	107.984
32	107.013
34	103.728
36	103.027
38	102.355
40	105.454
42	104.708

CSS (mm)	Calculated Power (kW)
44	103.992
46	101.731
48	101.155
50	100.607
52	100.103
54	99.623
56	99.145
58	98.685
60	98.245
62	97.806
64	97.386
66	96.983
68	96.582
70	96.198
72	95.829
74	95.459
76	95.102

Jaw crusher – granite

Table 45: Product PSDs for granite entering a jaw crusher with variable CSSs. Values were calculated using JKSimMet; continued overleaf.

Jaw crusher

CSS (mm)	10	12	14	16	18	20	22	24	26	28	30	32	34	36	38	40	42	44	46	48	50
Size (mm)	% retained																				
460	0.000	0.000	0.000	0.000	0.000	0.000	0.000	0.000	0.000	0.000	0.000	0.000	0.000	0.000	0.000	0.000	0.000	0.000	0.000	0.000	0.000
290	0.000	0.000	0.000	0.000	0.000	0.000	0.000	0.000	0.000	0.000	0.000	0.000	0.000	0.000	0.000	0.000	0.000	0.000	0.000	0.000	0.000
230	0.000	0.000	0.000	0.000	0.000	0.000	0.000	0.000	0.000	0.000	0.000	0.000	0.000	0.000	0.000	0.000	0.000	0.000	0.000	0.000	0.000
145	0.000	0.000	0.000	0.000	0.000	0.000	0.000	0.000	0.000	0.000	0.000	0.000	0.000	0.000	0.000	0.000	0.000	0.000	0.000	0.000	0.000
115	0.001	0.001	0.001	0.001	0.001	0.002	0.003	0.004	0.007	0.003	0.016	0.020	0.027	0.036	0.047	0.060	0.076	0.095	0.116	0.142	0.171
87	0.033	0.050	0.072	0.099	0.130	0.167	0.209	0.257	0.311	0.209	0.471	0.514	0.596	0.685	0.782	0.886	0.999	1.119	1.247	1.383	1.528
50	2.609	2.870	3.143	3.429	3.727	4.038	4.359	4.691	5.033	4.359	5.838	6.113	6.488	6.869	7.254	7.639	8.022	8.404	8.782	9.155	9.521
45	1.358	1.457	1.558	1.662	1.767	1.875	1.983	2.093	2.204	1.983	2.427	2.538	2.648	2.758	2.860	2.941	3.003	3.044	3.065	3.065	3.045
37.5	3.355	3.551	3.748	3.947	4.147	4.348	4.548	4.748	4.947	4.548	5.311	5.527	5.714	5.896	6.057	6.171	6.238	6.261	6.241	6.179	6.078
31.5	3.736	3.907	4.075	4.240	4.401	4.558	4.708	4.853	4.989	4.708	5.058	5.181	5.163	5.107	5.027	4.943	4.858	4.771	4.685	4.599	4.515
26.5	4.340	4.496	4.645	4.789	4.925	5.053	5.173	5.284	5.384	5.173	5.302	5.382	5.274	5.119	4.944	4.785	4.642	4.514	4.402	4.304	4.220
22.4	4.628	4.753	4.869	4.975	5.071	5.135	5.139	5.088	4.984	5.139	4.703	4.628	4.513	4.402	4.297	4.201	4.115	4.039	3.971	3.912	3.862
19	4.907	5.003	5.090	5.165	5.230	5.254	5.205	5.088	4.911	5.205	4.555	4.429	4.307	4.204	4.113	4.031	3.958	3.892	3.834	3.783	3.740
16	4.530	4.555	4.559	4.503	4.390	4.248	4.105	3.963	3.823	4.105	3.605	3.482	3.396	3.324	3.261	3.203	3.152	3.106	3.066	3.031	3.002
13.2	4.836	4.819	4.775	4.644	4.433	4.198	3.999	3.833	3.697	3.999	3.522	3.389	3.312	3.247	3.190	3.139	3.093	3.052	3.016	2.985	2.958
11.2	4.420	4.327	4.164	4.007	3.863	3.735	3.627	3.537	3.465	3.627	3.378	3.301	3.261	3.226	3.197	3.170	3.146	3.124	3.105	3.089	3.075
9.5	4.456	4.336	4.142	3.972	3.835	3.723	3.628	3.550	3.486	3.628	3.412	3.344	3.309	3.279	3.253	3.230	3.209	3.191	3.174	3.160	3.148
8	4.564	4.406	4.261	4.140	4.043	3.965	3.898	3.843	3.800	3.898	3.738	3.701	3.676	3.655	3.637	3.621	3.606	3.592	3.580	3.570	3.561
6.3	6.013	5.789	5.626	5.495	5.391	5.305	5.234	5.175	5.128	5.234	5.054	5.021	4.994	4.971	4.951	4.933	4.917	4.902	4.888	4.876	4.866
4.75	5.501	5.347	5.236	5.148	5.078	5.021	4.973	4.932	4.900	4.973	4.826	4.824	4.804	4.787	4.772	4.758	4.745	4.733	4.723	4.713	4.704
3.35	8.529	8.413	8.330	8.263	8.209	8.164	8.126	8.093	8.066	8.126	8.002	8.000	7.983	7.967	7.953	7.940	7.927	7.916	7.906	7.896	7.888
2.36	7.573	7.507	7.458	7.417	7.383	7.354	7.329	7.306	7.287	7.329	7.279	7.238	7.225	7.212	7.201	7.190	7.180	7.171	7.163	7.155	7.147
1.18	8.045	7.974	7.917	7.867	7.823	7.785	7.750	7.718	7.690	7.750	7.829	7.618	7.598	7.580	7.563	7.547	7.532	7.518	7.506	7.495	7.484
0.6	4.554	4.513	4.478	4.448	4.420	4.396	4.374	4.354	4.337	4.374	4.486	4.296	4.285	4.274	4.265	4.257	4.249	4.242	4.235	4.229	4.224
0.3	1.383	1.358	1.336	1.318	1.302	1.288	1.275	1.264	1.254	1.275	1.286	1.230	1.223	1.216	1.210	1.205	1.199	1.195	1.190	1.186	1.182
0.15	0.661	0.645	0.632	0.621	0.610	0.601	0.592	0.584	0.577	0.592	0.535	0.559	0.554	0.549	0.545	0.541	0.537	0.533	0.530	0.526	0.524
0	9.967	9.923	9.884	9.850	9.818	9.790	9.764	9.741	9.719	9.764	9.366	9.665	9.649	9.635	9.621	9.609	9.597	9.586	9.576	9.566	9.557

CSS (mm)	52	54	56	58	60	62	64	66	68	70	72	74	76
Size (mm)	% retained												
460	0.000	0.000	0.000	0.000	0.000	0.000	0.000	0.000	0.000	0.000	0.000	0.000	0.000
290	0.000	0.000	0.000	0.000	0.000	0.000	0.000	0.000	0.000	0.000	0.000	0.000	0.000
230	0.000	0.000	0.000	0.000	0.000	0.000	0.000	0.000	0.000	0.000	0.000	0.000	0.000
145	0.000	0.001	0.002	0.004	0.007	0.011	0.015	0.021	0.028	0.037	0.048	0.061	0.076
115	0.205	0.170	0.214	0.263	0.317	0.376	0.440	0.510	0.586	0.667	0.755	0.848	0.947
87	1.680	1.911	2.076	2.248	2.426	2.612	2.803	3.000	3.203	3.411	3.624	3.840	4.050
50	9.877	10.200	10.480	10.720	10.920	11.090	11.210	11.290	11.340	11.350	11.330	11.280	11.210
45	3.006	2.964	2.921	2.880	2.840	2.802	2.765	2.730	2.697	2.666	2.637	2.610	2.583
37.5	5.943	5.807	5.680	5.562	5.452	5.349	5.254	5.165	5.083	5.008	4.938	4.873	4.811
31.5	4.432	4.354	4.281	4.213	4.149	4.089	4.034	3.983	3.935	3.892	3.852	3.814	3.778
26.5	4.148	4.083	4.021	3.963	3.909	3.858	3.811	3.767	3.727	3.689	3.655	3.623	3.592
22.4	3.820	3.781	3.744	3.710	3.678	3.648	3.620	3.594	3.570	3.548	3.528	3.509	3.492
19	3.704	3.671	3.640	3.611	3.583	3.558	3.534	3.512	3.492	3.474	3.457	3.441	3.426
16	2.977	2.954	2.933	2.913	2.894	2.877	2.861	2.846	2.832	2.819	2.807	2.796	2.786
13.2	2.937	2.916	2.898	2.880	2.863	2.848	2.833	2.820	2.807	2.796	2.785	2.775	2.766
11.2	3.063	3.052	3.042	3.033	3.024	3.015	3.007	3.000	2.993	2.986	2.980	2.975	2.969
9.5	3.137	3.128	3.119	3.110	3.102	3.095	3.088	3.081	3.075	3.069	3.064	3.059	3.054
8	3.553	3.546	3.539	3.533	3.527	3.521	3.516	3.510	3.506	3.501	3.497	3.493	3.489
6.3	4.857	4.849	4.841	4.833	4.826	4.819	4.813	4.807	4.801	4.795	4.790	4.785	4.780
4.75	4.697	4.690	4.683	4.676	4.670	4.664	4.658	4.652	4.647	4.641	4.636	4.632	4.627
3.35	7.880	7.872	7.865	7.858	7.851	7.845	7.838	7.832	7.826	7.821	7.815	7.810	7.805
2.36	7.140	7.134	7.128	7.122	7.116	7.110	7.105	7.100	7.095	7.090	7.086	7.081	7.077
1.18	7.475	7.466	7.458	7.450	7.443	7.436	7.429	7.422	7.416	7.410	7.405	7.400	7.395
0.6	4.219	4.215	4.210	4.206	4.202	4.198	4.194	4.191	4.187	4.184	4.181	4.178	4.175
0.3	1.178	1.175	1.172	1.169	1.166	1.163	1.160	1.157	1.154	1.152	1.149	1.147	1.145
0.15	0.521	0.518	0.516	0.513	0.511	0.509	0.507	0.505	0.503	0.501	0.499	0.497	0.495
0	9.549	9.542	9.534	9.527	9.520	9.513	9.507	9.501	9.495	9.489	9.483	9.478	9.473

Jaw crusher – hard talc

Table 46: Product PSDs for hard talc entering a jaw crusher with variable CSSs. Power data is shown and values were calculated using JKSimMet; continued overleaf.

Jaw crusher

CSS (mm)	10	12	14	16	18	20	22	24	26	28	30	32	34	36	38	40	42	44	46	48	50
Size (mm)	% retained																				
460	0.000	0.000	0.000	0.000	0.000	0.000	0.000	0.000	0.000	0.000	0.000	0.000	0.000	0.000	0.000	0.000	0.000	0.000	0.000	0.000	0.000
290	0.000	0.000	0.000	0.000	0.000	0.000	0.000	0.000	0.000	0.000	0.000	0.000	0.000	0.000	0.000	0.000	0.000	0.000	0.000	0.000	0.000
230	0.000	0.000	0.000	0.000	0.000	0.000	0.000	0.000	0.000	0.000	0.000	0.000	0.000	0.000	0.000	0.000	0.000	0.000	0.000	0.000	0.000
145	0.000	0.000	0.000	0.000	0.000	0.000	0.000	0.000	0.000	0.000	0.000	0.000	0.000	0.000	0.000	0.000	0.000	0.000	0.000	0.000	0.000
115	0.001	0.001	0.001	0.001	0.001	0.002	0.003	0.005	0.007	0.011	0.016	0.022	0.030	0.040	0.052	0.066	0.084	0.104	0.128	0.156	0.189
87	0.036	0.055	0.079	0.108	0.142	0.182	0.227	0.279	0.338	0.403	0.476	0.556	0.644	0.740	0.843	0.954	1.073	1.201	1.336	1.479	1.630
50	2.790	3.064	3.349	3.647	3.956	4.276	4.606	4.946	5.293	5.649	6.011	6.379	6.751	7.127	7.503	7.877	8.248	8.613	8.972	9.324	9.666
45	1.430	1.530	1.631	1.734	1.839	1.944	2.050	2.156	2.262	2.367	2.472	2.575	2.677	2.778	2.869	2.941	2.995	3.029	3.044	3.041	3.019
37.5	3.504	3.697	3.891	4.084	4.278	4.469	4.660	4.847	5.032	5.213	5.390	5.562	5.729	5.890	6.029	6.124	6.176	6.187	6.159	6.095	5.995
31.5	3.839	4.001	4.158	4.311	4.458	4.599	4.734	4.861	4.980	5.069	5.118	5.131	5.107	5.048	4.968	4.886	4.802	4.718	4.634	4.551	4.470
26.5	4.416	4.558	4.693	4.820	4.939	5.050	5.151	5.243	5.324	5.364	5.351	5.290	5.183	5.035	4.870	4.720	4.585	4.464	4.358	4.265	4.184
22.4	4.652	4.760	4.859	4.948	5.027	5.075	5.070	5.014	4.912	4.796	4.682	4.570	4.461	4.355	4.255	4.165	4.084	4.011	3.947	3.891	3.843
19	4.899	4.979	5.048	5.107	5.155	5.167	5.112	4.998	4.831	4.660	4.510	4.378	4.263	4.165	4.079	4.002	3.932	3.869	3.814	3.766	3.725
16	4.473	4.486	4.478	4.417	4.307	4.171	4.035	3.901	3.769	3.648	3.541	3.448	3.367	3.298	3.238	3.183	3.135	3.091	3.053	3.019	2.991
13.2	4.745	4.718	4.665	4.537	4.338	4.119	3.933	3.777	3.650	3.541	3.444	3.360	3.286	3.224	3.170	3.121	3.078	3.039	3.004	2.974	2.949
11.2	4.339	4.247	4.094	3.947	3.812	3.693	3.592	3.508	3.440	3.381	3.330	3.285	3.246	3.214	3.185	3.160	3.137	3.116	3.098	3.082	3.068
9.5	4.372	4.257	4.077	3.920	3.792	3.687	3.598	3.524	3.465	3.414	3.369	3.330	3.296	3.268	3.243	3.221	3.201	3.183	3.167	3.153	3.141
8	4.497	4.350	4.215	4.103	4.012	3.938	3.876	3.824	3.783	3.747	3.716	3.689	3.665	3.645	3.628	3.612	3.598	3.585	3.573	3.563	3.554
6.3	5.934	5.727	5.576	5.454	5.356	5.276	5.209	5.153	5.109	5.070	5.036	5.007	4.981	4.959	4.940	4.922	4.906	4.892	4.879	4.867	4.857
4.75	5.444	5.301	5.199	5.116	5.050	4.996	4.950	4.912	4.881	4.854	4.830	4.808	4.790	4.773	4.758	4.745	4.732	4.721	4.711	4.701	4.693
3.35	8.480	8.372	8.294	8.231	8.180	8.137	8.101	8.070	8.044	8.021	8.000	7.981	7.964	7.949	7.936	7.923	7.912	7.901	7.891	7.882	7.873
2.36	7.536	7.474	7.428	7.390	7.358	7.330	7.306	7.284	7.266	7.249	7.234	7.220	7.207	7.196	7.185	7.175	7.166	7.157	7.149	7.141	7.134
1.18	7.988	7.921	7.868	7.821	7.781	7.744	7.712	7.682	7.656	7.632	7.610	7.590	7.571	7.554	7.538	7.524	7.510	7.498	7.486	7.476	7.466
0.6	4.516	4.479	4.447	4.419	4.394	4.372	4.352	4.335	4.319	4.305	4.293	4.282	4.271	4.262	4.254	4.246	4.239	4.233	4.227	4.221	4.217
0.3	1.364	1.341	1.322	1.305	1.291	1.278	1.267	1.257	1.248	1.240	1.232	1.226	1.219	1.213	1.208	1.203	1.198	1.193	1.189	1.185	1.181
0.15	0.655	0.641	0.630	0.619	0.609	0.601	0.593	0.585	0.579	0.573	0.567	0.561	0.557	0.552	0.548	0.544	0.540	0.536	0.533	0.530	0.527
0	10.090	10.040	9.998	9.960	9.926	9.894	9.865	9.838	9.814	9.792	9.771	9.752	9.734	9.717	9.701	9.687	9.673	9.660	9.648	9.637	9.626

CSS (mm)	52	54	56	58	60	62	64	66	68	70	72	74	76
Size (mm)	% retained												
460	0.000	0.000	0.000	0.000	0.000	0.000	0.000	0.000	0.000	0.000	0.000	0.000	0.000
290	0.000	0.000	0.000	0.000	0.000	0.000	0.000	0.000	0.000	0.000	0.000	0.000	0.000
230	0.000	0.000	0.000	0.000	0.000	0.000	0.000	0.000	0.000	0.000	0.000	0.000	0.000
145	0.000	0.001	0.003	0.005	0.008	0.011	0.017	0.023	0.031	0.041	0.053	0.067	0.083
115	0.226	0.185	0.233	0.286	0.344	0.408	0.477	0.552	0.633	0.720	0.813	0.912	1.017
87	1.788	2.035	2.206	2.383	2.566	2.756	2.950	3.149	3.353	3.561	3.773	3.985	4.192
50	9.996	10.290	10.550	10.760	10.940	11.080	11.180	11.240	11.280	11.270	11.240	11.180	11.100
45	2.980	2.938	2.897	2.857	2.818	2.781	2.746	2.712	2.680	2.650	2.621	2.594	2.568
37.5	5.865	5.735	5.615	5.502	5.396	5.298	5.206	5.121	5.042	4.969	4.902	4.838	4.778
31.5	4.391	4.316	4.246	4.181	4.119	4.062	4.009	3.960	3.914	3.872	3.833	3.796	3.761
26.5	4.116	4.053	3.994	3.938	3.886	3.837	3.791	3.749	3.710	3.673	3.640	3.608	3.578
22.4	3.802	3.764	3.729	3.696	3.665	3.636	3.609	3.584	3.561	3.540	3.520	3.502	3.484
19	3.690	3.658	3.628	3.599	3.573	3.548	3.526	3.504	3.485	3.467	3.450	3.435	3.420
16	2.967	2.945	2.925	2.905	2.887	2.870	2.854	2.840	2.826	2.814	2.802	2.791	2.781
13.2	2.928	2.908	2.890	2.872	2.856	2.841	2.827	2.814	2.802	2.791	2.780	2.771	2.761
11.2	3.057	3.046	3.036	3.027	3.018	3.010	3.002	2.995	2.988	2.982	2.976	2.970	2.965
9.5	3.131	3.122	3.113	3.105	3.097	3.090	3.083	3.077	3.071	3.065	3.060	3.055	3.050
8	3.547	3.540	3.533	3.527	3.521	3.515	3.510	3.505	3.500	3.496	3.492	3.488	3.484
6.3	4.849	4.841	4.833	4.825	4.818	4.812	4.805	4.799	4.794	4.788	4.783	4.778	4.773
4.75	4.686	4.679	4.672	4.666	4.659	4.654	4.648	4.642	4.637	4.632	4.627	4.623	4.618
3.35	7.866	7.859	7.852	7.845	7.839	7.832	7.826	7.820	7.815	7.809	7.804	7.799	7.794
2.36	7.128	7.122	7.116	7.110	7.105	7.099	7.094	7.089	7.085	7.080	7.076	7.072	7.068
1.18	7.458	7.450	7.442	7.435	7.428	7.421	7.415	7.409	7.403	7.398	7.393	7.388	7.384
0.6	4.212	4.208	4.204	4.200	4.196	4.193	4.189	4.186	4.183	4.179	4.176	4.173	4.171
0.3	1.178	1.175	1.172	1.168	1.166	1.163	1.160	1.157	1.155	1.152	1.150	1.148	1.145
0.15	0.524	0.522	0.519	0.517	0.515	0.512	0.510	0.508	0.506	0.504	0.502	0.500	0.499
0	9.617	9.607	9.599	9.590	9.582	9.573	9.566	9.558	9.551	9.544	9.537	9.530	9.524

CSS (mm)	Calculated Power (kW)
10	128.748
12	126.313
14	124.147
16	122.185
18	120.399
20	118.731
22	117.200
24	115.797
26	114.482
28	113.264
30	112.128
32	111.043
34	110.033
36	109.094
38	108.192
40	107.347
42	106.557

CSS (mm)	Calculated Power (kW)
44	105.796
46	105.087
48	104.427
50	103.795
52	103.210
54	102.652
56	102.098
58	101.566
60	101.056
62	100.547
64	100.059
66	99.590
68	99.122
70	98.672
72	98.239
74	97.805
76	97.387

Jaw crusher – lead-zinc ore

Table 47: Product PSDs for lead-zinc ore entering a jaw crusher with variable CSSs. Power data is shown and values were calculated using JKSimMet; continued overleaf.

Jaw crusher

CSS (mm)	10	12	14	16	18	20	22	24	26	28	30	32	34	36	38	40	42	44	46	48	50
Size (mm)	% retained																				
460	0.000	0.000	0.000	0.000	0.000	0.000	0.000	0.000	-	0.000	0.000	0.000	0.000	0.000	0.000	0.000	0.000	0.000	0.000	0.000	0.000
290	0.000	0.000	0.000	0.000	0.000	0.000	0.000	0.000	-	0.000	0.000	0.000	0.000	0.000	0.000	0.000	0.000	0.000	0.000	0.000	0.000
230	0.000	0.000	0.000	0.000	0.000	0.000	0.000	0.000	-	0.000	0.000	0.000	0.000	0.000	0.000	0.000	0.000	0.000	0.000	0.000	0.000
145	0.000	0.000	0.000	0.000	0.000	0.000	0.000	0.000	-	0.000	0.000	0.000	0.000	0.000	0.000	0.000	0.000	0.000	0.000	0.000	0.000
115	0.001	0.001	0.001	0.001	0.001	0.002	0.003	0.005	-	0.011	0.016	0.023	0.031	0.041	0.053	0.068	0.086	0.108	0.133	0.161	0.195
87	0.035	0.054	0.077	0.105	0.138	0.177	0.221	0.272	-	0.393	0.463	0.541	0.625	0.717	0.817	0.924	1.038	1.160	1.289	1.426	1.569
50	2.652	2.910	3.179	3.459	3.749	4.049	4.358	4.675	-	5.331	5.669	6.010	6.356	6.705	7.053	7.400	7.743	8.081	8.413	8.739	9.055
45	1.382	1.477	1.574	1.673	1.772	1.873	1.974	2.075	-	2.278	2.378	2.478	2.576	2.673	2.762	2.833	2.888	2.926	2.947	2.951	2.938
37.5	3.409	3.595	3.781	3.967	4.152	4.337	4.520	4.701	-	5.053	5.224	5.391	5.554	5.711	5.848	5.946	6.004	6.025	6.011	5.963	5.883
31.5	3.710	3.866	4.019	4.168	4.312	4.451	4.585	4.712	-	4.927	4.985	5.010	5.002	4.963	4.903	4.840	4.774	4.706	4.637	4.568	4.499
26.5	4.265	4.404	4.537	4.663	4.783	4.896	5.000	5.097	-	5.235	5.237	5.195	5.112	4.990	4.851	4.724	4.610	4.506	4.414	4.333	4.261
22.4	4.529	4.641	4.745	4.841	4.928	4.988	4.998	4.962	-	4.789	4.695	4.601	4.507	4.415	4.327	4.246	4.173	4.107	4.049	3.996	3.951
19	4.793	4.880	4.958	5.027	5.087	5.113	5.078	4.987	-	4.699	4.568	4.452	4.349	4.260	4.181	4.109	4.044	3.985	3.932	3.886	3.845
16	4.413	4.440	4.449	4.409	4.322	4.208	4.092	3.974	-	3.745	3.647	3.560	3.483	3.416	3.357	3.303	3.254	3.210	3.171	3.136	3.106
13.2	4.708	4.700	4.669	4.566	4.396	4.204	4.038	3.897	-	3.674	3.582	3.499	3.427	3.364	3.308	3.257	3.211	3.170	3.133	3.100	3.071
11.2	4.378	4.304	4.170	4.038	3.914	3.802	3.705	3.622	-	3.493	3.439	3.392	3.350	3.313	3.281	3.251	3.225	3.201	3.179	3.160	3.143
9.5	4.434	4.337	4.174	4.028	3.907	3.805	3.717	3.642	-	3.525	3.476	3.433	3.395	3.362	3.333	3.307	3.283	3.261	3.241	3.224	3.209
8	4.596	4.460	4.330	4.220	4.128	4.050	3.984	3.927	-	3.839	3.802	3.770	3.741	3.716	3.694	3.674	3.655	3.639	3.624	3.611	3.599
6.3	6.089	5.890	5.738	5.611	5.506	5.418	5.342	5.277	-	5.177	5.135	5.098	5.065	5.036	5.011	4.988	4.967	4.948	4.931	4.915	4.902
4.75	5.618	5.467	5.351	5.256	5.176	5.109	5.052	5.003	-	4.926	4.893	4.865	4.839	4.817	4.797	4.779	4.762	4.747	4.733	4.721	4.710
3.35	8.642	8.516	8.421	8.342	8.275	8.220	8.171	8.130	-	8.064	8.037	8.012	7.990	7.970	7.953	7.937	7.922	7.909	7.897	7.886	7.877
2.36	7.639	7.560	7.500	7.450	7.407	7.371	7.340	7.313	-	7.269	7.251	7.234	7.219	7.206	7.194	7.183	7.173	7.164	7.156	7.148	7.141
1.18	8.086	8.003	7.938	7.883	7.836	7.795	7.759	7.728	-	7.677	7.655	7.635	7.617	7.600	7.585	7.572	7.559	7.547	7.536	7.526	7.517
0.6	4.580	4.540	4.507	4.479	4.454	4.432	4.412	4.394	-	4.364	4.351	4.339	4.327	4.317	4.307	4.298	4.290	4.282	4.274	4.267	4.261
0.3	1.427	1.402	1.381	1.362	1.344	1.329	1.315	1.302	-	1.279	1.270	1.260	1.252	1.244	1.237	1.230	1.224	1.218	1.213	1.208	1.203
0.15	0.694	0.676	0.661	0.647	0.634	0.623	0.613	0.604	-	0.588	0.581	0.574	0.568	0.563	0.558	0.553	0.549	0.544	0.541	0.537	0.534
0	9.922	9.878	9.841	9.807	9.777	9.749	9.724	9.702	-	9.663	9.646	9.630	9.615	9.602	9.589	9.577	9.566	9.556	9.547	9.538	9.530

CSS (mm)	52	54	56	58	60	62	64	66	68	70	72	74	76
Size (mm)	% retained												
460	0.000	0.000	0.000	0.000	0.000	0.000	0.000	0.000	0.000	0.000	0.000	0.000	0.000
290	0.000	0.000	0.000	0.000	0.000	0.000	0.000	0.000	0.000	0.000	0.000	0.000	0.000
230	0.000	0.000	0.000	0.000	0.000	0.000	0.000	0.000	0.000	0.000	0.000	0.000	0.000
145	0.000	0.001	0.003	0.005	0.008	0.012	0.017	0.023	0.031	0.041	0.053	0.067	0.083
115	0.233	0.184	0.231	0.284	0.341	0.404	0.472	0.546	0.626	0.711	0.802	0.899	1.001
87	1.719	1.967	2.130	2.298	2.472	2.651	2.835	3.023	3.215	3.410	3.609	3.807	4.000
50	9.361	9.636	9.875	10.080	10.250	10.390	10.490	10.570	10.610	10.620	10.610	10.570	10.520
45	2.910	2.879	2.848	2.817	2.787	2.758	2.729	2.702	2.676	2.651	2.627	2.604	2.582
37.5	5.775	5.667	5.565	5.470	5.380	5.295	5.216	5.142	5.073	5.008	4.947	4.889	4.834
31.5	4.430	4.364	4.302	4.244	4.190	4.138	4.090	4.044	4.002	3.962	3.924	3.889	3.855
26.5	4.200	4.142	4.088	4.037	3.988	3.942	3.899	3.859	3.820	3.785	3.751	3.720	3.689
22.4	3.911	3.875	3.840	3.807	3.776	3.747	3.719	3.693	3.669	3.646	3.624	3.604	3.585
19	3.810	3.777	3.746	3.717	3.689	3.663	3.639	3.616	3.594	3.574	3.555	3.537	3.520
16	3.079	3.055	3.032	3.010	2.990	2.970	2.952	2.935	2.919	2.903	2.889	2.876	2.863
13.2	3.047	3.024	3.002	2.982	2.962	2.944	2.927	2.910	2.895	2.881	2.867	2.855	2.842
11.2	3.129	3.116	3.103	3.091	3.079	3.069	3.058	3.049	3.040	3.031	3.023	3.016	3.008
9.5	3.196	3.184	3.172	3.162	3.151	3.141	3.132	3.123	3.115	3.107	3.100	3.093	3.087
8	3.589	3.580	3.571	3.562	3.554	3.547	3.539	3.533	3.526	3.520	3.514	3.509	3.504
6.3	4.890	4.879	4.869	4.859	4.849	4.840	4.832	4.824	4.816	4.809	4.802	4.796	4.790
4.75	4.700	4.692	4.683	4.675	4.667	4.660	4.653	4.647	4.640	4.634	4.629	4.624	4.618
3.35	7.868	7.860	7.853	7.846	7.839	7.832	7.826	7.820	7.814	7.809	7.804	7.799	7.794
2.36	7.135	7.130	7.124	7.119	7.114	7.109	7.105	7.101	7.096	7.092	7.089	7.085	7.081
1.18	7.509	7.501	7.494	7.486	7.479	7.472	7.466	7.459	7.453	7.447	7.442	7.436	7.431
0.6	4.255	4.250	4.244	4.239	4.234	4.230	4.225	4.220	4.216	4.212	4.208	4.204	4.200
0.3	1.199	1.195	1.191	1.187	1.184	1.180	1.177	1.174	1.170	1.167	1.164	1.162	1.159
0.15	0.531	0.528	0.525	0.522	0.520	0.517	0.515	0.513	0.510	0.508	0.506	0.504	0.502
0	9.523	9.516	9.509	9.502	9.496	9.490	9.484	9.478	9.473	9.468	9.462	9.457	9.453

CSS (mm)	Calculated Power (kW)
10	127.872
12	125.488
14	123.371
16	121.456
18	119.714
20	118.089
22	116.598
24	115.233
26	113.954
28	112.771
30	111.669
32	110.616
34	109.636
36	108.725
38	107.853
40	107.036
42	106.272

CSS (mm)	Calculated Power (kW)
44	105.537
46	104.852
48	104.216
50	103.606
52	103.042
54	102.506
56	101.971
58	101.458
60	100.964
62	100.472
64	99.999
66	99.543
68	99.088
70	98.650
72	98.228
74	97.805
76	97.398

Jaw crusher – porphyry copper

Table 48: Product PSDs for porphyry copper entering a jaw crusher with variable CSSs. Power data is shown and values were calculated using JKSimMet; continued overleaf.

Jaw crusher

CSS (mm)	10	12	14	16	18	20	22	24	26	28	30	32	34	36	38	40	42	44	46	48	50
Size (mm)	% retained																				
460	0.000	0.000	0.000	0.000	0.000	0.000	0.000	0.000	0.000	0.000	0.000	0.000	0.000	0.000	0.000	0.000	0.000	0.000	0.000	0.000	0.000
290	0.000	0.000	0.000	0.000	0.000	0.000	0.000	0.000	0.000	0.000	0.000	0.000	0.000	0.000	0.000	0.000	0.000	0.000	0.000	0.000	0.000
230	0.000	0.000	0.000	0.000	0.000	0.000	0.000	0.000	0.000	0.000	0.000	0.000	0.000	0.000	0.000	0.000	0.000	0.000	0.000	0.000	0.000
145	0.000	0.000	0.000	0.000	0.000	0.000	0.000	0.000	0.000	0.000	0.000	0.000	0.000	0.000	0.000	0.000	0.000	0.000	0.000	0.000	0.000
115	0.001	0.001	0.001	0.001	0.001	0.002	0.003	0.004	0.007	0.010	0.014	0.020	0.027	0.036	0.047	0.061	0.076	0.095	0.117	0.143	0.172
87	0.032	0.050	0.071	0.097	0.128	0.164	0.205	0.252	0.306	0.365	0.432	0.505	0.585	0.672	0.767	0.869	0.979	1.097	1.222	1.355	1.496
50	2.543	2.796	3.062	3.340	3.630	3.931	4.243	4.566	4.898	5.239	5.589	5.946	6.310	6.680	7.053	7.427	7.799	8.170	8.537	8.899	9.255
45	1.335	1.432	1.531	1.633	1.737	1.842	1.949	2.058	2.167	2.276	2.386	2.496	2.606	2.715	2.815	2.898	2.960	3.004	3.027	3.031	3.016
37.5	3.310	3.502	3.697	3.893	4.091	4.289	4.487	4.685	4.881	5.076	5.268	5.458	5.644	5.826	5.987	6.103	6.174	6.203	6.189	6.136	6.044
31.5	3.681	3.850	4.017	4.182	4.342	4.499	4.650	4.796	4.935	5.044	5.113	5.142	5.132	5.085	5.014	4.940	4.862	4.784	4.704	4.624	4.545
26.5	4.279	4.434	4.584	4.728	4.866	4.996	5.119	5.233	5.337	5.400	5.405	5.358	5.261	5.118	4.955	4.806	4.672	4.552	4.445	4.352	4.272
22.4	4.584	4.712	4.831	4.942	5.044	5.114	5.127	5.084	4.992	4.881	4.771	4.662	4.554	4.448	4.348	4.256	4.173	4.099	4.033	3.976	3.926
19	4.873	4.974	5.066	5.147	5.219	5.251	5.211	5.105	4.939	4.768	4.616	4.482	4.365	4.265	4.177	4.097	4.025	3.960	3.902	3.852	3.809
16	4.522	4.556	4.568	4.522	4.420	4.288	4.153	4.018	3.883	3.758	3.648	3.550	3.466	3.393	3.329	3.272	3.220	3.173	3.131	3.095	3.064
13.2	4.843	4.837	4.803	4.685	4.486	4.262	4.070	3.909	3.777	3.662	3.560	3.471	3.393	3.326	3.267	3.214	3.166	3.123	3.085	3.052	3.024
11.2	4.460	4.375	4.220	4.068	3.927	3.801	3.694	3.604	3.530	3.466	3.410	3.360	3.317	3.280	3.248	3.218	3.192	3.168	3.147	3.128	3.113
9.5	4.506	4.394	4.205	4.040	3.904	3.791	3.695	3.615	3.549	3.493	3.443	3.399	3.361	3.328	3.300	3.274	3.250	3.229	3.211	3.194	3.180
8	4.629	4.473	4.328	4.207	4.107	4.025	3.955	3.897	3.850	3.809	3.772	3.740	3.712	3.689	3.668	3.649	3.631	3.616	3.602	3.590	3.579
6.3	6.103	5.880	5.714	5.579	5.468	5.377	5.300	5.236	5.183	5.138	5.097	5.062	5.031	5.004	4.980	4.959	4.939	4.922	4.906	4.892	4.880
4.75	5.590	5.428	5.309	5.212	5.134	5.069	5.013	4.966	4.928	4.895	4.865	4.838	4.815	4.794	4.776	4.759	4.744	4.730	4.718	4.707	4.697
3.35	8.597	8.470	8.376	8.299	8.236	8.183	8.138	8.099	8.067	8.039	8.013	7.990	7.970	7.952	7.936	7.921	7.908	7.895	7.884	7.874	7.865
2.36	7.598	7.522	7.465	7.417	7.377	7.344	7.314	7.289	7.267	7.248	7.230	7.215	7.200	7.188	7.176	7.166	7.156	7.147	7.138	7.131	7.124
1.18	8.021	7.941	7.879	7.826	7.780	7.741	7.706	7.675	7.648	7.624	7.602	7.582	7.564	7.548	7.533	7.519	7.506	7.494	7.484	7.474	7.465
0.6	4.517	4.478	4.446	4.418	4.394	4.372	4.353	4.336	4.322	4.308	4.296	4.285	4.275	4.266	4.258	4.250	4.243	4.236	4.230	4.225	4.220
0.3	1.367	1.344	1.325	1.308	1.294	1.281	1.269	1.258	1.249	1.241	1.233	1.225	1.219	1.212	1.207	1.201	1.196	1.191	1.187	1.183	1.179
0.15	0.655	0.640	0.627	0.616	0.606	0.597	0.588	0.581	0.574	0.568	0.562	0.556	0.551	0.547	0.542	0.538	0.534	0.531	0.528	0.524	0.522
0	9.955	9.912	9.874	9.840	9.809	9.781	9.756	9.733	9.712	9.693	9.675	9.659	9.643	9.629	9.616	9.604	9.592	9.581	9.571	9.562	9.554

CSS (mm)	52	54	56	58	60	62	64	66	68	70	72	74	76
Size (mm)	% retained												
460	0.000	0.000	0.000	0.000	0.000	0.000	0.000	0.000	0.000	0.000	0.000	0.000	0.000
290	0.000	0.000	0.000	0.000	0.000	0.000	0.000	0.000	0.000	0.000	0.000	0.000	0.000
230	0.000	0.000	0.000	0.000	0.000	0.000	0.000	0.000	0.000	0.000	0.000	0.000	0.000
145	0.000	0.001	0.002	0.004	0.007	0.010	0.015	0.021	0.028	0.037	0.048	0.061	0.076
115	0.206	0.168	0.212	0.260	0.313	0.372	0.436	0.505	0.579	0.660	0.746	0.838	0.936
87	1.645	1.875	2.036	2.204	2.378	2.559	2.745	2.937	3.135	3.338	3.545	3.754	3.959
50	9.603	9.917	10.190	10.430	10.630	10.790	10.920	11.010	11.060	11.080	11.070	11.030	10.970
45	2.982	2.944	2.907	2.870	2.834	2.799	2.766	2.734	2.704	2.675	2.648	2.622	2.597
37.5	5.919	5.793	5.675	5.564	5.461	5.364	5.274	5.191	5.113	5.041	4.974	4.911	4.851
31.5	4.467	4.393	4.323	4.258	4.196	4.139	4.086	4.036	3.990	3.947	3.907	3.870	3.834
26.5	4.204	4.140	4.080	4.024	3.971	3.921	3.875	3.831	3.791	3.753	3.719	3.686	3.655
22.4	3.884	3.845	3.808	3.773	3.741	3.710	3.682	3.655	3.630	3.607	3.586	3.566	3.547
19	3.772	3.738	3.706	3.676	3.648	3.621	3.596	3.573	3.551	3.532	3.513	3.496	3.479
16	3.038	3.014	2.991	2.970	2.949	2.930	2.912	2.896	2.880	2.866	2.853	2.840	2.828
13.2	3.000	2.978	2.957	2.937	2.918	2.901	2.885	2.869	2.855	2.842	2.830	2.818	2.807
11.2	3.099	3.087	3.075	3.064	3.053	3.043	3.034	3.025	3.017	3.009	3.002	2.995	2.989
9.5	3.168	3.157	3.147	3.137	3.127	3.118	3.110	3.102	3.095	3.088	3.081	3.075	3.069
8	3.570	3.561	3.553	3.546	3.538	3.532	3.525	3.519	3.513	3.508	3.503	3.498	3.493
6.3	4.869	4.859	4.850	4.841	4.832	4.824	4.817	4.810	4.803	4.796	4.790	4.785	4.779
4.75	4.688	4.680	4.672	4.665	4.658	4.651	4.644	4.638	4.633	4.627	4.622	4.617	4.612
3.35	7.857	7.849	7.842	7.835	7.828	7.822	7.816	7.810	7.804	7.799	7.794	7.789	7.784
2.36	7.118	7.112	7.107	7.102	7.097	7.092	7.087	7.083	7.079	7.075	7.071	7.067	7.063
1.18	7.457	7.450	7.443	7.436	7.430	7.424	7.418	7.412	7.407	7.402	7.397	7.392	7.388
0.6	4.215	4.211	4.207	4.203	4.199	4.195	4.192	4.188	4.185	4.181	4.178	4.175	4.172
0.3	1.176	1.173	1.169	1.166	1.163	1.161	1.158	1.155	1.153	1.150	1.148	1.145	1.143
0.15	0.519	0.517	0.514	0.512	0.510	0.508	0.505	0.503	0.502	0.500	0.498	0.496	0.494
0	9.546	9.538	9.531	9.524	9.517	9.511	9.504	9.498	9.493	9.487	9.481	9.476	9.471

CSS (mm)	Calculated Power (kW)
10	125.283
12	122.963
14	120.909
16	119.054
18	117.370
20	115.801
22	114.363
24	113.048
26	111.819
28	110.681
30	109.622
32	108.611
34	107.671
36	106.800
38	105.965
40	105.182
42	104.450

CSS (mm)	Calculated Power (kW)
44	103.747
46	103.093
48	102.487
50	101.909
52	101.375
54	100.867
56	100.361
58	99.875
60	99.409
62	98.944
64	98.499
66	98.071
68	97.644
70	97.235
72	96.841
74	96.446
76	96.065

Jaw crusher – copper carbonatitie

Table 49: Product PSDs for copper carbonatitie entering a jaw crusher with variable CSSs. Values were calculated using JKSimMet; continued overleaf.

Jaw crusher

CSS (mm)	10	12	14	16	18	20	22	24	26	28	30	32	34	36	38	40	42	44	46	48	50
Size (mm)	% retained																				
460	0.000	0.000	0.000	0.000	0.000	0.000	0.000	0.000	0.000	0.000	0.000	0.000	0.000	0.000	0.000	0.000	0.000	0.000	0.000	0.000	0.000
290	0.000	0.000	0.000	0.000	0.000	0.000	0.000	0.000	0.000	0.000	0.000	0.000	0.000	0.000	0.000	0.000	0.000	0.000	0.000	0.000	0.000
230	0.000	0.000	0.000	0.000	0.000	0.000	0.000	0.000	0.000	0.000	0.000	0.000	0.000	0.000	0.000	0.000	0.000	0.000	0.000	0.000	0.000
145	0.000	0.000	0.000	0.000	0.000	0.000	0.000	0.000	0.000	0.000	0.000	0.000	0.000	0.000	0.000	0.000	0.000	0.000	0.000	0.000	0.000
115	0.001	0.001	0.001	0.001	0.001	0.002	0.003	0.005	0.007	0.011	0.015	0.022	0.029	0.039	0.051	0.068	0.082	0.106	0.126	0.160	0.186
87	0.035	0.054	0.077	0.105	0.138	0.177	0.221	0.272	0.329	0.393	0.464	0.543	0.628	0.722	0.822	0.941	1.048	1.182	1.304	1.454	1.592
50	2.718	2.985	3.264	3.556	3.858	4.171	4.495	4.828	5.170	5.519	5.875	6.238	6.605	6.976	7.348	7.630	8.087	8.334	8.808	9.014	9.501
45	1.404	1.503	1.603	1.705	1.809	1.914	2.019	2.125	2.232	2.338	2.443	2.548	2.651	2.753	2.846	2.888	2.976	2.978	3.031	2.997	3.011
37.5	3.452	3.644	3.837	4.031	4.224	4.417	4.608	4.797	4.984	5.167	5.347	5.523	5.693	5.858	6.002	6.036	6.160	6.109	6.153	6.034	5.998
31.5	3.792	3.955	4.114	4.269	4.420	4.564	4.703	4.835	4.958	5.052	5.108	5.125	5.107	5.053	4.978	4.876	4.820	4.728	4.658	4.577	4.499
26.5	4.372	4.517	4.655	4.787	4.910	5.026	5.132	5.230	5.317	5.364	5.357	5.301	5.200	5.057	4.895	4.739	4.616	4.505	4.393	4.320	4.222
22.4	4.630	4.743	4.848	4.942	5.028	5.082	5.083	5.033	4.936	4.824	4.713	4.604	4.497	4.393	4.294	4.224	4.124	4.078	3.987	3.962	3.883
19	4.889	4.975	5.050	5.115	5.170	5.188	5.140	5.030	4.866	4.699	4.550	4.420	4.306	4.208	4.123	4.073	3.975	3.945	3.857	3.842	3.766
16	4.487	4.506	4.505	4.450	4.345	4.212	4.079	3.946	3.815	3.694	3.587	3.493	3.412	3.342	3.281	3.251	3.176	3.157	3.092	3.083	3.028
13.2	4.774	4.754	4.708	4.585	4.390	4.173	3.988	3.832	3.704	3.594	3.497	3.411	3.336	3.273	3.217	3.194	3.121	3.106	3.045	3.037	2.987
11.2	4.381	4.293	4.141	3.995	3.860	3.739	3.637	3.551	3.481	3.421	3.367	3.321	3.280	3.246	3.216	3.193	3.164	3.144	3.122	3.106	3.090
9.5	4.419	4.307	4.127	3.968	3.839	3.732	3.641	3.566	3.504	3.451	3.404	3.363	3.327	3.297	3.270	3.248	3.225	3.205	3.188	3.170	3.160
8	4.548	4.400	4.263	4.148	4.055	3.978	3.913	3.859	3.815	3.777	3.743	3.714	3.689	3.667	3.648	3.618	3.615	3.586	3.588	3.560	3.567
6.3	6.003	5.793	5.637	5.511	5.408	5.324	5.253	5.193	5.145	5.103	5.066	5.034	5.006	4.982	4.960	4.919	4.923	4.883	4.893	4.854	4.869
4.75	5.513	5.364	5.255	5.166	5.095	5.036	4.986	4.944	4.909	4.879	4.852	4.828	4.807	4.789	4.773	4.727	4.744	4.700	4.720	4.679	4.701
3.35	8.547	8.432	8.347	8.278	8.221	8.174	8.134	8.099	8.070	8.045	8.022	8.001	7.983	7.967	7.952	7.922	7.926	7.900	7.904	7.883	7.886
2.36	7.591	7.523	7.472	7.429	7.394	7.364	7.337	7.314	7.294	7.276	7.260	7.246	7.232	7.220	7.210	7.230	7.190	7.216	7.173	7.204	7.159
1.18	8.081	8.009	7.952	7.903	7.860	7.822	7.788	7.758	7.732	7.708	7.685	7.665	7.646	7.628	7.612	7.755	7.583	7.730	7.558	7.706	7.537
0.6	4.601	4.561	4.528	4.498	4.471	4.446	4.424	4.405	4.387	4.370	4.355	4.341	4.328	4.316	4.305	4.396	4.286	4.367	4.269	4.341	4.254
0.3	1.422	1.394	1.370	1.349	1.330	1.313	1.298	1.284	1.272	1.260	1.250	1.241	1.232	1.224	1.217	1.224	1.204	1.207	1.192	1.192	1.183
0.15	0.663	0.645	0.629	0.615	0.603	0.592	0.582	0.573	0.566	0.558	0.552	0.546	0.540	0.535	0.531	0.507	0.522	0.499	0.515	0.492	0.509
0	9.674	9.643	9.616	9.593	9.572	9.553	9.536	9.521	9.508	9.496	9.485	9.474	9.465	9.457	9.449	9.343	9.435	9.336	9.423	9.331	9.412

CSS (mm)	52	54	56	58	60	62	64	66	68	70	72	74	76
Size (mm)	% retained												
460	0.000	0.000	0.000	0.000	0.000	0.000	0.000	0.000	0.000	0.000	0.000	-	0.000
290	0.000	0.000	0.000	0.000	0.000	0.000	0.000	0.000	0.000	0.000	0.000	-	0.000
230	0.000	0.000	0.000	0.000	0.000	0.000	0.000	0.000	0.000	0.000	0.000	-	0.000
145	0.000	0.001	0.003	0.005	0.007	0.011	0.017	0.023	0.031	0.041	0.052	-	0.081
115	0.222	0.181	0.228	0.280	0.337	0.399	0.476	0.541	0.631	0.718	0.797	-	0.997
87	1.747	1.990	2.158	2.332	2.512	2.698	2.892	3.086	3.283	3.483	3.701	-	4.115
50	9.832	10.130	10.390	10.610	10.790	10.930	10.810	11.110	10.920	10.920	11.130	-	11.010
45	2.975	2.936	2.897	2.859	2.822	2.786	2.745	2.719	2.687	2.659	2.632	-	2.580
37.5	5.872	5.746	5.629	5.518	5.416	5.320	5.228	5.147	5.076	5.007	4.930	-	4.808
31.5	4.421	4.347	4.278	4.214	4.153	4.097	4.070	3.995	3.978	3.937	3.868	-	3.796
26.5	4.155	4.092	4.033	3.978	3.926	3.877	3.867	3.789	3.786	3.750	3.679	-	3.616
22.4	3.842	3.804	3.768	3.734	3.703	3.673	3.678	3.620	3.628	3.605	3.554	-	3.516
19	3.731	3.698	3.667	3.638	3.611	3.585	3.594	3.540	3.550	3.530	3.483	-	3.451
16	3.003	2.980	2.958	2.938	2.919	2.901	2.903	2.868	2.871	2.856	2.828	-	2.805
13.2	2.964	2.943	2.924	2.905	2.888	2.872	2.871	2.842	2.841	2.828	2.805	-	2.784
11.2	3.078	3.066	3.055	3.045	3.035	3.026	3.011	3.010	2.995	2.987	2.989	-	2.976
9.5	3.149	3.139	3.129	3.120	3.112	3.104	3.086	3.089	3.071	3.064	3.070	-	3.059
8	3.558	3.551	3.543	3.536	3.530	3.523	3.498	3.512	3.487	3.482	3.497	-	3.488
6.3	4.859	4.850	4.842	4.834	4.826	4.818	4.783	4.805	4.770	4.764	4.787	-	4.777
4.75	4.693	4.685	4.678	4.671	4.665	4.658	4.626	4.647	4.617	4.613	4.631	-	4.622
3.35	7.878	7.871	7.864	7.857	7.851	7.845	7.840	7.833	7.833	7.829	7.817	-	7.808
2.36	7.153	7.147	7.141	7.136	7.130	7.125	7.172	7.116	7.165	7.162	7.102	-	7.094
1.18	7.527	7.518	7.509	7.501	7.493	7.485	7.621	7.470	7.600	7.590	7.450	-	7.438
0.6	4.248	4.242	4.236	4.231	4.225	4.220	4.266	4.211	4.251	4.244	4.198	-	4.190
0.3	1.179	1.175	1.171	1.168	1.164	1.161	1.155	1.155	1.148	1.144	1.146	-	1.141
0.15	0.507	0.504	0.502	0.500	0.498	0.495	0.475	0.492	0.472	0.470	0.486	-	0.483
0	9.408	9.404	9.400	9.396	9.392	9.389	9.316	9.382	9.313	9.312	9.373	-	9.367

Affect of feed rate - basalt

Table 50: Product PSDs of basalt passing through a jaw crusher with varying feed rates. Power data is shown and values were calculated using JKSimMet.

CSS (mm)	75

		Product PSD		
Feed rate (t h^{-1})		10	333	657
Size (mm)	Feed			
460	0.000	0.000	0.000	0.000
290	10.000	0.000	0.000	0.000
230	6.124	0.000	0.000	0.000
145	8.876	0.000	0.000	0.000
115	6.273	0.035	0.035	0.035
87	5.808	3.199	3.199	3.199
50	7.576	23.740	23.740	23.740
45	3.841	5.616	5.616	5.616
37.5	6.366	9.893	9.893	9.893
31.5	5.695	7.909	7.909	7.909
26.5	5.173	7.049	7.049	7.049
22.4	3.604	4.852	4.852	4.852
19	3.030	4.063	4.063	4.063
16	2.544	3.322	3.322	3.322
13.2	2.476	3.192	3.192	3.192
11.2	4.355	4.734	4.734	4.734
9.5	4.008	4.412	4.412	4.412
8	4.017	4.246	4.246	4.246
6.3	4.442	4.738	4.738	4.738
4.75	4.704	5.080	5.080	5.080
3.35	1.087	1.667	1.667	1.667
2.36	0.001	0.573	0.573	0.573
1.18	0.000	0.863	0.863	0.863
0.6	0.000	0.441	0.441	0.441
0.3	0.000	0.207	0.207	0.207
0.15	0.000	0.094	0.094	0.094
0	0.000	0.078	0.078	0.078

Feed rate (t h^{-1})	Power draw (kW)
10	81.395
60	88.368
110	95.341
160	102.314
210	109.287
260	116.26
310	117.031
333	123.233
357	129.788
407	136.731
457	143.734
507	150.708
557	157.681
607	164.654
657	171.627

Affect of feed rate – BIF ore

Table 51: Product PSDs of BIF ore passing through a jaw crusher with varying feed rates. Power data is shown and values were calculated using JKSimMet.

CSS (mm)	75

		Product PSD		
Feed rate ($t\ h^{-1}$)		10	333	657
Size (mm)	Feed			
460	0.000	0.000	0.000	0.000
290	10.000	0.000	0.000	0.000
230	6.124	0.000	0.000	0.000
145	8.876	0.000	0.000	0.000
115	6.273	0.028	0.028	0.028
87	5.808	2.872	2.872	2.872
50	7.576	24.040	24.040	24.040
45	3.841	5.776	5.776	5.776
37.5	6.366	10.170	10.170	10.170
31.5	5.695	7.992	7.992	7.992
26.5	5.173	7.073	7.073	7.073
22.4	3.604	4.840	4.840	4.840
19	3.030	4.041	4.041	4.041
16	2.544	3.325	3.325	3.325
13.2	2.476	3.200	3.200	3.200
11.2	4.355	4.804	4.804	4.804
9.5	4.008	4.450	4.450	4.450
8	4.017	4.337	4.337	4.337
6.3	4.442	4.801	4.801	4.801
4.75	4.704	5.118	5.118	5.118
3.35	1.087	1.555	1.555	1.555
2.36	0.001	0.362	0.362	0.362
1.18	0.000	0.362	0.362	0.362
0.6	0.000	0.237	0.237	0.237
0.3	0.000	0.175	0.175	0.175
0.15	0.000	0.125	0.125	0.125
0	0.000	0.317	0.317	0.317

Feed rate ($t\ h^{-1}$)	Power draw (kW)
10	81.195
60	87.167
110	93.14
160	99.113
210	105.085
260	111.058
310	117.031
333	119.778
357	122.645
407	128.618
457	134.59
507	140.563
557	146.536
607	152.508
657	158.481

Affect of feed rate – granite

Table 52: Product PSDs of granite passing through a jaw crusher with varying feed rates. Power data is shown and values were calculated using JKSimMet.

CSS (mm)	75

		Product PSD		
Feed rate (t h^{-1})		10	333	657
Size (mm)	Feed			
460	0.000	0.000	0.000	0.000
290	10.000	0.000	0.000	0.000
230	6.124	0.000	0.000	0.000
145	8.876	0.000	0.000	0.000
115	6.273	0.029	0.029	0.029
87	5.808	3.114	3.114	3.114
50	7.576	24.620	24.620	24.620
45	3.841	5.635	5.635	5.635
37.5	6.366	9.876	9.876	9.876
31.5	5.695	7.784	7.784	7.784
26.5	5.173	6.904	6.904	6.904
22.4	3.604	4.707	4.707	4.707
19	3.030	3.932	3.932	3.932
16	2.544	3.236	3.236	3.236
13.2	2.476	3.120	3.120	3.120
11.2	4.355	4.742	4.742	4.742
9.5	4.008	4.424	4.424	4.424
8	4.017	4.302	4.302	4.302
6.3	4.442	4.794	4.794	4.794
4.75	4.704	5.126	5.126	5.126
3.35	1.087	1.615	1.615	1.615
2.36	0.001	0.408	0.408	0.408
1.18	0.000	0.430	0.430	0.430
0.6	0.000	0.294	0.294	0.294
0.3	0.000	0.227	0.227	0.227
0.15	0.000	0.171	0.171	0.171
0	0.000	0.514	0.514	0.514

Feed rate (t h^{-1})	Power draw (kW)
10	81.288
60	87.731
110	94.173
160	100.615
210	107.057
260	113.499
310	119.941
333	122.905
357	125.997
407	132.439
457	138.881
507	145.323
557	151.766
607	158.208
657	164.65

Affect of feed rate – hard talc

Table 53: Product PSDs of hard talc passing through a jaw crusher with varying feed rates. Power data is shown and values were calculated using JKSimMet.

CSS (mm)	75

		Product PSD		
Feed rate ($t\ h^{-1}$)		10	333	657
Size (mm)	Feed			
460	0.000	0.000	0.000	0.000
290	10.000	0.000	0.000	0.000
230	6.124	0.000	0.000	0.000
145	8.876	0.000	0.000	0.000
115	6.273	0.033	0.033	0.033
87	5.808	3.292	3.292	3.292
50	7.576	24.610	24.610	24.610
45	3.841	5.605	5.605	5.605
37.5	6.366	9.815	9.815	9.815
31.5	5.695	7.753	7.753	7.753
26.5	5.173	6.881	6.881	6.881
22.4	3.604	4.694	4.694	4.694
19	3.030	3.923	3.923	3.923
16	2.544	3.227	3.227	3.227
13.2	2.476	3.112	3.112	3.112
11.2	4.355	4.732	4.732	4.732
9.5	4.008	4.417	4.417	4.417
8	4.017	4.289	4.289	4.289
6.3	4.442	4.780	4.780	4.780
4.75	4.704	5.104	5.104	5.104
3.35	1.087	1.595	1.595	1.595
2.36	0.001	0.388	0.388	0.388
1.18	0.000	0.403	0.403	0.403
0.6	0.000	0.285	0.285	0.285
0.3	0.000	0.230	0.230	0.230
0.15	0.000	0.180	0.180	0.180
0	0.000	0.653	0.653	0.653

Feed rate ($t\ h^{-1}$)	Power draw (kW)
10	81.395
60	88.369
110	95.344
160	102.319
210	109.293
260	116.268
310	123.242
333	126.45
357	129.798
407	136.773
457	143.747
507	150.722
557	157.696
607	164.671
657	171.645

Affect of feed rate – lead-zinc ore

Table 54: Product PSDs of lead-zinc ore passing through a jaw crusher with varying feed rates. Power data is shown and values were calculated using JKSimMet.

CSS (mm)	75

Feed rate ($t\ h^{-1}$)		Product PSD		
Size (mm)	Feed	10	333	657
460	0.000	0.000	0.000	0.000
290	10.000	0.000	0.000	0.000
230	6.124	0.000	0.000	0.000
145	8.876	0.000	0.000	0.000
115	6.273	0.037	0.037	0.037
87	5.808	3.110	3.110	3.110
50	7.576	22.960	22.960	22.960
45	3.841	5.581	5.581	5.581
37.5	6.366	9.887	9.887	9.887
31.5	5.695	7.963	7.963	7.963
26.5	5.173	7.128	7.128	7.128
22.4	3.604	4.955	4.955	4.955
19	3.030	4.163	4.163	4.163
16	2.544	3.439	3.439	3.439
13.2	2.476	3.316	3.316	3.316
11.2	4.355	4.854	4.854	4.854
9.5	4.008	4.509	4.509	4.509
8	4.017	4.344	4.344	4.344
6.3	4.442	4.825	4.825	4.825
4.75	4.704	5.115	5.115	5.115
3.35	1.087	1.600	1.600	1.600
2.36	0.001	0.415	0.415	0.415
1.18	0.000	0.519	0.519	0.519
0.6	0.000	0.363	0.363	0.363
0.3	0.000	0.265	0.265	0.265
0.15	0.000	0.188	0.188	0.188
0	0.000	0.460	0.460	0.460

Feed rate ($t\ h^{-1}$)	Power draw (kW)
10	81.385
60	88.312
110	95.24
160	102.167
210	109.094
260	116.021
310	122.948
333	126.134
357	129.459
407	136.386
457	143.313
507	150.24
557	157.167
607	164.094
657	171.022

Affect of feed rate – porphyry copper

Table 55: Product PSDs of porphyry copper passing through a jaw crusher with varying feed rates. Power data is shown and values were calculated using JKSimMet.

CSS (mm)	75

		Product PSD		
Feed rate (t h^{-1})		10	333	657
Size (mm)	Feed			
460	0.000	0.000	0.000	0.000
290	10.000	0.000	0.000	0.000
230	6.124	0.000	0.000	0.000
145	8.876	0.000	0.000	0.000
115	6.273	0.030	0.030	0.030
87	5.808	3.027	3.027	3.027
50	7.576	23.930	23.930	23.930
45	3.841	5.646	5.646	5.646
37.5	6.366	9.943	9.943	9.943
31.5	5.695	7.916	7.916	7.916
26.5	5.173	7.045	7.045	7.045
22.4	3.604	4.851	4.851	4.851
19	3.030	4.061	4.061	4.061
16	2.544	3.346	3.346	3.346
13.2	2.476	3.223	3.223	3.223
11.2	4.355	4.802	4.802	4.802
9.5	4.008	4.459	4.459	4.459
8	4.017	4.319	4.319	4.319
6.3	4.442	4.791	4.791	4.791
4.75	4.704	5.094	5.094	5.094
3.35	1.087	1.559	1.559	1.559
2.36	0.001	0.370	0.370	0.370
1.18	0.000	0.407	0.407	0.407
0.6	0.000	0.287	0.287	0.287
0.3	0.000	0.222	0.222	0.222
0.15	0.000	0.167	0.167	0.167
0	0.000	0.507	0.507	0.507

Feed rate (t h^{-1})	Power draw (kW)
10	81.276
60	87.658
110	94.039
160	100.42
210	106.802
260	113.183
310	119.565
333	122.5
357	125.563
407	131.945
457	138.326
507	144.707
557	151.089
607	157.74
657	163.851

Affect of feed rate – copper carbonatitie

Table 56: Product PSDs of copper carbonatitie passing through a jaw crusher with varying feed rates. Power data is shown and values were calculated using JKSimMet.

CSS (mm)	75

		Product PSD		
Feed rate ($t\ h^{-1}$)		10	333	657
Size (mm)	Feed			
460	0.000	0.000	0.000	0.000
290	10.000	0.000	0.000	0.000
230	6.124	0.000	0.000	0.000
145	8.876	0.000	0.000	0.000
115	6.273	0.033	0.033	0.033
87	5.808	3.210	3.210	3.210
50	7.576	24.260	24.260	24.260
45	3.841	5.622	5.622	5.622
37.5	6.366	9.870	9.870	9.870
31.5	5.695	7.836	7.836	7.836
26.5	5.173	6.965	6.965	6.965
22.4	3.604	4.778	4.778	4.778
19	3.030	3.996	3.996	3.996
16	2.544	3.290	3.290	3.290
13.2	2.476	3.170	3.170	3.170
11.2	4.355	4.768	4.768	4.768
9.5	4.008	4.437	4.437	4.437
8	4.017	4.308	4.308	4.308
6.3	4.442	4.792	4.792	4.792
4.75	4.704	5.122	5.122	5.122
3.35	1.087	1.621	1.621	1.621
2.36	0.001	0.446	0.446	0.446
1.18	0.000	0.543	0.543	0.543
0.6	0.000	0.339	0.339	0.339
0.3	0.000	0.220	0.220	0.220
0.15	0.000	0.139	0.139	0.139
0	0.000	0.235	0.235	0.235

Feed rate ($t\ h^{-1}$)	Power draw (kW)
10	81.367
60	88.2
110	95.034
160	101.868
210	108.701
260	115.535
310	122.368
333	125.512
357	128.792
407	135.626
457	142.459
507	149.293
557	156.127
607	162.96
657	169.794

Appendix III – Blast vibration and acoustic readings

Blast 1

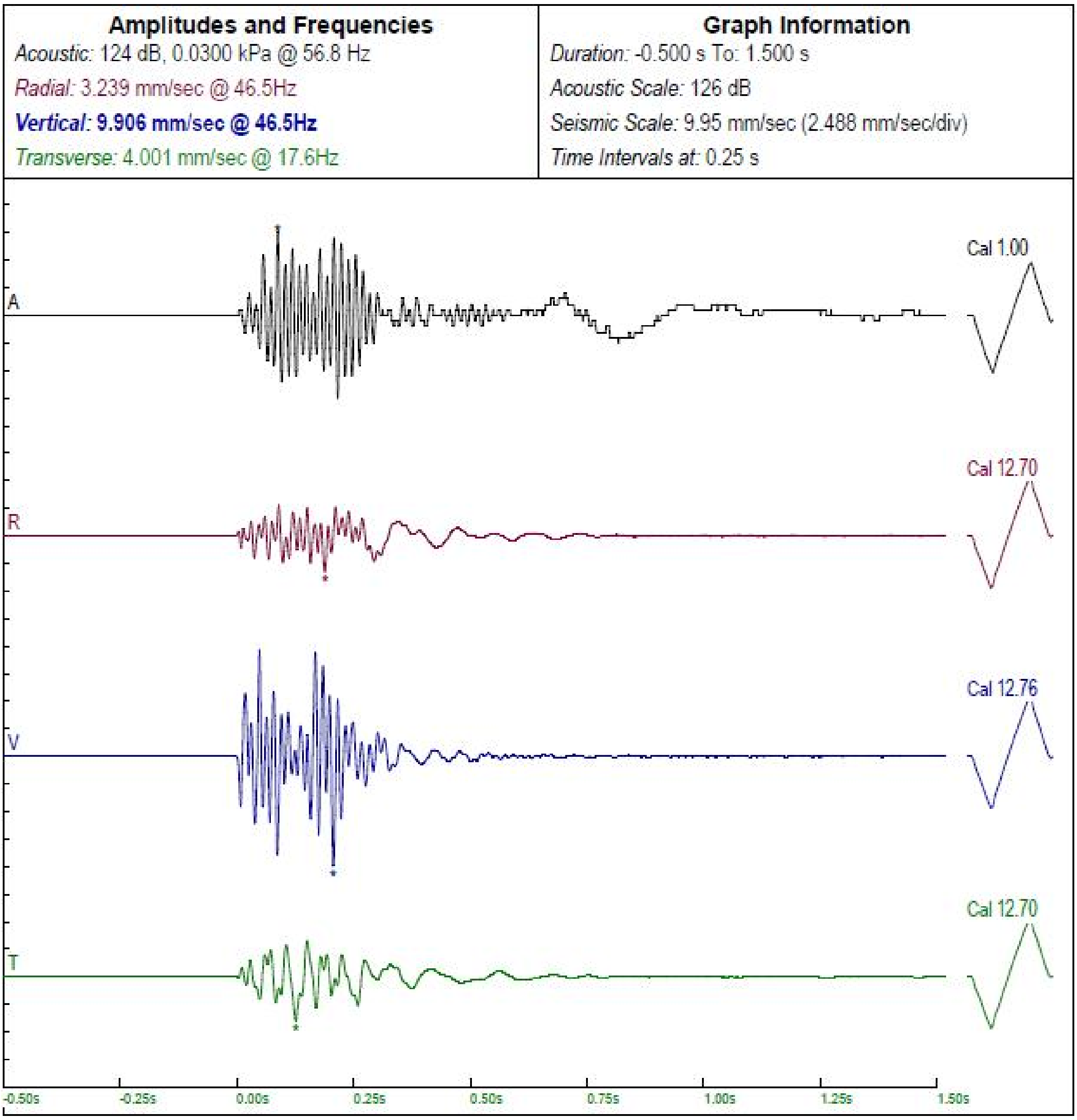

Figure 38: Acoustic and vibration readings from blast 1.

Blast 2

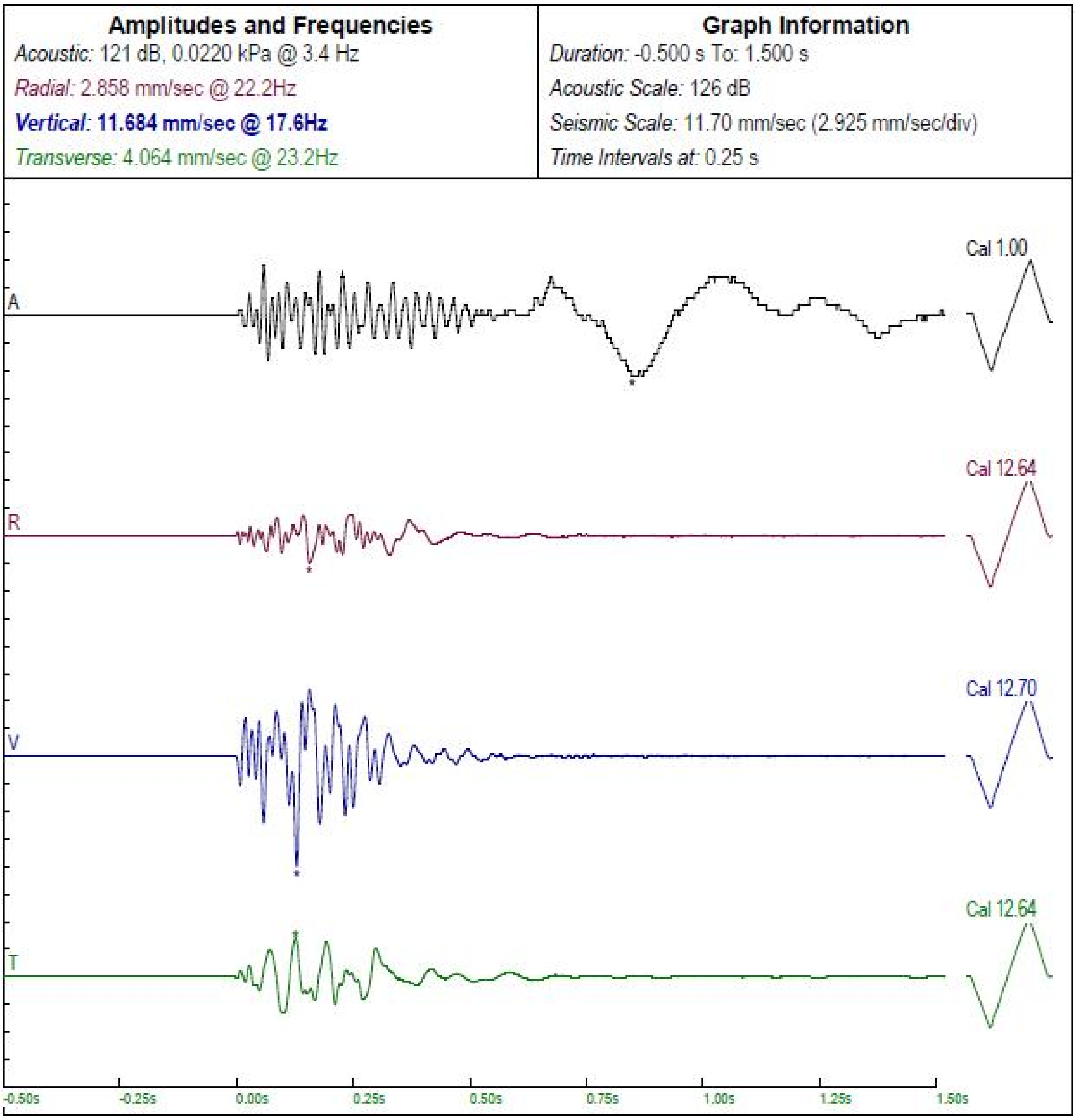

Figure 39: Acoustic and vibration readings from blast 2.